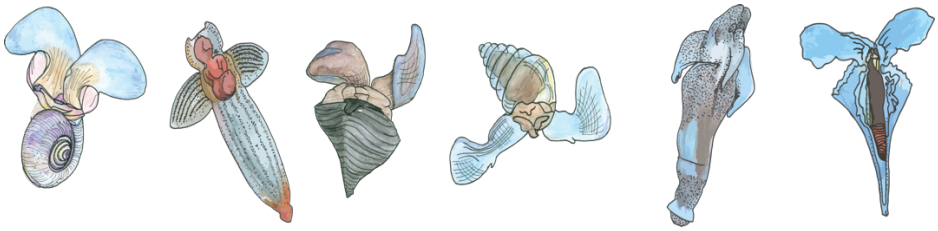

THE ECOLOGICAL FUNCTIONING OF SOUTHERN OCEAN PTEROPODS AND THE USE OF NOVEL FIELD- AND LABORATORY-BASED APPROACHES

By

Christine Kim Weldrick, BSc (UBC), MSc (UVic)

Submitted in fulfilment of the requirements for the Degree of

Doctor of Philosophy

University of Tasmania

Date 16 October 2019

"And what's more, they are all still smiling despite the long hours, roasting air temperatures, questionable coffee dispensed by the machine in the corridor and, for many of them, the repetitive, mind-numbing tasks—like counting sea butterflies."

Helen Scales

Spirals in Time:
The Secret Life and Curious Afterlife of Seashells

Statements and Declarations

Declaration of Originality

This thesis contains no material which has been accepted for a degree or diploma by the University or any other institution, except by way of background information and duly acknowledged in the thesis, and to the best of my knowledge and belief, no material previously published or written by another person where due acknowledgement is made in the text of the thesis, nor does the thesis contain any material that infringes copyright.

Statement of Authority of Access

The publishers of the papers comprising Chapters 2 and 3 hold the copyright for that content. Access to the material should be sought from the respective journals. The remaining non-published content of the thesis may be made available for loan and limited copying in accordance with the Copyright Act 1968.

Statement regarding published work contained in thesis

The publishers of the papers comprising Chapters 2 and 3 hold the copyright for that content, and access to the material should be sought from the journal. The remaining non published content of the thesis may be made available for loan and limited copying and communication in accordance with the Copyright Act 1968.

Statement of Ethical Conduct

The research associated with this thesis abides by the international and Australian codes on human and animal experimentation, the guidelines by the Australian Government's Office of the Gene Technology Regulator and the rulings of the Safety, Ethics and Institutional Biosafety Committees of the University. All research conducted for this thesis was approved by the University of Tasmania Animal Ethics Committee (Permit No. A0010843).

Signed:

Christine K. Weldrick

Date: 16 October 19

Statement of co-author contributions

The following people and institutions contributed to the publication of work undertaken as part of this thesis:

Christine K. Weldrick, Institute for Marine & Antarctic Studies, UTas

Dr. Kerrie M. Swadling, Institute for Marine & Antarctic Studies, UTas

Dr. Rowan Trebilco, Institute for Marine & Antarctic Studies, UTas

Dr. Diana M. Davies, CSIRO Oceans and Atmosphere, Hobart, TAS

Publications result from research, author details and their roles:

Paper 1, Can lipid removal affect interpretation of resource partitioning from stable isotopes in Southern Ocean pteropods?

Reproduced in Chapter 2; published in *Rapid Communications in Mass Spectrometry* – Wiley Publishing:

***Weldrick, C.K.**, Trebilco, R., Swadling, K.M., 2019. Can lipid removal affect interpretation of resource partitioning from stable isotopes in Southern Ocean pteropods?* Rapid Communications in Mass Spectrometry. *doi: 10.1002/rcm.8384*

- Christine K. Weldrick (70%)
- Dr. Kerrie M. Swadling (15%)
- Dr. Rowan Trebilco (15%)

Paper 2, Trophodynamics of Southern Ocean pteropods on the southern Kerguelen Plateau

Reproduced in Chapter 3; published in *Ecology & Evolution* – Wiley Publishing:

***Weldrick, C.K.**, Trebilco, R., Davies, D.M., Swadling, K.M. Trophodynamics of Southern Ocean pteropods south of the Kerguelen Plateau.* Ecology & Evolution. *doi: 10.1002/ece3.5380*

- Christine K. Weldrick (70%)
- Dr. Kerrie M. Swadling (10%)
- Dr. Rowan Trebilco (10%)
- Dr. Diana M. Davies (10%)

We the undersigned agree with the above stated "proportion of work undertaken" for each of the above published (or submitted) peer-reviewed manuscripts contributing to this thesis:

Signed:
Dr. Kerrie Swadling
Primary Supervisor
Institute for Marine & Antarctic Studies
University of Tasmania

Signed:
Prof. Craig Johnson
Head of Ecology & Biodiversity Centre
Institute for Marine & Antarctic Studies
University of Tasmania

Acknowledgements

Unquestionably, the successful completion of this degree was largely due the continued support, dedication, and generosity in knowledge and with time of my supervisory team, Drs. Kerrie Swadling and Rowan Trebilco. For them, I am forever grateful. During my time at IMAS, my team presented me with multiple opportunities for personal and professional growth and experience. They have enabled me to hone my writing and analytical skills, and further develop my critical thinking. Important to also stress is the great patience they possess, as they gave me the right amount of pressure while I grappled with numerous mental and physical health obstacles in my personal life. Kerrie and Rowan have granted me other notable opportunities for upskilling, including those related to voyage preparation, problem solving, fieldwork logistics and international relations. Undeniably, my confidence surrounding my ability to even call myself a marine ecologist is attributed entirely to my team.

I thank the organizations and institutes, including the Antarctic, Climate, & Ecosystems Cooperative Research Centre (ACE CRC), Australian Antarctic Division (AAD), Australian Nuclear Science and Technology Organization (ANSTO), Ecological Society of Australia (ESA), and Equity Trustees who provided opportunities and funding to enable the completion of this PhD research and research dissemination.

There are a great number of other people who have assisted immensely in my PhD journey. To the captain, crew, fellow researchers/expeditioners, and science technical support aboard the RV *Aurora Australis* and TRV *Umitaka-maru*, thank you for safe passage over the Southern Ocean, keeping me positive, helping with sampling, and in some cases, keeping me company while I work up to 20 hours per day. There was a rescue mission involved, and I am truly grateful for the concerted effort of a large group of individuals to keep things from "going south" (pun intended). It was during this time that I forged an everlasting friendship with my true blue PhD pal, Jake Wallis, who shocks me every day with his capacity to put others before himself, and I owe him the moon for the many ways he's helped me over the last few years. Ruth

Eriksen and Kohei Matsuno, thank you so much for being *sugoi* travel mates and for introducing me to wonderful Japanese culture. Thank you Lavy Ratnarajah for giving your time to help me navigate the world of grant proposals. I have deep gratitude for Wenneke ten Hout, and her incredible ability to make all things possible. Of special note, I would be remiss if I failed to thank Felipe Briceño for letting me recover in his dreamy Puerto Varas home after catching something truly awful from the IsoEcol conference.

Thanks to the anonymous examiners who dedicated their time and gave highly constructive feedback that greatly improved the quality of this work.

There were other beings and entities that require mentioning here, particularly for their role in keeping my mental health floating above water: Karen Kilgariff and Georgia Hardstark of the My Favorite Murder podcast, the various networks that made all of the episodes of Terrace House, Twin Peaks, and Game of Thrones available for much needed decompression. Some of my more stressful moments were significantly eased by several furry and feathered beings, including Yeti, Tino, Bella, Millie, Wavy, Benti, Zaph, Rosie, Robin, Susie, Tommy, Finn, Frankie, Gingy Ninjy and Scamps (or whatever your real names are), and even you, too, Rocky and Peanut. But not you Pixie and Ziggy: you know what you did.

Inevitably, this chapter of my life could not have been conceived if it weren't for the tireless support of my life partner, Tom. From the deep, deep bottom of my heart, I am truly indebted to you. I have a million reasons to thank you, but I will always be grateful that you picked me for life. I'm excited to see what sort of adventures we'll be getting ourselves into next.

During my time as doctoral candidate, my grandmother, Hubert Barr, lost her battle with Alzheimer's disease. She inspired me through her staunch leadership and community service through volunteerism. While I will always regret being so far away while she suffered. I've dedicated this work to her memory. This is for you, Nanny.

General Abstract

Southern Ocean (SO) thecosome pteropods are considered sentinels of anthropogenic ocean acidification (OA), and mounting evidence shows that rapid changes in ocean chemistry will affect their functional roles within marine ecosystems. However, there are major gaps in understanding of their current functional roles, along with the nature and magnitude of ongoing changes to these roles. There is urgency to address these gaps to establish a benchmark against which ongoing species-to-ecosystem scale responses may be assessed. The research in this thesis draws together state-of-the-art methodologies to provide new insights on the intra- and interspecific ecological roles of co-occurring SO pteropod species, focusing on the Indian sector of the Southern Ocean.

In the first two data chapters of this thesis, I used analysis of tissue stable isotope signatures to derive new insights into trophodynamics of among 3 key species of Southern Ocean pteropods. In Chapter 2, I first used isotopic niche metrics and a comparative analysis of several normalization models to show that it is important to account for lipids, either chemically or mathematically, before applying stable isotopes analysis (SIA) to estimate ecological niches for polar pteropods with moderate to high lipid content. In Chapter 3, I then extended the isotopic analysis to assess interspecific variability in feeding behaviour, including examining relationships between trophic position and body size. I found that *Clio pyramidata* f. *sulcata* occupied the lowest trophic position and smallest niche breadth relative to two gymnosomes, *Clione limacina antarctica* and *Spongiobranchaea australis*. This analysis also revealed dichotomous feeding and diet behaviour in gymnosomes, with *C. limacina antarctica* exhibiting either a more generalist behaviour than expected or a niche breadth reflective of food limitation.

In my third data chapter, I drew upon data from sediment traps to assess the contribution of pteropods to particle flux, which is a major (but poorly understood) mechanism by which pteropods contribute to carbon recycling in and export from Southern Ocean ecosystems. Two sediment traps were deployed to measure pteropod swimmer abundance and composition on two time scales. In both experiments, highest abundances were measured for *Limacina helicina antarctica* veligers. Fluorescence and sinking particulate organic and inorganic carbon possessed the most explanatory power for abundances of thecosome compositions, while gymnosome abundances were largely influenced by increasing adult *L. helicina antarctica* counts.

In my final data chapter, I examined fecundity, which is a key gap in knowledge of pteropod life histories (and information for their representation in population and ecosystem models). I assessed fecundity as the number of fertilized eggs per spawning event. I assessed egg and egg mass morphometrics, potential drivers of production, and presented a comprehensive description of the embryogenetic stages. Overall, egg dimensions change very little through successive embryonic stages, however egg areas decrease through the spawning season. Significant differences in egg and egg mass morphology between voyage samples were also discussed.

Together, these chapters represent a synthesis of emerging methods and broader ecological implications. Understanding of the key roles of pteropods in the Indian Sector of the Southern Ocean estimated here can enable better assessments of their impacts throughout the Southern Ocean and global marine ecosystems more broadly.

TABLE OF CONTENTS

List of Figures

List of Tables

Chapter 1

General Introduction and thesis overview

1.1 Pteropods, anthropogenic climate threats, and knowledge gaps

Global oceans absorb between 25 and 30% of the anthropogenic carbon emissions released into the atmosphere annually (Frölicher et al., 2016). While this absorptive ability has somewhat curtailed global warming, significant changes are still predicted for polar regions, such as increased warming, shallowing mixed layer depths, strengthening winds, declining sea ice and southward migration of oceanic frontal zones (Deppeler and Davidson, 2017). This is in addition to the significant chemical changes that have already occurred, including lowered surface seawater pH, carbonate ion concentration (CO_3^{-2}), and carbonate mineral saturation states (Orr et al., 2005). These changes have implications operating on all scales of biological systems that are enforced by abiotic changes to water circulation, nutrient cycling, and temperature. These abiotic changes could cause shifts in distribution and abundance of predator and prey communities, impact biodiversity, deter growth and respiration rates of species, and alter ecosystem services (Doney et al., 2009; Dupont et al., 2010; Perry et al., 2005; Sabine et al., 2004). Understanding these changes will require rigorous scientific data collection drawn from species and ecosystems that are sensitive to multiple stressors of climate change (Bednaršek et al., 2016).

Pteropods are opisthobranch gastropods comprising two taxonomic clades: Thecosomata and Gymnosomata. These clades are predominantly distinguished from one another by one major trait: thecosomes possess shells and gymnosomes do not. Both orders have a modified foot evolved into wings (parapodia) that they use for swimming (Lalli and Gilmer, 1989). Given the close trophic links with each other as well as with higher order species, both are potentially vulnerable to anthropogenic climate change. Studies highlighting the vulnerability of thecosome pteropods to ocean acidification primarily attribute it to their aragonite shells. Aragonite is a polymorph of calcium carbonate that is ~50 % more soluble to seawater than calcite (Mucci, 1983), thus suggesting that organisms such as pteropods are likely prone to dissolution, particularly as the partial pressure of carbon dioxide increases in global oceans as the aragonite saturation state (Ω_A) steadily decreases. Seawater that is greater than 1 ($\Omega_A > 1$), is conducive to shell formation, whereas seawater with $\Omega_A < 1$ means shell dissolution occurs to organisms that lack mechanisms to cope with acidic conditions (Yamamoto-Kawai et al., 2009).

In the Southern Ocean, aragonite undersaturation ($\Omega_A < 1$) is forecasted to occur in wintertime surface waters sometime between 2030 and 2038 (McNeil and Matear, 2008), and become more widespread on a seasonal long-term scale by 2050 (Hauri et al., 2016); however, *in situ* observations from sediment traps already reveal effects of ocean acidification on natural pteropod populations. In the sub-Antarctic, only 3% of pteropod shells sampled below the Ω_A horizon (depth where Ω_A falls below 1) exhibit ideal, or intact, preservation state, whereas 50% of shells sampled above this zone appear intact (Roberts et al., 2011). In the Terra Nova Bay polynya, Manno et al. (2007) also observed significant shell degradation among pteropods sampled below the Ω_A horizon, as well as low fluxes of *Limacina helicina* shells and carbonate. Shells from live pteropods sampled from undersaturated surface waters of the Scotia Sea (within 200 m), were diagnosed with severe dissolution, where prismatic layers of shells were completely missing (Bednaršek et al., 2012a). Furthermore, results from these Southern Ocean-based studies only mirror those reported from a significantly greater magnitude of research conducted on northern hemisphere assemblages (Manno et al., 2017).

These observations have collectively led to pteropods becoming increasingly widely-regarded as sentinels of ocean acidification (Bednaršek et al., 2017). However, a recent study revealed the production of an outer shell coating, or periostracum, that is produced by *L. helicina* to repair and maintain their shells from mechanical damage (Peck et al., 2018). It was proposed that, for many pteropods, mechanical damage occurs during attempted predation, which consequently exposes the damaged region to localised dissolution during winter months when Ω_A of the water column decreases beneath the sea ice. While these findings do not conclude that *L. helicina* is resistant to the effects of OA, they raise questions around the general assumptions regarding OA effects on pteropods, and highlights the need for further studies examining the energetic costs of shell repair. In light of these findings, this thesis will not discriminate other anthropogenic climate stressors, including warming and changing food supply, as potential threats to the functional ecological roles of pteropods, examined here as their biogeochemical and trophodynamic interactions.

Six species of pteropods are common within Southern Ocean waters (Hunt et al., 2008; Table 1.1). Among them, four are thecosomes that are believed to play a key role in the structure and function of Southern Ocean marine ecosystems (Hunt et al., 2008). Two species are gymnosomes, which are also believed to be vulnerable to climate change due largely to their monophagous (specialist) feeding behaviour on thecosomes. As with other dominant Southern Ocean mesozooplankton groups, such as copepods, euphausiids, and salps, pteropod distributions are closely linked to oceanographic frontal zones (Hosie et al. 2014).

Table 1.1 Species of both shelled (thecosome) and naked (gymnosome) pteropods most commonly found in the Southern Ocean. ACC = Antarctic Circumpolar Current (~60°S), PF = Polar Front (~55°S), STF = Sub-Tropical Front (~43°S). Typical distribution, biogeographic affinity, and depth range based on data compiled by Roberts et al. (2014) and Hunt et al. (2008).

Species	Authority	Order	Typical Distribution	Biogeographic Affinity	Depth Range
Clio piatkowskii	Bosc, 1802	Thecosomata	Weddell Sea	Antarctic	Bathypelagic
Clio pyramidata f. *sulcata*	Pfeffer, 1879	Thecosomata	South of PF to Antarctic coast	Antarctic	Epi-mesopelagic
Clione limacina antarctica	E.A. Smith, 1902	Gymnosomata	STF-Antarctic coast	Antarctic/sub-Antarctic	Epipelagic
Limacina helicina f. *antarctica*	Woodward, 1854	Thecosomata	South of ACC	Antarctic	Epipelagic
Limacina retroversa australis	Eydoux & Souleyet, 1840	Thecosomata	STF to PF	Sub-Antarctic	Epipelagic
Spongiobranchaea australis	D'Orbigny, 1834	Gymnosomata	STF-Antarctic coast	Sub/Antarctic	Epi-mesopelagic

Research has shown that Southern Ocean frontal zones are shifting southward, and it is believed that distribution of key plankton assemblages will also shift (Constable et al., 2014), potentially impacting trophic energy pathways throughout marine food webs. Field observations have already detected spatial changes in pteropod assemblages. In summers between 1993 and 2004, unusually higher densities of *L. helicina* were observed along the shelf waters of the northern and mid-western Antarctic Peninsula, as well as over the slope towards the south, than previously reported (Ross et al., 2008). In the following summers of 2009 and 2010 from the same region, Bernard et al. (2012) observed greater *L. helicina* densities towards coastal waters than along the shelf. In Terra Nova Bay, interannual peaks in summer abundance and biomass have shown shallow water (<50 m) zooplankton to be dominated by *L. helicina antarctica* (Guglielmo et al., 2007, 1998; Hopkins, 1987; Pane et al., 2004), and Minutoli et al., (2017) identified trends of increasing pteropod abundances from pelagic to coastal stations as well as northern to southern stations. Together, thecosomes and gymnosomes have accounted for up to 93 % of total macrozooplankton abundance in the East Antarctic at an interannual scale (Hunt

et al., 2008), yet despite this, there remains a lack of understanding of the magnitude of influence exerted by pteropods on the food web ecology of the Southern Ocean.

Over a decade ago, Hunt et al. (2008) published a review on Southern Ocean pteropods that, whilst a comprehensive synthesis of the data available at the time, highlighted many knowledge gaps in pteropod ecological research. The review encouraged future studies to focus largely on trophic behaviour, life history strategies, biogeochemical inputs, and any flow-on effects from human-induced variability of pteropod assemblages. What has emerged in pteropod-focused research since then? According to *Web of Science*, a search using the key word 'pteropod' results in 290 peer-reviewed publications spanning the last ten years. Among these results, ~71 studies feature Southern Ocean specimens though only four studies from the Indian sector, south of 60 °S (Fig. 1). Most of these Southern Ocean-based studies reported abundance (13 studies) and distribution (9 studies), whereas a comparatively small proportion reported data on aspects of functional roles of pteropods, including embryogenesis (1 study), flux potential (5 studies), population dynamics (1 study), and trophodynamics (4 studies). This thesis will explore significant gaps in our understanding of ecological roles of Southern Ocean pteropods, including biogeochemical and trophodynamic roles, from the relatively under-surveyed region of the Indian Sector.

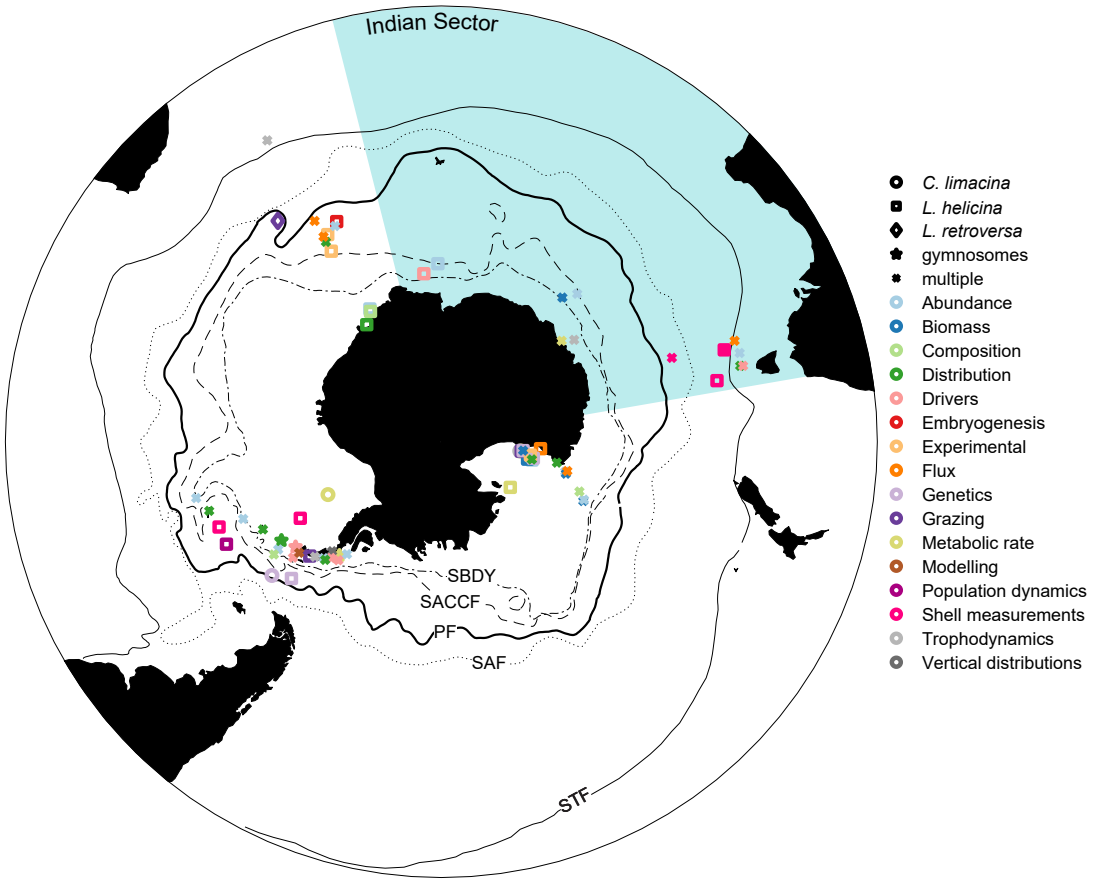

Figure 1.1 Locations of peer-reviewed studies related to pteropod-focused research. Shapes refer to taxa analysed; colours depict types of analysis; shaded region is the Indian Sector: black lines are oceanographic fronts, following Orsi et al. (1995), including PF = Polar Front, SACCF = Southern Antarctic Circumpolar Front, SAF = Subantarctic Front, SBDY = Southern Boundary, STF = Subtropic Front.

1.2 Ecological functioning of Southern Ocean pteropods

To measure the magnitude and dynamics of the functional roles that pteropods play in Southern Ocean ecosystems, it is essential to first define these roles. The following is an introduction to the major functional roles identified for Southern Ocean pteropod species.

1.2.1 Trophodynamic role

Thecosome pteropods feed on a wide range of phytoplankton and other food particles, ranging from bacteria to diatoms, dinoflagellates and small crustaceans and gastropod larvae (Hunt et al., 2008). One stable isotope study from East Antarctica reported a heavy reliance on sea ice biota by *L. helicina* (Jia et al., 2016). Gut contents analyses in thecosomes is minimal for Southern Ocean species (Hunt et al., 2008), however those that have been conducted revealed a high dietary proportion of diatoms, particularly in *L. helicina* sampled from the Ross Sea and South Georgia (Hopkins, 1987; Morton, 1954). A closely linked inter-seasonal relationship exists

between pteropod abundances and concentrations of primary producers. Bernard and Froneman (2009) found that whilst *L. retroversa* only comprised 5% of total mesozooplankton near the Polar Frontal (PF) zone of the Indian sector, they contributed up to 89% of total grazing impact per day. Previous stable isotopes and fatty acid analyses reveal a preference for *Clio pyramidata* by *Spongiobranchaea australis* (Hunt et al., 2008; Phleger et al., 1999). In contrast to *C. limacina*, *S. australis* feeds using two lateral arms, each with multiple suckers for grasping prey (Lalli and Gilmer, 1989).

Thecosomes and gymnosomes are important prey for a number of higher order trophic organisms, such as whales, seals, seabirds, squid, fishes, and other zooplankton (Hunt et al., 2008; Lalli and Gilmer, 1989; Pakhomov et al., 1996). A recent study from McMurdo Sound, Antarctica, reported diet preference for *C. limacina* by the giant sea spider, *Colossendeis magalonyx*, (Moran et al., 2018). Pteropods have also been shown to vary seasonally within diets of the myctophids from the Scotia Sea, with the highest proportion of pteropods found in spring-sampled *Electrona antarctica,* relative to other seasons (Saunders et al., 2018).

1.2.2 Biogeochemical role

Pteropods are conduits of organic and inorganic carbon export to the deep sea through numerous pathways. Significant grazing and predation rates mean they contribute significantly to organic carbon cycling through the production and release of negatively buoyant faecal pellets: flux up to 362 x 10^3 pellets m^{-2} $year^{-1}$ has been estimated in the Terra Nova Bay Polynya in the Ross Sea (Manno et al., 2010). The aggregation of un-grazed or dead particles by discarded mucous feeding webs produced by thecosomes is responsible for export of marine particulate organic carbon (POC) at depth (Noji et al., 1997). Thecosomes also play an important role in the sequestration of particulate inorganic carbon (PIC) of biological origin, through the synthesis and subsequent rapid-sinking of their aragonite shells when they die (Manno et al., 2007). Combined, the magnitude of these biogeochemical roles are such that when thecosomes seasonally dominate the calcifying communities in the Southern Ocean, they can impact total annual reduction of CO_2 transferred to the deep sea by up to twice that of other calcifying zooplankton, such as foraminifera and ostracods (Manno et al., 2018). The changes projected to occur within the Southern Ocean, and consequently to thecosome abundances, could mean significant changes to the efficiency of the carbon pump.

1.3 Innovative research techniques for addressing key knowledge gaps for Southern Ocean pteropods

A recent review of global pteropod research identified key knowledge gaps and acknowledged innovative research techniques to help address them (Manno et al., 2017). Some examples of gaps identified included coordinated research programs combining carbonate chemistry measurements with biological sampling, globally-scaled biomass estimates, and life history including life span and rate of shell growth. They highlighted innovative research techniques, including tomographic scanning, acoustics, video-imaging and molecular, trace elemental and stable isotopes analyses of shells. The following sections present additional novel techniques and approaches not featured within their report but used here to assess the ecological roles of Southern Ocean pteropods, including their contribution to the structure and function of Antarctic marine foodwebs.

1.3.1 Stable isotopes and lipid analysis

Ecologists view stable isotopes analysis (SIA) as a powerful analytical tool that can be applied to quantify trophic relationships, estimate ecological niches, and monitor seasonal food sources (Boecklen et al., 2011; Newsome et al., 2007). The majority of pteropod-based SIA research focuses on paleo-oceanographic records that use oxygen isotopic composition of their shells as climate proxies for seasonal variability of past sea surface temperatures (Keul et al., 2017). What is lacking are data estimating the carbon and nitrogen isotopic values from their soft tissues that provide valuable, time-integrated information about intra- and interspecific relationships in trophic connectivity.

When comparing the $\delta^{13}C$ values of species across a range of temporal and spatial scales it is important to first assess their lipid content to avoid bias. This is especially true for many polar organisms that possess large lipid stores used during winter months when prey availability is low (Phleger et al., 1997). The presence of highly variable ^{12}C-rich lipids in tissues can skew $\delta^{13}C$ values as lipids tend to be significantly more depleted in ^{13}C relative to other common macromolecules, including carbohydrates and proteins (Peterson and Fry, 1987). Without correcting for lipid content, either chemically or mathematically, $\delta^{13}C$ values from food sources may be masked. The aim is to measure the origin of carbon assimilated specifically through diet and tissues possessing moderate to high lipid content are often highly variable within and among tissues (DeNiro and Epstein, 1977).

Moderate lipid levels have been measured within *Limacina helicina* (8%), whereas the gymnosome *Clione limacina* has been reported to possess higher concentrations (37%) that are up

to 10 times as much lipid as other pteropod species (Kattner et al., 1998; Phleger et al., 1997). Triacylglycerols, and the alkyldiacylglycerol ethers that are specific to *C. limacina*, are the major lipid classes found within the few polar pteropod species examined (Kattner et al., 1998; Phleger et al., 1997). Kattner et al. (1998) used lipid compositions to measure the close trophic relationships between Arctic and Antarctic phytoplankton, *L. helicina* and *C. limacina* and found high amounts of 16:1(n-7), indicating diatom feeding by *L. helicina*, and significant levels of an uncommon lipid found in *C. limacina*. This lipid, known as 1-*O*-alkyldiacylglycerol ethers was not detected in its prey, *L. helicina*, and likely synthesized by *C. limacina* as a highly specialized biochemical adaptation to polar life. Given this information, it is clear that polar pteropods are most probably require lipid correction prior to SIA, and there is impetus to warrant further investigations into the effects of lipids on both $\delta^{13}C$ and $\delta^{15}N$ values in both polar pteropod clades.

1.3.2 Bayesian niche metrics

Classic ecological niche theories are developed to model the size and diversity of species coexisting within a particular space (Chase and Leibold, 2003). Hutchinson's ecological niche is defined as an *n*-dimensional hypervolume, bounded by axes representing the extent of environmental variables and resources required by an organism to persist (Hutchinson, 1957). The trophic niche is a version of the ecological niche that is primarily diet-focused. Carbon ($\delta^{13}C$) and nitrogen ($\delta^{15}N$) SIA has emerged as a standard method in ecology for gaining insight into the trophic relationships underlying food web dynamics. This method is particularly powerful in estimating carbon sources and nitrogen flow from primary producers to secondary consumers (Peterson and Fry, 1987). For 40 years, scientists have used stable isotope bi-plots to represent the niche, whereby the location of $\delta^{13}C$-$\delta^{15}N$ space occupied by an organism provides both an index of the basal resources from which consumers derive their energy, and the trophic level at which they feed (Fink et al., 2012). Bearhop et al., (2004) were among the first ecologists to infer trophic niche breadth using the variance of $\delta^{13}C$ and $\delta^{15}N$ values of consumers and food source tissues. This was followed by the development of quantitative spatial metrics to infer niche width, species spacing, density, overlapping, and clustering from the extent and spread of isotopic data points (Jackson et al., 2011; Layman et al., 2007; Swanson et al., 2014), all of which are emerging tools to approximate dimensionality of the spread of assemblages.

Southern Ocean zooplankton are an essential component of marine food webs in terms of providing top-down and bottom-up regulation of species composition, yet Southern Ocean-based niche research has focused primarily on higher trophic levels, including myctophid fishes

(Cherel et al., 2010), penguins (Cherel, 2008; Jaeger and Cherel, 2011), albatross and petrels (Cherel et al., 2017; Jaeger et al., 2010). These studies have provided valuable insights into spatial and seasonal foraging strategies of key Antarctic assemblages. However, there is a lack of similar data for lower trophic organisms, such as zooplankton, whose biological responses to climate change can influence the functioning of entire marine ecosystems given their significant trophic role as conduits of energy from primary producers to higher order predators (Tarling et al., 2017). Poleward range shifts by species assemblages in response to climate change is expected to result in overlapping niches (Walther et al., 2002), and consequently lead to changes in ecological interactions, including competition and/or predation, impacting many species, including pteropods, which rely heavily upon sea-ice biota (Jia et al., 2016; Urban et al., 2012).

1.3.3 Sinkers and 'Swimmers'

Classically, sediment traps have been the primary method for capturing passively sinking biogenic materials, enabling the estimation of particulate organic and inorganic carbon flux (POC and PIC, respectively) that lead to estimating the relative regional and global contributions of thecosomes to deep sea carbon and carbonate sequestration (Berger, 1978; Harbison and Gilmer, 1986). These studies traditionally assume that materials entrained within trap cups have arrived there passively as dead animals via vertical sinking, and as such, specimens identified as "swimmers" are initially removed from analyses. Pathways whereby swimmers could end up in traps include diurnal vertical migration, whereby thecosomes feed at the surface at night and sink to lower layers by day, and downward escape behaviour elicited by predation attempts (Harbison and Gilmer, 1986). While inappropriate for estimating their biogeochemical role (e.g. flux potential), trap-caught swimmers have been shown to provide valuable insight into seasonal fluctuations in polar zooplankton species and age composition and abundance (Makabe et al., 2010; Matsuno et al., 2014). In a study comparing the abundances of Arctic zooplankton taxa sampled by plankton net and sediment trap methods, pteropod abundances from both methods were significantly correlated, and relatively constant throughout the year (Makabe et al., 2016). This suggests that sediment traps can effectively gather ecological data on pteropods, and provide year-round data collection and monitoring in regions inaccessible to sampling, including by nets and continuous plankton recorders, as well as in deeper waters, under ice and during winter.

1.3.4 Microscopic image analyses

The quantitative analysis of physical form and shape, or morphometrics, can be a powerful tool when applied to investigating life history strategies of organisms. When the shape and size of organisms are microscopic, challenges in morphometric analyses can be minimized with the use of image analyses software platforms. Pteropod egg masses possess hundreds, sometimes thousands, of eggs within their matrices (Lalli and Gilmer, 1989; Manno et al., 2016; Paranjape, 1968), and manually estimating counts can be time consuming and prone to error. Image analyses can effectively automate processes involved with performing egg counts and early life stage morphometric measurements, and has shown to possess high levels of success compared to traditional manual methods (da Silva Júnior et al., 2018). Platforms such as ImageJ have been effectively employed in experimental work estimating the effects of future OA conditions on the brooding strategies of the marine gastropod *Crepidula fornicata* (Noisette et al., 2014). There is potential to expand this application towards estimations of fecundity in pteropods.

1.4 Study Region: The Indian Sector of the Southern Ocean

Research presented here was drawn from sampling expeditions that explored the Indian sector of the Southern Ocean (Fig. 2), a region which is under-surveyed compared to the Antarctic Peninsula and Weddell Sea, among others. Included in this region is the "Kerguelen Axis", a highly productive area, extending between the Kerguelen Plateau and the Antarctic continent. Satellite-based chlorophyll imagery of this region reveals an immense seasonal phytoplankton bloom that supports a diverse array of species, including large biomass of fish to the north and Antarctic krill to the south (Schallenberg et al., 2018). The iron-limited region towards the southern extent of the plateau is characterised by relatively low concentrations of primary productivity, whereas the plateau's eastern boundary near Princess Elizabeth Trough sustains long durations of summer phytoplankton blooms due to upwelling of iron-rich water (Schallenberg et al., 2018). While this biologically important region is undergoing change, including southward movement of the PF (Sokolov and Rintoul, 2009), reduction in sea-ice extent (De la Mare, 2009), and changes in overturning circulation of Antarctic Bottom Water (Purkey & Johnson, 2013; Rintoul, 2007; Shimada et al. 2012), their effects on adjacent marine ecosystems is not widely known, and the large fluctuating phytoplankton bloom reported here may mean that pteropods form a significant trophic link between primary productivity and higher level organisms.

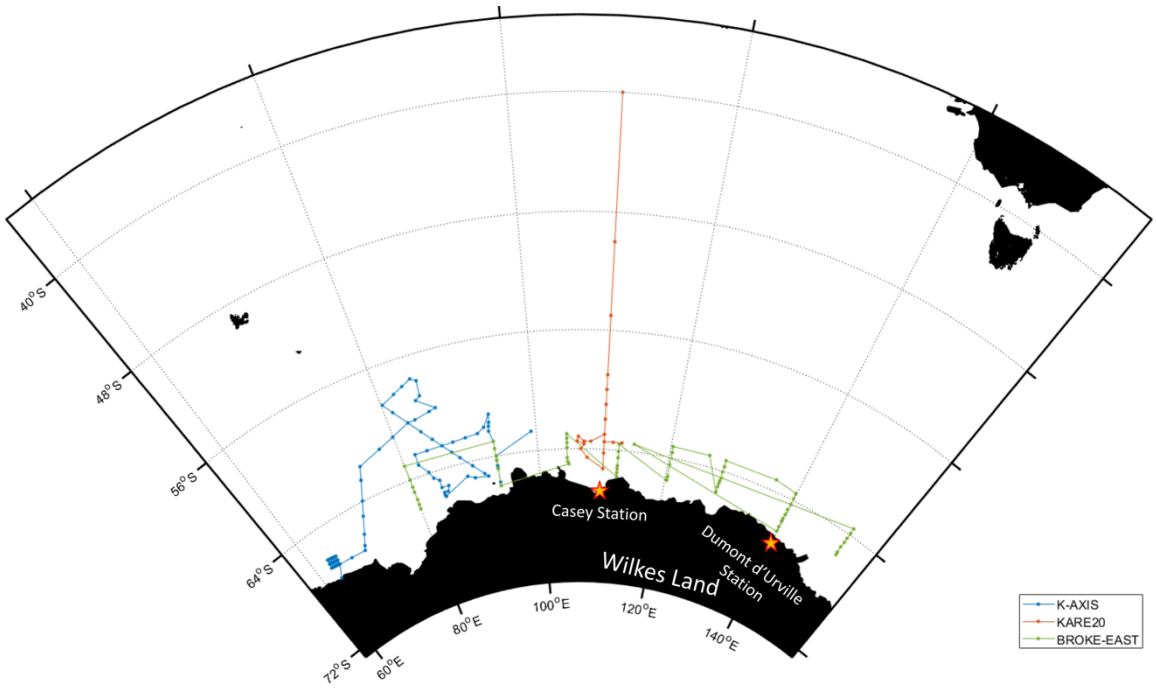

Figure 1.2 Ship's tracks of three Southern Ocean voyage programs along East Antarctica from which data is featured within this thesis, including K-Axis (2015/16), KARE20 (2016/17), and BROKE-EAST (1995/96). Locations of Antarctic bases Casey Station and Dumont d'Urville Station are marked by stars.

Research reported here also comes from samples retrieved from waters along Wilkes Land off Antarctica. This region is characterised by a pattern of variable chlorophyll concentrations between 83°E and 115°E, that transitions to low chlorophyll concentrations east of Casey Station, at 120°E (Comiso et al., 1993). The edge of the sea ice retreat along this coastline aligns with the bottom topography (Moteki et al., 2017). Previous oceanographic expeditions have detected freshening of Antarctic Bottom Water near Dumont d'Urville base, at 140°E, which may enforce flow-on effects to regional ecosystem functioning (Aoki et al., 2013).

1.5 Thesis Objectives, Questions and Approaches

The central objectives of this thesis were to improve current understanding of the functional roles of pteropods from an under-surveyed region of the Southern Ocean, as well as introduce novel techniques used to enable and advance pteropod-focused research. My focus was on understanding the structure and functional roles of sympatric species, as well as environmental variables that drive these species, through a survey of the lesser explored Indian Sector.

Specifically, this thesis asks:

1. What are the trophodynamic relationships between co-occurring pteropod species?
2. What is the relationship between trophic position and body size in adult pteropod species?
3. What information can be gained about abundance, flux potential and population dynamics from both sinking and swimmer pteropods?
4. What are the stages of embryogenesis and how does fecundity change over time and with variability in prey size?
5. What are the oceanographic and ecological drivers of adult and egg abundance and egg production in pteropods?

To answer these questions, the research presented in this thesis is based on samples collected during three Southern Ocean voyages spanning three separate summers along East Antarctica (Fig. 2), including BROKE-EAST (RV *Aurora Australis*, 1995/96), KAXIS (RV *Aurora Australis*, 2015/16), and KARE20 (TRV *Umitaka-maru*, 2016/17). Among these voyages, I directly participated on the latter three, spanning 2015 to 2017. I used novel research approaches, some of which have rarely, if ever, been used to study Southern Ocean pteropods, including Bayesian niche metrics, microscopic image analysis, the use of 'swimmers' and sinking specimens to estimate population dynamics and growth rate from sediment traps, and generalized additive models to estimate drivers of spatial variability in egg production.

Chapter 1 reviews previous research on species abundance, life history, feeding traits, and anthropogenic threats to Southern Ocean pteropods, and outlines potential knowledge gaps that remain since the last review on Southern Ocean pteropods, published over a decade ago.

Chapter 2 compares the stable isotopic values with and without chemical lipid extraction conducted prior to analyses, and assesses a suite of mathematical normalization models as an alternative to chemical extraction when estimating the isotopic niches of three co-occurring pteropod species.

Chapter 3 uses the correction formula established in Chapter 2, and estimates the isotopic niche breadth of the same species, calculates their trophic positions, and measures the relationship between trophic position and body size.

Chapter 4 uses passive sinking and active swimmer specimens retrieved from two, temporally distinct, sediment trap experiments and calculates species and age composition and flux, population dynamics and growth rate.

Chapter 5 uses *L. helicina antarctica* egg mass samples spanning three voyage programs to characterise the stages of embryogenetic development, estimate fecundity and identify potential environmental, ecological and physical drivers of spatial variability in egg production.

Chapter 6 synthesizes new insights into the functional roles of Southern Ocean pteropods provided by this thesis, and identifies future research directions that may assist in benchmarking these roles against variability caused by future climate change.

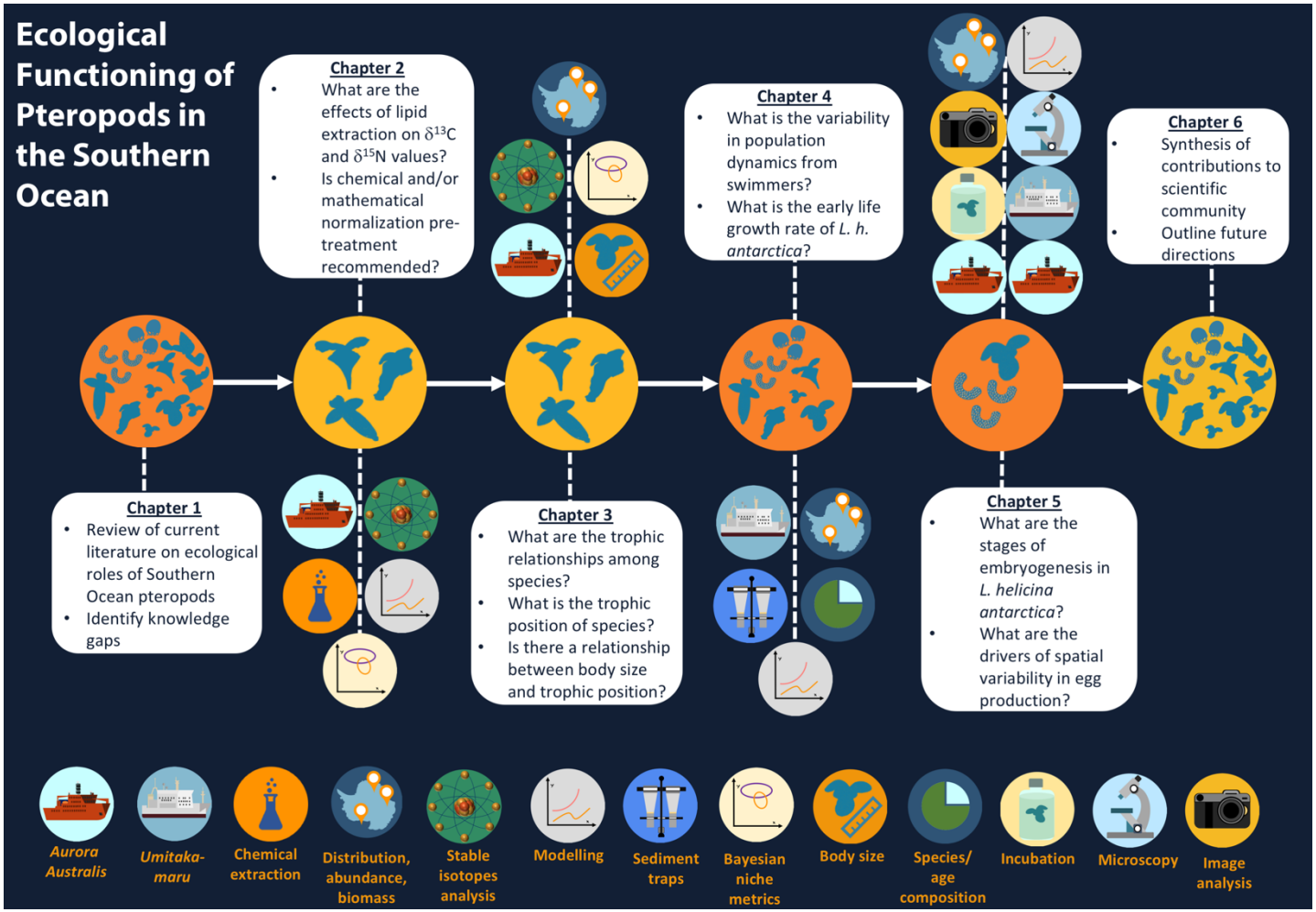

Figure 1.3 Graphical abstract depicting thesis outline covering research questions and topics addressed. Central icons depict the species and /or age classes featured in each chapter, including all species and age classes in Chapters 1 and 6, three adult species in Chapters 2 and 3, four species and some age classes of *L. helicina antarctica* in Chapter 4, and egg masses and adults of *L. helicina antarctica* in Chapter 5.

Chapter 2

Can lipid removal affect interpretation of resource partitioning from stable isotopes in Southern Ocean pteropods?[1]

2.1 Graphical Highlights

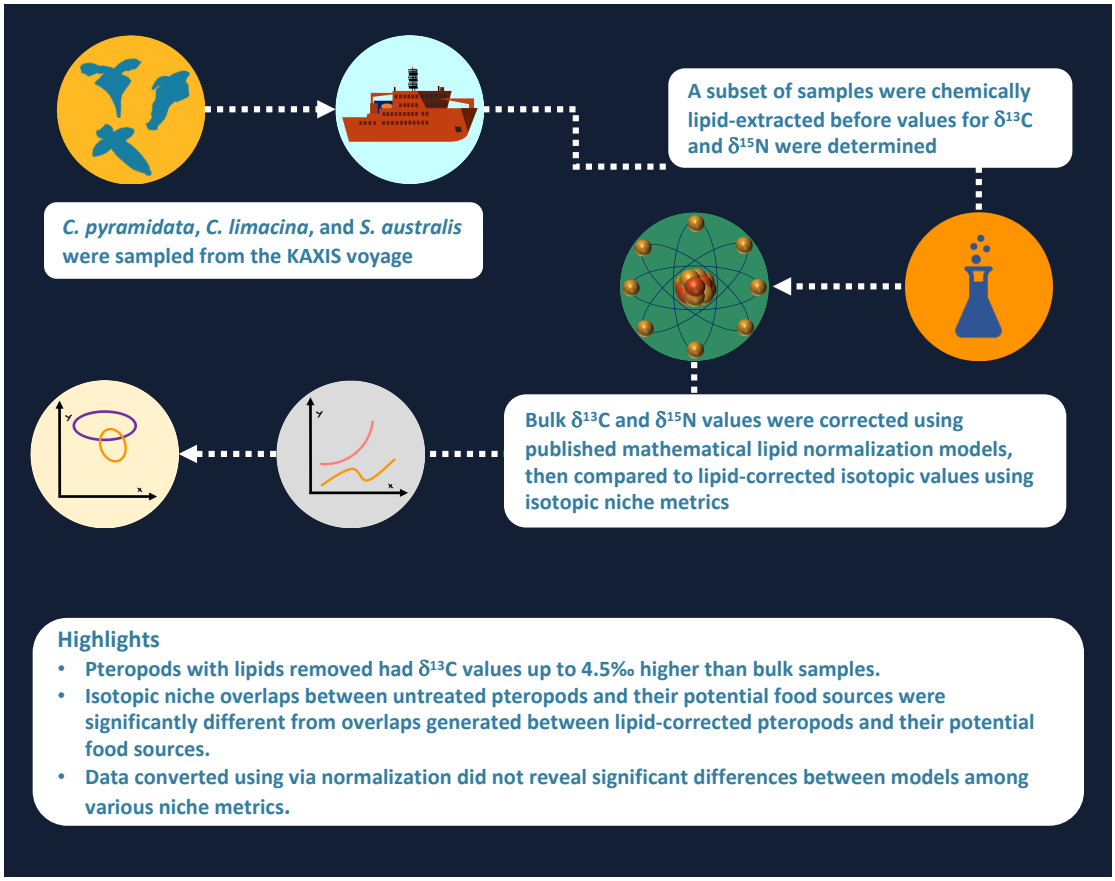

Figure 2.1 Graphical abstract for Chapter 2.

2.2 Key words

Lipid normalization, lipid correction, $\delta^{13}C$ and $\delta^{15}N$, niche dispersion metrics, polar, zooplankton

[1] *This work has been published in a refereed journal and is presented below in identical form. The citation for the original publication is:*
Weldrick, C.K., Trebilco, R., Swadling, K.M. 2019. Can lipid removal affect interpretation of resource partitioning from stable isotopes in Southern Ocean pteropods? *Rapid Communications in Mass Spectrometry*. doi: 10.1002/rcm.8384

2.3 Abstract

Stable isotopes analysis (SIA) is a powerful tool to estimate dietary links between polar zooplankton. However, the presence of highly variable ^{12}C-rich lipids may skew estimations as they are depleted in ^{13}C relative to proteins and carbohydrates, consequently masking carbon signals from food sources. Lipid effects on pteropod-specific values requires examining, since accounting for lipids is rarely conducted among the few existing pteropod-related SIA studies. It is currently unclear whether lipid correction is necessary prior to SIA of pteropods. Whole bodies of three species of pteropods (*Clio pyramidata* f. *sulcata*, *Clione limacina antarctica*, and *Spongiobranchaea australis*) sampled from the Southern Ocean were lipid-extracted chemically to test the effects on $\delta^{13}C$ and $\delta^{15}N$ values (n = 38 individuals in total). We determined the average change in $\delta^{13}C$ values for each treatment, and compared this offset to published normalization models. We tested lipid correction effects on isotopic niche dispersion metrics to compare interpretations surrounding food web dynamics.

Pteropods with lipids removed had $\delta^{13}C$ values up to 4.5‰ higher than bulk samples. However, lipid extraction also produced higher $\delta^{15}N$ values compared to bulk samples. Isotopic niche overlaps between untreated pteropods and their potential food sources were significantly different from overlaps generated between lipid-corrected pteropods and their potential food sources. Data converted using several published normalization models did not reveal significant differences among various calculated niche metrics, including standard ellipse and total area.

We recommend accounting for lipids via chemical extraction or mathematical normalization before applying SIA to calculate ecological niche metrics, particularly for organisms with moderate to high lipid content such as polar pteropods. Failure to account for lipids may result in misinterpretations of niche dimensions and overlap and, consequently, trophic interactions.

2.4 Introduction

Stable isotopes analysis (SIA) has emerged as a powerful tool for elucidating food web structure, including estimates of dietary niche breadths and degree of overlap for co-occurring species (Layman et al., 2007; Newsome et al., 2007). The most commonly used stable isotope values in ecological studies are the relatively enriched, heavier isotopes of carbon and nitrogen, with values denoted as $\delta^{13}C$ and $\delta^{15}N$, respectively (Fry, 2006). $\delta^{13}C$ values vary between different basal food sources, and show relatively little fractionation (~ 1‰) between trophic levels (DeNiro and Epstein, 1978; Peterson and Fry, 1987) while $\delta^{15}N$ typically shows greater trophic

fractionation (~ 1-4 ‰) (Minagawa and Wada, 1984; Peterson and Fry, 1987). SIA can be an effective means for estimating origins of consumer dietary sources and their trophic positions within food webs, but has limitations. Importantly, it is not known whether and how standardization (or the lack thereof) of treatment protocols for SIA (Marcus et al., 2017; Pomerleau et al., 2014) affects the interpretation of trophic patterns such as niches and their overlap.

Comparison of $\delta^{13}C$ values must take account of the potential effect of lipids, particularly when comparing samples with different lipid contents (e.g. different tissues and/or species). Lipids are depleted in ^{13}C (~ 2 to 8 ‰) relative to proteins and carbohydrates (Peterson and Fry, 1987), and can be a potential source of error in ecological studies if left uncorrected. The presence of lipids can lower ^{13}C values from animal tissues possessing relatively high lipid content (i.e. percent lipid content > 5%, mass C:N ratios > 3.5 (Post et al., 2007)), and mask the carbon values derived from diet (McConnaughey and McRoy, 1979). Zooplankton obtain lipids from food and they can also synthesize them via de novo biosynthesis (Kattner et al., 1998); these biosynthesized lipids can have different ^{13}C values from those obtained through diet (Smyntek et al., 2007). This is of particular importance when analyzing zooplankton from polar environments, such as pteropods, which have been shown to exhibit unique lipid biochemical adaptations (Kattner et al., 1998; Phleger et al., 2001, 1997) that vary both seasonally and latitudinally (Syväranta and Rautio, 2010). Among pteropods the highest lipid concentrations have been recorded for the polar gymnosome (unshelled) *Clione limacina*, which possesses fat reserves that permit them to survive long periods of food limitation during seasonally low abundances of their preferred prey, thecosome (shelled) pteropod *Limacina helicina* and *L. retroversa* (Conover and Lalli, 1972; Hunt et al., 2008).

Lipid removal is routinely achieved through chemical extraction (eg. chloroform/methanol) (Hussey et al., 2014) prior to SIA, enabling the standardization of carbon values across all samples (Post et al., 2007). However, chemical extraction can be time-consuming, costly, may alter $\delta^{15}N$ values, and adversely affect other sample-processing steps, including acidification used to remove inorganic carbon (Murry et al., 2006). Mathematical normalization models provide an alternative to the chemical removal of lipids from tissues; they are based on the relationship between bulk (uncorrected) C:N ratios and $\delta^{13}C$ values and have been shown to predict $\delta^{13}C$ values for other polar marine organisms (Pomerleau et al., 2014; Syväranta and Rautio, 2010). Polar zooplankton-focused studies (Pomerleau et al., 2014; Syväranta and Rautio, 2010) have measured significant depleting effects of lipids on isotopic

values and recommend correcting for these effects prior to further analyses. To our knowledge, no studies have tested these effects on isotopic values of polar pteropods.

This study investigates the effects of lipid removal on carbon and nitrogen stable isotopes ratios in pteropod assemblages from the Indian sector of the Southern Ocean. We extracted lipids from three pteropod species and sought to determine (1) whether $\delta^{13}C$ and $\delta^{15}N$ values from chemically extracted tissues differed from those from untreated tissues, (2) if mathematical normalization models were effective in correcting for lipids, and (3) if isotopic niche dispersion metrics were sensitive to chemical lipid-extraction and/or mathematical lipid correction. Few studies have employed SIA with Southern Ocean pteropods and, among them, fewer have accounted for lipids (Hunt et al., 2008; Jia et al., 2016), making between-study comparisons problematic. Given the essential roles of pteropods in contributing to deep sea CO_2 sequestration (Manno et al., 2018), and providing top down control on phytoplankton and smaller zooplankton concentrations (Lalli and Gilmer, 1989), there is urgency to perform climate impact assessments on a relatively understudied organism highly sensitive to changes in ocean temperature and chemistry (Orr et al. 2005, Manno et al. 2017). We hypothesize that lipid extraction will result in a statistically significant increase in $\delta^{13}C$ values relative to untreated values that will consequently lead to significantly different outcomes in isotopic niche estimations.

2.5 Methods

2.5.1 Sampling of pteropods and POM

Mesozooplankton were sampled with a Rectangular Midwater Trawl 8 (RMT8) (mesh size: 4.5 mm, mouth area: 8 m^2, Nitex nylon, Australian Filter Specialists, Huntingwood, NSW, Australia), equipped with a flow meter, and towed obliquely from the surface to 200 m. Ship speed during plankton net tows was 2-2.5 knots for an average duration of 45 minutes. Thecosome (shelled) and gymnosome (naked) pteropods were counted and identified to species level. One species of thecosome, *Clio pyramidata* f. *sulcata* (hereafter *C. pyramidata*), and two species of gymnosomes, *Clione limacina antarctica* (hereafter *C. antarctica*) and *Spongiobranchaea australis*, were separated into cryotubes, then stored in liquid nitrogen prior to analyses. Size-fractionated particulate organic matter (POM) was collected through large volume sequential filtration from the ship's underway water supply (~ 5 m depth), prescreened with an upstream 47 mm-diameter, 1 mm filter mesh for zooplankton removal, then collected onto 25 mm-diameter Sterlitech silver membrane (pore size = 1.2 μm; Sterlitech Corporation, Kent, WA, USA) and Nitex filters (pore size = 210 μm; Genesee Scientific, San Diego, CA, USA). Particles were

analyzed for two size fractions: 'large' >210 μm, and 'small' <210 μm. See Schallenberg et al. (2018) for further details on sampling POM.

2.5.2 Sample preparation and lipid extraction

Subsamples from the same sampling site and date were replicated in order to compare values with and without lipid extraction (LE). Prior to SIA, all pteropod samples were rinsed in filtered seawater and weighed. Whilst previous research recommends acidifying thecosome pteropods to remove carbonate content that could otherwise bias stable isotopes results (Pomerleau et al., 2014), the pressure from the RMT8 sampling method completely stripped entire shells from most *C. pyramidata* samples, and any shell fragments remaining on others were easily removed using forceps. As a result, we did not need to acid-treat our samples prior to further analyses.

Quantitative lipid extractions were conducted using a one-phase methanol/chloroform/Milli-Q water (2:1:0.8 *v/v/v*; modified from Bligh & Dyer (1959), following Phleger et al. (1997) overnight extraction. This was followed by additional methanol/chloroform/Milli-Q water solution (final ratio of 1:1:0.9 *v/v/v*) to allow phases to break. The lower lipid phase was removed and the upper mixture was filtered down to a pellet and dried for 24 hr at 60 °C to remove remaining solvents. Non-lipid-extracted ("bulk") samples and POM sample filters were also dried for 24 hr at 60 °C. After oven-drying, individual dry weights of both bulk and lipid-extracted samples were recorded. Small discs were punched from POM filters, and individual pteropods were ground to powder using an agate mortar and pestle, then all were weighed into tin cups in preparation for isotopic analysis.

2.5.3 Stable isotopes analysis

For pteropods, bulk and LE carbon and nitrogen stable isotope ratios were obtained using an automated Elementar vario PYRO cube analyser (Elementar Analysensysteme GmbH, Langenselbold, Germany) coupled with a continuous flow IsoPrime100 isotope ratio mass spectrometer (IsoPrime Ltd, Cheadle Hulme, United Kingdom); for POM, samples were analyzed using a Thermo Scientific Flash 2000HT elemental analyser (Thermo Fisher Scientific, Bremen, Germany) interfaced with a Thermo Fisher Delta V Plus IRMS through a Thermo Fisher Conflo IV. SIA of pteropods was conducted at the Central Science Laboratory (CSL), University of Tasmania (Hobart, Tasmania, Australia), and for POM, at the Australian Nuclear Science and Technology Organisation (ANSTO) in Lucas Heights, Sydney, Australia. Isotopic ratios were expressed in delta (δ) notation and reported as parts per thousand (‰) relative to

isotopic reference standards, Vienna Pee Dee Belemnite (for carbon) and atmospheric air (for nitrogen) (DeNiro and Epstein, 1978). To measure instrument stability, analytical precision, drift correction, and linearity performance at CSL, in-laboratory working standards of sulfanilamide, repeated every 6th sample, produced a standard deviation better than ±0.1‰ for both isotopes. At ANSTO, POM isotopic data are reported relative to IAEA secondary certified standards, with a standard error of analysis to 1 standard deviation (SD) measured at ± 0.3 mil. The carbon and nitrogen percentages were converted to atomic C:N ratios (%C/%N x 1.6667). Average standard deviations on triplicate measurements made from randomly selecting pteropod specimens was calculated as 0.15‰ for $\delta^{13}C$ values and 0.19‰ for $\delta^{15}N$ values.

2.5.4 Mathematical normalization and model comparison

The goal of a mathematical normalization model is to assess whether C:N ratios can be used as a predictor of the effect of LE on $\delta^{13}C$ values. This is typically achieved using paired samples (extracted versus untreated) at an individual level, and the relationship between the extraction effect at the individual level ($\Delta\delta^{13}C$) and C:N ratio (prior to LE) is used to 'correct' bulk samples. However, the small body size of our pteropod specimens meant that we were unable to subdivide them to enable direct comparison of the effect of LE within the same specimen. In lieu of testing treatment effects within the same individual, or duplicate aliquots of pooled individuals possessing potentially high individual variability that would otherwise be lost, we compared average bulk with chemically lipid-extracted $\delta^{13}C$ values of individuals from the same sampling sites. We achieved this through linear modeling $\delta^{13}C$ values by treatment method to estimate the mean effect of extraction (lm function in R). This simplified approach statistically compares averages and provides an estimate of the effect of LE on $\delta^{13}C$.

We compared our corrected $\delta^{13}C$ values with published normalization models. We first selected a variation of a standardized mathematical protocol (McConnaughey and McRoy, 1979) specific to fish tissues that was updated for freshwater zooplankton samples by Kiljunen et al. (2006). This model estimates the effect of lipids on non-lipid extracted $\delta^{13}C$ values by first calculating a lipid factor (L) from bulk C:N ratios (by mass):

$$L = \frac{93}{1 + [0.246 \times (\mathrm{C{:}\,N_{bulk}}) - 0.775]^{-1}} \quad (1a)$$

which is then applied to the following formula to calculate lipid-extracted $\delta^{13}C$ values ($\delta^{13}C_{LE}$):

$$\delta^{13}\mathrm{C_{LE}} = \delta^{13}\mathrm{C_{bulk}} + D \times \left(I + \frac{3.9}{1 + 287/L}\right) \quad (1b)$$

In this model, *D* is the average difference between $\delta^{13}C$ value of lipid extracted and bulk samples (representing the difference between lipids and proteins) and *I* is a constant. Kiljunen et al. (2006) used values of 7.018 and 0.048 for *D* and *I*, respectively.

The second model was developed by Logan et al. (2008) through comparing chemically- and mathematically-corrected collections of marine fishes and aquatic invertebrates. Like the model by Kiljunen et al. (2006), this model assumes a non-linear relationship between bulk C:N ratios (by mass) and $\Delta\delta^{13}C$ values:

$$\delta^{13}C_{LE} = \delta^{13}C_{bulk} + \beta_0 + \beta_1 \ln(C{:}\,N_{bulk}) \quad (2)$$

where values we used for β_0 (-2.06) and β_1 (1.91) are parameter estimates specifically applied to all invertebrate species tested (Logan et al., 2008).

Post et al. (2007) developed the following normalization model based on a strong positive predictive relationship between bulk C:N (by mass) and $\Delta\delta^{13}C$ values, estimated from a large variety of aquatic animal taxa:

$$\delta^{13}C_{LE} = \delta^{13}C_{bulk} - 3.32 + 0.99 \times C{:}\,N_{bulk} \quad (3)$$

The fourth model is based on a mass balance model (Fry et al., 2003) that was updated by Smyntek et al. (2007) for freshwater zooplankton incorporates both lipid-extracted and bulk atomic C:N ratios as well as D to estimate $\delta^{13}C_{LE}$:

$$\delta^{13}C_{LE} = \delta^{13}C_{bulk} + D \times \left[\frac{(C{:}\,N_{bulk} - C{:}\,N_{LE})}{C{:}\,N_{bulk}}\right] \quad (4)$$

where *D* was estimated by Smyntek et al. (2007) to be 6.3 and, for $C{:}N_{LE}$, we employed the average values that we empirically obtained for each pteropod species (Table 1).

Finally, we analyzed the mass balance-based model developed by Syväranta & Rautio (2010) for polar aquatic zooplankton:

$$\delta^{13}C_{LE} = \delta^{13}C_{bulk} + 7.95 \times \left[\frac{(C{:}\,N_{bulk} - 3.8)}{C{:}\,N_{bulk}}\right] \quad (5)$$

where mass $C{:}N_{bulk}$ ratios were used.

We applied these mass balance normalization models to our data and statistically compared the predicted results of each model with ours using a one-way ANOVA (base function in R). This allowed us to compare mean $\delta^{13}C$ and $\Delta\delta^{13}C$ (the change in $\delta^{13}C$ values from

bulk to corrected) values generated from data converted by our average offset value and by the several published normalization models. This was followed by a Tukey's Honest Significant Difference test (base function in R) to determine which published mathematical normalization model produces mean corrected $\delta^{13}C$ and $\Delta\delta^{13}C$ values not significantly different from our calculated average offset value.

2.5.5 Statistical analyses

Data analyses were conducted using the statistical software R, version 3.4.0(Team, 2014). We used the Shapiro-Wilk's (function in base R) and Levene's (from the car package, version 3.0-0 (Fox and Weisberg, 2011)) tests on bulk and LE isotopic values ($\delta^{13}C$ and $\delta^{15}N$) to measure normality and homogeneity of variance, respectively. A one-way multivariate analysis of variance (MANOVA; manova function in base R) was used on bulk and LE $\delta^{13}C$ and $\delta^{15}N$ values (as dependent variables) to test for species and treatment effects (as independent variables). Where not otherwise specified, variability is expressed in standard deviations (SD).

To test the effect of lipid correction on isotopic niches, we followed an analytical procedure similar to that of Choy et al. (2016), who measured the effects of lipid extraction on $\delta^{13}C$ values of beluga whales and prey using niche dispersion metrics as response variables. For each species, we tested the null hypothesis that the mean Euclidean distance between each centroid calculated from each of the niche breadths, estimated from the lipid corrected and unpublished bulk datasets, did not differ from zero. Null distributions were generated by using the residual permutation procedure (RPP) and were then used to compare with test statistics (Turner et al., 2010). Resultant empirical *P* values (the rank percentile of observed differences between groups) were compared with those generated using Hotelling's T^2 test. RPP and Hotelling's T^2 tests were performed following Turner et al. (2010)

Total and standard ellipse areas (TA and SEA, respectively) of each pteropod species and their potential food sources (POM fractions for *C. pyramidata* and *C. pyramidata* for *C. antarctica* and *S. australis*) were estimated using Stable Isotope Bayesian Ellipses in R (SIBER) version 2.1.3 package (Jackson et al., 2011). SIBER generates bivariate standard ellipses and convex hulls for isotopic niches. We also measured the proportion of dietary niche overlapping between species using the R package nicheRover version 1.0 (Swanson et al., 2014), which produces probable pairwise comparisons between the niche region of each species combination within a Bayesian framework. The niche region of a species is considered to be the 95% probability that a species will be located within isotopic bivariate space, and the niche overlap is defined as 95% probability that the niche region of one species will overlap with another.

2.6 Results

2.6.1 Effect of lipid-extraction on isotopic values

Thirty-eight pteropod individuals representing three species and sampled from 12 sites were lipid-extracted (LE) (Table A.1 in Appendix A). Significant isotopic enrichment for all species in $\delta^{13}C$ values (mean Δ = 2.43 ± 0.2‰) and in $\delta^{15}N$ values (mean Δ = 1.11 ± 0.8‰) occurred in samples with lipids removed prior to SIA as compared to untreated (n = 61) samples from the same sampling sites (MANOVA: Wilk's λ: $F_{2,74}$ = 105.1, P < 0.001; Table A.2 in Appendix A). Multivariate analysis also detected significant differences in mean $\delta^{13}C$ and $\delta^{15}N$ values between species (MANOVA, Wilk's λ: species: $F_{4,148}$ = 28.6, P < 0.001; Table 2.1).

The bulk C:N ratios for all species ranged from 3.6 to 8.0 (average 4.6 ± 1.3), which was more variable than LE C:N ratios that ranged from 3.2 to 4.1 (Fig. A.1 in Appendix A, Table 2.1). The largest magnitude of increase in $\delta^{13}C$ values (LE – bulk) was detected in the gymnosome pteropods (*S. australis*: +4.0‰; *C. antarctica*: +4.5‰; Table A.1 in Appendix A).

Table 2.1 Species-specific average (± SD) bulk, lipid-extracted (LE), and lipid-corrected (LC) $\delta^{13}C$ values and bulk and LE C:N ratios. LC values were obtained using our calculated average offset value of $\Delta\delta^{13}C$ = 2.4 ± 0.2‰ from our simplified modelling approach.

Species	Bulk $\delta^{13}C$	LE $\delta^{13}C$	LC $\delta^{13}C$	C:N (bulk)	C:N (LE)
C. pyramidata	-28.1 ± 0.9	-25.4 ± 0.6	-25.7 ± 0.9	3.9 ± 0.3	3.3 ± 0.1
C. antarctica	-28.3 ± 1.0	-26.6 ± 1.2	-23.7 ± 0.8	6.4 ± 1.4	3.8 ± 0.4
S. australis	-27.9 ± 1.0	-24.0	-25.3 ± 0.9	5.1 ± 0.4	3.3

The average (by site) bulk C:N ratio for all pteropods was 5.0 ± 1.5, with a range that varied between and within species (3.7 – 7.4); however, lipid extracted samples possessed a more reduced intersample range (3.2 – 4.1), along with a much lower average C:N ratio of 3.4 ± 0.2 (Table A.1 in Appendix A). The largest variation in bulk C:N ratio in a given species was measured in *C. pyramidata* (3.7 – 4.4). *C. antarctica* was the only species to measure >7.0 in mean bulk C:N ratio, whereas *C. pyramidata* had the smallest mean bulk C:N ratio (4.0 ± 0.2).

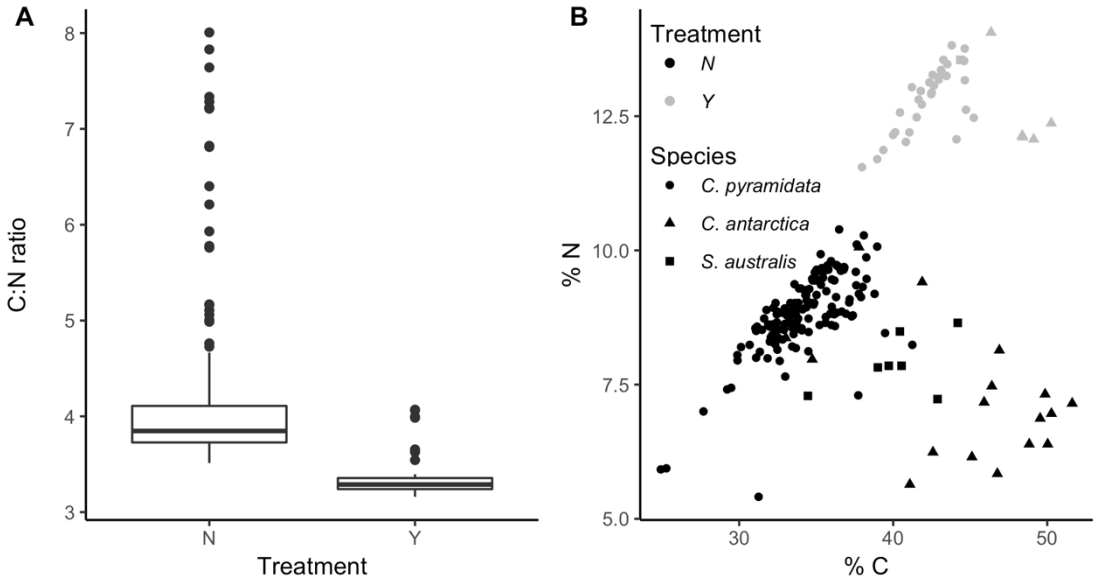

Figure 2.2 (A) Relationship between treatment (N = bulk, Y = lipid-extracted) and C:N ratio; (B) relationship between percent carbon and percent nitrogen for both treatments (N = bulk (black), Y = lipid-extracted (grey)) and grouped by species (circle = *C. pyramidata*, triangle = *C. antarctica*, square = *S. australis*).

Treatment also affected carbon and nitrogen content, whereby the range of both % carbon and % nitrogen were reduced relative to untreated values, while also demonstrating a net overall increase in both (Fig. 2.2B). The net effect of reduced C:N ratios from extraction was a result of a relatively greater effect on % nitrogen (Fig. 2.3A and B).

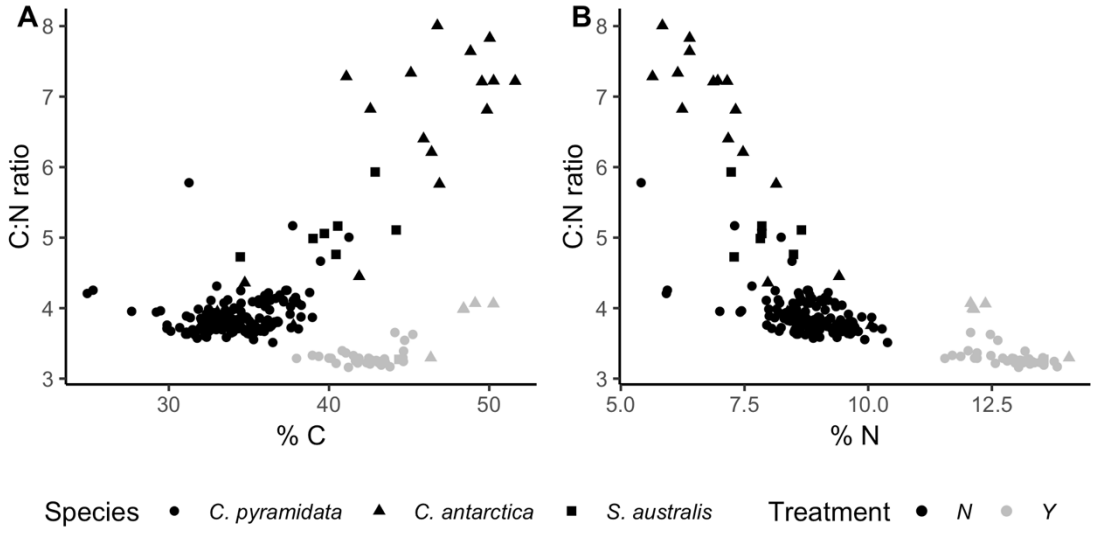

Figure 2.3 Relationship between (A) % carbon, and (B) % nitrogen and C:N ratio for each treatment (N = bulk (black), Y = lipid-extracted (grey)) and species (circle = *C. pyramidata*, triangle = *C. antarctica*, square = *S. australis*).

2.6.2 Lipid normalization model comparison and selection

The results from our modelling approach ($\delta^{13}C$ ~ treatment) determined that 63% of the variation in $\delta^{13}C$ values was accounted for by extraction treatment alone (Fig. 2.4).

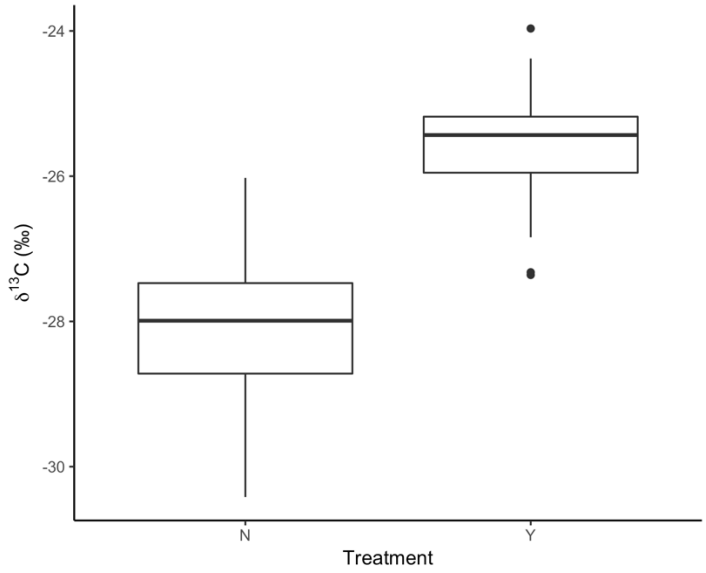

Figure 2.4 Relationship between each treatment (N = bulk, Y = lipid-extracted) and $\delta^{13}C$ values.

Multiple pairwise comparisons made between each model- and offset-corrected mean $\delta^{13}C$ value revealed statistically significant differences between datasets except for the models developed by Kiljunen et al. (2006) and Syväranta & Rautio (2010) (Fig. 2.5, Table A.3 in Appendix A).

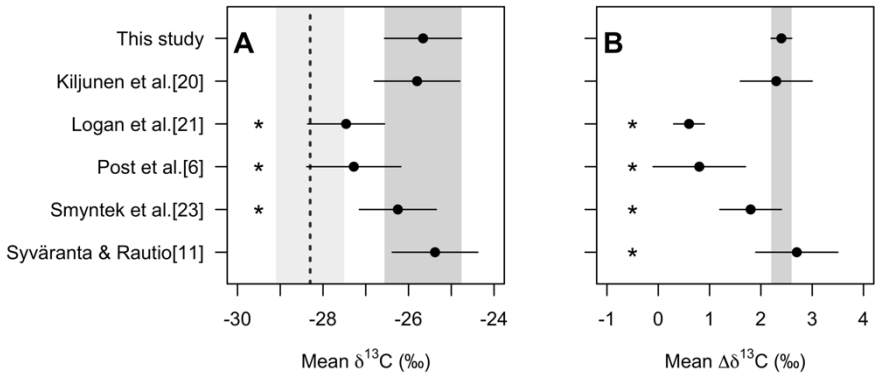

Figure 2.5 Summary results of multiple pairwise comparisons made between (A) mean $\delta^{13}C$ values (black dots) derived from correcting $\delta^{13}C_{bulk}$ values by each model with the mean $\delta^{13}C_{corrected}$ value derived from our offset value ("This study"); and (B) $\Delta\delta^{13}C$ values ($\delta^{13}C_{bulk}$ - $\delta^{13}C_{corrected}$) derived from each model with the $\Delta\delta^{13}C$ values obtained from our offset value. Dark grey vertical bands denote standard deviations of the mean values obtained from using our offset value to correct bulk. The mean $\delta^{13}C_{bulk}$ values in (A) are denoted by the dashed vertical lines with the standard deviations of the mean shown by the light grey vertical bands. Horizontal error bars refer to standard error of the means. Asterisks refer to values that are significantly different from the means obtained from this study.

Comparisons made on the average corrected change from bulk to corrected values with our average offset value, all values were significantly different except for the model by Kiljunen et al. (2006).

2.6.3 Effect of lipids on niche dispersion metrics

The total area was larger for bulk than for lipid-extracted samples, whereas lipid-extracted SEAs and SEA_cs were larger than those measured for the bulk dataset (Fig. 2.6, Table 2.2).

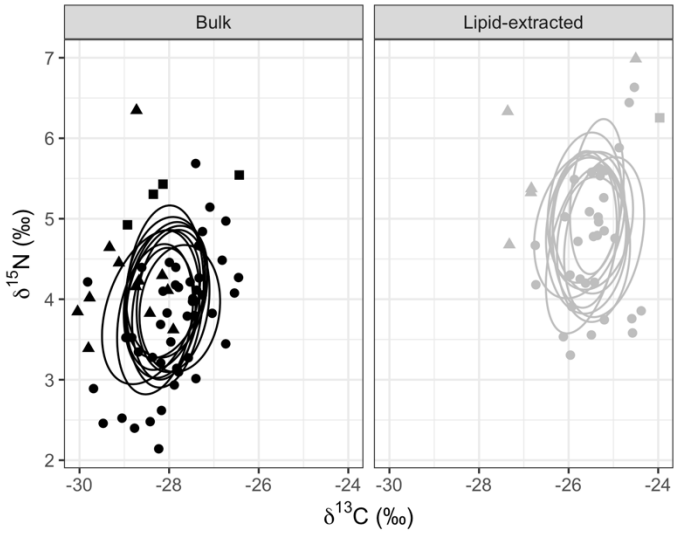

Figure 2.6 Bulk (black) versus LE (grey) $\delta^{13}C$ and bulk $\delta^{15}N$ values for *C. pyramidata* (circles), *C. antarctica* (triangles), and *S. australis* (squares). Ellipses represent ten random elliptical projections of trophic niche space and contain ~40% of the data.

RPP and Hotelling's T^2 tests revealed that Euclidean distances between centroids of isotopic niches measured before and after lipid correction differed significantly from zero for all species (*C. pyramidata* distance = 2.38; $p = 0.001$; Hotelling's $T^2 = 99.81$; $P < 0.0001$; *C. antarctica* distance = 2.84; $p = 0.001$; Hotelling's $T^2 = 97.3$; $P < 0.001$; *S. australis* distance = 2.61; $p = 0.001$; Hotelling's $T^2 = 30.41$; $P < 0.001$). This means that there were statistically significant differences in the distances between centroids calculated for treated and untreated pteropods of each species.

Table 2.2 Total area (TA), standard ellipse area (SEA) and SEA corrected for small sample sizes (SEAc) for all pteropod species combined.

	TA (‰^{2})	SEA (‰^{2})	SEAc (‰^{2})	*N*
Bulk	10.38	2.29	2.33	61
Lipid-extracted	9.35	2.35	2.41	38

The total and standard ellipse areas (TA and SEA, respectively) for both large (>210 μm) and small (<210 μm)-fractionated POM samples were calculated (small fraction: TA = 1.86‰^{2}, SEA = 1.22‰^{2}; large fraction: TA = 2.18‰^{2}, SEA = 1.47‰^{2}), then subsequently combined as one potential food source to compare niche overlaps with the SEAs calculated for bulk and lipid-corrected (LC) *C. pyramidata* (Fig 2.7A). 95% probabilistic niche area overlaps of bulk and

POM standard ellipses were higher than overlaps between LC and POM standard area ellipses of both bulk and LC *C. pyramidata* (bulk + POM: 0.34%; LC + POM: 0.04%). However, when the SEAs of *S. australis* were compared to that of their potential food source, represented by bulk *C. pyramidata*, overlapping with corrected samples was higher than with bulk samples (Fig. 2.7B; bulk + POM, 29.0%; LC + POM, 90.7%).

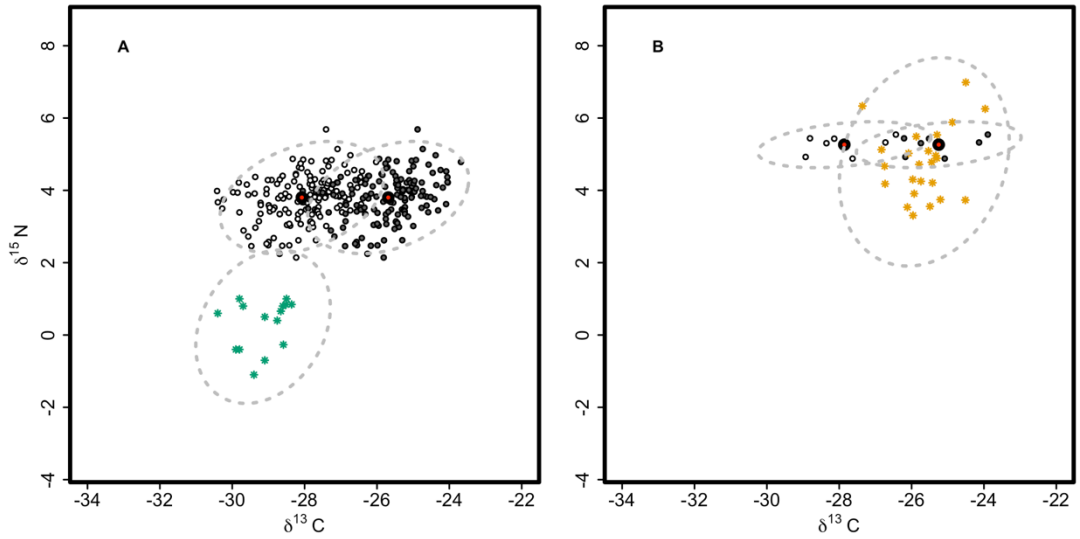

Figure 2.7 Isotopic niches including standard ellipses (grey dashed line) of pteropod species applied to bulk (white circles) and lipid-corrected (LC) $\delta^{13}C$ values (dark grey circles) for (A), *C. pyramidata*, and (B), *S. australis*. Red points are centroid values. Green and yellow stars represent standard area ellipse of marine POM and lipid extracted *C. pyramidata*, respectively.

Comparisons made between pteropod data corrected using our average offset value and data corrected using normalization models revealed no significant differences for each niche dispersion metric (Fig. 2.8; Table A.4 in Appendix A), including TA ($F_{(3, 7)} = 0.05$, $p = 0.985$) and SEA ($F_{(3, 7)} = 0.11$, $p = 0.949$).

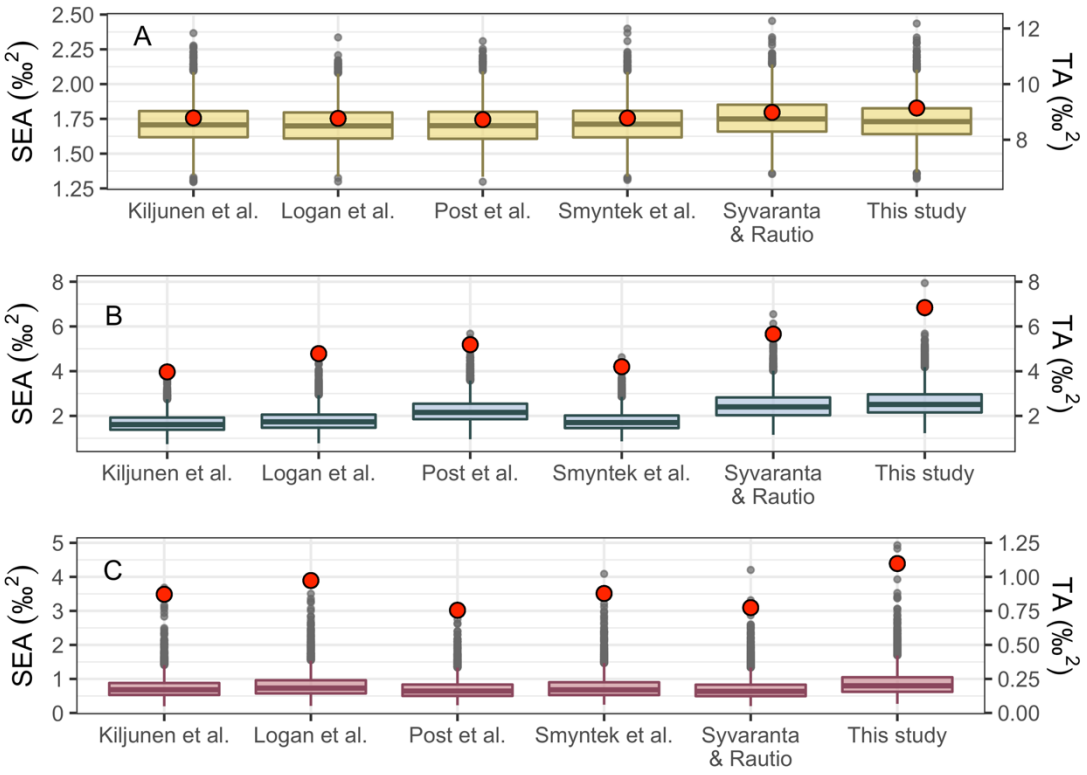

Figure 2.8 Differences in standard area ellipses (SEA) and total area of the convex hull (red circles) between data that was not lipid-corrected (bulk), and corrected using each normalization model for (A) *C. pyramidata*, (B) *C. antarctica*, and (C) *S. australis*. The bottom and top of the box are the 25th and 75th percentiles, respectively; the horizontal line bisecting the box is the 50th percentile. The whiskers span the highest to the lowest value observations; outliers (grey circles) are the observations plotted outside of this range.

2.7 Discussion

2.7.1 Chemical lipid extraction vs. bulk samples

Lipid extraction consistently produced statistically significant differences in $\delta^{13}C$ values for all pteropod species and sampling sites examined, with a 2.4 ± 0.2‰ average increase compared to bulk values. When we modelled the mean effect of treatment on $\delta^{13}C$ values, 63% of the variation in $\delta^{13}C$ values was accounted for by lipid extraction alone. We also found that, for all species combined, lipid extracted samples were significantly higher for $\delta^{15}N$ by 1.1 ± 0.8 ‰, relative to bulk samples. This difference in $\delta^{15}N$ values is not uncommon in marine species and is well within the variable offset range (-2.3 to +1.8 ‰) reported by Svensson et al. (2016) for several fish and invertebrates. This is likely a function of variable loss of solvent-soluble nitrogenous materials and proteins depleted in ^{15}N relative to bulk tissues, such as the amino acid serine, from lipids (Svensson et al., 2016; Sweeting et al., 2006). This was also demonstrated by

the net increase in % nitrogen in all species that may have significantly impacted the decreasing C:N ratios.

We observed an increase in variability within extracted versus untreated bulk $\delta^{13}C$ values, which some previous studies have reported as a function of removing lipids (DeNiro and Epstein, 1977; Murry et al., 2006; Pinnegar and Polunin, 1999). We did detect a decrease in variance calculated in C:N ratios of lipid-extracted relative to bulk samples. C:N ratios are commonly used as a proxy for lipid content, with high C:N ratios assumed to indicate higher lipid content (Kiljunen et al., 2006; Post et al., 2007). They are calculated from % carbon and nitrogen values, which also each possessed decreased variances after lipid extraction. The Bligh and Dyer method (Bligh and Dyer, 1959) employed in our analysis produced C:N ratios ranging from 3.2 to 4.1 (average = 3.4 ± 0.2) from all species combined, in comparison to the higher variance measured in bulk C:N ratios, ranging from 3.6 to 8.0 (average = 4.6 ± 1.3). Taken separately, the gymnosome *C. antarctica* yielded the highest average bulk and lipid-extracted C:N ratios, whereas the other gymnosome analyzed, *S. australis*, showed the greatest difference in $\delta^{13}C$ between treatments. These results could point to an incomplete delipidation for *C. antarctica*, particularly given that it is less clear to see the net increase in % carbon from extracted samples as compared to *C. pyramidata* and *S. australis*. They may also suggest a potentially strong species-specific response to lipid extraction, consequently pointing to greater difficulty when inferring a strong relationship between bulk C:N ratios and lipid content. This conclusion is further corroborated by similar responses to lipid extraction and acidification of many Arctic and sub-Arctic marine zooplankton assemblages (Pomerleau et al., 2014). Unfortunately, due to low sample sizes of gymnosomes, we were unable to model a species-specific lipid normalization in order to determine whether C:N ratios can appropriately serve as a proxy for lipid content at species level. Choy et al. (2016) found no relationship between bulk C:N ratios and $\Delta\delta^{13}C$ values in isopod and shrimp species, and questioned the utility of approximating C:N ratios for % lipid in many species of marine invertebrates and fish (Kiljunen et al., 2006; Pomerleau et al., 2014). Future directed studies measuring species-specific proportion of lipids (measured in dry weight) and its relationship to untreated C:N ratios of pteropods are encouraged, with, wherever possible, larger sample sizes.

2.7.2 Normalization model selection and the effect of lipid correction on niche dispersion metrics

The normalization model by Kiljunen et al. (2006) most accurately predicted extracted $\delta^{13}C$ values for all pteropod species combined, and can provide a suitable alternative to chemical lipid

extraction in pteropod-based isotopic research. This outcome is surprising, considering model efficiency tests in other studies have shown this model to be appropriate for correcting $\delta^{13}C$ values from high lipid content tissues such as fish liver (Skinner et al., 2016). Though their own model provided the best fit (R^2 = 0.86) for their subarctic and boreal lakes zooplankton data, Syväranta & Rautio (2010) found the model by Kiljunen et al. (2006) to fit their data closer (R^2 = 0.65) than any other normalization model tested. The model by Syväranta & Rautio (2010) also produced an average $\delta^{13}C$ value closely resembling the average value calculated by data corrected via our offset value. This, however, is not surprising considering this model was developed for polar zooplankton. Our results indicate minor differences in the effect of mathematical normalization model selection on the niche dispersion metrics of standard ellipses and total areas, though not sufficient enough to distort the interpretation of overall trophic structure. Due to our relatively small sample sizes, particularly when accounting for species separately, we understand that total and standard ellipse areas can be inaccurate when used as a proxy for isotopic niche areas (Syväranta et al., 2013), and thus exercise considerable caution when interpreting these results. Syväranta et al. (2013) generated simulations of varying sample sizes from among two fish populations and found that sizes greater than 30 were still insufficient in improving uncertainty surrounding niche analyses, particularly using total area estimations. Further research is required to determine the appropriate minimum samples sizes needed to perform robust estimations of trophic niche breadth in pteropods using standard ellipse and total areas.

Murry et al. (2006) found that, relative to bulk samples, lipid extraction of tissues from an entire fish community altered the $\delta^{13}C$ and $\delta^{15}N$ values to significantly shift the position of the entire food web, rather than induce smaller scale impacts such as relative trophic positions among species. Since our normalization model was based on all species combined, applying this to correct bulk tissues of all species produced a similar result, wherein the entire community significantly shifted without affecting positioning of each species relative to other species. We also calculated species-specific standard area ellipses and centroid locations separately for both lipid-corrected and bulk $\delta^{13}C$ values to determine the existence of isotopic niche overlapping with potential food sources, and whether the magnitude of overlapping could bias interpretations of resource partitioning. Higher within-sample variability was measured in bulk versus lipid-extracted and lipid-corrected $\delta^{13}C$ values, particularly in total area measurements, which was similar to the results Choy et al. (2016) found in a number of polar organisms and tissues. Unlike Murry et al. (2006), Choy et al. (2016) did not detect community-level change with respect to differences in niche dispersion metrics, and pointed at the need to examine

community-based niche dynamics at the species level. We measured varying degrees of overlapping between standard area ellipses of pteropod species and their potential food sources, with bulk *C. pyramidata* displaying higher overlapping with POM than corrected *C. pyramidata*, and corrected gymnosome species (*C. antarctica* and *S. australis*) displaying higher overlapping with *C. pyramidata* than bulk gymnosome species niches. This variability highlights the need to correct for lipids in untreated samples, and shows how ignoring this procedure can affect interpretations of trophic relationships between and among species assemblages, particularly if species are directly connected through ecologically significant predator-prey interactions or competition.

2.8 Conclusions

Given we observed variability in niche overlapping measured between untreated versus mathematically corrected isotopic ratios of pteropods with their diet preferences, we strongly encourage the incorporation of lipid correction within the development of research protocols involving pteropod-focused niche breadth analyses. Without lipid correction of $\delta^{13}C$ values, be it through chemical extraction or a posteriori mathematical normalization, the magnitude of species interactions and resource partitioning can be over- or underestimated within polar pteropod assemblages. When analysing samples possessing similar untreated C:N ratios observed here (3.5-8.0), and chemical extraction of a subset is not an option, we recommend selecting models calibrated to similar ratios and organisms (e.g. Kiljunen et al. 2006, Syväranta & Rautio 2010). We found high species-specific variability in relationships between untreated C:N ratios and $\Delta\delta^{13}C$ values, and thus strongly encourage incorporation of larger sample sizes, though it may be challenging for less common species, such as polar gymnosomes. Lipid extraction also affected $\delta^{15}N$ values, and we consequently support analytical treatments of $\delta^{13}C$ and $\delta^{15}N$ values separately (Choy et al., 2016; Ryan et al., 2012). We advocate well-developed research protocols as doing so will further research into a taxonomic group particularly sensitive to anthropogenic change to ocean chemistry.

Chapter 3

Trophodynamics of Southern Ocean pteropods on the southern Kerguelen Plateau[2]

3.1 Graphical Highlights

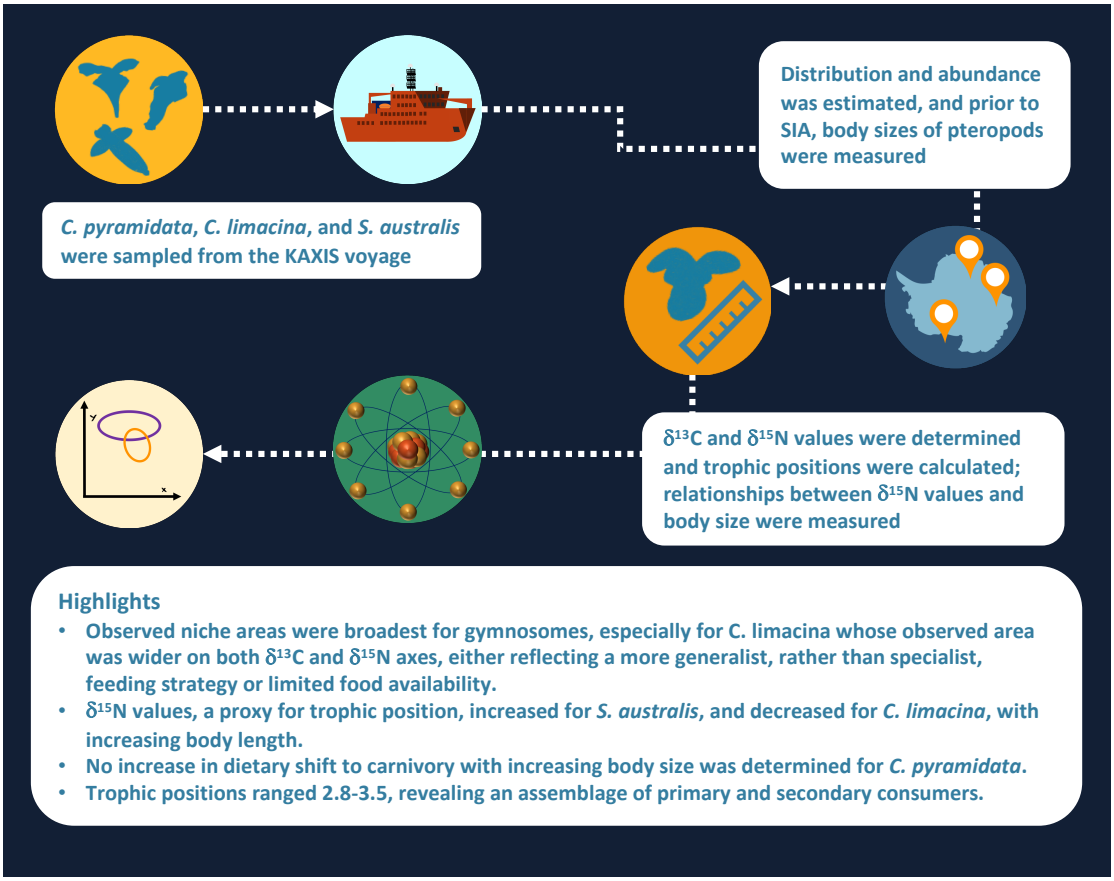

Figure 3.1 Graphical abstract for Chapter 3.

3.2 Key words

Clio pyramidata, *Clione limacina*, isotopic niche, size-based, *Spongiobranchaea australis*, trophic position

[2] *This work has been published in a refereed journal and is presented below in identical form. The citation for the original publication is:* Weldrick, C.K., Trebilco, R., Davies, D.M., Swadling, K.M. 2019. Trophodynamics of Southern Ocean pteropods south of the Kerguelen Plateau *Ecology & Evolution.* doi: 10.1002/ece3.5380

3.3 Abstract

Pteropods are a group of small marine gastropods that are highly sensitive to multiple stressors associated with climate change. Their trophic ecology is not well studied, with most research having focused primarily on the effects of ocean acidification on their fragile, aragonite shells. Stable isotopes analysis (SIA) and isotope-based Bayesian niche metrics are useful for characterizing the trophic structure of biological assemblages and can provide a benchmark against which future climate-driven ecological change can be assessed. These approaches have not been implemented for pteropod assemblages.

We used isotopes-based Bayesian niche metrics to investigate the trophic relationships of three co-occurring pteropod species, with divergent feeding behaviours, sampled from the Southern Kerguelen Plateau area in the Indian Sector of the Southern Ocean - a biologically and economically important but poorly-studied region. Two of these species were gymnosomes (shell-less pteropods), which are traditionally regarded as specialist predators on other pteropods, and the third species was a thecosome (shelled pteropod), which are typically generalist omnivores. For each species, we aimed to understand (1) variability and overlap among isotopic niches; and (2) whether there was a relationship between body size and trophic position.

Observed isotopic niche areas were broadest for gymnosomes, especially *Clione limacina antarctica*, whose observed isotopic niche area was wider on both $\delta^{13}C$ and $\delta^{15}N$ value axes, possibly reflecting either a more generalist, rather than specialist, feeding strategy, or limited food availability. We also found that $\delta^{15}N$ values increased for *Spongiobranchaea australis*, and decreased for *C. limacina antarctica*, with increasing body length. We found no indication of a dietary shift towards increased carnivory with increasing body size for *Clio pyramidata* f. *sulcata*. Trophic positions ranged from 2.8 to 3.5, revealing an assemblage composed of both primary and secondary consumer behaviours.

This study is the first comprehensive comparative analysis on trophodynamics in Southern Ocean pteropod species. Combined, our results illustrate differences in intraspecific trophic behaviour that may be attributed to differential feeding strategies at species level.

3.4 Introduction

Human-driven climate change is causing significant chemical and physical changes to global oceans, leading to demonstrable direct and indirect ecological impacts to Southern Ocean assemblages across all trophic levels (Constable et al., 2014). Among these changes is ocean acidification, which causes dissolution of shell-secreting organisms (Fabry et al., 2008; Orr et al., 2005). Acidification and warming of polar waters is also expected to lead to changing size and

composition of phytoplankton and microbial communities, which could have severe bottom-up effects on marine food webs (Davidson et al., 2016). Many shell-secreting organisms rely on these basal food sources, and if the availability of these sources is altered, it is unclear how this will impact grazing organisms, be it through range redistribution, in situ adaptation, or localized extinction.

The pitting of aragonite shells produced by thecosome (shelled) pteropods makes them a useful biological indicator of ocean acidification due to increased atmospheric CO_2 (Bednaršek et al., 2016). Thecosomes are often dominant in macrozooplankton communities within the Southern Ocean (Hunt et al., 2008), and often regarded as strict herbivores (Hopkins, 1987; Karleskint et al., 2012) capable of exerting significant top-down control of phytoplankton assemblages (Perissinotto, 1992). However, gut contents have revealed the presence of metazoans such as tintinnids, copepods, and larval thecosome pteropods, indicating that they are more likely omnivorous (Hopkins and Torres, 1989). Gut content and fatty acid analyses of gymnosome (shell-less) pteropods point to a highly specialized carnivorous diet, preying exclusively on thecosomes (Conover and Lalli, 1972). Both thecosomes and gymnosomes are important food for higher trophic level organisms (Lalli and Gilmer, 1989; Pakhomov et al., 1996), so changes to pteropod assemblages in the Southern Ocean will have flow on effects up the food web (Suprenand and Ainsworth, 2017). Despite their importance, our knowledge of pteropod trophodynamics is very patchy, particularly in the Southern Ocean, and based almost entirely on visual analysis of their stomach contents. Co-occurring Southern Ocean pteropods could provide a unique model community to understand how different functional traits (eg. feeding structures, body size) correlate with the trophic structure of communities consisting of both monophagous specialists and generalists.

The niche concept has been popular for over 100 years as it is a useful way of considering how different organisms fit into communities and ecosystems, and the roles they play (Grinnell, 1917; Sexton et al., 2017). Several different versions of the niche concept have been introduced over time that focus on different aspects of species' ecologies including traits, trophic interactions (resource use) and environmental (habitat) requirements (Elton, 1927; Hutchinson, 1957). Over the last decade, stable isotopes have gained popularity as an approach for quantifying the trophic niche (thus being most closely analogous to the Eltonian niche, and the resource axes of the Hutchinsonian niche) (Newsome et al., 2007). This approach is based on the detectable average enrichments of 3-5 ‰ and ~1 ‰ in the isotopic ratios for nitrogen and carbon, respectively, per tropic level (Post, 2002). Measuring space occupied by consumers $\delta^{13}C$ and $\delta^{15}N$ enables insight into both trophic and ecological niches, as it provides both an index of

the basal resources from which consumers derive their energy, and the trophic position at which they feed, respectively (Fink et al., 2012). As for the latter, $\delta^{15}N$ values of predators rarely overlap with those of their prey, and are thus effective at estimating trophic position (Vanderklift and Ponsard, 2003).

The extent of stable isotopic values representing all resources used by a consumer is commonly used as a proxy for trophic and ecological niche (Bearhop et al., 2004; Jackson et al., 2011). Bearhop et al. (2004) first inferred the qualitative description of the trophic niche breadth by using $\delta^{13}C$ and $\delta^{15}N$ values of consumers and food source tissues, which was followed by the development of quantitative metrics to measure niche width, species spacing, density, overlapping, and clustering from the extent and spread of isotopic data points (Jackson et al., 2011; Layman et al., 2007; Swanson et al., 2014). It is often assumed that smaller isotopic niches are associated with trophic specialists due to a low diversity of dietary resources that is consequently translated to small ranges in isotopic composition (Bolnick et al., 2003).

The niche variation hypothesis (Van Valen, 1965) proposed that broader, population-level dietary niches are associated with greater individual-level resource use, in relation to populations possessing narrower niches. Assuming the niche variation hypothesis, our objective was to measure trophodynamic variability in sympatric pteropod species in an under-surveyed region on the southern Kerguelen Plateau. Here, we enlisted prior knowledge of gymnosome and thecosome pteropod feeding preferences (Lalli and Gilmer, 1989) and predicted that specialist gymnosomes will exhibit narrower isotopic niche areas than generalist thecosomes, with little variability over space and time scales. Based on studies using nitrogen stable isotopes and a range of biomass size-spectra to show positive relationships between trophic position and body size (France et al., 1998; Jennings et al., 2002), we assumed that larger individuals will have higher trophic positions than smaller individuals due increasing ability to access larger, higher trophic-level prey with increasing body size. The effects of climate change are expected to cause shifts in the trophodynamics of many polar organisms (Gutt et al., 2015), including predictions made that may see narrowing of niche areas due to decreased prey diversity, an increase in niche overlapping due to shifts in species distribution (Bas et al., 2019), and an increase in trophic positions of key marine predators due to expected diet shifts towards higher trophic prey (Tarroux et al., 2016). The trophic niches estimated here provide a benchmark for pteropods and a piece of the puzzle for ongoing efforts to understand trophic structuring of pelagic communities and ecosystems more generally.

3.5 Methods

3.5.1 Study area & sampling

Samples were collected during the Kerguelen Axis (K-Axis) research voyage aboard the RV *Aurora Australis* between 11 January and 24 February 2016. 47 stations spanned the region from 62.7 °E to 93.5 °E, and from 57.6 °S to 65.2 °S, covering the southern extent of the Kerguelen Plateau in the Indian sector of the Southern Ocean (Fig. 3.2). Station depths ranged from 1276 m to 4770 m.

Macrozooplankton were sampled with a Rectangular Midwater Trawl (RMT8; mesh size: 4.5 mm, mouth area: 8 m^2), equipped with a flow meter, and towed obliquely from the surface to 200 m. Ship speed during plankton net tows was 2-2.5 knots for an average duration of 45 minutes. Pteropods were counted and identified to species level, placed in cryotubes, then stored in liquid nitrogen prior to analyses. Abundances of each species were quantified in terms of individuals per 1000 m^{-3} of seawater filtered.

Size-fractioned particulate organic matter (POM) was retrieved from the ship's underway water supply (~ 5 m depth) via large volume sequential filtration, pre-screened using an upstream 47 mm-diameter, 1 mm filter mesh for zooplankton removal, and collected onto 25 mm-diameter Sterlitech silver membrane (pore size = 1.2 μm) and Nitex filters (pore size = 210 μm). Two particle size fractions were analysed as 'large' > 210 μm and 'small' < 210 μm, predominantly phytoplankton. The large fraction on Nitex filters was cleanly transferred to silver membranes for analysis. Filters were acidified and air dried at 60 °C prior to stable isotopes analysis (SIA).

3.5.2 SIA sample preparation

Individual pteropods were rinsed in filtered seawater and weighed prior to drying in an oven for 24 h at 60 °C. Whilst previous research recommends acidifying thecosomatous pteropods to remove carbonate material that would otherwise bias stable isotopes results (Pomerleau et al., 2014), the pressure from the RMT8 sampling method completely stripped entire shells from most shelled pteropods, and we did not need to acid-treat our samples prior to further analyses as shell fragments could be easily removed using forceps. Individual dry weights were measured and samples were ground to powder using an agate mortar and pestle, then weighed into tin cups in preparation for isotopic analysis. Since lipids may bias carbon isotope ratios (Post et al., 2007), a pteropod-specific correction offset value determined by Weldrick et al., (2019) was used to correct bulk samples. POM sample filters were acidified dried for 48 h at 60 °C prior subsampling 5 mm diameter aliquots into silver capsules (Sercon SC0037).

3.5.3 Stable isotopes analysis

Bulk carbon and nitrogen stable isotope ratios were obtained using an automated Elementar vario PYRO cube analyser (Langenselbold, Germany) interfaced with a continuous flow IsoPrime100 isotope ratio mass spectrometer (Cheadle Hulme, United Kingdom) for pteropods, and a Thermo Scientific Flash 2000HT analyser (Bremen, Germany) coupled with a Thermo Fisher Delta V Plus mass spectrometer through a Thermo Fisher Conflo IV for POM. For pteropods, SIA was performed at the Central Science Laboratory (CSL), University of Tasmania (Sandy Bay, Tasmania), and for POM, at the Australian Nuclear Science and Technology Organisation (ANSTO, Lucas Heights, Sydney). Isotopic ratios were expressed in delta (δ) notation and reported as parts per thousand (‰) deviations from conventional certified isotopic reference standards, Vienna Pee Dee Belemnite (for carbon) and atmospheric air (for nitrogen) (DeNiro and Epstein, 1978). At CSL, laboratory working standards of sulfanilamide were repeated every 6th sample for both isotopes to measure instrument stability and precision. Average standard deviations on triplicate measurements were 0.15 ‰ and 0.19 ‰ for $\delta^{13}C$ and $\delta^{15}N$ values of pteropods, respectively. At ANSTO, POM isotopic data are reported relative to IAEA secondary certified standards with a standard error of analysis to 1 standard deviation (SD) measured at ± 0.3 mil. The carbon and nitrogen percentages, by weight, were converted to atomic C:N ratios.

3.5.4 Statistical analyses

Data analyses were conducted using the statistical software R, version 3.4.0 (R Development Core Team, 2017). We used the Shapiro-Wilk's and Levene's tests on isotopic values ($\delta^{13}C$ and $\delta^{15}N$) to assess normality and homogeneity of variance, respectively. A multivariate analysis of variance (MANOVA; using the manova function in base R) was also used to test for spatial (latitude, longitude, and site depth) and species effects (independent variables) on bulk isotopic values (dependent variables). Simple linear regressions were used to test the relationships between each isotopic values ($\delta^{13}C$ and $\delta^{15}N$) and time, latitude, longitude and site depth, as well as relationships between body size and trophic position (lm function, base R). Intraspecific comparisons of niche metrics could not be conducted by site as sample sizes of gymnosome species were lower than empirically determined recommended sizes (Syväranta et al., 2013).

3.5.5 Niche dispersion metrics, trophic position, and body size

Interspecies isotopic niche widths were estimated using the Stable Isotope Bayesian Ellipses package in R (SIBER) version 2.1.3 (Jackson et al., 2011). SIBER calculates bivariate standard ellipses corresponding to isotopic niches, and standard ellipse areas (SEA) representing standard deviation of the data. Standard area ellipses corrected for sample sizes (SEAc) were also calculated (Jackson et al., 2011). Interspecies dietary niche area overlaps were calculated using nicheRover in R version 1.0 (Swanson et al., 2014), which uses a Bayesian framework to produce probable pairwise comparisons between the niche region of each species combination. The niche region of a species was defined at 95 and 99 % probability that a species will be located within isotopic bivariate space; similarly, the niche overlap is defined at 95 and 99 % probability that the niche region of one species will overlap with that of another.

We also calculated multiple probability estimates of the trophic positions of each pteropod species. Unlike the trophic level, which refers to categories of trophic modes based on integer values, the trophic position of a species is a continuous, numerical measure that represents the relative location of a particular species within a trophic hierarchy (Carscallen et al., 2012). Trophic positions were calculated for each pteropod species separately using the R package tRophicPosition version 0.7.5 (Quezada-Romegialli et al., 2018). This package calculates consumer trophic positions within a Bayesian framework based on the stable isotopes of both consumers and baselines as well as user-specified trophic enrichment factors (TEF). We adopted TEF values (± standard error) of 0.5 ± 0.13 ‰ for carbon ($\Delta\delta^{13}C$ values) and 2.3 ± 0.18 ‰ for nitrogen ($\Delta\delta^{15}N$ values) based on those measured for similarly sized marine gastropods previously reported in the literature (McCutchan et al., 2003). We also converted $\delta^{15}N$ values to trophic positions on specimens used to compare with body size. Body lengths (mm) from a subset of intact pteropods were measured using ImageJ/Fiji software (Schindelin et al., 2012). Results from individuals sampled for SIA were plotted against $\delta^{15}N$ values to determine the effect of body size on trophic position.

3.6 Results

3.6.1 Species abundance and composition

One thecosome (shelled) and two gymnosome (shell-less) pteropod species were identified: *Clio pyramidata*, *Clione limacina antarctica* (hereafter referred to as *C. pyramidata* and *C. antarctica*, respectively), and *Spongiobranchaea australis*. *C. pyramidata* was the most abundant pteropod in the region, followed by the gymnosome species, with averages of 22 (maximum:

272) and 2 (maximum: 47) ind. 1000 m^{-3}, respectively. Relative abundances were 89.6% for *C. pyramidata*, 4.8% for *C. antarctica*, 0.4% for *S. australis*, and 5.2% for gymnosomes unidentified to species level that were not used in the subsequent SIA (Fig. 3.1). Latitudinal ranges were narrowest for *S. australis* (60.4 °S - 62.7 °S), followed by *C. antarctica* (61.4 °S - 67.0 °S), and *C. pyramidata* (57.7 °S - 67.0 °S).

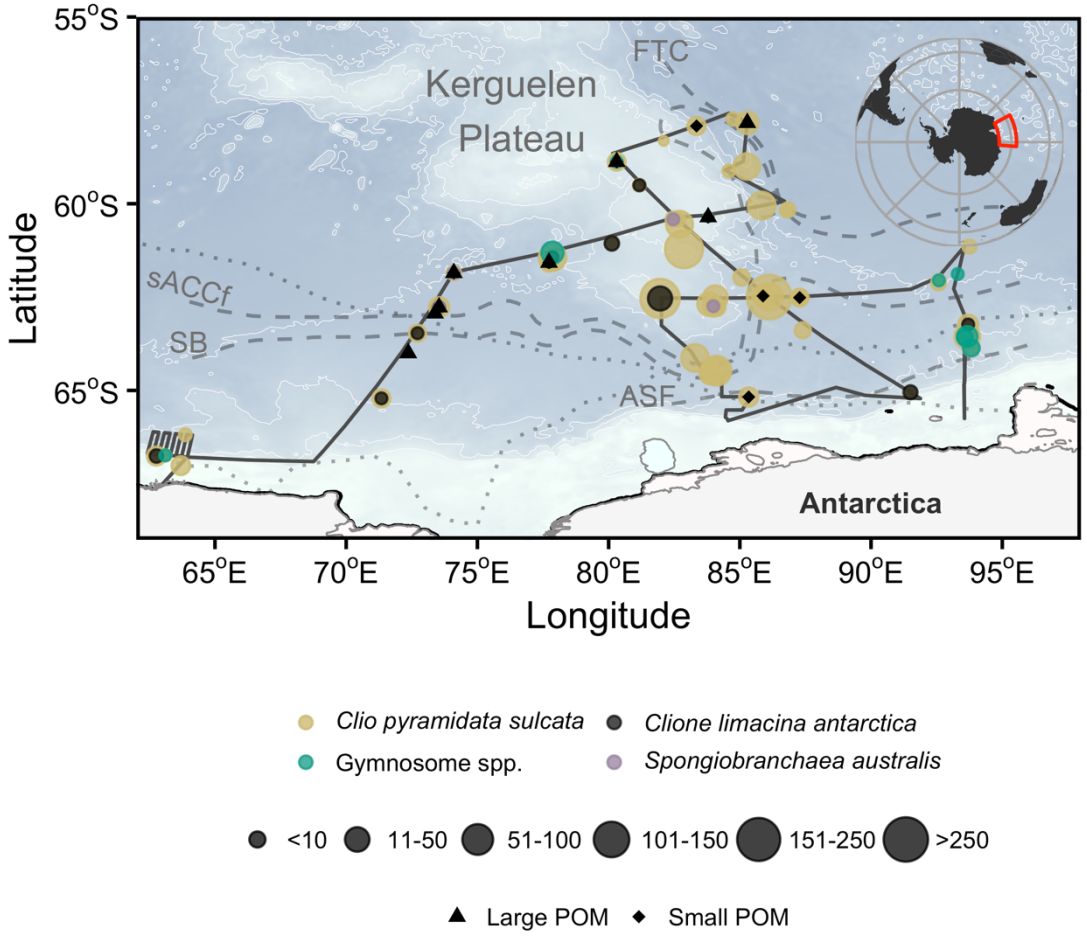

Figure 3.2 Relative abundance (size of circle, ind. 1000m^{-3}) of pteropod species sampled from RMT8 plankton nets during the K-Axis voyage. Some gymnosome individuals were unable to be identified to species level and were not used in stable isotopes analysis. Large-fraction (triangles) and small-fraction (diamonds) are also featured here. Oceanographic features and front locations (dashed lines) determined by (Bestley et al. (2018) include: the southern ACC front (sACCf), the Southern Boundary (SB), the Antarctic Slope Front (ASF), and the Fawn Trough Current (FTC). Upper and lower dotted lines are October and January average sea ice extent, respectively.

3.6.2 Bulk isotopic values of pteropods

$\delta^{13}C$ and $\delta^{15}N$ values were obtained from 185 individuals representing all three pteropod species from the RMT8 samples (*C. pyramidata*: $n = 152$; *C. antarctica*: $n = 24$; *S. australis*: $n = 9$). Pairwise comparison tests indicated significant differences among stable isotopic values associated with parameters tested (MANOVA, $\delta^{13}C$ and $\delta^{15}N$ values, $p < 0.001$; see Table B.1 in Appendix B). $\delta^{13}C$ values were strongly associated with spatial attributes, including latitude, longitude and depth modeled together. Variation in $\delta^{15}N$ values was primarily predicted by longitude and species. Linear regression models of species-specific relationships between each isotopic value versus spatio-temporal variables (date, depth, latitude and longitude) showed statistically significant positive relationships for the following: *C. pyramidata* between $\delta^{15}N$ and sampling dates and latitude (Figs 3.3 and 3.5, respectively), and between $\delta^{13}C$ and longitude (Fig 3.6); and *C. antarctica* between $\delta^{15}N$ and $\delta^{13}C$ and sampling dates (Fig 3.3). Statistically significant negative relationships were measured for the following: *C. pyramidata* between $\delta^{13}C$ and sampling dates and longitude (Figs 3.3 and 3.6, respectively); and *C. antarctica* between $\delta^{13}C$ and longitude (Fig 3.6).

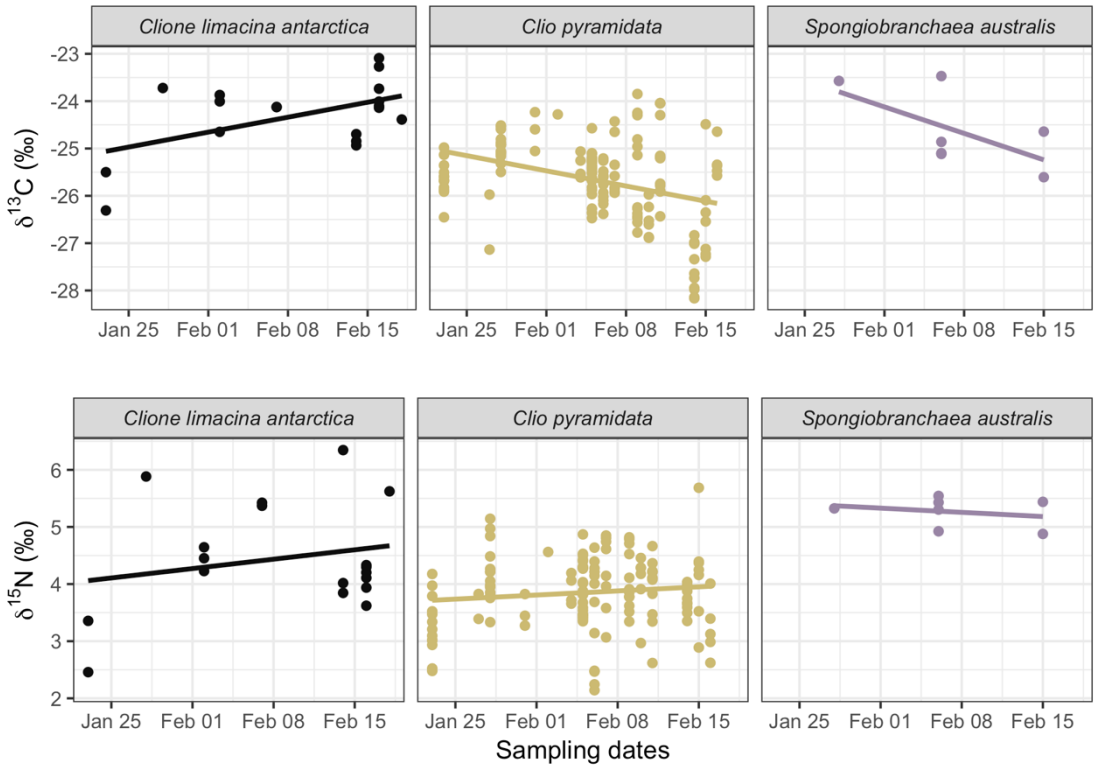

Figure 3.3 Linear relationships between $\delta^{13}C$ (upper plots) and $\delta^{15}N$ (lower plots) and sampling dates. For *C. antarctica*: $\delta^{13}C$, $R^2 = 0.50$, $p < 0.05$, $\delta^{15}N$, $R^2 = 0.34$, $p < 0.05$; *C. pyramidata*: $\delta^{13}C$, $R^2 = 0.21$, $p < 0.05$, $\delta^{15}N$, $R^2 = 0.06$, $p < 0.05$; *S. australis*: $\delta^{13}C$, $R^2 = 0.11$, $p = 0.35$, $\delta^{15}N$, $R^2 = -0.39$, $p = 0.85$.

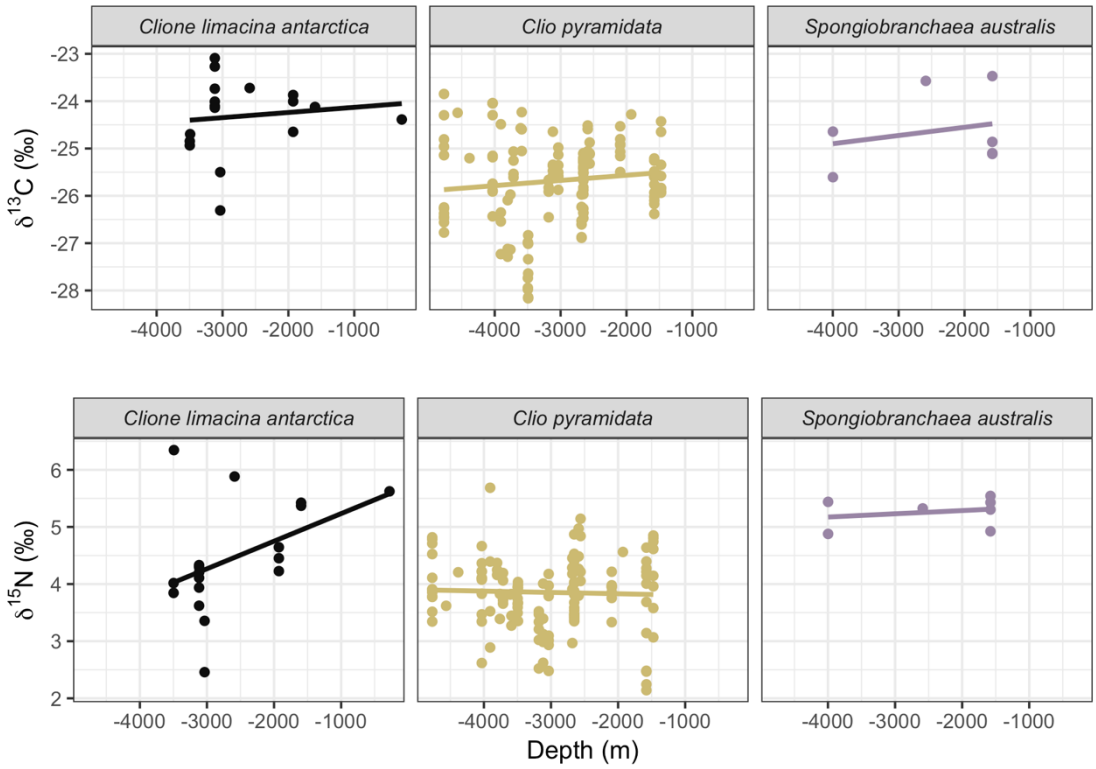

Figure 3.4 Linear relationships between $\delta^{13}C$ (upper plots) and $\delta^{15}N$ (lower plots) and depth (m). For *C. antarctica*: $\delta^{13}C$, R^2 = -0.05, p = 0.62, $\delta^{15}N$, R^2 = 0.14, p = 0.07; *C. pyramidata*: $\delta^{13}C$, R^2 = 0.006, p = 0.17, $\delta^{15}N$, R^2 = -0.006, p = 0.67; *S. australis*: $\delta^{13}C$, R^2 = -0.13, p = 0.60, $\delta^{15}N$, R^2 = -0.13, p = 0.59.

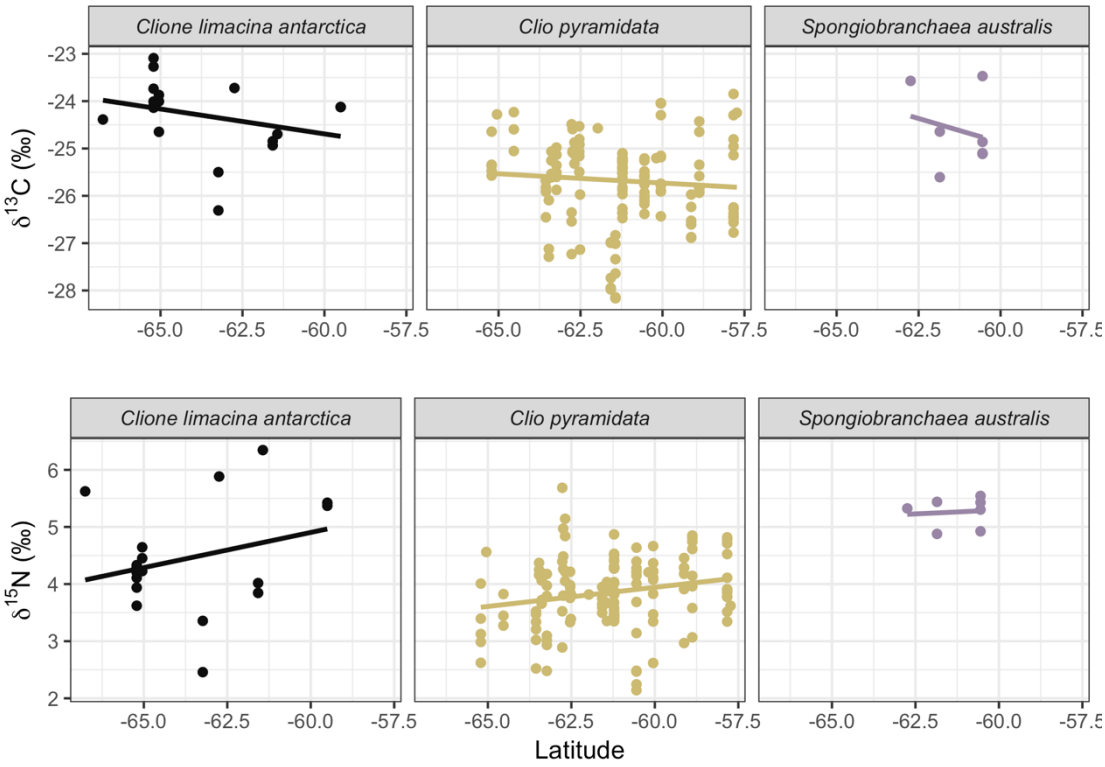

Figure 3.5 Linear relationships between $\delta^{13}C$ (upper plots) and $\delta^{15}N$ (lower plots) and latitude (°S). For *C. antarctica*: $\delta^{13}C$, R^2 = 0.03, p = 0.24, $\delta^{15}N$, R^2 = 0.02, p = 0.27; *C. pyramidata*: $\delta^{13}C$, R^2 = -0.0001, p = 0.32, $\delta^{15}N$, R^2 = 0.04, $p < 0.05$; *S. australis*: $\delta^{13}C$, R^2 = -0.14, p = 0.62, $\delta^{15}N$, R^2 = -0.19, p = 0.84.

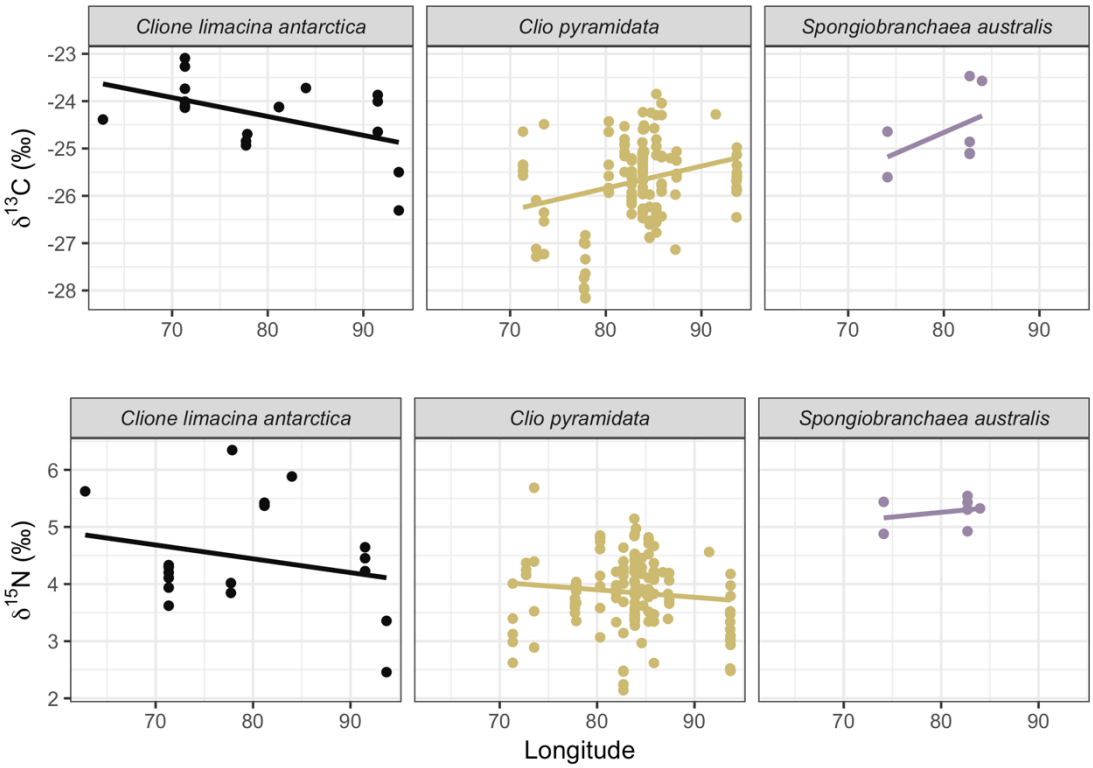

Figure 3.6 Linear relationships between $\delta^{13}C$ (upper plots) and $\delta^{15}N$ (lower plots) and longitude (°E). For *C. antarctica*: $\delta^{13}C$, $R^2 = 0.20$, $p < 0.05$, $\delta^{15}N$, $R^2 = -0.001$, $p = 0.34$; *C. pyramidata*: $\delta^{13}C$, $R^2 = 0.06$, $p < 0.05$, $\delta^{15}N$, $R^2 = 0.06$, $p < 0.05$; *S. australis*: $\delta^{13}C$, $R^2 = 0.07$, $p = 0.28$, $\delta^{15}N$, $R^2 = -0.11$, $p = 0.55$.

Table 3.1 Bulk stable isotopes ($\delta^{13}C$ and $\delta^{15}N$) signatures (± SD) averaged over all sampling sites and species, as well as results from the same Southern Ocean species from other studies. Some values are listed as approximate ranges where exact values and standard deviations are unavailable.

Species	Region	*n*	$\delta^{13}C$	$\delta^{15}N$	Reference
C. pyramidata	S. Kerguelen Plateau	152	-28.1 ± 0.9	3.8 ± 0.6	This study
	Lazarev Sea[a]	6	~-26 - -29.5	~1-2	Hunt et al. 2008
	SW Indian Ocean, N of STC	3	-20.3 ± 0.5**	5.6 ± 0.2	Richoux and Froneman, 2009†
	SW Indian Ocean, mid-STC	--	-20.7**	4.1	Richoux and Froneman, 2009†
	SW Indian Ocean, S of STC	2	-20.6**	0.4 ± 0.3	Richoux and Froneman, 2009†
C. limacina	S. Kerguelen Plateau	24	-28.3 ± 1.1	4.5 ± 0.9	This study
	Lazarev Sea[a]	3	~-28.5 - -29.7	~2.5-3.7	Hunt et al. 2008
	E. Antarctica[b]	3	-30.8	5.1 ± 0.9	Jia et al. 2016
S. australis	S. Kerguelen Plateau	9	-27.9 ± 1.0	5.3 ± 0.3	This study
	Lazarev Sea[a]	3	~-27.5- -30	~5.5-6.5	Hunt et al. 2008
	Prince Edward Islands[c]	3	--	~2.8 – 3.5*	Hunt et al. 2008

[a]April 2004

[b]Sept to Nov 2012

[c]April 1999

* Lipid-corrected

**Carbonate-corrected

†Study pooled thecosome pteropod species which included *C. pyramida*

3.6.3 Between-species isotopic niche widths, overlap, and body size effects

Between-species comparisons of pteropods revealed the largest mean total niche area was for *C. antarctica* (8.15 ‰^{2}), followed by *C. pyramidata* (7.90 ‰^{2}), and *S. australis* (4.19 ‰^{2}) (Fig 3.7; Table B.2 in Appendix B). POM exhibited mean total niche areas of 1.86 ‰^{2} (large fraction; n = 7) and 2.18 ‰^{2} (small fraction; n = 8). Mean (95 % credibility limits) standard ellipse areas (SEA and SEAc) between species showed the largest estimates for gymnosomes *C. antarctica* and *S. australis* (Fig 3.7; see Table B.2 in Appendix B).

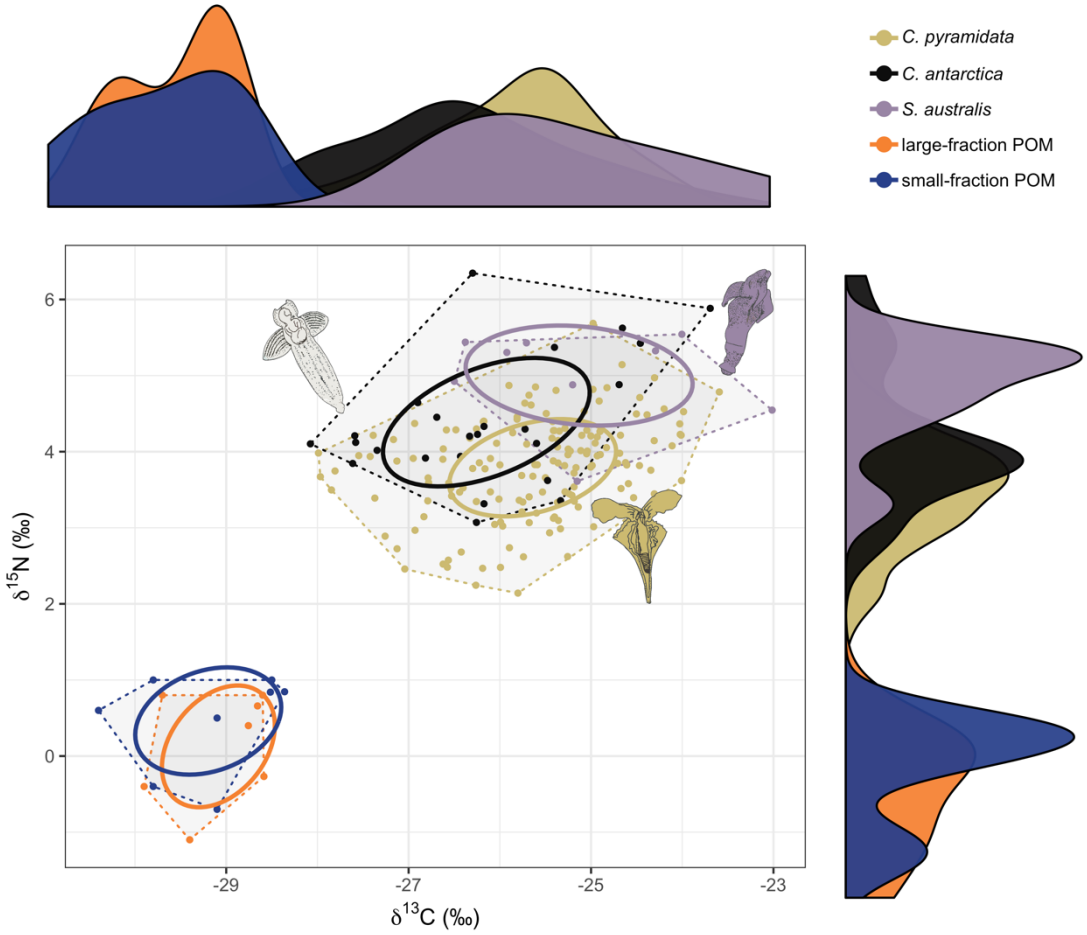

Figure 3.7 $\delta^{13}C$-$\delta^{15}N$ biplot of isotopes values, standard ellipses (solid lines; 40 % probability level), convex hulls (dashed lines), and density plots (outer axes) for each pteropod species and large- and small-fraction (grey) POM.

Probability niche overlap was high among all pteropod species (Fig 3.7, see Appendix B Table B.3), with the highest overlap observed between *C. antarctica* and *C. pyramidata* (85.6% at α = 0.95; 95.0% at α = 0.99 probabilistic niche regions (PNR)), followed by *C. antarctica* and *S.*

australis (79.5% at α = 0.95; 89.9% at α = 0.99 PNR) and *C. pyramidata* and *S. australis* (48.0% at α = 0.95; 64.8% at α = 0.99 PNR). We found small niche overlap between *C. pyramidata* and large-fraction POM (0.19% at α = 0.95; 0.65% at α = 0.99) and small-fraction POM (0.14% at α = 0.95; 0.74% at α = 0.99).

Only *S. australis* revealed a positive linear relationship between body length (mm) and $\delta^{15}N$ value, whereas the other two species, *C. pyramidata* and *C. antarctica*, showed negative relationships (Fig 3.8); only the relationship for *S. australis* was statistically significant (r^2 = 0.39, p = 0.05).

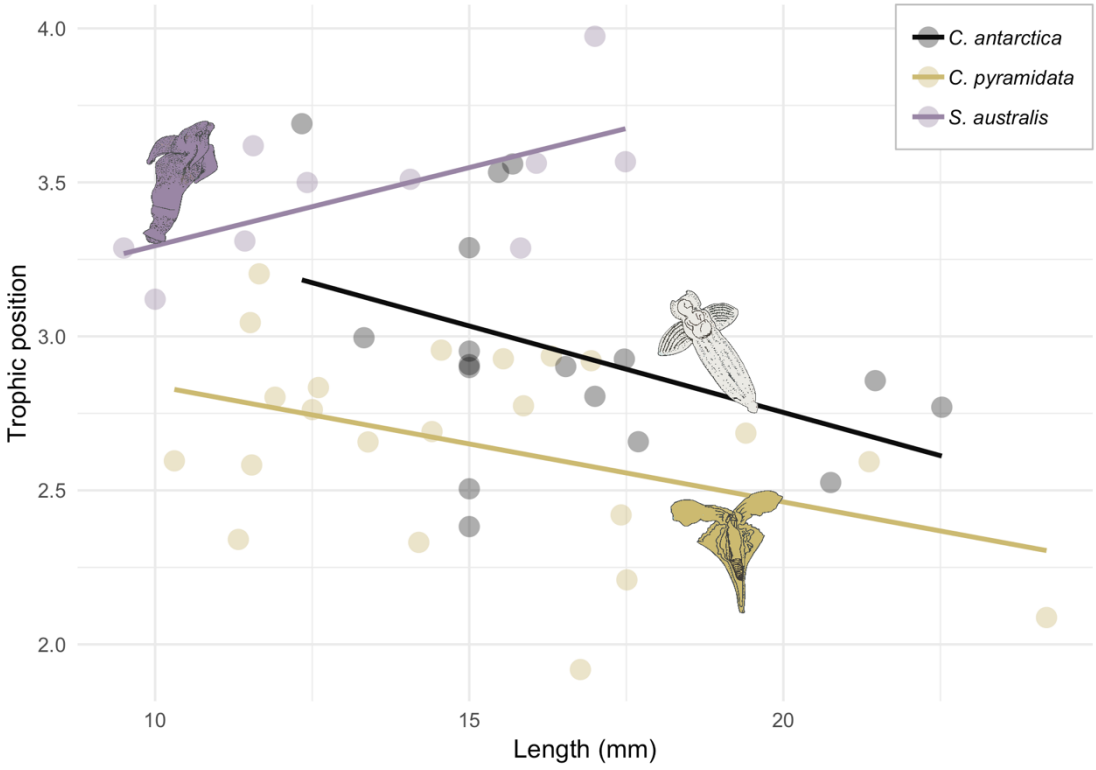

Figure 3.8 Relationship between body length (mm) and trophic position of pteropods *C. pyramidata*, *C. antarctica*, and *S. australis*. Equations for regression lines are: *C. pyramidata*, y = 4.74 – 0.08x (n = 21, r^2 = 0.17, p = 0.06); *C. antarctica*, y = 6.06 – 0.11x (n = 17, r^2 = 0.18, p = 0.09); *S. australis*, y = 3.88 + 0.10 (n = 9, r^2 = 0.39, $p < 0.05$).

3.6.4 Trophic positions

Average and modal trophic positions were determined for all species (Fig. 3.9), with *S. australis* exhibiting the highest trophic position (TP average: 3.46 ± 0.18; TP mode = 3.39) followed by *C. antarctica* (TP average: 3.20 ± 0.17; TP mode = 3.12), and *C. pyramidata* (TP average: 2.84 ± 0.14; TP mode = 2.75).

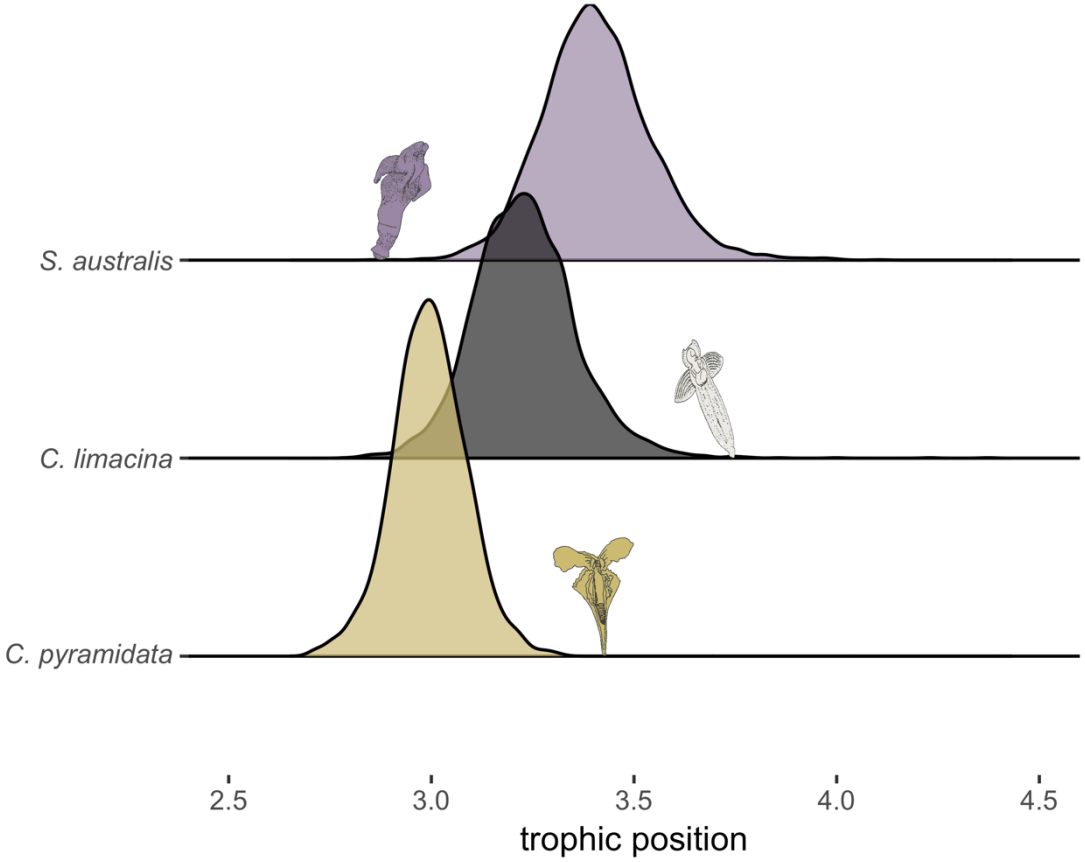

Figure 3.9 Bayesian estimates of trophic position created from 20000 Markov Chain Monte Carlo iterations for each pteropod species.

3.7 Discussion

We hypothesized that Southern Ocean pteropods would reveal variability in isotopic niche areas that reflect *a priori* knowledge of species-specific feeding preferences, with specialists, the gymnosomes, exhibiting smaller niche areas than generalists, the thecosomes. We expected narrow isotopic niches for gymnosomes possessing monophagous diets, consisting of a single species or genus, with *C. antarctica* preferring to prey on *Limacina* spp. and *S. australis* preying only on *C. pyramidata*. Instead, we measured broader than expected isotopic niche areas for gymnosomes *C. antarctica* and *S. australis*, compared to the value estimated for thecosome *C. pyramidata*. The generally accepted idea that niche width positively correlates with diet breadth is based on a common assumption that has emerged from the niche variation hypothesis (Van Valen, 1965). Empirical work involving an isotopically heterogenous range of consumers has revealed broader isotopic niches occupied by populations of dietary specialists in relation to those of generalists (Flaherty and Ben-David, 2010). Modelling efforts focused on the isotopic

composition of marine assemblages have confirmed that estimations of an organism's trophic niche can be confounded by isotopic variability in prey, regardless of both the source of isotopic variation and/or the diet behaviour (Cummings et al., 2012). Below, we discuss factors that may explain these patterns, but note that distinguishing among these mechanisms would require additional sampling and analysis and would be a fruitful direction for future work.

The isotopic variation within pteropod species measured here suggests niche partitioning and could point to their distinctive functional traits as observed through anatomical structures associated with feeding. Thecosomes such as *C. pyramidata* particle feed on marine snow by deploying an external mucus web to capture suspended materials of all sizes, which are then transported to the mouth by ciliary pathways, where particle sorting and ingestion occur (Gilmer, 1974; Gilmer, 1990). Gut content data from the Weddell Sea have revealed an omnivorous diet for *C. pyramidata* (Hopkins and Torres, 1989), corroborated by the broad range of $\delta^{15}N$ values measured within the present study. In contrast to thecosomes, the feeding apparatus of gymnosomes varies among species. *C. antarctica* possess six buccal cones that capture prey, and a series of hooks and the radula remove and swallow the soft tissue whole from the shell (Conover and Lalli, 1972), whereas *S. australis* captures prey using two lateral arms, each possessing a series of suckers (Lalli and Gilmer, 1989). Whilst both gymnosomes revealed broad $\delta^{13}C$ value ranges, which closely matched that of *C. pyramidata*, the variable ranges in $\delta^{15}N$ values displayed between each gymnosome may be a result of these species-specific feeding strategies.

Published $\delta^{13}C$-$\delta^{15}N$ biplots featuring Southern Ocean pteropod species place *S. australis* trophically higher than any other pteropod species common to the region (Hunt et al., 2008; Table 3.1). By our estimates, *S. australis* was one trophic level above its prey *C. pyramidata*, however despite obtaining a similar outcome to previous isotopic work evaluating the interaction between these two species (Table 3.1), these results alone cannot confirm a direct trophic relationship without supplemented by other lines of evidence, such as direct observation, genetic, and/or gut content analyses (Nielsen et al., 2018). More work is required to better understand prey size preference for this species. Meanwhile, *C. pyramidata* possessed a larger total niche area than those measured for gymnosomes, which likely reflecting omnivory.

We predicted narrow isotopic niche widths for both gymnosomes relative to that of *C. pyramidata*; however, our results demonstrate significant trophic diversity not only between orders, but also between gymnosome species. For *S. australis*, this may be a function of latitude, as this least-abundant species was sampled within the narrowest latitudinal range, however linear relationships did not reveal any statistically significant spatial correlations. We expected the isotopic niche width of both gymnosomes to be narrow because of *a priori* knowledge of their

specialist feeding preference for thecosomes (Phleger et al., 1997). However, the niche width of *C. antarctica* was significantly broader along the δ^{15}N-axis than hypothesized, which might be a function of their wider geographical range within our voyage transect, relative to that of *S. australis* more commonly found north of the Polar Front (PF) and the northern extent of our sampling effort (Hunt et al., 2008).

The unexpectedly wide niche area of *C. antarctica* might be a function of either diet switching to other unrecorded food sources, and/or driven by nutritional stress. One study posited that *C. limacina* diet may include other taxa when the preferred prey *Limacina* species are limited. DNA-based approaches used to investigate prey within Arctic *C. limacina* stomach contents revealed alternative prey items, such as amphipods and calanoid copepods (Kallevik, 2013). Further, laboratory observations have demonstrated that *C. limacina* can survive between 260 and 365 days without prey due to an adaptive ability to reduce body size and metabolic rate as a consequence of efficient utilization of lipids and phospholipids stores (Böer et al., 2007, 2006; Falk-Petersen et al., 2001). However, no studies have tested how these changes affect *C. limacina* isotopically. Among the numerous studies examining how a range of nutritional stresses affect isotopic compositions of various animals, enrichment in ^{15}N is the response most likely to confound interpretations of isotopic niches, particularly given that isotopic niche metrics rely on the assumption that inter-individual variability in enrichment between consumer and prey is insignificant (Karlson et al., 2018; McCue and Pollock, 2008). One experiment-based study on the amphipod *Monoporeia affinis* revealed wider niche widths among specimens exposed to nutrient and chemical stress relative to control animals (Karlson et al., 2018). It is understood that increases in isotopic niche areas are a function of inter-individual variability in the responses of consumers to stress exposure through changes in their metabolic pathways. Further laboratory testing is needed to understand how exposure to physiological stress, such as food limitation, can affect the magnitude of the isotopic compositions and niche metrics of *C. antarctica,* with special focus on the scale of individual. Furthermore, results of laboratory tests will need to be compared with *in situ* estimates of niche metrics taken from *C. limacina* sampled in years where prey species, *L. helicina*, were also abundant.

The qualitative concept of niche breadth can be fundamental to understanding the adaptive capabilities of an organism or assemblage, and is potentially useful for investigating responses of climate-driven changes to prey availability (Sexton et al., 2017). Recently, Henschke et al., (2015) employed isotopic niche analysis of co-occurring zooplankton and suspended POM assemblages from the Tasman Sea under three different oceanographic water types and found that omnivorous zooplankton became more carnivorous under low chlorophyll *a* conditions.

They concluded that niche breadth among different zooplankton groups was a function of the responses of phytoplankton and POM to oceanographic conditions. Narrower niches have been observed among CO_2-enriched hydrothermal vent communities relative to controls, whereby near-future predicted pCO_2 concentrations are directly associated with decreased higher trophic species diversity and simplified habitats (Agostini et al., 2018; Vizzini et al., 2017).

Clione antarctica showed the highest average bulk C:N ratio (6.8 ± 1.4), which is lower than reported for spring to early summer 2012 (C:N = 10.2; Table 3.1) in East Antarctica (Jia et al., 2016). Seasonal build-up of lipid deposits may be contributing to this difference, as C:N ratios in zooplankton are often positively related to lipid content (Syväranta and Rautio, 2010) which is depleted in ^{13}C relative to carbohydrates and proteins (Tieszen et al., 1983). Empirical evidence has shown that lipid extraction has a significant influence on stable isotope ratios of Southern Ocean pteropods, including *C. antarctica* (Weldrick et al., 2019). *Clione* spp. have developed a unique metabolic adaptation through *de novo* biosynthesis of large deposits of 1-*O*-alkyldiacylglycerol ethers (DAGE) for long-term energy storage (Kattner et al., 1998) necessary to cope with food limitation and overwintering survival (Böer et al., 2005; Phleger et al., 2001). Meanwhile, similar studies on *S. australis* (C:N = 5.1 ± 0.4, C content = 34.5 – 44.2 %; N content = 7.23 – 8.65 %) and its prey, *C. pyramidata* (C:N = 3.9 ± 0.3; C content = 24.9 – 41.2 %; N content = 5.4 – 10.4 %), have reported low to no levels of DAGE, respectively (Phleger et al., 1999).

Trophic positions of many aquatic species are, in many cases, more strongly predicted by body size than by taxonomy (Jennings et al., 2001; Soler et al., 2016) and distinctive feeding strategies specialize ontogenetically for many Southern Ocean zooplankton (Schmidt et al., 2003; Zhang et al., 2017). Generally, food preference in pteropods varies with age and season, and depends on food particle size and availability; with veliger- and juvenile-aged thecosomes primarily relying on marine POM, and adults consuming a largely diatom-based diet in spring and summer ahead of a switch to detrital materials between late autumn and winter when phytoplankton blooms are depleted (Gannefors et al., 2005; Manno et al., 2010). As our study focused on macrozooplankton greater than 2000 μm, we only present adult stages for each species, and further research is required to explore size-trophic position relationships that also incorporate earlier life stages.

For *C. pyramidata*, we did not observe an increase in trophic position with body size that would signify a possible shifting from herbivory to omnivory. Positive correlations between *C. pyramidata* abundance and phytoplankton blooms have been linked to high ingestion rates, with pteropods contributing up to 53 % to total grazing impact within the Spring ice edge whilst

contributing only 13 % to total biomass in the region (Pakhomov and Froneman, 2004). Gut content analyses from Weddell Sea specimens showed *C. pyramidata* f. *sulcata* diets primarily composed of diatoms, however larger motile organisms such as tintinnids, foraminiferans, copepods and polychaetes appeared in larger sized *C. pyramidata*, pointing to omnivorous feeding habits (Hopkins and Torres, 1989). Fatty acid profiles linked to crustacean biomarkers have also been measured in *C. pyramidata* from the Antarctic Peninsula (Phleger et al., 2001).

For gymnosomes, our results imply a continuous change in dietary preference throughout adult stages, which may vary spatially and depend on prey availability. A laboratory-based feeding experiment using Arctic *C. limacina* sampled in mid-summer measured low prey assimilation rates that increased towards the end of the experiment (Boissonnot et al., 2019). Results from their study suggested that sampling period overlapped with a seasonal period of low prey availability followed by high reproductive activity and subsequent body shrinkage. Among the RMT1 samples taken from the same research program (K-Axis) analyzed here, Matsuno et al. (submitted) identified and counted *L. helicina,* the preferred prey of *C. limacina*, however all specimens were juveniles with an average shell diameter of 0.4 ± 0.1 mm (see Table B.4 in Appendix B), and laboratory-based feeding experiments have shown that adult *C. antarctica* rarely consume *L. helicina* smaller than ~1 mm (Conover and Lalli, 1972). For *C. antarctica,* the negative relationship between trophic position and body size measured here could point to stress-induced isotopic enrichment within nutrient-limited body tissues causing body shrinkage (Boag et al., 2006). However, while this result aligns with the wider than expected niche width obtained for this species, the relationship was not statistically significant and conclusions cannot be drawn from this result.

Pteropod abundances throughout the Southern Ocean indicate highly variable yet sometimes dominant densities, and in proportion to other zooplankton groups, contributing up to 93 % of total macrozooplankton (Hunt et al., 2008), and strongly tied to El Niño events, sea ice retreat, and the presence of prey (Thibodeau et al., 2019). Our maximum abundance of 272 ind. 1000 m^{-3} for *C. pyramidata* is within the range of 2—996 ind. 1000 m^{-3} previously recorded for other macrozooplankton samples (4.5 mm mesh size) throughout the Southern Ocean (Hunt et al., 2008). Maximum abundance for both gymnosome species combined, 47 ind. 1000 m^{-3}, was high compared to macrozooplankton samples throughout the Southern Ocean, including the maximum abundances ranging 2.0—27 ind. 1000 m^{-3} of gymnosome species combined (Hunt et al., 2008).

Linear regressions revealed a statistically significant positive relationship between $\delta^{13}C$ and longitude for *C. pyramidata*, which may relate to the cluster of enriched values overlapping the

same region (just north of the sACCf on the Plateau) we measured high abundances of this species, towards the eastern flank of the Plateau. Particulate organic nitrogen (PON) measurements revealed enriched values along this region, indicating nitrate uptake which suggests new production was occurring here (Schallenberg et al., 2018). However, we also detected a statistically significant negative relationship between $\delta^{13}C$ and longitude for *C. antarctica*, whose highest abundances generally overlapped with those of *C. pyramidata*. A weakly positive significant linear relationship was measured between $\delta^{15}N$ and latitude for *C. pyramidata*, who displayed gradients of isotopic enrichment from deeper regions of the transect towards the coastlines and towards shallower areas towards Banzare Bank, at 60°S and 80°E. Regions along the transect where abundances were lowest (between 70°E to 80°E) overlapped with the lowest $\delta^{13}C$ and $\delta^{15}N$ values measured for all species, combined. Incidentally, this region, which covers the western area of the Plateau, also measured the most ^{15}N-depleted in PON, suggesting nitrogen recycling and ammonia uptake (Schallenberg et al., 2018).

The pteropod species sampled from the southern extent of the Kerguelen Plateau are among the four common species regularly found south of the PF (Loeb and Santora, 2013). The notable absence was that of adults of the most common thecosome species, *L. helicina antarctica,* and could be a result of environmental factors affecting primary productivity. A similar absence was first documented in McMurdo Sound in December 2001, a year following a 50 to 75% reduction in phytoplankton biomass and high sea ice cover which resulted in nutrient stress-related decreases in metabolic rates in both *L. helicina antarctica* and its monophagous predator *C. antarctica* (Seibel and Dierssen, 2003). In 1989, low densities were also recorded in the East Antarctic and may be attributed to low chlorophyll *a* biomass resulting from late winter sea-ice retreat (Hunt et al., 2008). Satellite observations for the region and period surveyed here exhibited comparatively low average chlorophyll *a* concentration, ranging from 0.45 to 0.55 mg m^{-3} (see Fig. B.1 in Appendix B for monthly interannual time series (2008-2017) of average chlorophyll *a* concentration from satellite observations). However, in 2015, the Kerguelen Plateau region experienced lower than average maximum chlorophyll *a* concentration (<0.5 mg m^{-3}) preceded by much lower averages (<0.3 mg m^{-3}) since December 2012. These values are less than the lowest value of 1.0 mg m^{-3} observed by Seibel and Dierssen (2003) the year prior to their observed absence of *L. helicina*. It is possible that with chlorophyll *a* concentration decreasing to less than 0.8 mg m^{-3} since 2008, this region may not provide enough resources to sustain growth and development of *L. helicina* assemblages beyond juvenile stage.

3.8 Concluding remarks

While the Southern Ocean supports a range of diverse ecosystems, it is also among the most rapidly changing regions on a global scale, and it is an ongoing challenge to predict how these ecosystems and species will respond (Murphy et al., 2012). Climate-driven changes in ocean temperature, ocean frontal positions, seasonal ice cover, and CO_2 uptake are expected to significantly alter abundance, distribution, and trophodynamics of key polar organisms (Constable et al., 2014), including pteropods, as a response to changing metabolic fitness, prey availability and diversity, and competition. Given the complex spatial and temporal dynamics of the Southern Ocean, future research focused on understanding species responses due to human-induced physical and chemical changes need to be small scale and regionally comparative (Allan et al., 2013). Monitoring variation between pteropod species in their isotopic niches coupled with their regional abundance and distribution could play a key role in understanding oceanographic and ecological drivers of change, for instance, due to their intraspecific reliance on sea ice primary production (Jia et al., 2016), and close associations with ocean frontal zones and biogeochemical provinces (Burridge et al., 2017). Additionally, such work will need to account for the magnitude of phenotypic plasticity in pteropods, including if and how their metabolic responses to multiple stressors of climate change are driving variability in isotopic niches. The work presented here concludes that isotopic niches in Southern Ocean pteropod communities are not merely driven by diet diversity nor follow the niche variation hypothesis of Van Valen (1965). To our knowledge the present study represents the first comprehensive assessment involving measurement and interpretation of isotopic niche widths among pteropod assemblages. Our findings highlight the utility of employing isotopic niche metrics and dispersion analyses to reconstruct the trophic structure of co-occurring Southern Ocean pteropods, and the need to expand this research to understand drivers of diet behaviour.

Chapter 4

The use of swimmers from sediment traps to measure summer community structure of Southern Ocean pteropods[3]

4.1 Graphical Highlights

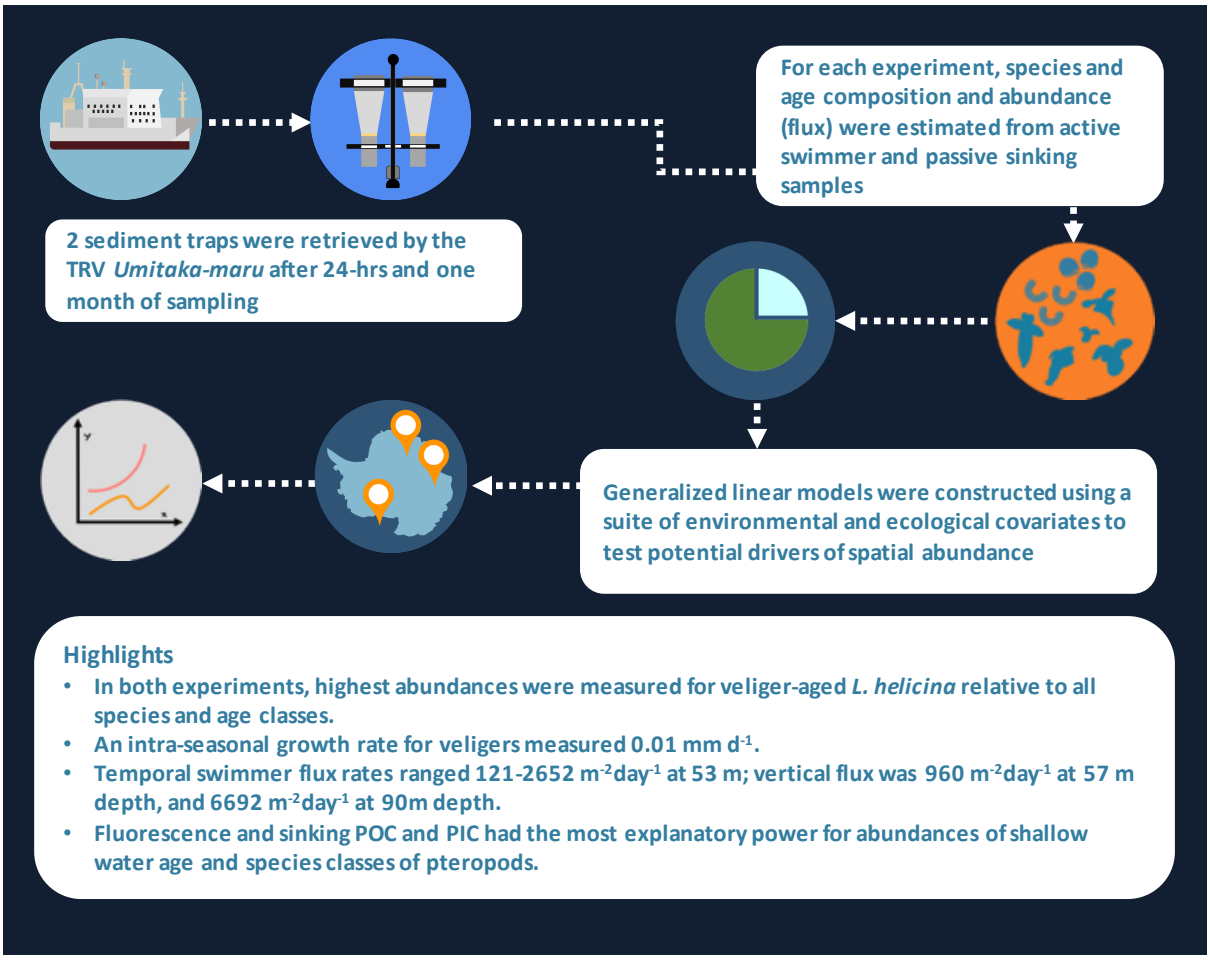

Figure 4.1 Graphical abstract for Chapter 4.

4.2 Key words

Swimmers, sediment traps, Southern Ocean, population dynamics, thecosomes, gymnosomes

[3] R. Makabe, S. Takao, K. Mizobata, M. Moteki, T. Odate, R. Trebilco, and K.M. Swadling are coauthors on this chapter, which is currently in preparation for journal submission.

4.3 Abstract

In the Southern Ocean, pteropods play an important role in biogeochemical cycling, and sediment traps are a valuable tool for quantifying this role through the collection of passively sinking matter from productive surface waters to deep sea layers. However, observations of 'swimmers' (e.g. organisms that actively swim into traps) can also prove valuable in studying zooplankton community structure. In this study, population and flux dynamics of pteropods were analysed from two separate sediment trap experiments during the 2016-17 summer. In both experiments, highest fluxes were measured for veliger-stage *Limacina helicina antarctica* (0.09 – 0.3 mm) relative to all species and age classes. Increases in shell diameters of veligers in all traps over time allowed enabled the calculation of an intraseasonal growth rate of 0.0068 mm d^{-1}. Swimmer flux rates ranged from 121 to 2674 ind. m^{-2} d^{-1} at 53 m depth, and vertical flux measured 960 ind. m^{-2} d^{-1} at 57 m depth and 6692 m^{-2} d^{-1} at 90 m depth. Among a suite of environmental and biological covariates tested, fluorescence and sinking particulate organic and inorganic carbon (POC and PIC) had the most explanatory power for the abundances of shallow water pteropod age class and species composition. Gymnosome abundances were largely influenced by increasing adult *L. helicina antarctica* counts. Changes to pteropod population and community dynamics in response to near-future climate change will have cascading effects throughout Antarctic epipelagic food webs, and these results provide a small-scale regional snapshot of patterns in structure and sedimentation from an under-surveyed region of the Southern Ocean.

4.4 Introduction

Pteropods are marine holoplanktonic gastropods with a cosmopolitan distribution (Bednaršek et al., 2012a; Hunt et al., 2008). There are two clades: thecosome pteropods, which possess aragonite shells and gymnosome pteropods, which, as adults, do not (Lalli and Gilmer, 1989). In the Southern Ocean, periods of increased thecosome abundance can significantly impact ecological functioning of Antarctic and sub-Antarctic ecosystems, providing food for higher trophic levels, top-down control of primary producers, and contributions to biogeochemical organic and inorganic carbon cycles (Elliott et al., 2009; Hunt et al., 2008). Thecosome pteropods are recognized as early responders to ocean climate change due to the damaging effects of ocean acidification on their aragonite shells (Bednaršek et al. 2017; Manno et al. 2017). Estimating and monitoring pteropod diversity, life history, and vertical flux over varying spatial and temporal scales will help improve understanding of the magnitude of their ecological roles, particularly in polar regions that are undergoing anthropogenic changes in marine chemistry.

Many large planktonic microphages contribute significantly to the organic carbon transport to the deep sea, particularly during blooms. As marine calcifiers, thecosomes facilitate direct, downward fluxing of both particulate organic and inorganic carbon to the mesopelagic zone through three mechanisms (Manno et al., 2017): (1) they can repurpose organic matter from grazing into faecal pellets (Manno et al., 2010); (2) the mucous webs they use for feeding are discarded, likely in response to predation, along with the aggregated organic particles adhered to them (Noji et al., 1997); and (3) they undergo interannual mass mortality events that export large concentrations of both organic soft tissues and inorganic aragonite shells (Manno et al., 2007). Thecosomes thus contribute to both biological carbon and the calcium carbonate counter pumps, causing either removal or release of CO_2 to and from the atmosphere (Manno et al., 2018). The role that thecosomes play in regulating the balance between the two outcomes results from both the deep-sea export and production of particulate inorganic carbon (PIC) from $CaCO_3$ shells.

Sediment trap samples are routinely used for estimating carbon flux, including identifying regional influences on marine food webs and the global biological carbon and carbonate counter pumps (Buesseler et al., 2007; Manno et al., 2010, 2007; Rembauville et al., 2016). They can be used for longer-term monitoring studies in pelagic environments at depths not easily or regularly accessible (Makabe et al., 2016). Many pteropod-focused sediment trap studies from the Southern Ocean concentrate efforts on estimating carbon and carbonate flux potential primarily through the analysis of aragonite shells and faecal pellets (Manno et al., 2010; Roberts et al., 2011; 2014; Teniswood et al., 2016), but intentionally remove 'swimmers' prior to analyses as they are treated as sinking particles (Table 4.1). Swimmers are live zooplankton that are suspected to actively swim into trap cups, and most trap-based studies regard them as contaminants, as they confound quantitative measurements from passively sinking particles, which should only include faecal pellets, detritus, and mucous webs, that flux from productive surface layers to the deep sea (Buesseler et al., 2007; Michaels et al., 1990). Swimmers are often difficult to distinguish from passive particles (Accornero et al., 2003; Knauer et al., 1984; Michaels et al., 1990). Diel vertical migration by pteropods means that species exist throughout in the mesopelagic zone, however highest densities are generally found within the upper 50 m (Hunt et al., 2008), thus their presence in shallow water traps may provide valuable insights into estimations of abundance, composition, and population dynamics that are commonly estimated through more traditional net-caught sampling techniques (Matsuno et al., 2014).

Table 4.1 Details of peer-reviewed pteropod-focused sediment trap studies.

Region	Focus	Species	Sample	Trap depth (m)	Year	Reference
South of Australia, north of SACCF	Abundance and POC biomass	*L. helicina* and *L. retroversa*	Sinkers and swimmers	70	2010	Akiha et al., 2017
Sargasso Sea	Seasonal flux	Euthecosomes, multiple species	Swimmers	3200 ± 100 below surface; 1000 above sea floor	1977, 1978, 1978-1982	Almogi-Labin et al., 1988
Norwegian Sea	Autumn sedimentation	*L. retroversa*	Sinkers and swimmers	50, 100, 250, 500, 1000, 1300	1988	Bathmann et al., 1991
Eastern Fram Strait	Long term patterns in sedimentation	*Limacina* spp.	Sinkers and swimmers	300	2000-2009	Bauerfeind et al., 2014
Eastern Fram Strait	Long term patterns in sedimentation	*Limacina* spp.	Sinkers and swimmers	Multiple, 80 - 2565	2008-2012	Busch et al., 2015
North Pacific	Species-specific variability in $\delta^{18}O$ from shells	Euthecosomes and atlantids, multiple species	Swimmers	100, 400	1981	Grossman et al., 1986
Greenland	Estimating sediment traps as attractants to swimmers	*Limacina* spp.	Swimmers and sinkers	25	1985	Harbison and Gilmer, 1986
Subantarctic	Seasonal flux	Euthecosome pteropods and heteropods	Sinkers	2100	2003-2004	Howard et al., 2011

Western Sargasso Sea	Species-specific variability in $\delta^{13}C$ and $\delta^{18}O$ from shells	*L. inflata* and *S. subula*	Sinkers and swimmers	500	1991-1992	Juranek et al., 2003
Terra Nova Bay	Estimate effect of carbonate saturation state on shells	*L. helicina*	Sinkers	260, 880	1999, 2000, 2003	Manno et al., 2007
Terra Nova Bay	Quantification of flux from faecal pellets	*L. helicina*	Sinkers	180	1998-2001	Manno et al., 2010
Norwegian Sea	Carbonate and individual flux rates, $\delta^{18}O$ from shells	*L. helicina* and *L. retroversa*	Sinkers and swimmers	400-500 above sea floor (depths: 1700 m and 2800 m)	1983-1985	Meinecke and Wefer, 1990
Western Arabian Sea	Abundance, carbonate, and organic carbon flux	Euthecosomes, multiple species	Sinkers	919	1993	Mohan et al., 2006
Subantarctic	Diversity, preservation state, and shell flux above and below aragonite saturation horizon	Euthecosomes, multiple species	Sinkers	Above 1000, below 2000	1997-2006	Roberts et al., 2011
Subantarctic	Long term shell mass and number flux	*Limacina* spp.	Sinkers	800	1997-2007	Roberts et al., 2014
Somali Basin, Arabian Sea	9-month time series of numerical and mass flux	Euthecosomes, multiple species	Sinkers	1032	1992-1993	Singh and Conan, 2008
Subantarctic	Microstructure of shells	*L. helicina antarctica*	Sinkers and swimmers	2000	1997/1998	Teniswood et al., 2016
North Pacific	Deep sea abundances	*L. helicina* and *C. pyramidata*	Assumed to be sinkers	200, 1000, 3800	1983-2000	Tsurumi et al., 2005

Studies comparing both net- and sediment trap samples have revealed significant correlations in abundance for pteropods, thus demonstrating the utility of sediment traps as an alternative or supplement to traditional net-sampling (Almogi-Labin et al., 1988; Makabe et al., 2016). Almogi-Labin et al. (1988) found that the spring arrival of pteropod shells to traps seasonally matched both the composition of the net-sampled living communities and the peak food availability observed at the surface. Furthermore, sediment traps can sample continuously, which is particularly effective in estimating how depth-stratified environmental and ecological properties influence the vertical structure of shallow water zooplankton compositions over varying time scales (Willis et al., 2006).

Both swimmer and sinker specimens have been used in long-term sediment trap studies to observe sedimentation patterns in Arctic Euthecosome pteropods (Bauerfeind et al., 2014; Busch et al., 2015). These studies have revealed significant interannual changes in pteropod species composition, including communities once dominated by cold-water adapted *L. helicina* shifting towards communities dominated primarily by the subarctic *L. retroversa* in later sampling years. Furthermore, long term length-frequency data of trap-caught amphipod swimmers have enabled the calculation of life spans for Arctic species, *Themisto compressa* and *T. libellula* (Kraft et al., 2012). Similar life cycle patterns have only previously been assessed using pteropods sampled from plankton nets possessing mesh sizes of 50 – 150 μm (Bednaršek et al., 2012c; Wang et al., 2017), a range of which is sufficient to capture all life stages though not commonly used in polar zooplankton research (Ashjian et al., 2003; Hopcroft et al., 2005).

The need to gather early age population structure data on Southern Ocean pteropods stems from growing research reporting harmful effects on ontogenetic development caused by multiple stressors of anthropogenic climate change (Comeau et al., 2012; Thabet et al., 2015). Gardner et al. (2018) found high larval mortality and shell malformation and dissolution in laboratory-cultivated *L. helicina antarctica* veligers exposed to increased temperature and aragonite undersaturation. *L. helicina* shell diameters were measured to assess age structure, early development, and possible timing of spawning events, all data contributing to a valuable baseline from which to monitor spatial and temporal changes to early life stages of a species highly sensitive to environmental changes.

The Japanese Antarctic Research Expedition (JARE) has been conducting oceanographic data and plankton sampling along the 110°E meridian within the Indian sector of the Southern Ocean since 1987 (Moteki et al., 2017). In this region, observations from one long-term time-series dataset have revealed considerable interannual variation in Euthecosome pteropod abundances, with samples consistently dominated by *L. helicina antarctica* possessing average shell

sizes between 150 μm and 300 μm (Nishizawa et al., 2016). These observations were based on individuals sampled using plankton nets of 110 μm mesh size and were therefore unable to account for early life stages (< 110 μm). In this study, both passive sinking and active swimmer pteropods from two sediment trap sampling events were analysed as a means to determine spatial and temporal variation in community structure of pteropods. The identity of environmental and ecological covariates that may drive pteropod assemblages were also sought within this Chapter.

4.5 Methods

4.5.1 Field sampling

Two separate sampling experiments were performed within the Indian sector of the Southern Ocean, both located north of the Southern Boundary of the Antarctic Circumpolar Current (SB-ACC) front (Orsi et al., 1995; Sokolov and Rintoul, 2009). Two GPS-equipped surface drifters attached to sensors and time-series sediment traps (Nichiyu 7S; 0.02 m2 aperture) were deployed to collect zooplankton swimmers and sinking particles at two sites for different durations and depths (Fig. 4.2). The first drifter was deployed during the Southern Ocean cruise of the ice breaker Shirase as part of the 58th Japanese Antarctic Research Expedition, then retrieved during the Southern Ocean research voyage aboard the Tokyo University of Marine Science and Technology (TUMSAT) training vessel Umitaka-maru. The second drifter was deployed and retrieved during the Umitaka-maru cruise. These traps thus provide one month of continuous pteropod sampling, followed by another sampling time point 10 days later during the

start of austral summer.

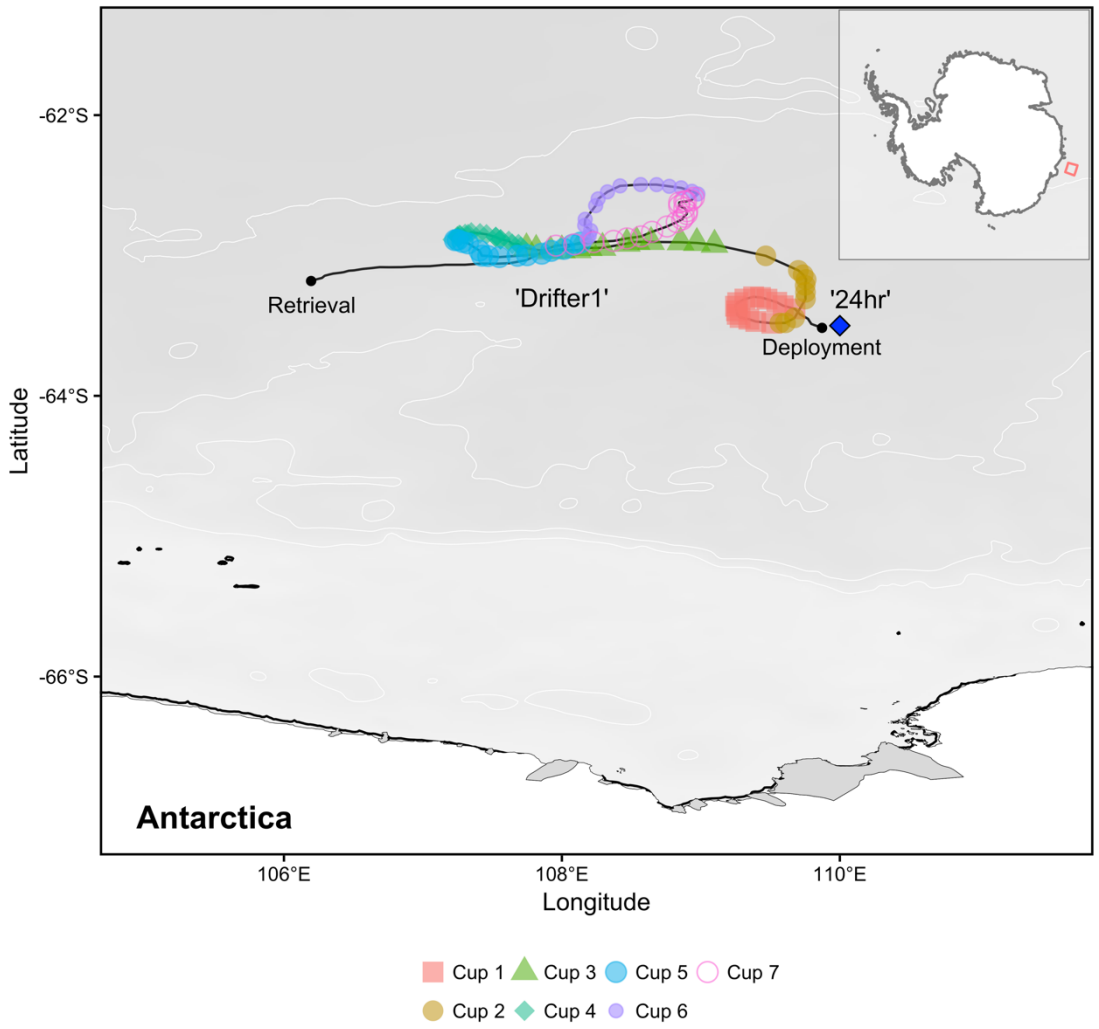

Figure 4.2 Positions of drifter1 and 24-hr (diamond) sediment traps. Numbers in bottom legend refer to each drifer1 sediment trap cup.

The first, 7-cup sediment trap ("drifter1") sampled from 10 December 2016 until 7 January 2017 (109.9 °E, -63.5 °S). Attached to it at various depths was a series of sensors collecting oceanographic data including temperature, salinity, and in situ fluorescence (Table 4.2; see Table C.1 in Appendix C for details of each sensor and trap). Each cup sampled every 4 days, and at an average depth of 52.7 ± 0.2 m (Table 4.2). Previously acquired long-term temperature-salinity profiles at 110 °E and 64 °S have identified a seasonal surface mixed layer shallower than 50 m between December and January (Nishizawa et al., 2016), and this depth was chosen as cups could capture export production. Cups were initially filled with filtered seawater containing neutral Lugol's solution (final conc. 5%, salinity ca. 50 NaCl). The drifter1 buoy was recovered at

106.2 °E, -63.2 °S on 14 January 2017 and sampling cups were kept in darkness at 4 °C until analyses in Tachikawa, Japan.

Table 4.2 Location, depths, dates, and environmental variables recorded for all time-series sediment trap (drifter1) sampling cups. (± standard deviation shown in parentheses).

	Cup 1	Cup 2	Cup 3	Cup 4	Cup 5	Cup 6	Cup 7
Latitude (°S)	-63.4	-63.3	-62.9	-62.9	-63.0	-62.6	-62.7
Longitude (°E)	109.4	109.7	108.4	107.4	107.6	108.5	108.7
Deployment depth (m)	52.9 (0.1)	52.9 (0.1)	52.7 (0.2)	52.6 (0.3)	52.8 (0.1)	52.6 (0.2)	52.7 (0.2)
Sampling period:							
Start	10/12	14/12	18/12	22/12	26/12	30/12	3/1
End	14/12	18/12	22/12	26/12	30/12	3/1	8/1
Temperature (°C)	-0.9 (0.3)	-1.4 (0.3)	-1.2 (0.5)	-1.4 (0.1)	-1.3 (0.1)	-1.2 (0.2)	-1.3 (0.2)
Salinity (PSU)	34.2 (0.0)	34.9 (0.0)	34.2 (0.1)	34.0 (0.1)	34.1 (0.1)	34.1 (0.1)	34.1 (0.1)
Fluorescence (μgL^{-1})	1.94 (0.8)	2.29 (0.9)	2.08 (0.9)	0.58 (0.2)	0.57 (0.2)	0.51 (0.2)	0.72 (0.4)

The second sediment trap ("24hr") was deployed on 17 January 2017 (110.0°E, 63.5°S). It was secured to a GPS buoy along with a CTD (Seabird SBE-37+©), and fitted with a series of sensor frames at 4 depths, and an Aquadopp acoustic doppler current profiler (ADCP) at 65 m depth (see Table C.1 in Appendix C for more details on trap and sensor equipment). Also attached to the trap were 4 sampling cups: with 2 cups each positioned at 57 and 90 m depths. The trap was recovered after 24-hours, on 18 January 2017 (109.9°E, 63.4°S). A CTD cast before deployment was conducted to determine trap and sensor depths. The shallower trap (57 m) was positioned just below the subsurface chlorophyll maximum layer, and the deeper trap (90 m) was positioned just below the temperature minimum layer, which is considered the winter mixed layer. On a seasonal scale, this winter maximum layer is equivalent to the maximum depth of the surface mixed layer, and carbon sequestration from this layer is assumed to have vertically fluxed approximately one or more years ago. Prior to deployment, sample cups were filled with

filtered sea water with the addition of NaCl (50 PSU in salinity) and, upon retrieval, maintained at 4°C until analyses. One sampling cup per each "24hr" depth was preserved with neutralized 5% (v/v) buffered formalin-seawater while the other cups from each depth were filled with 5% neutral Lugol's solution. Whilst I conducted swimmer analyses using both preservatives, the purpose of using each was for another study (Sano et al., in prep), and inconsequential to this study.

4.5.2 Swimmer size and flux estimates

All species of pteropod swimmers were removed from the whole sinking POM sample, then identified to the highest taxonomic level and enumerated (following Lalli and Wells (1978)) using a Nikon SMZ18 stereomicroscope. The number of empty shells were also noted. Both intact individual pteropods and empty pteropod shells were placed on petri dishes and photographed using a Nikon DS-Fi2 CCD camera mounted to the stereomicroscope in connection with the NIS-Elements software (version 4.30, Nikon Instruments, Japan). Shell diameters (in mm) of *Limacina helicina antarctica* were measured following Bednaršek et al., (2012b) for *L. helicina antarctica* from the Scotia Sea. To measure shell diameter from images, I used the open-source image analysis software, ImageJ/Fiji (Schindelin et al., 2012). I classified developmental stages based on shell diameters, whereby veligers, immature juveniles, and adults are <0.3, 0.3-4.0, and >4.0 mm, respectively (Lalli and Wells, 1978). It is important to note that this classification was previously determined for Arctic *L. helicina*, which may possess different growth rates to the Antarctic species sampled within this study.

Swimmer abundance was expressed as swimmer flux (ind. m^{-2} d^{-1}) and calculated by the following equation:

$$N \, x \frac{1}{d} x \frac{1}{0.02} \tag{1}$$

where N is the number of individuals per sample, d is the number of sampling days, and 0.02 (m^2) is the mouth area of each sediment trap.

4.5.3 Sinking POM sampling

While at sea, seawater was collected at 8 m from the underway pump, at the surface by bucket, and at 50 m using Niskin bottles and a bucket. For sinking POM, samples preserved with 5 % neutral Lugol's solution were initially stored at 4 °C while at sea, then filtered onto pre-

combusted GF/F filters and desalinated using a drop of ultrapure water in the laboratory. Filtered samples of sinking POM were exposed to HCl fumes for 24 hours to remove inorganic carbon fractions, then dried at 60°C for another 24 hours.

4.5.4 Sinking PIC, POC and PON

After removal of all swimmers, samples were divided into several aliquots using a Motoda-box plankton splitter (Motoda, 1985) for chemical measurements, including particulate organic carbon and nitrogen (POC and PON, respectively) and microscopic analysis of sinking particles. Analyses of POC and PON concentrations were performed using a mass spectrometer (Callisto CF-IRMS, SerCon, UK). Sinking POC and PIC were determined using the same method as sinking POM, but without exposure to HCl fumes. Sinking PIC was calculated by subtracting organic carbon from total particulate carbon. Most of the PIC contents here were composed of foraminiferans, as all pteropod and ostracod specimens were identified as swimmers and had been removed. Furthermore, no coccolithophores were detected in any of the sediment trap samples (Ayuko Kagesawa, personal communication).

4.5.5 Cohort analysis and daily growth rate estimates

Cohort generations of *L. helicina antarctica* were determined using the package mixdist v.0.5-4 (Macdonald and Du, 2015) in R (R Development Core Team 2018). I used 726 shell length measurements pooled from all sediment trap samples to construct length-frequency histograms from which discrete modal peaks were identified, by mixdist, using finite mixture distribution modelling. Each modal peak was assumed to represent a distinct spawning event.

The average intra-seasonal daily growth rate (mm d^{-1}) of veliger *L. helicina antarctica* was calculated by taking the difference in average shell length (in mm) between each two consecutive time steps (i.e. trap cups) divided by the length of time (in days) between time steps. Maximum intra-seasonal daily growth rate was calculated by subtracting the minimum shell length in the earliest trap from the maximum shell length from the final trap sample, following Bednaršek et al. (2012b) for net-sampled *L. helicina antarctica* from the Scotia Sea. These calculations assume all species represent an homogeneous population, unaltered by recruitment or emigration.

4.5.6 Egg mass morphometric analyses

A series of morphometric measurements was conducted on pteropod egg masses to identify patterns in fecundity throughout both sediment trap experiments in this study. Egg masses were placed on glass petri dishes and photographed using the same protocol used for

shell diameter measurements. ImageJ/Fiji freeware was used to conduct morphometric analyses and ontogenetic determination of pteropod eggs, including clutch length (CL), clutch area (CA), clutch-to-egg ratio (C:E), egg count (EC) and area (EA) from each photograph. Ontogenetic stages of egg development were identified following Wakabayashi, (2017) and Thabet et al., (2015) for similar pteropod species. Fecundity rate was calculated as the number of eggs per egg mass.

4.5.7 Statistical analyses

All statistical analyses were performed using RStudio, version 1.1.442 (R Development Core Team 2018). Analysis of variance (ANOVA) and post-hoc Tukey Honest Significant Difference (HSD) tests were performed to measure differences in total pteropod flux between each drifter1 sampling cup and within pteropod swimmer composition. *F*-tests were used to test for differences in variances between the two sample sets, with respect to depth or preservation techniques. Significance for these tests was based on p value < 0.05. Environmental data for each time-step (cups in drifter1) were summarized (Table 4.2), and means were tested for statistical differences using Welch's t-test, due to heterogeneity of variances.

4.5.8 Covariate selection and generalized linear modeling

Generalized linear models (GLMs) were developed to explore how environmental, ecological, and spatial explanatory covariates influence pteropod swimmer abundance (flux) for all species and age classes. Despite measuring low abundances for some groups in this study (see Results), all pteropod species and age classes were included due to the need for baseline data given their vulnerability to multiple stressors of climate change (Bednaršek et al., 2016). Environmental covariates included fluorescence, salinity, and temperature. Fluorescence was selected as an estimate of chlorophyll a, which was used here as a proxy for phytoplankton biomass, and thus food for the thecosomes (Noji et al., 1997; Seibel and Dierssen, 2003). Salinity was selected as it may exert a secondary influence on *L. helicina antarctica* densities through its direct effect on its food source, sea ice algae (Jia et al., 2016; Ryan et al., 2011). Temperature was chosen as previous research has identified all age classes of thecosome pteropods to be particularly vulnerable to ocean warming (Bednaršek et al., 2016) and it is believed that latitudinal distributions will shift in response to Southern Ocean warming (Mackey et al., 2012). Based on predator-prey interactions between Southern Ocean gymnosomes, *Clione limacina antarctica* and *Spongiobranchaea australis*, and thecosomes, *Limacina helicina antarctica* and *Clio pyramidata*, respectively (Hunt et al., 2008), ecological covariates included gymnosome densities (for

thecosome models only), thecosome densities (for the gymnosome model only), and densities of other zooplankton species collected from the sediment traps. Other covariates related to potential prey for primary consumers, including particulate inorganic and organic carbon, were used in model building. Spatial covariates, including latitude, longitude, and depth, all averaged for each cup, were used because they were found to drive spatial patterns in egg masses (Chapter 5). A priori hypotheses related to drivers of shallow water densities of Southern Ocean pteropod species informed covariate selection. I employed a negative binomial distribution and log-link function to correct for overdispersion detected within the data, using the MASS and AER packages in R (Kleiber and Zeileis, 2008; Venables and Ripley, 2002). The most parsimonious model, as determined by the lowest Akaike Information Criterion (AIC), was chosen through backwards selection.

4.6 Results

4.6.1 Time series and age composition

The composition of all pteropod species and age classes collected from the time-series sediment trap (drifter1) was variable, and included veliger (81.9 %), immature juvenile (3.2 %) and adult *Limacina helicina antarctica* (10.1 %), juvenile *Clio pyramidata* f. *sulcata* (1.7 %), juvenile gymnosomes (indeterminate species, 1.6 %), and egg masses (1.5 %). Sizes of *L. helicina antarctica* ranged from 0.091 to 6.708 mm, and, given this relatively large maximum size and geographic location, is likely to be morphotype *L. helicina antarctica* f. *antarctica* (van der Spoel et al., 1999). Notably, there were no individuals sampled with shell diameters falling between the maximum value for *L. helicina antarctica* juveniles, 0.43 mm, and the minimum value for *L. helicina antarctica* adults, 3.38 mm. Adult *L. helicina antarctica* were only found from 22 December to 8 January.

The total swimmer flux of all pteropod species and age classes throughout the drifter1 sampling period was 2673.6 ind. m^{-2} d^{-1} (Fig. 4.3a-c; Table C.2 in Appendix C). The highest total flux among age and species classes was comprised of veligers (< 0.3 mm) in all but one of the sample cups [$F(5,36) = 4.15$, $P = 0.004$]. In sample cup 4 (22-25 December), adult *L. helicina antarctica* were most abundant of all species and age classes collected. Though not significant, the highest pteropod swimmer flux (2469.6 ind. m^{-2} d^{-1}) was observed in sample cup 7 (3-8 January), and 92.4% of this total was composed of *L. helicina antarctica* veliger age class [$F(6,35) = 0.775$, $P = 0.60$]. The lowest period of pteropod flux (120.8 ind. m^{-2} d^{-1}) was observed in the first sample cup (10-13 December).

Average chlorophyll-*a* concentration was highest (>2 μg L^{-1}) during 14-18 December sample period (cup 2; Fig. 4.3a), then strongly decreased to <1 μg L^{-1} between 18 to 22

December (cup 3; Fig. 4.3a) where it remained throughout the remainder of the experiment. Average temperature steadily increased throughout the sampling duration, starting at -0.7 °C (± 0.2 °C; Fig. 4.3b) and reaching to 0.5 °C (± 0.4 °C; Fig. 4.3b) by the end of the drifter1 experiment. As for biogeochemical results, sinking POC spiked (62 mg C m^{-2} d^{-1}) during 14-18 December (cup 2; Fig. 4.3c) before decreasing just below 20 mg C m^{-2} d^{-1} by 22 December, where it remained for the duration of the experiment. Also during 14-18 December (cup 2; Fig. 4.3c), sinking PIC measured lowest (-4.4 mg C m^{-2} d^{-1}) but remained below 6 mg C m^{-2} d^{-1} throughout the experiment. C:N remained between 4.2 and 6.4 through the sampling duration (Fig. 4.3c).

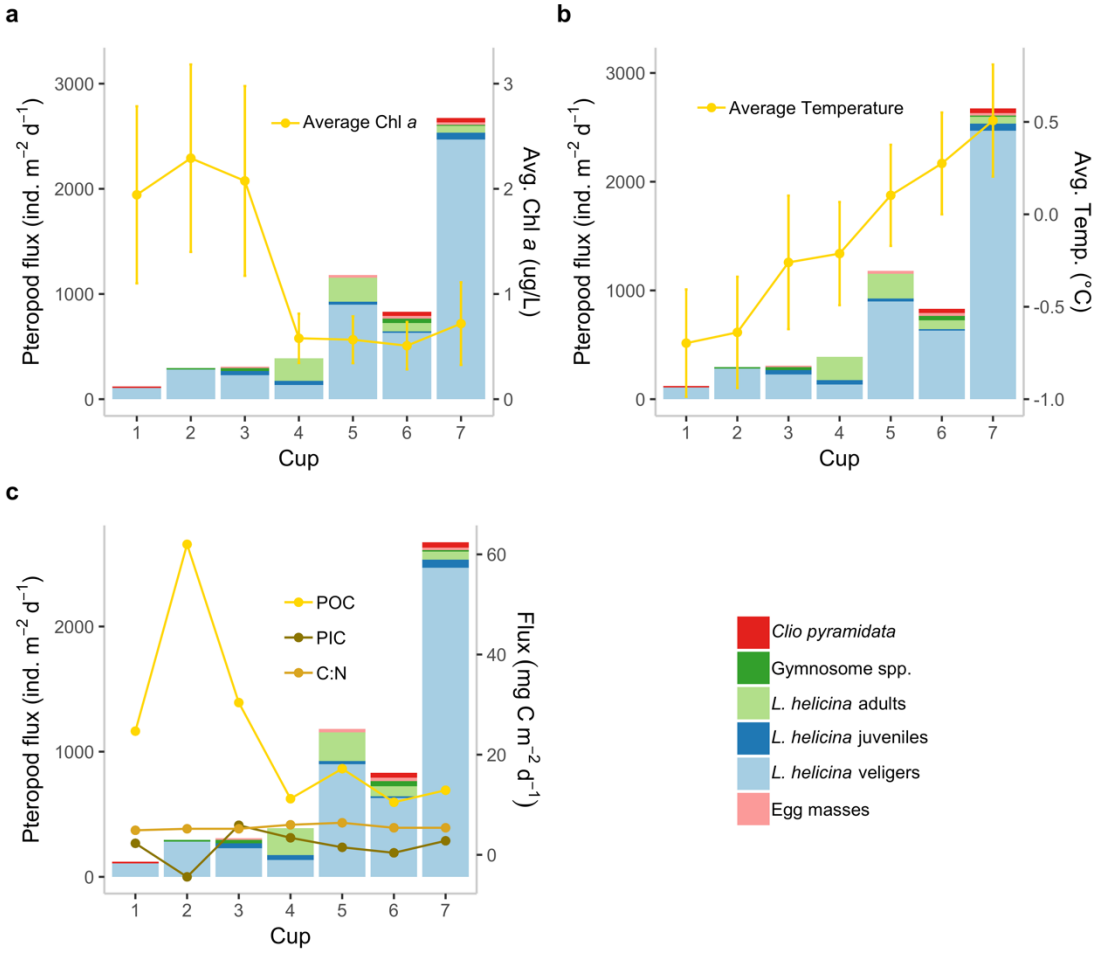

Figure 4.3 Pteropod (swimmer) flux (ind. m^{-2} d^{-1}) of all species and age classes observed at ~52 m for each sampling cup from 10 December 2016 – 7 January 2017. Environmental and physical parameters (lines) measured for each cup were: (a) average Chla, (b) temperature, and (c) sinking POC, PIC, and C:N flux. Vertical lines are error bars. Veliger size class (< 0.4 mm) made up the highest proportion (82 %) of age class for nearly all sampling periods (cups).

4.6.2 24-hour vertical distribution

L. helicina antarctica was the only pteropod species identified within the 24hr sediment traps. Adults (11.1 %), juveniles (38.9 %), veligers (44.4 %), and egg masses (5.6 %) were observed within both 57 m traps, whereas only veligers were sampled within the deeper (90 m) cups (Fig. 4.4a; Table C.3 in Appendix C). Average shell diameters of pteropods collected from 57 m were 1.62 ± 2.1 and 0.71 ± 1.4 mm from the formalin- and Lugol's-poisoned cups, respectively; while the average shell diameter of pteropods was 0.10 ± 0.02 mm for both cups sampled at 90 m (Fig. 4.4b). Similar to the earlier drifter1 experiment, there were no shell lengths observed between 0.31 and 4.35 mm.

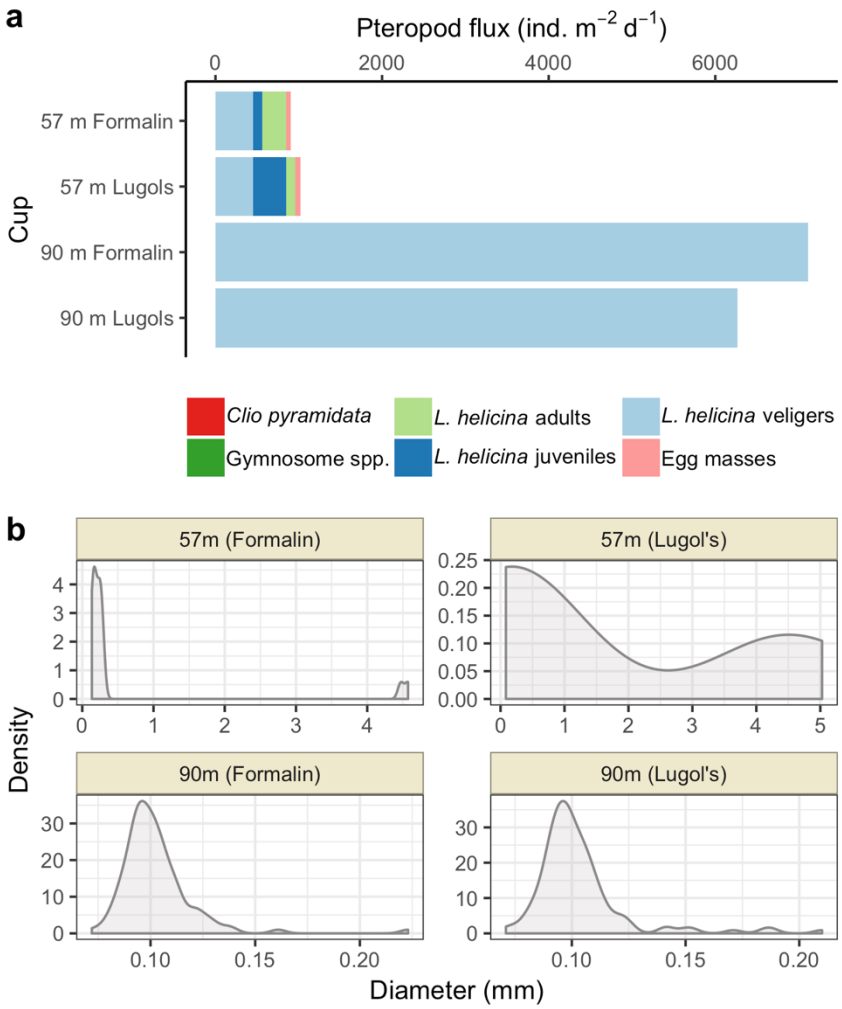

Figure 4.4 Results from 24-hr sediment trap experiment including: (a), total pteropod (species and age class) flux (ind. m^{-2} d^{-1}) observed at ~57 m and 90 m within each preservation medium; and (b), densities of thecosomatous *L. helicina* shell diameters, ranging 0.07 to 5.0 mm. The majority of *L. helicina* sampled were within veliger age class for each cup, with no adults found within deeper cups.

The *F*-test revealed a significant difference in variances ($p < 0.05$) between pteropod flux to 57 and 90 m depth. Maximum fluxes of *L. helicina antarctica* occurred at 90 m depth, where 7115 veligers m^{-2} d^{-1} and 6268 veligers m^{-2} d^{-1} were counted within the formalin-poisoned and Lugol's-poisoned cups, respectively (Table A4.3). As with the time-series (drifter1) experiment results, there were significantly more veligers tallied than any other *L. helicina antarctica* age class [$F(3,12) = 3.7$, $p = 0.043$], with 47.1 % and 100 % of the total composition represented within both 57 m and 90 m depth samples, respectively. Pteropod flux sampled at 57 m depth was 1011 and 904 ind. m^{-2} d^{-1} for Lugol's-poisoned and formalin-poisoned cups, respectively. The *F*-test determined no statistically significant differences in variances measured between sampling cup poison treatments ($p = 0.749$).

4.6.3 Cohort structure and growth rate estimations

The length-frequency analysis identified the presence of two, possibly three, cohorts, including the smallest size class, possessing shell lengths ranging 0.1 – 0.4 mm, and one, possibly two, overlapping older generation(s) of sizes ranging from 3.4 – 7.2 mm. However low sample sizes of adult shell lengths, as well as the absence of juveniles, did not permit a clear distinction between a possible 1-year and/or 2-year generation(s) (Fig. 4.5).

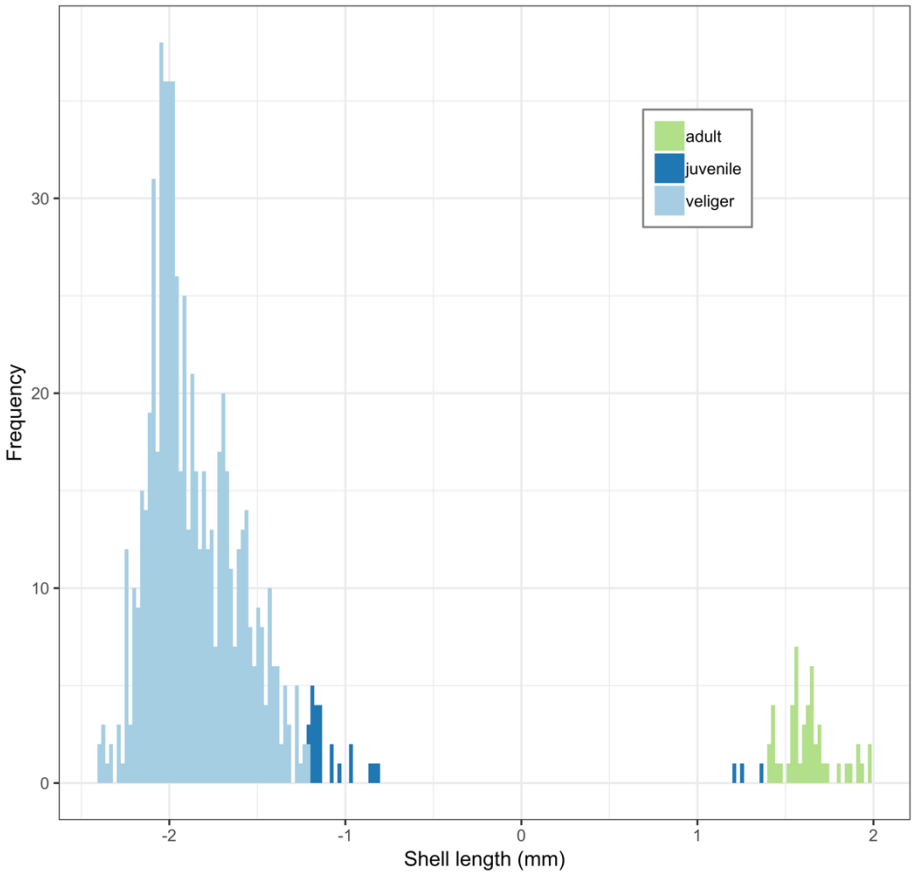

Figure 4.5 Log-transformed shell length-frequency distribution of veliger, juvenile, and adult size classes of sediment trap-sampled *Limacina helicina* (from all trap cups).

For the veliger size class, we calculated an average intra-seasonal daily growth rate of 0.0068 mm d^{-1} from average shell lengths measured between cups 1 and 4 (10 – 26 Dec). This is due to the appearance of a steady increase in average shell lengths between these trap cups, immediately followed by consecutive decreases in average shell lengths between cups 5 to 7, and likely related to new recruits from a spawning event during this time (Fig. 4.6). Subtracting the minimum veliger size class shell length from cup 1 (0.1 mm) from the maximum veliger size class shell length (0.4 mm) from the upper depth cup (24hr) resulted in a maximum intra-seasonal growth rate of 0.0078 mm d^{-1}. For the adult generation (>4 mm), average shell length in cup 4 was 4.82 ± 0.4 mm, and the average shell length in the upper traps of the 24-hour sediment experiment was 6.25 ± 0.9 mm, giving an average intra-seasonal daily growth rate of 0.057 mm d^{-1}. Minimum shell length of adults in cup 4 was 4.05 mm, and maximum shell length in upper depth 24-hour traps was 7.24 mm, giving a maximum intra-seasonal rate of 0.128 mm d-

[1]. There were insufficient samples from the juvenile generation to effectively estimate daily growth rates.

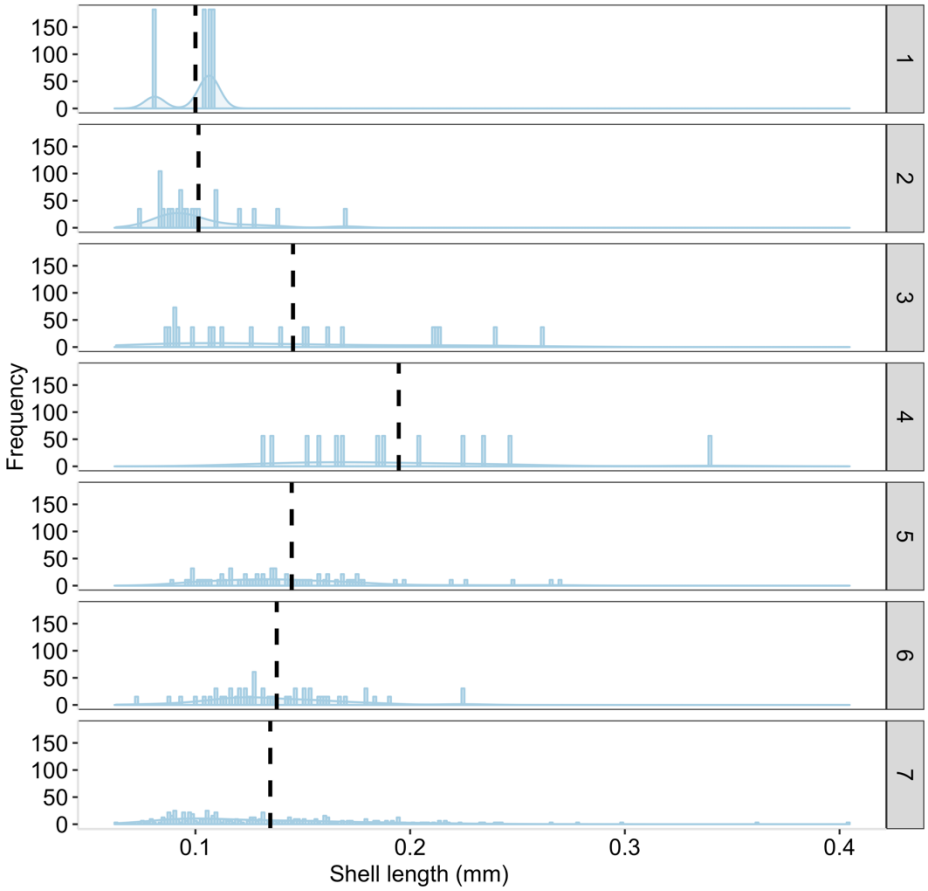

Figure 4.6 Shell length-frequency distributions of veliger and juvenile age classes of *Limacina helicina* separated by sediment trap cups 1-7. Density curves were fitted to each distribution to demonstrate small-scale temporal change in distributional patterns. Vertical dotted lines represent means.

4.6.4 Environmental drivers of pteropod swimmer flux

According to the GLM (Table C.4 in Appendix C for output), decreasing fluorescence and increasing sinking PIC and sinking POC emerged as covariates primarily associated with increasing abundance for all pteropod species and age classes combined. Analysed separately, each species and age class responded differently to the covariates tested. Also based on GLM results, decreasing fluorescence and temperature, and to a lesser extent salinity, were correlated with increasing abundances of adult *L. helicina antarctica*. Juvenile *L. helicina antarctica* were also primarily associated with decreasing fluorescence and temperature, although abundances also increased with increasing sinking PIC and sinking POC. Veliger *L. helicina antarctica* increased

with decreasing depth, sinking POC, and temperature, whereby their increasing abundances were primarily correlated with increasing abundances of other zooplankton species, primarily copepods, copepod nauplii, and appendicularians, present in the traps. A weak positive relationship was observed between increasing veligers and gymnosomes. Increasing *C. pyramidata* abundance correlated with increasing fluorescence and longitude, and with decreasing sinking POC. When modelling gymnosome abundances specifically, extra biological interaction variables were tested including all *L. helicina antarctica* age classes and *C. pyramidata* as potential food sources. While increasing abundances of gymnosomes were primarily driven by decreasing salinity, comparisons made with other species resulted in a relatively strong relationship with decreasing abundances of both adult *L. helicina antarctica* and increasing *C. pyramidata*, versus a relatively weak relationship with increasing juvenile-aged abundances. For all species and size classes, AIC values indicated that simplified models were the best fitting models, as opposed to the saturated model incorporating all variables.

4.6.5 Developmental stage compositions of egg masses

All eggs within clutches appeared to be within the earliest stage (2-cell) of ontogenetic development (Lalli and Wells, 1978; Wakabayashi, 2017). Multiple comparisons for each morphometric trait revealed no statistically significant difference ($p > 0.05$, Fig. C.1 in Appendix C), and given the low sample sizes, analyses on egg mass morphometrics can only be considered qualitative (Table C.6 in Appendix C). Among the nine egg masses sampled throughout this study, I enumerated an average fecundity rate of 735 eggs individual^{-1} ($\pm$ 193 eggs individual^{-1}). During the time-series experiment (drifter1), the first egg clutch appeared in the sampling cups during 18 – 22 December, and then again between 26 December and 8 January. Egg masses were observed within the shallower sampling cups (<57 m depth) during the 24-hour sediment trap experiment (January 17-18).

4.7 Discussion

4.7.1 Species and age composition

Adding to the small but growing number of shallow water datasets that exist for the relatively under-surveyed Indian sector, this research enhances the potential of using both Southern Ocean pteropod swimmers and sinkers for filling current knowledge gaps in our understanding of their community structure. The results of these sediment trap experiments provide both high resolution data and a promising alternative to net sampling techniques for describing population dynamics and flux patterns of a taxonomic group highly sensitive to

anthropogenic changes in ocean chemistry. A species composition similar to other, more often-surveyed regions of the Southern Ocean situated between the SACCF and the SB-ACC was observed. This regional band is primarily composed of *L. helicina antarctica* f. *antarctica* and the lesser abundant *C. pyramidata* f. *sulcata*, as well as gymnosomes *Clione limacina antarctica* and *Spongiobranchaea australis* (Hunt et al., 2008). Nearly all of the time-series sampling cups were dominated by the veliger size class, with juvenile-aged *L. helicina antarctica* starting to appear in samples from 18-22 December, and adult *L. helicina antarctica* from 22-26 December. The presence of young *C. pyramidata*, gymnosomes, and egg masses within cups was infrequent and random (combined: 4.8% total) throughout the sampling duration, as also noted by Howard et al. (2011), and thus patterns in growth rate or abundance for these taxa could not be identified.

Pteropod age composition differed between 57 and 90 m. Within the 24-hour duration, a heterogeneous age composition was obtained in the upper trap depth (57 m) that was dominated by veligers, followed by juvenile *L. helicina antarctica*, adult *L. helicina antarctica*, and egg masses. No other pteropod species were collected within the 24hr trap cups, and the deeper sampling cups were entirely composed of veligers. The adult shell diameter range sampled within the shallower cups (4.3 to 5.0 m) exceeded the maximum sizes reported for *L. helicina antarctica* f. *rangi* (~3.5 mm) and *L. retroversa australis* (~1.5 mm) (Dadon and de Cidre, 1992; van der Spoel et al., 1999) and were within the maximum size class reported for forma *antarctica* (Lalli and Gilmer, 1989). While advection may explain the high abundance of veligers in the deeper traps, sensor data revealed very little movement by the trap, including a 3.1 m vertical range (see Appendix C, Table C.6). Vertical stratification in species and age composition has been recorded for pteropods elsewhere, and considered to be driven by season and size (Kobayashi, 1974; Wormuth, 1981), however no studies have closely examined swimming in pteropod veligers. Other pelagic molluscan larvae, such as bivalves, can adjust their vertical positioning within the water column through swimming (Bayne, 1986), and many species demonstrate diel feeding behaviour (Tremblay and Sinclair, 2007). Furthermore, higher abundances of bivalve larvae have been found below the pycnocline in highly stratified waters, whereas abundances of well-fed larvae have been shown to be equal throughout well mixed and highly turbulent water columns (Raby et al., 1994).

It should also be noted that while the recovery of traps from the water column, and consequently the entering of new material into cups, may introduce some bias, there are several reasons to believe this is not an issue. Firstly, as traps are lifted out of the water, cups are filled with sea water thus preventing new material from entering. Secondly, other larger plankton taxa were present in the deeper traps, though will be reported in another study (Makabe, in prep).

And finally, zooplankton abundance estimated at the same time and station using a Vertical Multiple-opening Plankton Sampler (VMPS) revealed no presence of pteropods in the upper 100 m (Okubo, et al. in prep). Okubo et al. (in prep) also reported that *L. helicina antarctica* were less abundant at 0-50 m compared to >50 m, at surrounding station that same year.

Juvenile *L. helicina antarctica* from the Scotia Sea have been shown to occur in different regions than adults (Bednaršek et al., 2012c), and may account for the lack of *Limacina* sp. with shell diameters ranging 0.4 – 2.9 mm (drifter1) and 0.3 – 4.3 mm (24hr) from the sampling cups. Moreover, resource partitioning between *L. helicina* age classes may be occurring due to vertical stratification in species and size classes of their primary food sources (Rines et al., 2010). Food preference in Antarctic thecosome veligers is relatively unknown, however fatty acid data from Arctic *L. helicina* veligers suggests particulate organic matter (Gannefors et al., 2005), while temperate *Limacina* sp. have been cultured successfully using filtered seawater supplemented with crytophytes, haptophytes, dinoflagellates, and small diatoms (Paranjape, 1968; Thabet et al., 2015). The GLM revealed a weak relationship between increasing veliger abundances in association with decreasing suspended POC, which could point to a reliance on phytoplankton for food by veligers, with an inverse response resulting from a lag effect from post-bloom feeding (Almogi-Labin et al., 1988). Additional sampling experiments are required to determine environmental and/or ecological covariates driving short term vertical patterns in age and species stratification.

Interestingly, egg masses were only found in the shallowest trap cups, although they were mostly sampled between 100-200 m by a suite of multi-depth net-sampling techniques as reported for a different study conducted at the same time and location (see Fig. C.2 in Appendix C for unpublished results). Downward fluxing of fertilized egg masses and/or spawning adults, observed for many dominant Antarctic zooplankton (Ross et al., 1996), may have occurred at the time of the 24hr experiment, which a spawning event may signal adults to release egg masses that hatch at depth, and migrate upward as veligers. This may also account for why deeper traps captured more veligers than the shallower traps; however veligers have not yet developed parapodia (wings) and instead possess restricted movement driven by cilia (Lalli and Gilmer, 1989). It is not clear whether spawning adults release egg masses at a particular depth, but, given this behaviour, two theories may explain the pattern observed here. The first posits high predation that may have occurred on egg masses within the winter water layer (>50 m) at the time of this experiment, whereas the second points to patchiness and/or relatively low egg mass productivity unable to be captured by the traps. Given that sample sizes were low, I can only

speculate, but strongly encourage future net-sampling and trap-caught observations to report presence of pteropod egg masses.

Few studies have attempted morphometric measurements or reported egg counts on newly fertilized pteropod egg masses. Akiha et al. (2017) recorded mean length measurements of egg masses (6.0 mm) they found within net samples taken within the upper water column (0-50 m) which is within the range of lengths measured in this Chapter (4.4 – 8.3 mm), sampled from the same region of the Southern Ocean. Lengths of *L. helicina* egg masses sampled from Friday Harbor, Washington were smaller, at approximately 3-4 mm. From the nine total egg masses collected from both sediment trap experiments, the calculated average fecundity rate of 735 eggs individual^{-1} matched observations by Paranjape (1968), who measured an average fecundity rate of 565 eggs individual^{-1} for *L. helicina* collected from Friday Harbor, Washington. These results are less than the number of eggs counted by Manno et al. (2016), who sampled egg masses of captive *L. helicina antarctica* from the Scotia Sea from December 2013, but more than those observed within Arctic *L. helicina* in a study by Gannefors et al. (2005). Manno et al. (2016) has suggested that high variability in spawning demonstrates the strong influence of environmental conditions in driving pteropod fecundity. In this study, the inability to incorporate egg mass abundance into the GLM was a consequence of recording a low sample size for egg masses. Bearing adequate sample sizes, future studies designed to measure how environmental conditions affect pteropod fecundity would be fruitful.

4.7.2 Growth rate and cohort structure

Limacina spp. eggs hatch within a few days after spawning, grow to veligers within 2-6 days, and become juveniles within a month (Lalli and Wells, 1978; Paranjape, 1968; Thabet et al., 2015). The presence of egg masses, though sparse, in traps from both experiments could point to a protracted period of spawning that occurs throughout December and towards the end of January, as reported for *L. helicina* from western Canada (Wang et al., 2017), rather than one or two discrete events, as observed in studies featuring other polar *L. helicina* assemblages (Bednaršek et al., 2012c; Gannefors et al., 2005). Average shell diameter for veligers appear to be typical for the sampling region and period surveyed in this Chapter (Nishizawa et al., 2016). Between 10-26 December, the average veliger shell diameter increased, followed by a slightly steady decrease towards the end of the time-series experiment; suggesting a steady growth rate resulting from an early spring spawning event followed by a subsequent spawning event during 22-26 December that decreased the average size. This is corroborated by the presence of juvenile *L. helicina antarctica* that began to appear by 18-22 December, when egg masses also began

appearing. From these observations, I calculated average and maximum intraseasonal daily growth rates of 0.0068 and 0.0078 mm d^{-1}, respectively, closely matching the rate of 0.0073 mm d^{-1} derived from multi-year preserved net samples from the Scotia Sea (Bednaršek et al., 2012c). Similarly, Wang et al., (2017) measured a growth rate of 0.006 mm d^{-1} for their estimated spring *L. helicina* cohort (mean size 0.2 mm) observed from Queen Charlotte Sound, British Columbia.

Depending on the region, *L. helicina* undergo one to two spawning events per year within a life span of 3+ years, with the first event occurring in spring and the second in late summer (Bednaršek et al. 2012b). The late summer generation overwinters as veligers and metamorphoses to juvenile age by spring (Gannefors et al., 2005; Hunt et al., 2008; Paranjape, 1968). Given the that time-series sampling program began in late spring, veligers retrieved from the earliest sampling cups were likely members of the spring spawning generation (October – November), and the result of wider reproductive periods as observed by several cohort peaks.

The lack of trap-sampled *L. helicina antarctica* representing diameters ranging 0.43 to 3.38 mm reveals the presence of only two separate, non-overlapping cohorts in this study. Bednaršek et al. (2012b) found a pattern of three distinct, non-overlapping cohorts of *L. helicina antarctica* based on interannual net samples from spring to autumn in the Scotia Sea. While the discrete cohorts measured in this Chapter are similar to those determined for December and January within their study, the additional juvenile-aged cohort absent from the traps may be a function of sampling strategies. Since these samples only represent the upper 90 m of the water column, it is possible this year-old cohort, mainly consisting of juveniles hatched late summer-autumn, overwintered at depth, and thus were distributed deeper than the traps were placed. For net sampling, Bednaršek et al. (2012b) found that vertically hauled Bongo nets were most effective at sampling pteropods within the 0.1-4 mm size range. This, combined with their patchy distribution and stronger swimming ability, all contribute to the low abundance of this cohort in the traps. Given most estimations of *L. helicina* life cycle are based on data retrieved from net samples that span multiple years (Wang et al., 2017), a comprehensive life cycle reassessment of *L. helicina antarctica* using sediment trap swimmer specimens would benefit from continuous, interannual sampling periods over greater depth ranges. The current study provides a high-resolution snapshot of ~1.5 months of sampling at a single depth and demonstrates the potential to employ sediment traps to assess *L. helicina* life cycle.

4.7.3 Patterns in swimmer flux

Pteropod swimmer flux for all species combined increased throughout the time-series sediment trap sampling period, with the highest abundance recorded during the final period of

sampling, in early January 2017. In December 2010, Akiha et al. (2017) observed notably higher pteropod fluxes in sediment trap cups placed at 70 m, slightly north (60°S, 110°E) of the present study. They reported an average flux of early age *Limacina* sp. as 5.1 ± 1.6 x 103 ind. m^{-2} d^{-1}, with the highest flux (23.8 x 103 ind. m^{-2} d^{-1}) observed over a smaller sampling period. This value is higher than the average flux of 0.89 ± 0.89 x 103 ind. m^{-2} d^{-1} collected over the entire drifter1 sampling period, including all species and age classes. Despite both studies occurring within the same region, it is likely that the variability between sample years is a function of interannual variability of environmental parameters, such as temperature and food availability (ie. timing of phytoplankton blooms).

4.7.4 Environmental drivers of swimmer flux

The complex relationships between pteropod abundances and environmental covariates underlines the need to explore species-specific and ontogenetic responses to climate change. Since the time-series drifter buoy moved location throughout the sampling duration, it was important to also incorporate a spatial element to this analysis, and determine whether changes in latitude, longitude, and depth affected pteropod flux. The modelling approach developed here suggested changes in chlorophyll fluorescence, latitude, sinking PIC and sinking POC flux as the environmental covariates most likely driving pteropod assemblages.

Chlorophyll fluorescence is commonly used as a proxy for phytoplankton biomass, and therefore food resources for primary consumers, and the negative relationship found with adult *L. helicina antarctica* may point to a lag effect, whereby a decrease in phytoplankton concentration was likely the result of grazing by the pteropods. Fatty acid profiles from Arctic *L. helicina* reflect diet shifting behaviour in thecosomes, particularly between spring and summer/early autumn when primary producers transition from diatom-dominated to dinoflagellates within the water column (Gannefors et al., 2005). Calanoid copepod markers in fatty acid profiles of adult female *L. helicina* have also been detected (Gannefors et al., 2005), pointing to an adaptation to fluctuating food availability. *Limacina helicina* responds strongly to changes in primary productivity (Maas et al., 2011; Seibel et al., 2012). Phytoplankton blooms fuel increases in thecosome abundances, which likely also includes increased egg mass production and growth in shell diameters. Furthermore, a study using stable isotopes analysis to elucidate a winter-spring transitional East Antarctic food web composed of a zooplankton community beneath the pack ice has revealed a diet preference for sea ice biota over water column-sampled POM by *L. helicina antarctica* (Jia et al., 2016). In addition to fluorescence, abundances in adult *L. helicina antarctica* were correlated with temperature and salinity, which have shown to also affect physiological

responses of Antarctic bottom-ice algae (Arrigo and Thomas, 2004; Ryan et al., 2011). Enhanced seasonal ice melt may expose sea ice algae to abnormally low salinities, followed by considerably higher than normal irradiances, and consequently lead to restricted photosynthetic activity by ice algal communities. This implies that environmental stresses may alter the availability of preferred food sources to primary consumers, thus altering the integrity of coastal Antarctic food webs.

Spatio-temporal heterogeneity in surface waters is related to dynamic phytoplankton productivity in that blooms are immediately followed by temporary decreases in both pCO_2 concentrations and population growth of thecosomes (Seibel and Dierssen, 2003). As such, it may appear that enhanced reproductive and growth activity in *L. helicina* occurs in concert with low pCO_2 conditions, though indirectly related. This could also mean that as the season progresses, chlorophyll-*a* concentration may not be the only resource-related parameter driving pteropod assemblages (Gannefors et al., 2005). Abundances of early age *L. helicina antarctica* and *C. pyramidata* were also closely associated with PIC and POC flux. In this study, POC flux was closely linked to chlorophyll-*a* concentrations and associated with early-aged thecosomes, which likely reveals the importance of spring phytoplankton blooms to fuel the growth of recently hatched pteropods. PIC flux, which in this study was primarily composed of planktonic foraminiferans, was correlated with juvenile *L. helicina antarctica*, and likely demonstrates close coupling of abundances and distributions of both calcifier taxa by the same parameters: temperature, salinity, and chlorophyll-*a* concentration (Bergami et al., 2009). For comparison, further investigating parameters that drive foraminiferan and other marine calcifiers may provide valuable insight into their relationships.

Thecosome abundances may also be driven by other ecological factors, such as reproductive activity, mortality, and/or predation pressure. Gymnosome abundances had a strong positive relationship with increasing numbers of adult *L. helicina antarctica*, which are considered exclusive prey for the Antarctic gymnosome *C. limacina antarctica* (Hopkins, 1987) This result was similar to those of Thibodeau et al., (2019) who measured long-term environmental and ecological covariates from the Western Antarctic Peninsula. Monophagous feeding behaviour by gymnosomes has been observed as early as the polytrochous larval stage, and has been described as an example of close-coupling of life histories in both predator and prey, along with other adaptations that indicate co-evolution of both species (Kattner et al., 1998; Lalli and Gilmer, 1989).

4.8 Conclusions

This chapter presents a time-integrated examination of shallow water age and species compositions of Southern Ocean pteropod assemblages from late spring to summer, as well as estimates of the timing of multiple spawning events by *L. helicina antarctica* that occurred within the one and a half months of sampling duration. It also provides insight into the degree of weekly and daily flux, displaying significant variation in both depth and age class, and how these were influenced by a suite of species- and age-associated environmental covariates. This research reveals that while fluorescence, salinity and temperature were important predictors of adult *L. helicina antarctica* abundances, earlier age classes may be driven by predation pressure based on the presence of gymnosomes and, to a lesser degree, the presence of other zooplankton assemblages. I also report morphometric data on pteropod egg masses and encourage future pteropod-related sampling studies to include similar data to monitor changes in ontogenetic development that may reveal responses to changing climate. Finally, this research supports the utility of sediment trap swimmer samples to gather a suite of data beneficial to ground-truthing responses to future anthropogenic climate change by a taxonomic group highly sensitive to changes in ocean chemistry.

Chapter 5

Estimating fecundity, egg morphometrics and embryogenesis in *Limacina helicina antarctica*[4]

5.1 Graphical Highlights

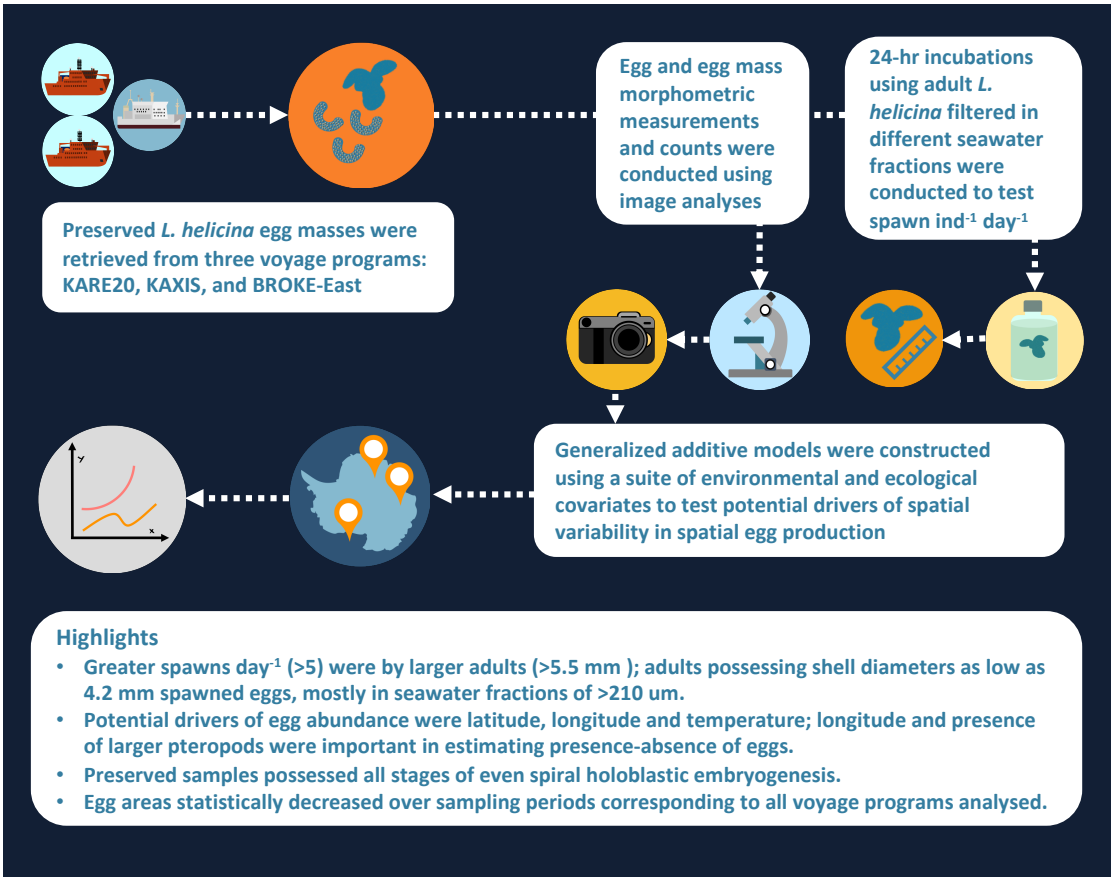

Figure 5.1 Graphical abstract for Chapter 5.

5.2 Key words

Embryogenesis, GAMs, image analysis, morphometrics, reproductive success

[4] I. Seiffert, R. Trebilco, and K.M. Swadling are coauthors on this chapter, which is currently in preparation for journal submission.

5.3 Abstract

Shelled pteropods are ecologically and functionally important to Southern Ocean ecosystems, but there is little understanding of key aspects of their biology, notable fecundity. Using preserved samples retrieved from three different research voyages, as well as data collected from 24-hr live incubations, I aimed to understand: (1) drivers of spatial distribution and abundance of egg masses, (2) the effect of adult shell diameter and prey availability on spawning, (3) quantitative morphometric traits of embryogenesis, and (4) variability in morphometric traits over time. Using generalized additive models, I explored the association of *Limacina helicina antarctica* egg production with potential drivers, including latitude, longitude, temperature, and density of juvenile- to adult-aged *L. helicina antarctica*. At-sea incubation experiments where ambient sea-water was filtered into size-fractions showed highest numbers of egg masses (>5 24-hrs^{-1}) released by adults with shell diameters >5.5 mm and incubated within a seawater size fraction of >210 μm. Adults possessing shell diameters as narrow as 4.2 mm released egg masses. Preserved samples appeared to possess all stages of holoblastic embryogenesis, typical in developmental patterns of molluscan species. Among embryogenetic traits measured, egg area (mm^2) statistically significantly decreased over the time spanning early January to mid-February, as estimated from sampling dates representing all voyage programs. Understanding potential spatial, environmental and ecological drivers of spawning can improve estimates of fecundity, which will be important for anticipating likely responses of *Limacina* populations to future change. This in turn will underpin the potential utility of *Limacina* as a sentinel species for Southern Ocean ecosystems.

5.4 Introduction

The Southern Ocean is experiencing rapid change, and work is needed to identify drivers of the reproductive success in key taxa considered as both functionally important and highly sensitive to change (Boyd et al., 2018). Thecosome (shelled) pteropods, such as *Limacina helicina antarctica,* contribute numerous ecological functional roles to Southern Ocean ecosystems. They are major contributors to the organic and inorganic carbon flux, provide a direct trophic link between primary producers and higher level organisms, and are considered early responders to climate change (Manno et al., 2017). Despite often representing a dominant component of the macrozooplankton, many aspects of pteropod early life history strategies have yet to be formally described (Manno et al., 2017). Research on the effects of ocean acidification on early development of Southern Ocean pteropods is beginning to gain traction (Gardner et al., 2018; Manno et al., 2016), however benchmark information on pteropod fecundity are only available

from only a few studies, none of which focus on Southern Ocean species (Gannefors et al., 2005; Lalli and Wells, 1978; Paranjape, 1968).

Most pteropod species are protandrous hermaphrodites (Lalli and Gilmer, 1989). They initially function as males before reaching a threshold size (~5 mm for *Limacina* spp.) that signals resorption of male reproductive organs and replacement by female organs (Lalli and Gilmer, 1989; Lalli and Wells, 1978). Females broadcast spawn buoyant strings of fertilized, phospholipid-rich eggs protected within a gelatinous matrix egg mass (Gannefors et al., 2005). The earliest stages of development, from egg to veliger larvae, take place entirely within these egg masses over approximately seven days (Lalli and Wells, 1978). Shape dimensions, or morphometrics, of eggs and egg masses are relatively unknown, however Lalli and Wells, (1978) reported significant interspecific differences in several morphometric traits between *L. helicina* and *L. retroversa*. It is not known whether these morphometrics differ, if at all, over variable space and time scales within a species, and how this relates to offspring provisioning by ovigerous adult females.

In this Chapter, I present qualitative and quantitative traits of early life history strategies of adult and early-aged *L. helicina antarctica* forma *antarctica* (hereafter referred to as *L. helicina antarctica*) from samples collected during three East Antarctic research voyages. I conducted live incubation experiments, developed and employed image analytical techniques, and constructed generalized additive models (GAMs) with the aims of: (1) estimating the effect of prey size availability and shell diameter on egg production in adults, (2) describing the stages of, and morphometric relationships among traits associated with, egg development, (3) modelling trends in egg production as functions of spatial, environmental and ecological variability, and (4) measuring egg trait variability over time to understand seasonal reproductive investment. Additionally, I tested the accuracy of a technique developed to automate egg counting using image analysis software.

5.5 Methods

5.5.1 Study sites

Pteropod egg masses were separated from preserved mesozooplankton samples collected during three summer voyages within the Indian sector of the Southern Ocean. These voyages were the Baseline Research on Oceanography, Krill and the Environment - East (BROKE-EAST) in 1995/96, the Kerguelen Axis (KAXIS) in 2015/16, and the 20th Kaiyodai Antarctic Research Expedition (KARE20) in 2016/17. Zooplankton samples from BROKE-East and K-Axis were obtained aboard the RV *Aurora Australis* from a Rectangular Midwater Trawl (RMT

1+8) net with a mouth area of 8 m^2 and a mesh size of 4.5 mm that tapered to a mesh size of 1.5 mm in the last 1.8 m of net (see Hosie et al., 2000 for more details). Only specimens collected with the RMT1 net, with a mesh size of 315 μm, and a mouth area of 1 m^2, were measured for this study. Samples from KARE20 were obtained aboard the TRV *Umitaka-maru* using an Ocean Research Institute (ORI) net with a mouth diameter of 160 cm and a mesh size of 500 μm (see Sakurai et al., 2018 for more details). Both zooplankton collection methods sampled from a maximum depth of 200 m. All samples were preserved in 5% formalin.

5.5.2 Live incubations

During KARE20, two 24-hr incubation experiments (13 and 17 December, 2017) were conducted to estimate fecundity rate in adult *L. helicina antarctica*. Live, actively swimming adult (shell length >4 cm) pteropods were selected from mesozooplankton samples collected using a ring net (200 μm mesh, 80 cm mouth area) within the upper 200 m, then examined under a light microscope to ensure shells and body showed no signs of damage. To test the effects of different available prey sizes on fecundity, seawater was filtered at different size fractions, < 20 μm, 20-210 μm, and > 210 μm, from the ship's underway supply, then added to 1-L Nalgene bottles before live *L. helicina antarctica* adults were placed in them for 24-hrs (one adult per bottle) to avoid changes to prey quality by bacteria, and to ensure maintenance of ambient conditions (within incubation unit) suitable to pteropods are met while ship is in constant motion. Bottles were placed in a purpose-built, on deck incubation unit, within which surface seawater continuously flows allowing experimental bottles to maintain ambient water temperatures. The unit was artificially shaded to prevent blooming of algal species within experimental bottles. After incubation, the bottles were checked for actively swimming pteropods and egg masses were counted. Adult pteropods and egg masses were removed and preserved in 5% buffered formalin for follow-up analyses in the laboratory.

5.5.3 Image analyses

For image analysis, egg masses were first separated, enumerated, and photographed using a Canon EOS Mark II 5D camera mounted on a Leica M165 C stereoscopic microscope and using EOS Utility software (Canon USA). Images were further analysed using ImageJ software (Schindelin et al., 2012) for the following morphometric traits: egg mass length and area, clutch area and proportion within egg mass area, egg area and diameter, and egg count per mass area. Eggs were counted using a method I developed employing ImageJ software to automate the process (see Supplementary Methods D.1 in Appendix D). A threshold cell size of 10 μm was

set due to both the large concentration of non-egg debris (eg. phytoplankton cells) and egg overlapping within the egg masses. Manual enumeration of eggs using a subsample (n = 32; Table 5.1) of egg masses was performed from images to compare counts from the automated technique using ImageJ software. Identification of embryonic developmental stages for each egg mass was conducted..

5.5.4 Statistical analyses

All statistical analyses were performed using RStudio, version 1.1.442 (Team, 2014). Two-sample *t*-tests were used to statistically compare manual with automated ImageJ estimations of egg per mass area (mm^2), and to detect differences in egg and egg mass morphometric trait means between voyages. Exponential curves were fit to data representing each size fraction (from incubation experiments) as log – log using lm function in base R. A multivariate analysis of variance (MANOVA) was used to test if the entire suite of morphological estimations based on eggs and egg masses varied among independent variables, year and sites, fitted with the MANOVA function in R. For each voyage, several linear regression models were used to assess relationships between mass area (mm^2) and egg count, as well as with sampling date and egg area (μm^2) and clutch-to-mass area ratio.

5.5.5 Generalized additive model

Based on the occurrence of non-linear relationships between dependent and independent variables during preliminary inspection, generalized additive models (GAMs; Hastie and Tibshirani, 1986) were used to investigate the influence of latitude, longitude, mean temperature at surface maximum layer (SML), and density of combined pteropod species on the abundance of eggs sampled, expressed here as the number of eggs · mass mm^{-2}, and presence/absence of egg masses; the latter was recommended given the large number of absences (zero observations) in the data (Borchers et al., 2011). Explanatory covariates included mean temperature at 200 m depth and at the lower layer of the surface mixed layer (SML), mean salinity at the lower layer of SML, integrated chlorophyll *a*, latitude, longitude, depth, and abundance of juvenile- to adult-aged *L. helicina antarctica* sampled. A priori hypotheses related to drivers of spatial patterns in egg mass production by other marine organisms (Borchers et al., 2011), as well as density of adult Southern Ocean *L. helicina antarctica* (Thibodeau et al., 2019), informed covariate selection. Selected covariates each met assumptions of multiple linear regression, including normal distribution, homogeneity of variance, and no multicollinearity. Negative binomial and binomial distributions were used for abundances and presence-absences, respectively, and lowest Akaike's

Information Criterion (AIC) scores were selected as the best model. GAMs were fitted using the 'mgcv' library (version 1.8-26; Wood, 2006) in R.

Table 5.1 Data sources for this study.

Analysis	Voyage	Sampling net	*n*
Abundance and distribution	BROKE-EAST, KAXIS, KARE20	RMT 1, ORI	435
Generalized additive modelling	KAXIS	RMT 1	37
Incubation experiment	KARE20	Ring	16
Method validation	KAXIS, KARE20	RMT1, ORI	32
Morphometrics:			
• Egg mass length (mm)	BROKE-EAST, KAXIS, KARE20	RMT1, ORI	412
• Egg mass area (mm^2)	BROKE-EAST, KAXIS, KARE20	RMT1, ORI	411
• Clutch area (mm^2)	BROKE-EAST, KAXIS, KARE20	RMT1, ORI	410
• Clutch : mass areas	BROKE-EAST, KAXIS, KARE20	RMT1, ORI	412
• Egg count	BROKE-EAST, KAXIS, KARE20	RMT1, ORI	411
• Eggs egg $mass^{-1}$(mm^2)	BROKE-EAST, KAXIS, KARE20	RMT1, ORI	398
• Egg area (mm^2)	BROKE-EAST, KAXIS, KARE20	RMT1, ORI	226
• Egg diameter (μm)	KARE20	ORI	24
• Embryogenetic stage identification	BROKE-EAST, KAXIS, KARE20	RMT1, ORI	435

5.6 Results

5.6.1 Distribution and abundance

A total of 435 egg masses and mass fragments was enumerated from preserved samples at 19 stations from the three sampling programs within a combined region extending between 79° and 110°E, and 60° and 67°S (Fig. 5.2, Table D.1 in Appendix D). Non-zero densities ranged from 41.8 to 3783.5 eggs mass area^{-1}mm^{2}, with the highest proportion of egg masses retrieved between 60° S and 66° S, and between 60° E and 110° E (Fig. 5.2).

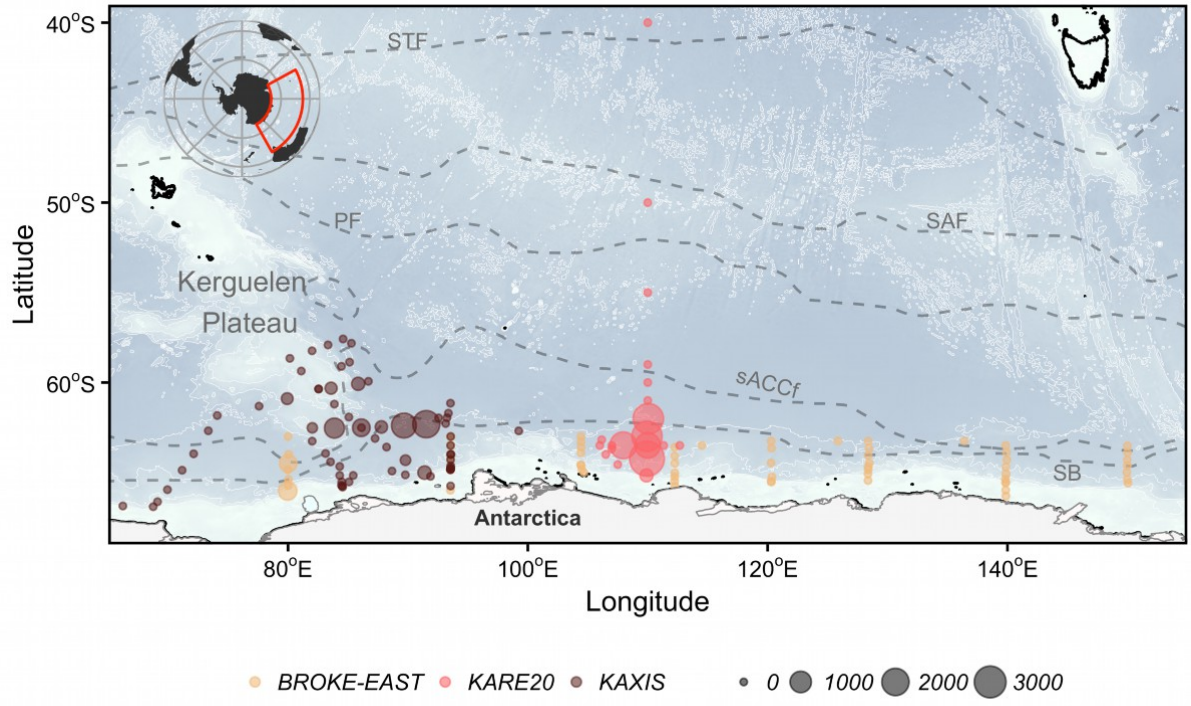

Figure 5.2 Locations and relative abundances (size of points) of *L. helicina antarctica* eggs × mass mm^{-2} sampled for each voyage. Colours represent each voyage. Dashed lines show approximate locations of major fronts (Orsi et al., 1995), including the Subtropical Front (STF), Subantarctic Front (SAF), Polar Front (PF), Southern Antarctic Circumpolar Front (SACCF), and the Southern Boundary (SB). The inset map shows the study region within a global scale.

5.6.2 GAM analysis

The final models for egg abundance and egg mass presence encompassed three and two, respectively, of the nine covariates tested. Latitude was included in both models. The preferred model for egg mass abundance was given by:

(1) Egg abundance ~ latitude$_s$ + longitude$_s$ + mean temperature (at lower SML)$_s$

and for presence/absence of eggs, by:

(2) Egg presence ~ latitude$_s$ + pteropod abundance$_s$

where subscript *s* represents spline smooths. Of the series of one-, two-, three- and four-term models tested for each model, the simplest model was preferred as determined by the lowest AIC (Table 5.2).

Table 5.2 Parameters and fit of the final generalized additive models for both (1) egg mass abundance and (2) presence-absence of egg masses. All covariates were significant in the model (p<0.05).

(1) Model for egg mass abundance				
	df	*k*	*Chi*^{2}	*p*-value
Latitude	4.159	9	24.158	<0.001
Longitude	4.941	9	31.203	<0.001
Mean Temperature (lower SML)	41.000	9	7.095	<0.05
Fit: Negative binomial	Adjusted R^2	Deviance explained	*n*	
	0.897	98%	37	
(2) Model for egg mass presence-absence				
	df	*k*	*Chi*^{2}	*p*-value
Longitude	5.817	9	5.899	0.472
Pteropod abundance	1.00	9	4.567	<0.05
Fit: Binomial	Adjusted R^2	Deviance explained	*n*	
	0.651	68.3%	37	

The modelled egg abundances reveal a nonlinear dependence on the explanatory variables (Figs. 5.3 and 5.4). In terms of model performance, both procedures resulted in high adjusted R^2 and deviance explained values, indicating that both were reliable at capturing variation (Table 5.2).

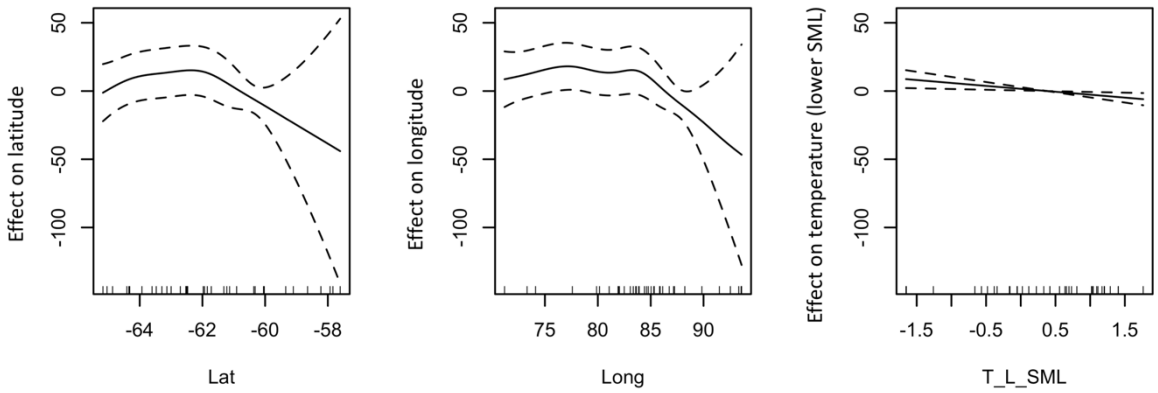

Figure 5.3 Shapes of the smooths for the covariates tested in the *L. helicina antarctica* egg mass abundance GAM possessing the lowest AIC value. Covariates include latitude, longitude, and mean temperature at the lower layer of the SML. Zero on y-axis refers to no effect of the explanatory covariate. Dashed lines correspond to 95 % confidence limits for the smooth. X-axis tick marks refer to relative density of observations.

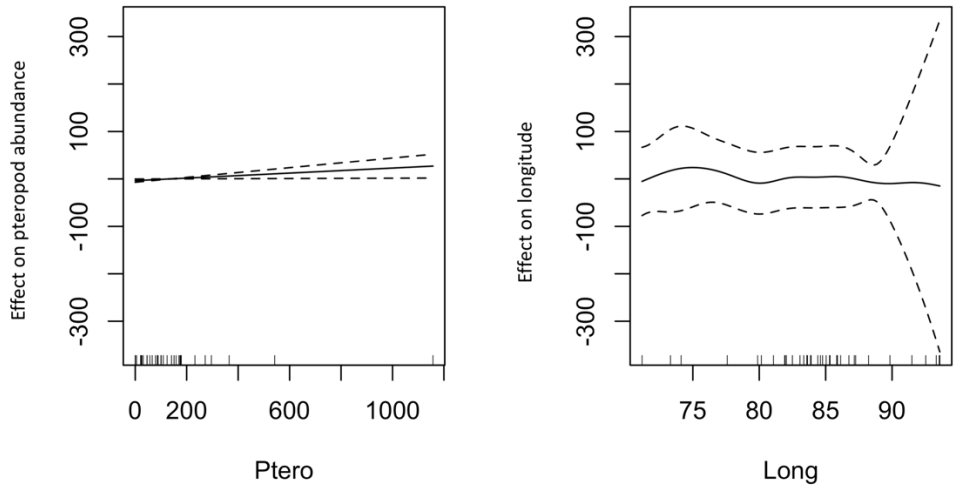

Figure 5.4 Shapes of the smooths for the covariates tested in the presence of *L. helicina antarctica* egg masses GAM possessing the lowest AIC value. Covariates include adult pteropod abundance and longitude. Zero on y-axis refers to no effect of the explanatory covariate. Dashed lines correspond to 95 % confidence limits for the smooth. X-axis tick marks refer to relative density of observations.

5.6.3 Live incubations

Significant variability was observed in the number of egg masses released by adults possessing different shell lengths (range = 4.2-7.0 mm; $F_{(1,14)} = 6.751$, $p < 0.05$; Fig. 5.5), with the majority of egg masses (5-15 masses 24-hr^{-1}) spawned by pteropods with shell lengths >6 mm (Table D.2 in Appendix D). All adults incubated in >210 µm and 20-210 µm seawater fractions released egg masses, whereas only two pteropods released egg masses when incubated in the <20 µm fraction. Of the exponential curves fit to data representing each size fraction, only the curve for > 210 µm was statistically significant (Fig. 5.5). The variation of egg masses spawned between size fractions was not statistically significant ($F_{(2,13)} = 1.839$, $p = 0.198$; Fig. 5.5).

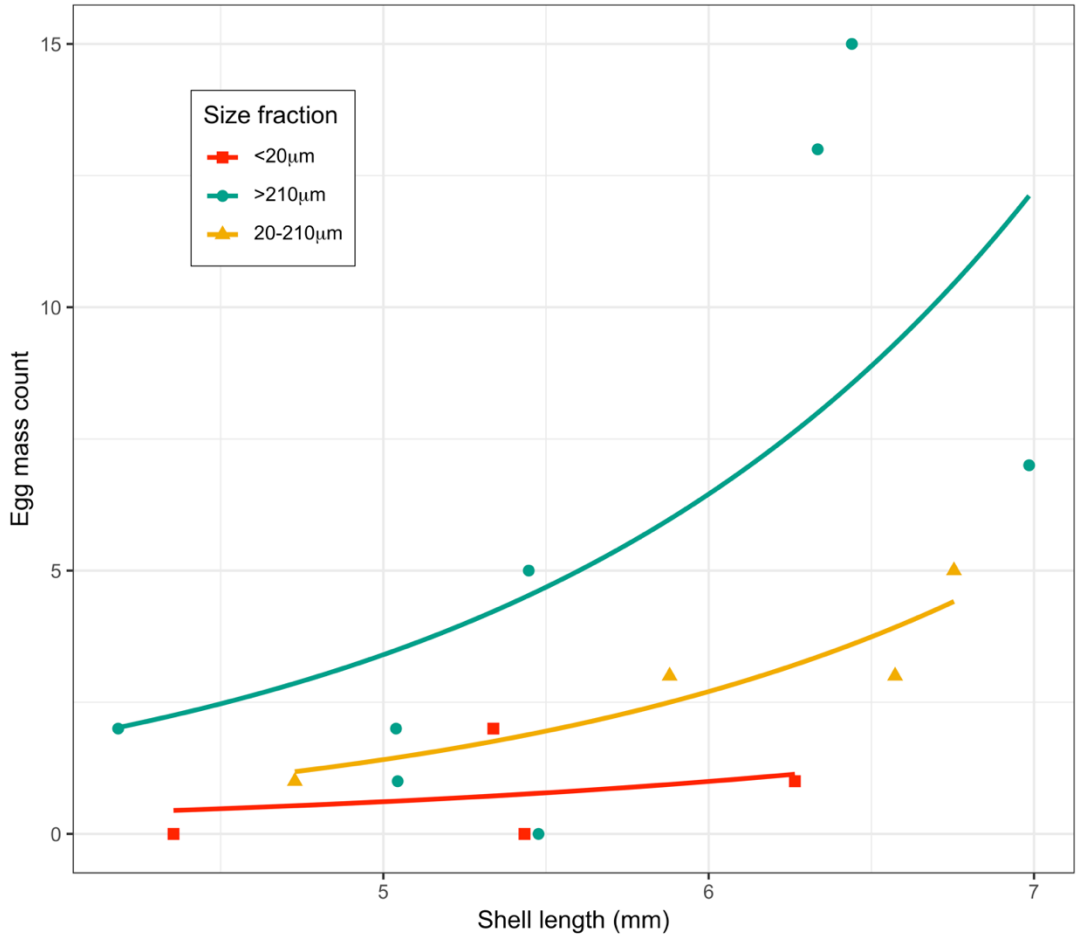

Figure 5.5 Relationships between egg mass counts and adult *L. helicina antarctica* shell length (mm) for each seawater size fraction (µm). Exponential curves were fit with data for each size fraction, including '< 20 µm': $y = e^{-2.93x + 0.49}$, $R^2 = 0.10$, $p = 0.60$; '> 210 µm': $y = e^{0.64x+1.97}$, $R^2 = 0.39$, $p < 0.05$; and '20-210 µm': $y = e^{-2.91x+0.65}$, $R^2 = 0.81$, $p = 0.10$.

5.6.4 Accuracy of egg count automation

The comparison of egg counting techniques showed a statistically significant correlation between manual and automated egg counts ($R^2 = 0.92$, $p < 0.05$; Fig. 5.6). When egg counts were divided by the egg mass areas (mm^2), these values were compared between the manual and automated methods and there was no significant difference ($t(29.6) = 1.98$, $p = 0.06$; Fig. 5.6).

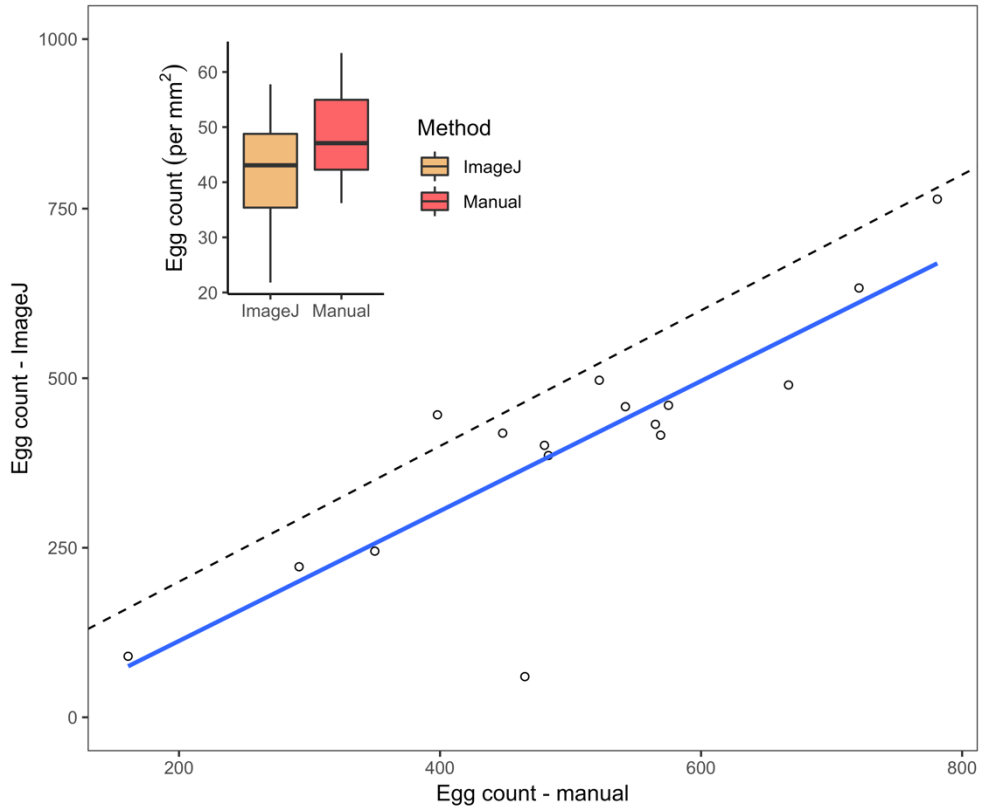

Figure 5.6 Estimated counts of eggs within *L. helicina antarctica* egg masses. Linear regression from the correlation calculated between manual and automated counts obtained through ImageJ is y = 0.9787x – 55.9883, where y is the predicted number of eggs estimated through automation, and x is manual count variable; $R^2 = 0.9217$, $p < 0.05$. Dashed line is 1:1 reference. Inset plot: Results of *L. helicina antarctica* egg counts mm^{-2} conducted by automation and manually. Median values of egg counts per area are depicted by horizontal lines within the 50% interquartiles (boxes). Upper and lower vertical lines, or "whiskers" refer to maximum and minimum dependent values, respectively. No significant difference was observed between methods, $p > 0.05$.

A linear regression for each voyage was conducted on egg mass lengths (mm) versus automated egg counts to determine whether mass areas could be used to predict number of eggs (Fig. 5.7). There were moderately strong, statistically significant levels of predictability for each voyage (BROKE-EAST: $R^2 = 0.80$; $p < 0.05$; KARE20: $R^2 = 0.58$; $p < 0.05$; KAXIS: $R^2 = 0.61$; $p < 0.05$). The linear regression performed on egg mass areas (mm^2) versus automated egg counts

produced a similarly moderately strong, statistically significant relationship ($R^2 = 0.61$, $p < 0.05$). The equation from this relationship was used to calculate mean egg counts mass area^{-1} for further analyses.

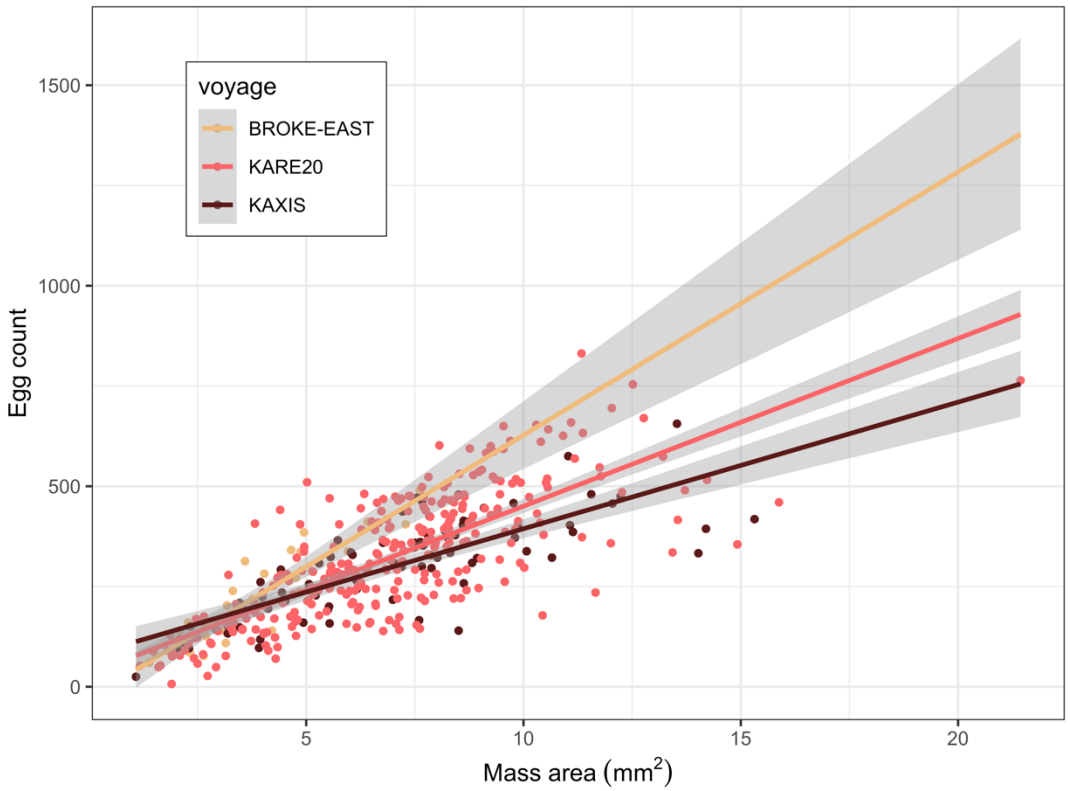

Figure 5.7 Linear relationships examined between mass areas (x axis, mm^2) and egg counts (y axis) for each voyage. Linear regression for BROKE-EAST: y = 65.61x - 28.57; R^2 = 0.80, $p < 0.05$; for KARE20: y = 41.8x + 32.4; R^2 = 0.58, $p < 0.05$; for KAXIS: y = 31.57x + 78.35; R^2 = 0.61, $p < 0.05$. Shaded region is the 95% confidence interval on the fitted values.

5.6.5 Morphometrics

Each egg mass was crescent-shaped with rounded edges, consisting of a transparent, gelatinous matrix encasing a ribbon of spherically-shaped eggs (Fig. 5.8). Eggs were yellow in colour, and embedded within oval egg membranes, or chorions. Many egg masses appeared to have non-egg mass related organic material, including colonies of phytoplankton species (eg. *Chaetoceros cryophilus*), adhered to surfaces of their gelatinous matrices. Some eggs within egg masses appeared misshapen, fused together or deformed, and consequently omitted from morphometric trait measurements (Fig. D.1 in Appendix D).

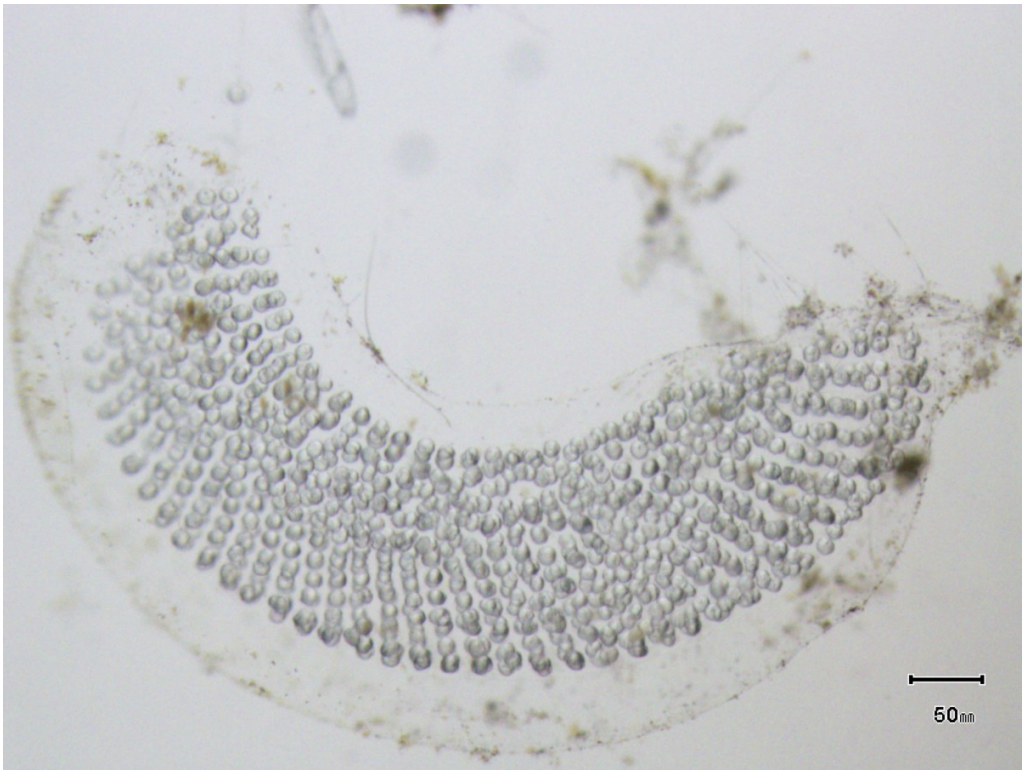

Figure 5.8 Newly hatched egg mass consisting of hundreds of oval-shaped eggs arranged in a ribbon and embedded within an outer gelatinous matrix.

Of the 435 egg masses sampled, 122 masses were fragments and thus not used in egg mass length (mm) and area (mm^2) calculations (Table 5.3). Whole egg masses averaged 6.2 ± 1.5 mm in length (Table 5.3; ranging 2.2—12.2 mm) and 7.7 ± 2.6 mm^2 in area (Table 5.3; ranging 1.1—12.4 mm^2). While samples from KARE20 produced the highest number of eggs per single egg mass (831 eggs $mass^{-1}$), BROKE-EAST samples possessed the highest mean number of eggs $mass\ area^{-1}$ (57 mm^2 ± 15 mm^2; Table 5.3) (see Table D.3 in Appendix D for statistical results for comparisons of morphometric characters between voyages).

Table 5.3 Mean (± SD) morphological variables measured for preserved egg masses and eggs sampled from each research voyage. Egg mass count (n) refers to both whole and fragmented egg masses; however mean mass length and area values did not incorporate fragmented egg masses in calculations. Clutch area refers to the region within the gelatinous matrix encompassing the string of eggs.

Voyage	Egg mass count (*n*)	Egg mass length (mm)*	Egg mass area (mm^2)*	Clutch area (mm^2)	Clutch:Mass Area (%)	Eggs/mass area (Eggs · mass mm^{-2})	Egg area (μm^2)
BROKE-EAST	31	5.1 ± 0.9	5.6 ± 1.1	2.9 ± 1.2	71.4 ± 10	57 ± 15	59 ± 2.9
KAXIS	90	5.6 ± 1.7	7.2 ± 3.0	4.3 ± 1.7	61.7 ± 10	44 ± 11	59 ± 3.8
KARE20	314	6.4 ± 1.4	8.0 ± 2.4	4.8 ± 1.7	68.9 ± 10	47 ± 15	73 ± 8.0
All samples	435	6.2 ± 1.5	7.7 ± 2.6	4.6 ± 2.0	67.7 ± 10	47 ± 15	72 ± 8.5

* Estimates did not include egg mass fragments

5.6.6 Embryogenesis and temporal variation in morphometric traits

Nine stages of embryonic development within all preserved egg masses were recognized (Fig 5.9). Mean egg area estimated from all samples, regardless of embryogenetic stage, was 72 ± 8.5 μm^2 (mean diameter, 96 ± 4 μm), including the surrounding egg membrane (Table 5.3). The shape remained ovoid, and polar bodies were observed attached to the surface of embryos at the animal pole, throughout egg development. Four stages of major embryonic cleavage appeared as spiral holoblastic in pattern (Fig. 5.9A-D), with micromeres appearing to have formed, doubled and rotated perpendicular and symmetrical relative to the animal-vegetal axis with each successive subdivision before developing into a compact 16-cell mass, or morula (Fig. 5.9E-F). Preserved samples also possessed embryos in the post-cleavage stages of embryogenesis, early to late gastrulation (Fig. 5.9G-I), whereby embryos become multilayered masses, blastula walls transform through invagination, and indentations known as blastopores (Fig. 5.9G), deepen and develop into archenterons (Fig. 5.9H) that eventually form the gut.

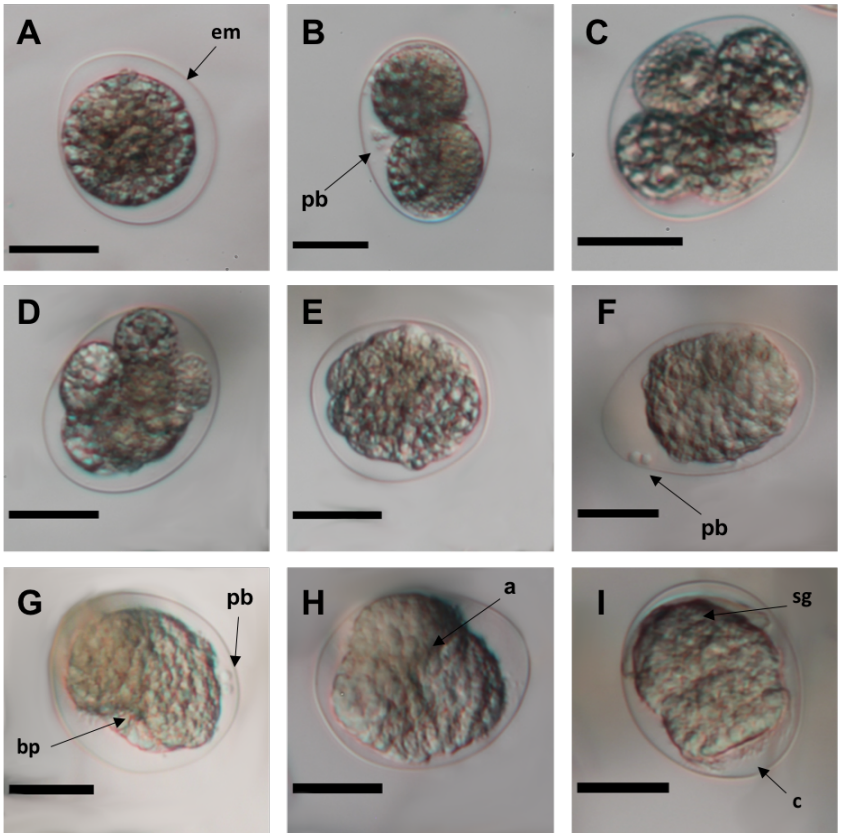

Figure 5.9 Egg areas (in um) measured against embryonic (pre-larval) developmental stage of *L. helicina antarctica*. (A) fertilized egg, (B) 2-cell stage, (C) 4-cell stage, (D) 8-cell stage, (E) early morula, (F) morula, (G) early gastrula, (H) gastrula, (I) late gastrula. a: archenteron, bp: blastopore, c: cilia, em: egg membrane, pb: polar body, sg: shell gland. Scale bar is 50 μm.

Many morphometric measurements (egg mass length (mm), egg mass area (mm^2), and eggs per egg mass area (eggs · mm^{-2})) were estimated for each embryogenetic stage (Fig. 5.10). Morphometric measurements remained consistent across each embryogenetic stage, (Fig. 5.10C).

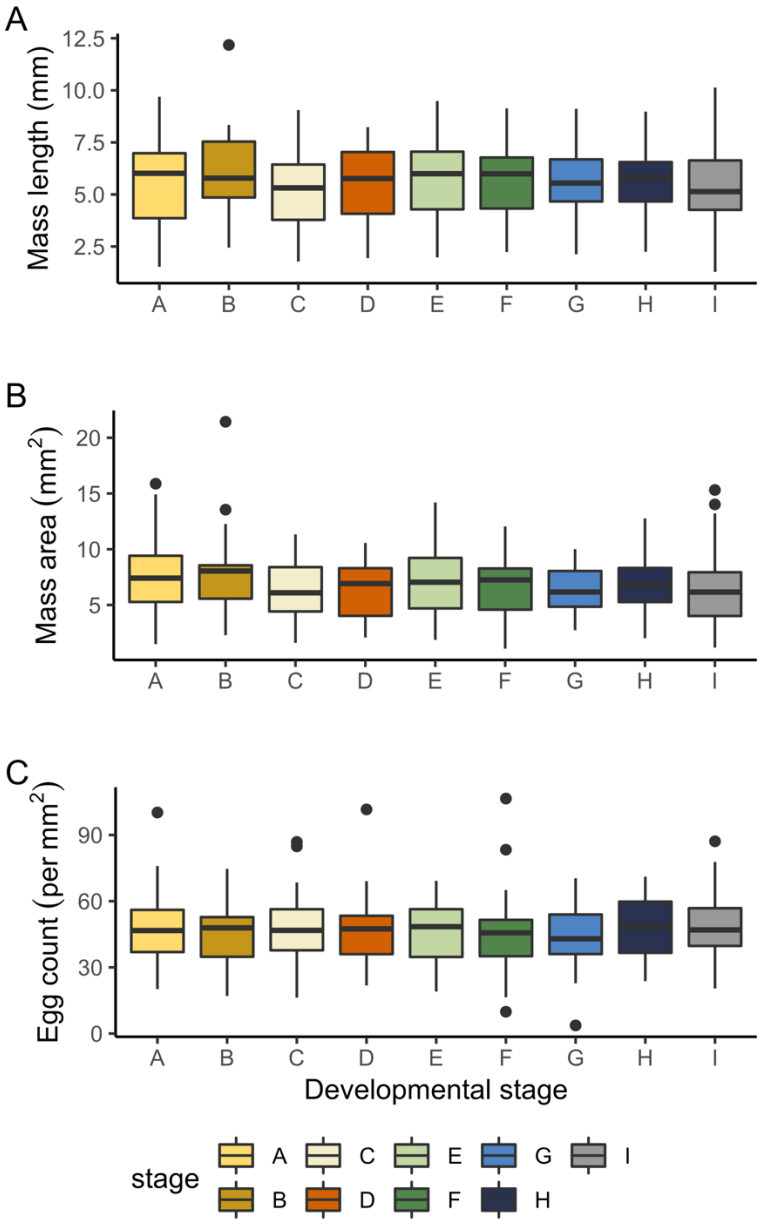

Figure 5.10 Egg mass morphometrics versus developmental stage. Horizontal lines within the boxes refer to median values, upper and lower vertical whiskers from the box depict minimum and maximum dependent values.

The highest frequency of egg masses were observed primarily from the KARE20 voyage, (Fig. 5.11). The maximum number of egg masses, 87, was sampled at site C07 on 10 January, 2017, with a composition that includes every embryonic stage, including 23% consisting of 4-cell (Fig. 5.11C) and 21% of early gastrula (Fig. 5.11G) stages. The later stages of egg development,

early to late gastrula (Fig. 5.11G-I) were most common among preserved specimens from BROKE-EAST (64 – 85%) and KAXIS (46 – 85%), though only 0 – 45% were represented in KARE20 samples. For KARE20, early embryogenetic cell dividing stages (Fig. 5.11A-D) were dominant among sample sites (26 – 73%).

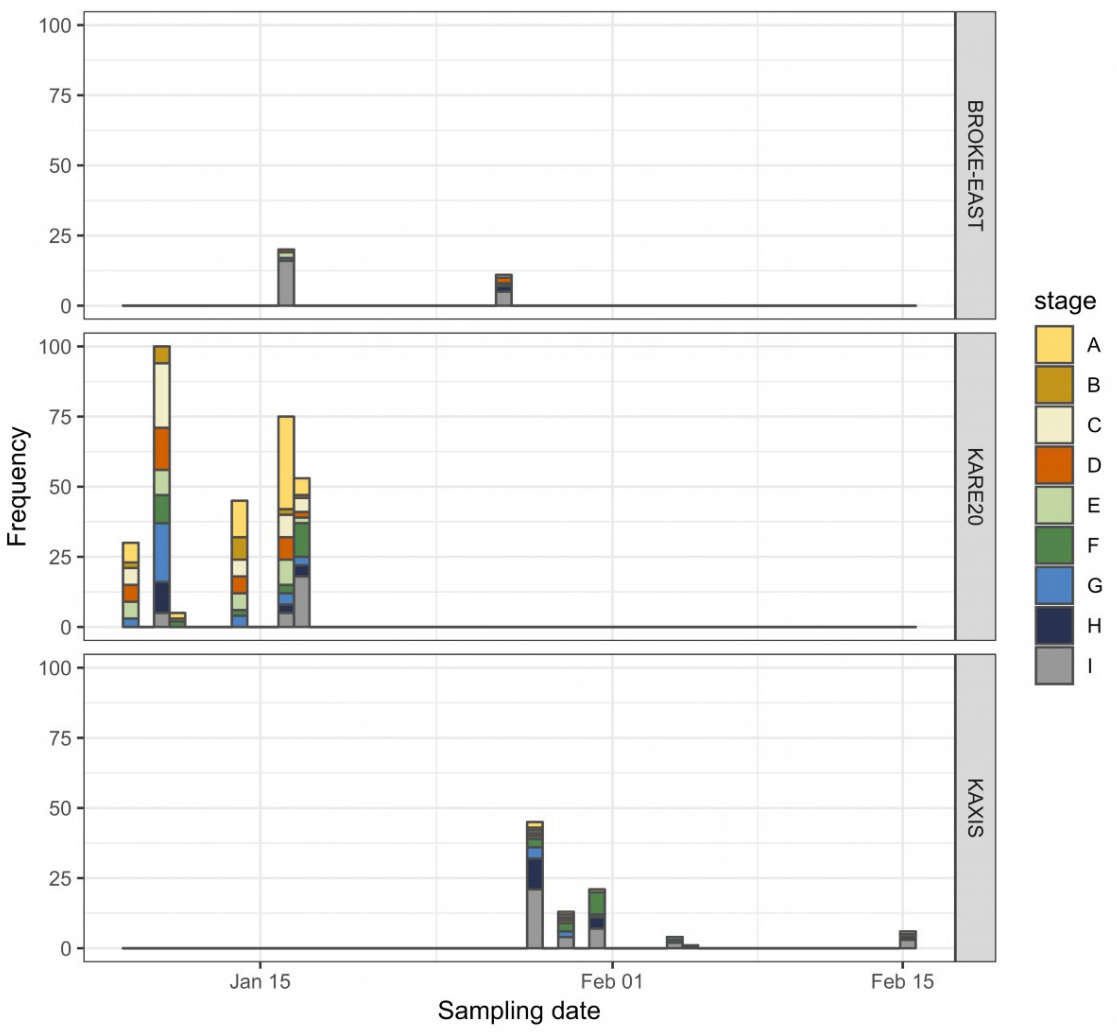

Figure 5.11 Frequency of egg developmental stages detected at sampling dates separated by voyage.

Egg area (mm^2) and proportion of clutch area-to-egg mass area (%) were measured against sampling date for each voyage to estimate rates of fecundity change over time (Fig. 5.12). Egg areas (Fig. 5.12A) and clutch-to-egg mass areas (Fig. 5.12B) significantly decreased over the sampling season for both KAXIS and KARE20 voyages. No statistically significant change was detected for BROKE-EAST samples.

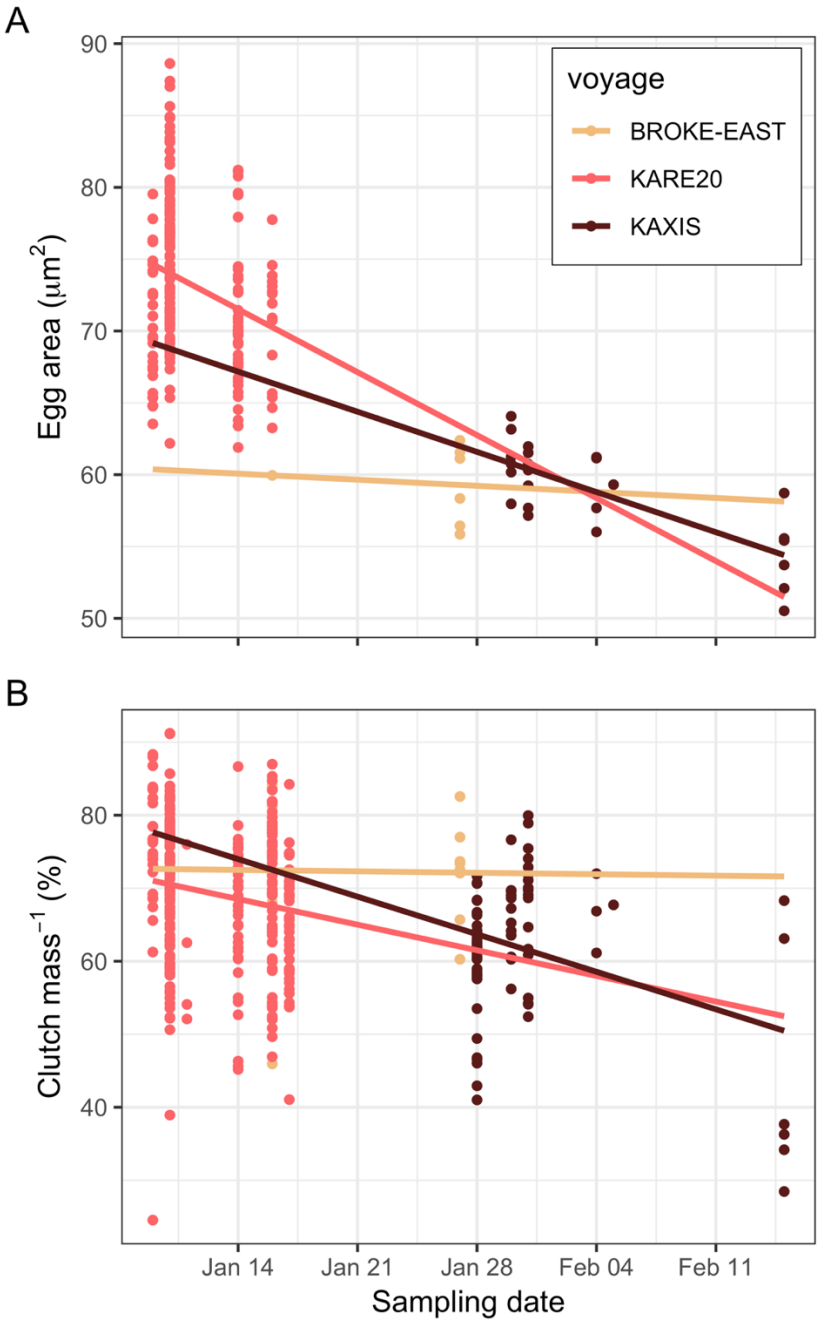

Figure 5.12 Egg and egg mass morphometric traits over sampling dates from preserved samples, per voyage, including (A) egg areas (mm^2), (B) proportion of clutch area to egg mass area. Linear relationships between sampling date and egg area for BROKE-EAST: y = $-6.05e^{-6}x + 1.12e^{-1}$; R^2 = -0.19, p = 0.83; for KARE20: y = $-6.30e^{-5}x$ + 1.13; R^2 = 0.06, p < 0.05; for KAXIS: y = $-3.99e^{-5}x + 7.22e^{-1}$; R^2 = 0.57, p < 0.05. Linear relationships between sampling date and clutch per egg mass area for BROKE-EAST: y = $-0.028e^{-6}x$ + 575.7; R^2 = -0.04, p = 0.94; for KARE20: y = -0.50x + 9050.3; R^2 = 0.02, p < 0.05; for KAXIS: y = -0.74x + 13233.1; R^2 = 0.11, p < 0.05.

5.7 Discussion

This is a first report of patterns and processes in early life strategies of *L. helicina antarctica* based on quantitative estimations and quantitative observations drawn from preserved specimens and live incubation experiments. Here, I have shown that egg mass abundances are strongly correlated with spatial and environmental covariates, whereas presence/absence of egg masses is correlated with spatial and ecological covariates. The largest ovigerous females spawned the most egg masses while exposed to largest sea water size fraction. I also provide a photographic representation of embryogenetic developmental stages, and present several morphometric estimates of embryogenesis that do not vary among individuals or among voyages. However, I have also shown that some morphometrics decrease over a typical spawning season, thus possessing implications on the influence of maternal age on the survival of pteropods.

5.7.1 Drivers of spatial variability of egg masses

GAMs have been shown to perform substantially better than previously-used methods, including acoustic surveys, employed to estimate biomass of economically valuable fish species based on modelling spatial variations of annual and daily egg production (Augustin et al., 2011; Borchers et al., 2011). To my knowledge, this study is the first time that the GAM approach has been used to model spatial patterns in abundance and distribution of pteropod egg production. For pteropods, there are potential gains in the use of modeling procedures that could predict how spatial, ecological, and/or environmental cues may affect variability in egg production that could in turn aid our understanding of how sentinel species to ocean acidification respond to chemical changes to oceans. In this study, the highest abundances of egg masses (eggs · mm^{-2}) were observed south of 60 ºS and west of 110 ºE. Latitude and longitude, along with temperature, were the strongest parameters determining spatial variability in densities, as estimated through the GAMs method.

Presence and absence was also modelled using the GAM, and, as with abundance, latitude exerted a strong influence on the distributional patterns of *L. helicina antarctica*. This outcome of modeling presence-absence also introduced an ecological covariate driver: abundance of older *L. helicina antarctica*. Since data were based on KAXIS samples retrieved from RMT1 and not RMT8 plankton samples, these older *L. helicina antarctica* abundance values are based on specimens ranging 1.5—4.5 mm, thus equating to mid-sized juveniles, adult males and small adult females. It is unlikely here that presence-absence of egg masses is driven by spawning females, but more associated with other aged members of the assemblage. In the 24-hr depth-stratified sediment

trap experiment deployed mid-January within the KARE20 sampling region (Chapter 4), I recovered egg masses along with veliger-, juvenile-, and adult-aged *L. helicina antarctica* within the shallower (57 m) cups, as opposed to the deeper (90 m) cups that possessed 100 % veliger-aged *L. helicina antarctica* composition. Conversely, unpublished results from the same KARE20 research program revealed that egg masses were also sampled between depths of 50-200 m from a variety of depth-stratified net-sampling techniques.

5.7.2 Effect of body size and prey size availability on spawning

During the incubation experiment, the smallest *L. helicina antarctica* adult that spawned egg masses measured 4.2 mm in shell diameter. This is smaller than the average size at reproductive maturity previously reported for *Limacina helicina* (Lalli and Wells, 1978); however different sizes at reproductive maturity may vary with season, where smaller sizes have been reported for some species spawned during summer than during spring (Dadon and de Cidre, 1992; Wang et al., 2017). Due to the timing of each incubation experiment (13 and 17 December, 2017), the smaller mature adults that spawned in this study were likely part of a new generation that were spawned in spring by the generation that spawned the previous year, prior to overwintering in larval form (Lischka and Riebesell, 2012).

I did not directly measure duration of each embryogenetic stage transition, however after 24 hours in incubation, eggs did not appear to be beyond early morula (blastula) stage. Thabet et al. (2015) found that the much smaller *Limacina retroversa* from the Gulf of Maine reached blastula stage within 16-hours of culture. By my estimation, it is likely that it takes approximately 24 hours (± 1-2 hours) to reach morula development, although it is possible that some adults may not have spawned immediately after transfer. Both Gardner et al. (2018) and Manno et al. (2016) observed *L. helicina antarctica* adults spawning within 2 hours of being placed in incubation. Furthermore, many studies observed increased spawning events in *L. helicina antarctica* under laboratory conditions, with some concluding the cause was likely the stresses of handling and exposure to changing environmental conditions (Maas et al., 2011; Manno et al., 2016).

Compared to adult shell size, exposure to different seawater fractions revealed a lesser effect on spawning events (eggs ind^{-1}). The growth curve for number of spawning events by adults incubated in the largest seawater size fraction was the only significant relationship in relation to the other sea-water size fractions. However, if this experiment could be repeated to permit greater sample sizes, these results have implications on thecosome reproductive success under future climate conditions, namely, if and how pteropods can adapt to changes to concentrations and abundances of primary producers in the Southern Ocean (reviewed by

Deppeler and Davidson, 2017). Perhaps a smaller size fraction (e.g. <2 μm) may be a more appropriate control that would enable the assessment of impact on the community, not only on spawning events but also on rates of embryogenesis.

5.7.3 Embryogenesis and morphometrics

Samples in this study featured representatives from all stages of embryogenesis typical to molluscan development, including holoblastic spiral cleavage producing two and four equal and parallel macromeres at the 4-cell and 8-cell stage, respectively, as was also recorded for *L. retroversa* (Thabet et al., 2015). Samples with eggs showing early gastrula stage were identified by a blastopore, which eventually forms the mouth by ectodermal invagination by the blastula (McMurrich, 1886). As with other pteropod species, eventually cilia appear, and it is at this stage that the embryo begins to rotate within its egg membrane prior to metamorphosing into trochophore larvae that hatch. Many samples analysed here showed the egg membrane in various degrees of deterioration and surrounding highly ciliated embryos that were likely in the process of hatching. Comparing our results to other studies highlights close similarities among embryogenesis among pteropod species.

Morphometrics includes the quantitative analysis of physical form and shape and can provide useful insights concerning early life history phenomena of aquatic organisms (Timms and Lindsay, 2011). The morphometric results for *L. helicina antarctica* determined here show that mean egg mass length of 6.2 mm is slightly longer than the 5.2 mm measured for sediment trap-caught *L. helicina antarctica* from Chapter 4, but highly similar to lengths (~6.0 mm) measured by Akiha et al. (2017) off Wilkes Land, Antarctica, and for *L. helicina* in the northern Davis Strait, Labrador Sea by (Lalli and Wells, 1978). Egg masses measured in the present study contained an average of 47 eggs mm^{-2}, which was larger than the 35 eggs mm^{-2} reported for Canadian Atlantic and Subarctic specimens of *L. helicina* (Lalli and Wells, 1978), and less than the 81.5 eggs mm^{-2} reported for San Juan Island, Washington, specimens of *L. helicina* (Paranjape, 1968).

Several egg and egg mass morphometric traits measured from BROKE-EAST samples varied significantly from KAXIS and KARE20 samples, which were similar to each other. This may be an artefact of long-term preservation for the BROKE-EAST samples that have been stored since re-analysis 22 years later. Though work has been done to measure impacts of various preservation techniques on adult shell condition of pteropods (Oakes et al., 2018), research has yet to verify the effects of short- and long-term preservation techniques on pteropod egg and egg mass morphometric traits. One study on early-aged *Calanus finmarchicus* found that short-term (5 years) preservation fixed in 4 % buffered formaldehyde made no

difference to egg production rate estimates (Runge, 1987). With the smallest sample size among all voyage programs, BROKE-EAST samples occupied only 7 % total sample size and likely did not influence morphometric results.

5.7.4 Relationships between embryogenetic characteristics and time

In this study, it was important to incorporate a temporal element to establish whether preserved samples capture the effects of seasonal energetic investment on egg morphometrics (eg. size) in *L. helicina antarctica*. For many gastropods, availability of resources, changing environmental variables, and maternal age dictate the reproductive strategies of spawning females (Ito, 1997). Manno et al., (2016) found that egg to ribbon ratio decreased with successive spawning events, and that exposure intensity and duration to acidified ocean conditions affected egg quality, morphometrics, and egg numbers differently, suggesting that, aside from stress, maternal age also impacts fecundity. Furthermore, the results presented in this chapter support the theory that as maternal age increases, and as the breeding season progresses, spawning *L. helicina antarctica* females exert less energy on reproduction as the rate of maternal mortality increase. Over the combined voyage sampling period, data obtained from the preserved egg mass samples revealed decreasing size and number of eggs as well as, to a lesser magnitude, decreasing clutch size areas per egg masses. More experimental work is needed to better understand how maternal age determines growth and survival in euthecosomatous pteropods, and how these natural processes change in a rapidly changing ocean.

5.7.5 Future directions

When focusing on microscopic organisms, challenges in measuring fecundity can be minimized with the use of image analyses platforms. Several studies have employed the ImageJ platform to automatically enumerate microscopic eggs of invertebrates with high degrees of success (Collin, 2010; da Silva Júnior et al., 2018; Rosati et al., 2015). Due to the high number of microscopic eggs embedded within each egg mass, manually counting eggs within an egg mass can be time consuming and estimating fecundity using abundance of mature-aged adults is a relatively inaccurate alternative given the range of egg masses released by each adult *L. helicina antarctica*. Before discussing the ecological implications associated with the egg counting outputs originating from the ImageJ platform, it is critical to determine the reliability of these results. Many of the images depicted egg mass samples surrounded by non-pteropod particles, such as phytoplankton cells, that would likely also be counted by the software. The inability by the platform to distinguish eggs from other materials, identify egg and egg mass abnormalities or

differentiate between eggs within close proximity are all limitations of this technique. Precision is enhanced through pre-analysis image preparation, involving setting size threshold limits and drawing regions of interest (ROIs) encompassing high concentrations of intended materials. Despite these caveats, the statistically significant similarity obtained between manual and automated techniques validate the latter as a suitable solution for estimating fecundity.

Manno et al. (2016) found that *L. helicina antarctica* each spawned approximately 1200 eggs under ambient conditions, which was higher than the 500—700 eggs · spawn^{-1} reported for a northern congener of *Limacina*, *L. helicina* from the San Juan Islands, Washington (Paranjape, 1968). Results here ranged from 145—831 eggs · spawn^{-1} (average for all voyages combined: 379 ± 49 eggs · spawn^{-1}). Using the same automated egg counting technique, in Chapter 4, I measured an average of 735 eggs spawn^{-1}, and though this was higher than the average from the present study, it was within our range of estimates. These values come from the early to late summer period (9 December, KARE20—5 February, KAXIS), and as discussed in detail below, studies have shown that eggs · spawn^{-1} decrease through successive spawning events (Manno et al., 2016). Average eggs · spawn^{-1} measured here decreased by 62% from the early to late summer sampling dates. Future research should focus on validating regional and seasonal differences in fecundity in order to monitor how rates they may respond to changing ocean conditions.

Chapter 6

Synthesis: Key highlights, implications and future directions

6.1 Key research findings

The Southern Ocean, a vast circumpolar region extending from the Antarctic continent towards 40°S, is currently experiencing rapid shifts in physical and oceanographic properties due to climatic shifts (Rintoul, 2018; Stark et al., 2019). These changes will inevitably affect marine species, and some have been identified as sentinels of climate change due to their sensitivities to change (Ropert-Coudert et al., 2019; Xavier et al., 2016). Notably, thecosome pteropods have been called 'canaries in the coalmine' as they have shown pitting and malformation of their aragonite shells when exposed to ocean acidification (Bednaršek et al., 2017). Recent research has revealed physiological responses of pteropods that might mitigate damage due to exposure to ocean acidification, despite metabolic costs (Peck et al., 2018). However, at present, a larger body of work indicates that climate stressors, such as increasing sea surface temperatures, deoxygenation, freshening, and enhanced stratification, as well as OA, are significant threats to shelled pteropods (Bednaršek et al., 2016; Manno et al., 2017). Moreover, pteropods contribute important ecological functional roles within Southern Ocean ecosystems, and understanding these roles formed the impetus for the research presented in this thesis.

In this thesis, I addressed knowledge gaps in our fundamental understanding of the ecological functional roles of co-occurring Southern Ocean pteropod species. My research focused on the relatively under-surveyed yet highly biologically and ecologically productive Indian Sector of the Southern Ocean. The identification of patterns pertaining to the ecological functional roles presented here, including trophodynamics, abundance, and life history strategies, were drawn from three voyages, two separate sediment trap experiments, and represent the most comprehensive pteropod assessment for the Indian Sector. Furthermore, this work featured all age classes as well as four of the six most common pteropod species south of the Polar Frontal Zone. While most studies focus specifically on the sensitivity of thecosomes to multiple stressors of climate change, I recognised that gymnosomes are just as much at risk of such stressors, and have consequently not excluded them, wherever possible, in assessments provided within this thesis.

As with the recent review by Manno et al. (2017) that synthesized recent technological advances introduced to pteropod-based research, I have also used novel technologies and methodologies to fill knowledge gaps in fundamental biology and ecology of Southern Ocean pteropod species. I made important advances in using stable isotopes to understand the trophic ecology of Southern Ocean pteropods. While chemical lipid extraction is not new to pteropod research, the effect of lipid removal on stable carbon and nitrogen is an advancement to our knowledge, and the effect this has on a variety of niche metrics is an important contribution to our understanding of the biochemistry of polar pteropods. Similarly, stable carbon and nitrogen isotopes analyses have previously been used to estimate the ecological niches of pteropods, however my expansion into using Bayesian niche metrics is a first in this field. Identifying the benefit of using swimmer specimens from sediment traps in ecological studies is gaining more attention (Busch et al., 2015; Makabe et al., 2016), especially in polar regions where traps can continue to sample even when sites are seasonally inaccessible. The research presented here is the first to demonstrate that ecological processes, such as early age growth rates, obtained from trap-caught swimmer specimens, can closely match information obtained through traditional plankton net-sampled techniques. Finally, the egg mass measurements presented in the final data chapter were facilitated through the use of an open source image analysis platform, ImageJ/Fiji. This technique had not been used before to enumerate and measure eggs within pteropod egg masses.

To summarize , this thesis found the following based on stable isotopes analyses (Chapters 2 and 3):

- Pteropods with lipids removed had $\delta^{13}C$ values up to 4.5‰ higher than bulk samples.
- Isotopic niche overlaps between untreated pteropods and their potential food sources were significantly different from overlaps generated between lipid-corrected pteropods and their potential food sources.
- Data converted via normalisation models did not reveal significant differences either between the models or among various niche metrics.
- Observed niche areas were broadest for gymnosomes, especially for *C. limacina*, whose observed area was wider on both $\delta^{13}C$ and $\delta^{15}N$ axes, either reflecting a more generalist, rather than specialist, feeding strategy or limited food availability.
- Trophic position increased for *S. australis* with increasing body length.
- No dietary shift to carnivory with increasing body size was inferred for *C. pyramidata.*
- Trophic positions among all species ranged 2.8-3.5, revealing an assemblage composed of both primary and secondary consumers.

Based on shallow water sediment trap experiments (Chapter 4), this thesis also found:

- Highest abundances were measured for veliger-aged *L. helicina*, relative to all other species and age classes.
- Intra-seasonal growth rate for veligers was estimated to be 0.01 mm d^{-1}.
- Temporal swimmer flux rates ranged from 121 - 2,652 $m^{-2}d^{-1}$ at 53 m; vertical flux was 960 m^{-2} d^{-1} at 57 m depth, and 6,692 m^{-2} d^{-1} at 90 m depth.
- Fluorescence and sinking POC and PIC had the most explanatory power for abundances of shallow water age and species classes of pteropods.

Finally, based on fecundity estimates involving both live and preserved *L. helicina antarctica* specimens sampled from the Indian Sector of the Southern Ocean (Chapter 5):

- Larger adults (>5.5 mm shell diameters) spawned more egg masses per 24 hours (>5 egg masses), with adults as small as 4.2 mm (shell diameter) spawning eggs.
- Ovigerous females spawned more egg masses while incubated in larger seawater fractions (>210 μm).
- Potential drivers of egg abundance were latitude, longitude and temperature, whereas longitude and presence of larger pteropods were important in estimating presence-absence of eggs.
- Preserved samples possessed all stages of holoblastic embryogenesis, typical developmental patterns observed in gastropods molluscs.
- Egg areas decreased over sampling periods equivalent to spawning seasons and corresponding to all voyage collections analysed.
- The automated method of counting eggs within egg masses using the image analysis platform ImageJ/Fiji was ~92 % effective when compared to results from manual counting of images.

6.2 Implications of this research

The research presented within these chapters offers a substantial contribution of new data drawn from innovative analytical techniques that have rarely been used in pteropod-focused studies. Stable isotopes analyses are a useful tool employed by ecologists to estimate the ecological and trophic niches of organisms. However, among its limitations is the bias presented by the presence of lipids within soft tissues and it is essential to not only quantify these concentrations, but also correct for them prior to further analyses. Prior to the research presented in Chapter 2, we had not known the effect lipids had on stable carbon and nitrogen

isotopes of pteropods, nor had we confirmation of the suitability of chemical versus mathematical lipid correction procedures on pteropods. This thesis provides strong support for the pre-treatment of lipids, either chemically or mathematically, from Southern Ocean pteropod specimens prior to work involving stable isotopes analyses.

The process of estimating niche breadth in co-occurring pteropods raised more questions than it answered. While the sampling effort conducted during the KAXIS research voyage was the most regionally extensive of its kind, it was difficult to determine whether the pteropod species composition observed here was typical. In fact, the low abundance of the species considered the most abundant south of the Polar Front, *L. helicina antarctica*, seemed the most likely explanation for the wider than expected niche widths of its monophagous predator, *C. limacina antarctica*. This observation emerged from three conclusions about Southern Ocean pteropods based on similar research:

1) That the niche breadth of pteropods, at least Southern Ocean species, may not be directly or closely associated with dietary diversity, consequently not adhering to the niche variation hypothesis posited by Van Valen (1965);
2) That gymnosome species, such as *C. limacina antarctica*, may possess a high inter-individual variability due to metabolic responses to stresses, such as food limitation, which can be observed through a greater stable carbon and nitrogen isotopic range (Karlson et al., 2018);
3) That 'low *Limacina* years' have previously occurred in the Southern Ocean (Hunt et al., 2008; Seibel and Dierssen, 2003).

The results from Chapter 4, along with the work of Makabe et al. (2016), support the use of sediment trap-caught swimmer specimens in ecological studies, including estimations of population dynamics, early stage growth rates, and species and age abundances and compositions. Sediment traps are particularly useful as, unlike traditional plankton net sampling techniques, they do not bias against smaller size fractions and can provide realistic species age structure profiles with the potential to expand these profiles over interannual time scales. I also provided estimations on the rate of particulate organic and inorganic matter, which are useful to understand the magnitude of passive contributions by pteropods to the global carbon and carbonate pump, at a regional scale. Sediment traps are most commonly employed for gathering these types of data. Moreover, the data presented in this chapter show swimmer flux at two separate time scales within the same austral season, which enabled the identification of pulsed spawning events, and also made it a useful dataset with which to determine potential drivers of a variety of ecological patterns and processes among co-occurring pteropod species. Future work

should also investigate any influence carbonate chemistry may also have on pteropod distributions.

An important goal for this thesis was to highlight fecundity and embryogenetic development in pteropods, specifically the common *Limacina helicina antarctica*. Southern Ocean-based research focusing on responses to ocean acidification by early-stage pteropods is emerging, yet gaps remain in our understanding of in situ patterns and strategies of early life stages, and reproductive success of ovigerous females. Moreover, the research presented in Chapter 5 is a first attempt at measuring the abundance of egg masses and determining environmental drivers of patterns in abundance of egg masses. While the effects of ocean acidification cannot be ignored, it was important to identify whether these patterns are driven by other processes, and this study revealed possible spatial and oceanographic influences (ie. latitude, longitude and temperature). Data presented in this chapter represent a first step in the process of forecasting reproductive success of thecosome pteropods and highlights the importance of incorporating egg masses into species abundance and composition assessments for the Southern Ocean.

6.3 Future directions

As pteropods are gaining more attention as early indicators of climate change, our understanding of the magnitude of their ecological roles remains limited. Designing future pteropod-focused ecological research should incorporate both empirical and theoretical approaches. Below I outline promising directions for future research building upon the work presented in this thesis (not an exhaustive list).

6.3.1 Assessments in pteropod variability, trends over time, and prognoses

Returning to the same transects to repeat sampling efforts is highly encouraged. This will enable a better understanding of the dynamic community structure and oceanographic processes acting on co-occurring pteropod species, at interannual time scales. This is especially important for relatively under-surveyed regions, such as the southern Kerguelen Plateau where, during summer 2015/16, we observed significantly higher densities of *C. pyramidata* f. *sulcata* than the common *L. helicina antarctica*, as observed in Chapter 3. Without prior knowledge of regional interannual variation in abundance and isotopic values for these species, we cannot be sure that this represented a "low *Limacina* year" or a species composition typically observed for the southern Kerguelen Plateau.

6.3.2 Biochemical responses to changing climate conditions

An important aim in pteropod-related trophodynamic research is to investigate how multiple stressors affect their isotopic niches. For instance, as addressed in Chapter 3, the breadth of pteropod isotopic niches may not be influenced solely by diet diversity, as indicated by the larger niche widths occupied by the specialist gymnosome species relative to omnivorous *C. pyramidata* f. *sulcata*. The data presented Chapter 3 provides an impetus to better understand how various stressors, such as food limitation, affect their stable carbon and nitrogen isotope signatures. I propose several different approaches to reach this aim. Empirically, this can be achieved through inducing physiological stress (e.g. starvation) on live pteropod specimens and testing how these conditions affect stable isotopic values. In the field, pteropods should be sampled for stable isotopes analyses over long time scales, and assessed against a suite of oceanographic and physical covariates, thus enabling the identification of a baseline isotopic range that can be used to monitor biochemical responses to changing climate conditions. Explicit model representation of the evolution of isotope signatures could also give more powerful comparisons with observed signatures (McCormack et al., 2019).

6.3.3 Changing primary production and effects on fecundity

Given the threat of changing species and size compositions of phytoplankton in the Southern Ocean, understanding how this will affect fecundity in herbivorous pteropods motivated the incubation experiments conducted in Chapter 5. Due to the small number of live, ovigerous *L. helicina antarctica* females retrieved during the KARE20 voyage, these results can only be regarded as preliminary. An expansion of this work is recommended to include a greater sample size. This would enable a better understanding of the ecological and energetic requirements of thecosome pteropods (particularly *L. helicina antarctica*) optimal for reproductive success. As research continues to investigate regional changes to phytoplankton size and species concentrations under future climate scenarios, this could in turn lead to enhanced forecasting of the effects on the trophic dynamics and reproductive success of herbivorous pteropod assemblages.

6.3.4 Drivers of early life history and reproductive success

Knowledge pertaining to key oceanographic and environmental variables that drive early life history strategies and reproductive success of Southern Ocean pteropods remains underdeveloped. Future studies should investigate the environmental features that form suitable habitat for co-occurring pteropod species, and identify any species- and age-specific responses

should any of these features reach a tipping point. For instance, in Chapter 5, I presented results from a first attempt to model oceanographic drivers of egg production in *L. helicina antarctica* using generalized additive modelling procedures; however, this effort was based on data sampled from a single voyage transect (KAXIS). It would be fruitful to explore regional egg production over greater time and spatial scales, thus enabling a better understanding of how future climate change scenarios directly affect reproductive success of this species.

6.3.5 Explore the role of the Chaetoceros species link to egg masses

During both the KAXIS and KARE20 voyages, and briefly discussed in Chapter 5, high concentrations of the centric diatom *Chaetoceros* spp., primarily *C. cyrophilus*, were observed which were associated with zooplankton samples at sites containing *L. helicina antarctica* egg masses. The mechanism of this association is not clear; for instance, it is not well known whether *C. cryophilus* is a preferred food source for adult *L. helicina antarctica*, and low concentrations of *Chaetoceros* sp. skeletal remains have been found in the gut contents of *L. helicina* sampled from northern temperate regions (Paranjape, 1968) as well as in other thecosome species (Bednaršek et al., 2016). *Chaetoceros* spp. is a dominant phytoplankton genus that has high lipid and fatty acid concentrations, and is an important food source for many organisms (Bloom et al., 2002). It would be useful to investigate this pteropod egg mass-*Chaetoceros* relationship in depth, particularly given the growing research identifying varying sensitivities of Southern Ocean *Chaetoceros* spp. under different climate scenarios (Sackett et al., 2013; Trimborn et al., 2019).

6.3.6 Incorporate all life stages into ecosystem models

Recent work in ecosystem modelling has explicitly represented both gymnosomes and thecosomes, as individual functional groups, rather than grouping them together as 'zooplankton', or other larger groupings (Suprenand and Ainsworth, 2017). Using Ecopath with Ecosim (EwE) to simulate changes in food web dynamics under forecasted changes to primary production in the western Antarctic Peninsula, results have predicted positive trends in terms of biomass and trophic position (Suprenand and Ainsworth, 2017). The development of ecosystem models that investigate diet linkages need to incorporate all life stages of species and/or functional groups, and is rarely practiced in Antarctic food web models (McCormack et al., 2017). Key needs to enable robust representation of pteropods in future ecosystem modelling efforts include parameterization of largely unknown characteristics of life cycle, such as fecundity, growth rate, life span, and mortality (Manno et al. 2017). Ontogenetic diet shifts that have been observed in both gymnosome and thecosome pteropod species suggest that multi-

stanza or size-based representations will be appropriate. Data for such research requires sampling techniques that preserve the integrity of shells and body tissue (e.g. ring net), and captures a greater range of early age classes through smaller mesh sized nets.

References

Accornero, A., Manno, C., Esposito, F., Gambi, M.C., 2003. The vertical flux of particulate matter in the polynya of Terra Nova Bay. Part II. Biological components. Antarct. Sci. 15, 175–188. doi:10.1017/S0954102003001214

Agostini, S., Harvey, B.P., Wada, S., Kon, K., Milazzo, M., Inaba, K., Hall-Spencer, J.M., 2018. Ocean acidification drives community shifts towards simplified non-calcified habitats in a subtropical−temperate transition zone. Sci. Rep. 8, 5–10. doi:10.1038/s41598-018-29251-7

Akiha, F., Hashida, G., Makabe, R., Hattori, H., Sasaki, H., 2017. Distribution in the abundance and biomass of shelled pteropods in surface waters of the Indian sector of the Antarctic Ocean in mid-summer. Polar Sci. 1–7. doi:10.1016/j.polar.2017.02.003

Allan, E.L., Froneman, P.W., Durgadoo, J. V., Mcquaid, C.D., Ansorge, I.J., Richoux, N.B., 2013. Critical indirect effects of climate change on sub-Antarctic ecosystem functioning. Ecol. Evol. 3, 2994–3004. doi:10.1002/ece3.678

Almogi-Labin, A., Hemleben, C., Deuser, W.G., 1988. Seasonal variation in the flux of euthecosomatous pteropods collected in a deep sediment trap in the Sargasso Sea. Deep Sea Res. Part A, Oceanogr. Res. Pap. 35, 441–464. doi:10.1016/0198-0149(88)90020-9

Aoki, S., Kitade, Y., Shimada, K., Ohshima, K.I., Tamura, T., Bajish, C.C., Moteki, M., Rintoul, S.R., 2013. Widespread freshening in the Seasonal Ice Zone near 140°E off the Adélie Land Coast, Antarctica, from 1994 to 2012. J. Geophys. Res. Ocean. 118, 6046–6063. doi:10.1002/2013JC009009

Arrigo, K.R., Thomas, D.N., 2004. Large scale importance of sea ice biology in the Southern Ocean. Antarct. Sci. 16, 471–486. doi:10.1017/S0954102004002263

Ashjian, C.J., Campbell, R.G., Welch, H.E., Butler, M., Van Keuren, D., 2003. Annual cycle in abundance, distribution, and size in relation to hydrography of important copepod species in the western Arctic Ocean. Deep. Res. Part I Oceanogr. Res. Pap. 50, 1235–1261. doi:10.1016/S0967-0637(03)00129-8

Augustin, N.H., Borchers, D.L., Clarke, E.D., Buckland, S.T., Walsh, M., 2011. Spatiotemporal modelling for the annual egg production method of stock assessment using generalized additive models. Can. J. Fish. Aquat. Sci. 55, 2608–2621. doi:10.1139/f98-143

Bas, M., Briz i Godino, I., Álvarez, M., Vales, D.G., Crespo, E.A., Cardona, L., 2019. Back to the future? Late Holocene marine food web structure in a warm climatic phase as a predictor of trophodynamics in a warmer South-Western Atlantic Ocean. Glob. Chang. Biol. 25, 404–419. doi:10.1111/gcb.14523

Bathmann, U. V., Noji, T.T., von Bodungen, B., 1991. Sedimentation of pteropods in the Norwegian Sea in autumn. Deep Sea Res. Part A, Oceanogr. Res. Pap. 38, 1341–1360. doi:10.1016/0198-0149(91)90031-A

Bauerfeind, E., Nöthig, E.M., Pauls, B., Kraft, A., Beszczynska-Möller, A., 2014. Variability in pteropod sedimentation and corresponding aragonite flux at the Arctic deep-sea long-term observatory HAUSGARTEN in the eastern Fram Strait from 2000 to 2009. J. Mar. Syst. 132, 95–105. doi:10.1016/j.jmarsys.2013.12.006

Bayne, B.L., 1986. Marine mussels: their ecology and physiology. Cambridge University Press, Cambridge.

Bearhop, S., Adams, C.E., Waldron, S., Fuller, R.A., Macleod, H., 2004. Determining trophic niche width: A novel approach using stable isotope analysis. J. Anim. Ecol. 73, 1007–1012. doi:10.1111/j.0021-8790.2004.00861.x

Bednaršek, N., Harvey, C.J., Kaplan, I.C., Feely, R.A., Možina, J., 2016. Pteropods on the edge: Cumulative effects of ocean acidification, warming, and deoxygenation. Prog. Oceanogr. 145, 1–24. doi:10.1016/j.pocean.2016.04.002

Bednaršek, N., Klinger, T., Harvey, C.J., Weisberg, S., McCabe, R.M., Feely, R.A., Newton, J., Tolimieri, N., 2017. New ocean, new needs: Application of pteropod shell dissolution as a biological indicator for marine resource management. Ecol. Indic. 76, 240–244. doi:10.1016/j.ecolind.2017.01.025

Bednaršek, N., Mozina, J., Vogt, M., O'Brien, C., Tarling, G.A., 2012a. The global distribution of pteropods and their contribution to carbonate and carbon biomass in the modern ocean. Earth Syst. Sci. Data 1, 1–20. doi:10.5194/essd-1-1-2012

Bednaršek, N., Tarling, G.A., Bakker, D.C.E., Fielding, S., Jones, E.M., Venables, H.J., Ward, P., Kuzirian, A., Lézé, B., Feely, R.A., Murphy, E.J., 2012b. Extensive dissolution of live pteropods in the Southern Ocean. Nat. Geosci. 5, 881–885. doi:10.1038/ngeo1635

Bednaršek, N., Tarling, G.A., Fielding, S., Bakker, D.C.E., 2012c. Population dynamics and biogeochemical significance of *Limacina helicina antarctica* in the Scotia Sea (Southern Ocean). Deep Sea Res. Part II Top. Stud. Oceanogr. 59–60, 105–116. doi:10.1016/j.dsr2.2011.08.003

Bergami, C., Capotondi, L., Langone, L., Giglio, F., Ravaioli, M., 2009. Distribution of living planktonic foraminifera in the Ross Sea and the Pacific sector of the Southern Ocean (Antarctica). Mar. Micropaleontol. 73, 37–48. doi:10.1016/j.marmicro.2009.06.007

Berger, W.H., 1978. Deep-sea carbonate: pteropod distribution and the aragonite compensation depth. Deep. Res. 25, 447–452. doi:10.1016/0146-6291(78)90552-0

Bernard, K.S., Froneman, P.W., 2009. The sub-Antarctic euthecosome pteropod, *Limacina retroversa*: Distribution patterns and trophic role. Deep. Res. Part I Oceanogr. Res. Pap. 56, 582–598. doi:10.1016/j.dsr.2008.11.007

Bernard, K.S., Steinberg, D.K., Schofield, O.M.E., 2012. Summertime grazing impact of the dominant macrozooplankton off the Western Antarctic Peninsula. Deep. Res. Part I 62, 111–122. doi:10.1016/j.dsr.2011.12.015

Bestley, S., van Wijk, E., Rosenberg, M., Eriksen, R., Corney, S., Tattersall, K., Rintoul, S., 2018. Ocean circulation and frontal structure near the southern Kerguelen Plateau: The physical context for the Kerguelen Axis ecosystem study. Deep Sea Res. Part II Top. Stud. Oceanogr. 0–1. doi:10.1016/j.dsr2.2018.07.013

Bligh, E.G., Dyer, W.J., 1959. A rapid method of total lipid extraction and purification. Can. J. Biochem. Physiol. 37, 911–917. doi:dx.doi.org/10,1139/cjm2014-0700

Bloom, B., Larouche, P., Bélanger, S., Klein, B., Amiel, D., Mei, Z.-P., 2002. Dynamics of *Chaetoceros socialis* blooms in the North Water. Deep Sea Res. Part II 49, 5003–5025.

Boag, B., Neilson, R., Scrimgeour, C.M., 2006. The effect of starvation on the planarian *Arthurdendyus triangulatus* (Tricladida: Terricola) as measured by stable isotopes. Biol. Fertil. Soils 43, 267–270. doi:10.1007/s00374-006-0108-3

Boecklen, W.J., Yarnes, C.T., Cook, B.A., James, A.C., 2011. On the use of stable isotopes in trophic ecology. Annu. Rev. Ecol. Syst. 42, 411–440. doi:doi:10.1146/annurev-ecolsys-102209-144726

Böer, M., Gannefors, C., Kattner, G., Graeve, M., Hop, H., Falk-Petersen, S., 2005. The Arctic pteropod *Clione limacina*: Seasonal lipid dynamics and life-strategy. Mar. Biol. 147, 707–717. doi:10.1007/s00227-005-1607-8

Böer, M., Graeve, M., Kattner, G., 2007. Exceptional long-term starvation ability and sites of lipid storage of the Arctic pteropod *Clione limacina*. Polar Biol. 30, 571–580. doi:10.1007/s00300-006-0214-6

Böer, M., Graeve, M., Kattner, G., 2006. Impact of feeding and starvation on the lipid metabolism of the Arctic pteropod *Clione limacina*. J. Exp. Mar. Bio. Ecol. 328, 98–112. doi:10.1016/j.jembe.2005.07.001

Boissonnot, L., Niehoff, B., Ehrenfels, B., Søreide, J., Hagen, W., Graeve, M., 2019. Lipid and fatty acid turnover of the pteropods *Limacina helicina*, *L. retroversa* and *Clione limacina* from Svalbard waters. Mar. Ecol. Prog. Ser. 609, 133–149. doi:10.3354/meps12837

Bolnick, Svanbäck, Fordyce, Yang, Davis, Hulsey, Forister, 2003. The ecology of individuals: Incidence and implications of individual specialization. Am. Nat. 161, 1.

doi:10.2307/3078879

Borchers, D.L., Buckland, S.T., Priede, I.G., Ahmadi, S., 2011. Improving the precision of the daily egg production method using generalized additive models. Can. J. Fish. Aquat. Sci. 54, 2727–2742. doi:10.1139/f97-134

Boyd, P.W., Collins, S., Dupont, S., Fabricius, K., Gattuso, J.P., Havenhand, J., Hutchins, D.A., Riebesell, U., Rintoul, M.S., Vichi, M., Biswas, H., Ciotti, A., Gao, K., Gehlen, M., Hurd, C.L., Kurihara, H., McGraw, C.M., Navarro, J.M., Nilsson, G.E., Passow, U., Pörtner, H.O., 2018. Experimental strategies to assess the biological ramifications of multiple drivers of global ocean change—A review. Glob. Chang. Biol. 24, 2239–2261. doi:10.1111/gcb.14102

Buesseler, K.O., Antia, A.N., Chen, M., Fowler, S.W., Gardner, W.D., Gustafsson, O., Harada, K., Michaels, A.F., Rutgers van der Loeff, M., Sarin, M., Steinberg, D.K., Trull, T., 2007. An assessment of the use of sediment traps for estimating upper ocean particle fluxes. J. Mar. Res. 65, 345–416. doi:10.1357/002224007781567621

Burridge, A.K., Goetze, E., Wall-Palmer, D., Le Double, S.L., Huisman, J., Peijnenburg, K.T.C.A., 2017. Diversity and abundance of pteropods and heteropods along a latitudinal gradient across the Atlantic Ocean. Prog. Oceanogr. 158, 213–223. doi:10.1016/j.pocean.2016.10.001

Busch, K., Bauerfeind, E., Nöthig, E.M., 2015. Pteropod sedimentation patterns in different water depths observed with moored sediment traps over a 4-year period at the LTER station HAUSGARTEN in eastern Fram Strait. Polar Biol. 38, 845–859. doi:10.1007/s00300-015-1644-9

Carscallen, W.M.A., Vandenberg, K., Lawson, J.M., Martinez, N.D., Romanuk, T.N., 2012. Estimating trophic position in marine and estuarine food webs. Ecosphere 3, 1–20. doi:10.1890/ES11-00224.1

Chase, J.M., Leibold, M.A., 2003. Ecological Niches: Linking Classical and Contemporary Approaches, The University of Chicago Press. University of Chicago Press, Chicago, IL.

Cherel, Y., 2008. Isotopic niches of emperor and Adélie penguins in Adélie Land, Antarctica. Mar. Biol. 154, 813–821. doi:10.1007/s00227-008-0974-3

Cherel, Y., Fontaine, C., Richard, P., Labat, J.-P., 2010. Isotopic niches and trophic levels of myctophid fishes and their predators in the Southern Ocean. Limnol. Oceanogr. 55, 324–332. doi:10.4319/lo.2010.55.1.0324

Cherel, Y., Xavier, J.C., De Grissac, S., Trouvé, C., Weimerskirch, H., 2017. Feeding ecology, isotopic niche, and ingestion of fishery-related items of the wandering albatross *Diomedea*

exulans at Kerguelen and Crozet Islands. Mar. Ecol. Prog. Ser. 565, 197–215. doi:10.3354/meps11994

Choy, E.S., Roth, J.D., Loseto, L.L., 2016. Lipid removal and acidification affect nitrogen and carbon stable isotope ratios of beluga whales (*Delphinapterus leucas*) and their potential prey species in the Beaufort Sea ecosystem. Mar. Biol. 163, 220. doi:10.1007/s00227-016-2992-x

Collin, R., 2010. Repeatability of egg size in two marine gastropods: brood order and female size do not contribute to intraspecific variation. Mar. Ecol. Prog. Ser. 410, 89–96. doi:10.3354/meps08638

Comeau, S., Alliouane, S., Gattuso, J.P., 2012. Effects of ocean acidification on overwintering juvenile Arctic pteropods *Limacina helicina*. Mar. Ecol. Prog. Ser. 456, 279–284. doi:10.3354/meps09696

Comiso, J.C., McClain, C.R., Sullivan, C.W., Ryan, J.P., Leonard, C.L., 1993. Coastal zone color scanner pigment concentrations in the Southern Ocean and relationships to geophysical surface features. J. Geophys. Res. 98, 2419–2451. doi:10.1029/92JC02505

Conover, R.J., Lalli, C.M., 1972. Feeding and growth in *Clione limacina* (Phipps), a pteropod mollusc. J. Exp. Mar. Bio. Ecol. 9, 279–302. doi:10.1016/0022-0981(72)90038-X

Constable, A.J., Melbourne-Thomas, J., Corney, S.P., Arrigo, K.R., Barbraud, C., Barnes, D.K.A., Bindoff, N.L., Boyd, P.W., Brandt, A., Costa, D.P., Davidson, A.T., Ducklow, H.W., Emmerson, L., Fukuchi, M., Gutt, J., Hindell, M.A., Hofmann, E.E., Hosie, G.W., Iida, T., Jacob, S., Johnston, N.M., Kawaguchi, S., Kokubun, N., Koubbi, P., Lea, M.-A., Makhado, A., Massom, R.A., Meiners, K., Meredith, M.P., Murphy, E.J., Nicol, S., Reid, K., Richerson, K., Riddle, M.J., Rintoul, S.R., Smith, W.O., Southwell, C., Stark, J.S., Sumner, M., Swadling, K.M., Takahashi, K.T., Trathan, P.N., Welsford, D.C., Weimerskirch, H., Westwood, K.J., Wienecke, B.C., Wolf-Gladrow, D., Wright, S.W., Xavier, J.C., Ziegler, P., 2014. Climate change and Southern Ocean ecosystems I: how changes in physical habitats directly affect marine biota. Glob. Chang. Biol. 20, 3004–3025. doi:10.1111/gcb.12623

Cummings, D.O., Buhl, J., Lee, R.W., Simpson, S.J., Holmes, S.P., 2012. Estimating niche width using stable isotopes in the face of habitat variability: A modelling case study in the marine environment. PLoS One 7. doi:10.1371/journal.pone.0040539

da Silva Júnior, F.A., Monteiro da Silva, C., de Almeida, F.B., Rodrigues-Silva, R., 2018. Digital image analysis to estimate the minimum number of *Eurytrema coelomaticum* eggs in the uterus of adult specimens. Helminthologia 55, 204–212. doi:10.2478/helm-2018-0014

Dadon, J.R., de Cidre, L.L., 1992. The reproductive cycle of the Thecosomatous pteropod *Limacina retroversa* in the western South Atlantic. Mar. Biol. 114, 439–442.

Davidson, A.T., McKinlay, J., Westwood, K., Thomson, P.G., Van Den Enden, R., De Salas, M., Wright, S., Johnson, R., Berry, K., 2016. Enhanced CO_2 concentrations change the structure of Antarctic marine microbial communities. Mar. Ecol. Prog. Ser. 552, 93–113. doi:10.3354/meps11742

DeNiro, M.J., Epstein, S., 1978. Influence of diet on the distribution of carbon isotopes in animals. Geochim. Cosmochim. Acta 42, 495–506. doi:10.1016/0016-7037(78)90199-0

DeNiro, M.J., Epstein, S., 1977. Mechanism of carbon isotope fractionation associated with lipid synthesis. Science (80-.). 197, 261–263. doi:10.1126/science.327543

Deppeler, S.L., Davidson, A.T., 2017. Southern Ocean phytoplankton in a changing climate. Front. Mar. Sci. 4. doi:10.3389/fmars.2017.00040

Doney, S.C., Fabry, V.J., Feely, R.A., Kleypas, J.A., 2009. Ocean acidification: The other CO2 problem. Ann. Rev. Mar. Sci. 1, 169–192. doi:10.1146/annurev.marine.010908.163834

Dupont, S., Dorey, N., Thorndyke, M., 2010. What meta-analysis can tell us about vulnerability of marine biodiversity to ocean acidification? Estuar. Coast. Shelf Sci. 89, 182–185. doi:10.1016/j.ecss.2010.06.013

Elliott, D.T., Tang, K.W., Shields, A.R., 2009. Mesozooplankton beneath the summer sea ice in McMurdo Sound, Antarctica: Abundance, species composition, and DMSP content. Polar Biol. 32, 113–122. doi:10.1007/s00300-008-0511-3

Elton, C., 1927. Animal Ecology. New York, MacMillan Co.

Fabry, V.J., Seibel, B.A., Feely, R.A., Orr, J.C., 2008. Impacts of ocean acidification on marine fauna and ecosystem processes. ICES J. Mar. Sci. 65, 414–432. doi:10.1093/icesjms/fsn048

Falk-Petersen, S., Sargent, J.R., Kwasniewski, S., Gulliksen, B., Millar, R.M., 2001. Lipids and fatty acids in *Clione limacina* and *Limacina helicina* in Svalbard waters and the Arctic Ocean: Trophic implications. Polar Biol. 24, 163–170. doi:10.1007/s003000000190

Fink, P., Reichwaldt, E.S., Harrod, C., Rossberg, A.G., 2012. Determining trophic niche width: An experimental test of the stable isotope approach. Oikos 121, 1985–1994. doi:10.1111/j.1600-0706.2012.20185.x

Flaherty, E.A., Ben-David, M., 2010. Overlap and partitioning of the ecological and isotopic niches. Oikos 119, 1409–1416. doi:10.1111/j.1600-0706.2010.18259.x

Fox, J., Weisberg, S., 2011. An R Companion to Applied Regression, Second. ed. Sage Publications, Thousand Oaks, CA.

France, R., Chandler, M., Peters, R., 1998. Mapping trophic continua of benthic foodwebs:body size-δ^{15}N relationships. Mar. Ecol. Prog. Ser. 174, 301–306. doi:10.3354/meps174301

Frölicher, T.L., Rodgers, K.B., Stock, C.A., Cheung, W.W.L., 2016. Sources of uncertainties in

21st century projections of potential ocean ecosystem stressors. Environ. Microbiol. 18, 1088–1089. doi:10.1111/1462-2920.13280

Fry, B., 2006. Stable Isotope Ecology, 1st ed. Springer-Verlag, New York. doi:10.1007/0-387-33745-8

Fry, B., Baltz, D.M., Benfield, M.C., Fleeger, J.W., Gace, A., Haas, H.L., Quiñones-Rivera, Z.J., 2003. Stable isotope indicators of movement and residency for brown shrimp (*Farfantepenaeus aztecus*) in coastal Louisiana marshscapes. Estuaries 26, 82–97. doi:10.1007/BF02691696

Gannefors, C., Böer, M., Kattner, G., Graeve, M., Eiane, K., Gulliksen, B., Hop, H., Falk-Petersen, S., 2005. The Arctic sea butterfly *Limacina helicina*: Lipids and life strategy. Mar. Biol. 147, 169–177. doi:10.1007/s00227-004-1544-y

Gardner, J., Manno, C., Bakker, D.C.E., Peck, V.L., Tarling, G.A., 2018. Southern Ocean pteropods at risk from ocean warming and acidification. Mar. Biol. 165, 8. doi:10.1007/s00227-017-3261-3

Gilmer, R.W., 1990. In situ observations of feeding behavior of thecosome pteropod mollucs. Am. Malacol. Bull. 8, 53–59.

Gilmer, R.W., 1974. Some aspects of feeding in thecosomatous pteropod molluscs. J. Exp. Biol. Ecol. 1, 127–144. doi:10.1016/0022-0981(74)90039-2

Grinnell, J., 1917. The niche-relationships of the California thrasher. Auk 34, 427–433. doi:10.1152/ajplegacy.1972.222.5.1121

Grossman, E.L., Betzer, P.R., Dudley, W.C., Dunbar, R.B., 1986. Stable isotopic variation in pteropods and atlantids from North Pacific sediment traps. Mar. Micropaleontol. 10, 9–22.

Guglielmo, L., Granata, A., Greco, S., 1998. Distribution and abundance of postlarval and juvenile *Pleuragramma antarcticum* (Pisces, Nototheniidae) off Terra Nova Bay (Ross Sea, Antarctica). Polar Biol. 19, 37–51. doi:10.1007/s003000050214

Guglielmo, L., Zagami, G., Saggiomo, V., Catalano, G., Granata, A., 2007. Copepods in spring annual sea ice at Terra Nova Bay (Ross Sea, Antarctica). Polar Biol. 30, 747–758. doi:10.1007/s00300-006-0234-2

Gutt, J., Bertler, N., Bracegirdle, T.J., Buschmann, A., Comiso, J., Hosie, G., Isla, E., Schloss, I.R., Smith, C.R., Tournadre, J., Xavier, J.C., 2015. The Southern Ocean ecosystem under multiple climate change stresses - an integrated circumpolar assessment. Glob. Chang. Biol. 21, 1434–1453. doi:10.1111/gcb.12794

Harbison, G.R., Gilmer, R.W., 1986. Effects of animal behavior on sediment trap collections: implications for the calculation of aragonite fluxes. Deep Sea Res. Part A, Oceanogr. Res.

Pap. 33, 1017–1024. doi:10.1016/0198-0149(86)90027-0

Hastie, T., Tibshirani, R., 1986. Generalized Additive Models. Stat. Sci. 1, 297–318. doi:10.2307/2246134

Hauri, C., Friedrich, T., Timmermann, A., 2016. Abrupt onset and prolongation of aragonite undersaturation events in the Southern Ocean. Nat. Clim. Chang. 6, 172–176. doi:10.1038/nclimate2844

Henschke, N., Everett, J.D., Suthers, I.M., Smith, J.A., Hunt, B.P. V, Doblin, M.A., Taylor, M.D., 2015. Zooplankton trophic niches respond to different water types of the western Tasman Sea: A stable isotope analysis. Deep. Res. Part I Oceanogr. Res. Pap. 104, 1–8. doi:10.1016/j.dsr.2015.06.010

Hopcroft, R.R., Clarke, C., Nelson, R.J., Raskoff, K.A., 2005. Zooplankton communities of the Arctic's Canada Basin: The contribution by smaller taxa. Polar Biol. 28, 198–206. doi:10.1007/s00300-004-0680-7

Hopkins, T.L., 1987. Midwater food web in McMurdo Sound, Ross Sea, Antarctica. Mar. Biol. 96, 93–106. doi:10.1007/BF00394842

Hopkins, T.L., Torres, J.J., 1989. Midwater food web in the vicinity of a marginal ice zone in the western Weddell Sea. Deep Sea Res. Part A, Oceanogr. Res. Pap. 36, 543–560. doi:10.1016/0198-0149(89)90005-8

Hosie, G.W., Schultz, M.B., Kitchener, J.A., Cochran, T.G., Richards, K., 2000. Macrozooplankton community structure off East Antarctica (80-150°E) during the Austral summer of 1995/1996. Deep Sea Res. Part II 47, 2437–2463.

Howard, W.R., Roberts, D., Moy, A.D., Lindsay, M.C.M., Hopcroft, R.R., Trull, T.W., Bray, S.G., 2011. Distribution, abundance and seasonal flux of pteropods in the Sub-Antarctic Zone. Deep. Res. Part II Top. Stud. Oceanogr. 58, 2293–2300. doi:10.1016/j.dsr2.2011.05.031

Hunt, B.P.V., Pakhomov, E.A., Hosie, G.W., Siegel, V., Ward, P., Bernard, K., 2008. Pteropods in Southern Ocean ecosystems. Prog. Oceanogr. 78, 193–221. doi:10.1016/j.pocean.2008.06.001

Hussey, N.E., MacNeil, M.A., McMeans, B.C., Olin, J.A., Dudley, S.F.J., Cliff, G., Wintner, S.P., Fennessy, S.T., Fisk, A.T., 2014. Rescaling the trophic structure of marine food webs. Ecol. Lett. 17, 239–250. doi:10.1111/ele.12226

Hutchinson, G.E., 1957. Cold spring harbor symposium on quantitative biology. Concluding remarks. 22, 415–427.

Ito, K., 1997. Egg-size and -number variations related to maternal size and age, and the

relationship between egg size and larval characteristics in an annual marine gastropod, *Haloa japonica* (Opisthobranchia; Cephalaspidea). Mar. Ecol. Prog. Ser. 152, 187–195. doi:10.3354/meps152187

Jackson, A.L., Inger, R., Parnell, A.C., Bearhop, S., 2011. Comparing isotopic niche widths among and within communities: SIBER - Stable Isotope Bayesian Ellipses in R. J. Anim. Ecol. 80, 595–602. doi:10.1111/j.1365-2656.2011.01806.x

Jaeger, A., Cherel, Y., 2011. Isotopic investigation of contemporary and historic changes in penguin trophic niches and carrying capacity of the Southern Indian Ocean. PLoS One 6. doi:10.1371/journal.pone.0016484

Jaeger, A., Connan, M., Richard, P., Cherel, Y., 2010. Use of stable isotopes to quantify seasonal changes of trophic niche and levels of population and individual specialisation in seabirds. Mar. Ecol. Prog. Ser. 401, 269–277. doi:10.3354/meps08380

Jennings, S., Pinnegar, J., Polunin, N., Warr, K., 2002. Linking size-based and trophic analyses of benthic community structure. Mar. Ecol. Prog. Ser. 226, 77–85. doi:10.3354/meps226077

Jennings, S., Pinnegar, J.K., Polunin, N.V.C., Boon, T.W., 2001. Weak cross-species relationships between body size and trophic level belie powerful size-based trophic structuring in fish communities. J. Anim. Ecol. 70, 934–944. doi:10.1046/j.0021-8790.2001.00552.x

Jia, Z., Swadling, K.M., Meiners, K.M., Kawaguchi, S., Virtue, P., 2016. The zooplankton food web under East Antarctic pack ice – A stable isotope study. Deep. Res. Part II Top. Stud. Oceanogr. 131, 189–202. doi:10.1016/j.dsr2.2015.10.010

Juranek, L.W., Russell, A.D., Spero, H.J., 2003. Seasonal oxygen and carbon isotope variability in euthecosomatous pteropods from the Sargasso Sea. Deep. Res. Part I Oceanogr. Res. Pap. 50, 231–245. doi:10.1016/S0967-0637(02)00164-4

Kallevik, I.H.F., 2013. Alternative prey choice in the pteropod *Clione limacina* (Gastropoda) studied by DNA-based methods. The Arctic University of Norway; The University Centre in Svalbard.

Karleskint, G., Turner, R., Small, J., 2012. Introduction to Marine Biology, 4th ed. Cengage Learning, Inc.

Karlson, A.M.L., Reutgard, M., Garbaras, A., Gorokhova, E., 2018. Isotopic niche reflects stress-induced variability in physiological status. R. Soc. Open Sci. 5. doi:10.1098/rsos.171398

Kattner, G., Hagen, W., Graeve, M., Albers, C., 1998. Exceptional lipids and fatty acids in the pteropod *Clione limacina* (Gastropoda) from both polar oceans. Mar. Chem. 61, 219–228. doi:10.1016/S0304-4203(98)00013-9

Keul, N., Peijnenburg, K.T.C.A., Andersen, N., Kitidis, V., Goetze, E., Schneider, R.R., 2017.

Pteropods are excellent recorders of surface temperature and carbonate ion concentration. Sci. Rep. 7, 1–11. doi:10.1038/s41598-017-11708-w

Kiljunen, M., Grey, J., Sinisalo, T., Harrod, C., Immonen, H., Jones, R.I., 2006. A revised model for lipid-normalizing $\delta^{13}C$ values from aquatic organisms, with implications for isotope mixing models. J. Appl. Ecol. 43, 1213–1222. doi:10.1111/j.1365-2664.2006.01224.x

Kleiber, C., Zeileis, A., 2008. Applied econometrics with R. Springer Science and Business Media.

Knauer, G.A., Karl, D.M., Martin, J.H., Hunter, C.N., 1984. In situ effects of selected preservatives on total carbon, nitrogen and metals collected in sediment traps. J. Mar. Res. 42, 445–462. doi:10.1357/002224084788502710

Kobayashi, H.A., 1974. Growth cycle and related vertical distribution of the thecosomatous pteropod *Spiratella ("Limacina") helicina* in the central Arctic Ocean. Mar. Biol. 26, 295–301. doi:10.1007/BF00391513

Kraft, A., Bauerfeind, E., Nöthig, E.M., Bathmann, U. V., 2012. Size structure and life cycle patterns of dominant pelagic amphipods collected as swimmers in sediment traps in the eastern Fram Strait. J. Mar. Syst. 95, 1–15. doi:10.1016/j.jmarsys.2011.12.006

Lalli, C.M., Gilmer, R.W., 1989. Pelagic Snails: The Biology of Holoplanktonic Gastropod Mollusks. Stanford University Press.

Lalli, M., Wells, F.E., 1978. Reproduction in the genus *Limacina* (Opisthobranchia: Thecosomata). J. Zool. London 186, 95–108.

Layman, C.A., Quattrochi, J.P., Peyer, C.M., Allgeier, J.E., 2007. Niche width collapse in a resilient top predator following ecosystem fragmentation. Ecol. Lett. 10, 937–944. doi:10.1111/j.1461-0248.2007.01087.x

Lischka, S., Riebesell, U., 2012. Synergistic effects of ocean acidification and warming on overwintering pteropods in the Arctic. Glob. Chang. Biol. 18, 3517–3528. doi:10.1111/gcb.12020

Loeb, V.J., Santora, J.A., 2013. Pteropods and climate off the Antarctic Peninsula. Prog. Oceanogr. 116, 31–48. doi:10.1016/j.pocean.2013.05.030

Logan, J.M., Jardine, T.D., Miller, T.J., Bunn, S.E., Cunjak, R.A., Lutcavage, M.E., 2008. Lipid corrections in carbon and nitrogen stable isotope analyses: Comparison of chemical extraction and modelling methods. J. Anim. Ecol. 77, 838–846. doi:10.1111/j.1365-2656.2008.01394.x

Maas, A.E., Elder, L.E., Dierssen, H.M., Seibel, B.A., 2011. Metabolic response of Antarctic pteropods (Mollusca: Gastropoda) to food depriviation and regional productivity. Mar.

Ecol. Prog. Ser. 441, 129–139. doi:10.3354/meps09358

Macdonald, P., Du, J., 2015. mixdist: Finite Mixture Distribution Models. R package, version 0.5-4. (http://CRAN.R-project.org/package=mixdist).

Mackey, A.P., Atkinson, A., Hill, S.L., Ward, P., Cunningham, N.J., Johnston, N.M., Murphy, E.J., 2012. Antarctic macrozooplankton of the southwest Atlantic sector and Bellingshausen Sea: Baseline historical distributions (Discovery Investigations, 1928-1935) related to temperature and food, with projections for subsequent ocean warming. Deep. Res. Part II Top. Stud. Oceanogr. 59–60, 130–146. doi:10.1016/j.dsr2.2011.08.011

Makabe, R., Hattori, H., Sampei, M., Darnis, G., Fortier, L., Sasaki, H., 2016. Can sediment trap-collected zooplankton be used for ecological studies? Polar Biol. 39, 2335–2346. doi:10.1007/s00300-016-1900-7

Makabe, R., Hattori, H., Sampei, M., Ota, Y., Fukuchi, M., Fortier, L., Sasaki, H., 2010. Regional and seasonal variability of zooplankton collected using sediment traps in the southeastern Beaufort Sea, Canadian Arctic. Polar Biol. 33, 257–270. doi:10.1007/s00300-009-0701-7

Manno, C., Bednaršek, N., Tarling, G.A., Peck, V.L., Comeau, S., Adhikari, D., Bakker, D.C.E., Bauerfeind, E., Bergan, A.J., Berning, M.I., Buitenhuis, E., Burridge, A.K., Chierici, M., Flöter, S., Fransson, A., Gardner, J., Howes, E.L., Keul, N., Kimoto, K., Kohnert, P., Lawson, G.L., Lischka, S., Maas, A., Mekkes, L., Oakes, R.L., Pebody, C., Peijnenburg, K.T.C.A., Seifert, M., Skinner, J., Thibodeau, P.S., Wall-Palmer, D., Ziveri, P., 2017. Shelled pteropods in peril: Assessing vulnerability in a high CO_2 ocean. Earth-Science Rev. 169, 132–145. doi:10.1016/j.earscirev.2017.04.005

Manno, C., Giglio, F., Stowasser, G., Fielding, S., Enderlein, P., Tarling, G.A., 2018. Threatened species drive the strength of the carbonate pump in the northern Scotia Sea. Nat. Commun. 1–7. doi:10.1038/s41467-018-07088-y

Manno, C., Peck, V.L., Tarling, G.A., 2016. Pteropod eggs released at high pCO_2 lack resilience to ocean acidification. Nat. Publ. Gr. 1–10. doi:10.1038/srep25752

Manno, C., Sandrini, S., Tositti, L., Accornero, A., 2007. First stages of degradation of *Limacina helicina* shells observed above the aragonite chemical lysocline in Terra Nova Bay (Antarctica). J. Mar. Syst. 68, 91–102. doi:10.1016/j.jmarsys.2006.11.002

Manno, C., Tirelli, V., Accornero, A., Fonda Umani, S., 2010. Importance of the contribution of Limacina helicina faecal pellets to the carbon pump in Terra Nova Bay (Antarctica). J. Plankton Res. 32, 145–152. doi:10.1093/plankt/fbp108

Marcus, L., Virtue, P., Nichols, P.D., Meekan, M.G., Pethybridge, H., 2017. Effects of sample treatment on the analysis of stable isotopes of carbon and nitrogen in zooplankton,

micronekton and a filter-feeding shark. Mar. Biol. 164, 124. doi:10.1007/s00227-017-3153-6

Matsuno, K., Yamaguchi, A., Fujiwara, A., Onodera, J., Watanabe, E., Imai, I., Chiba, S., Harada, N., Kikuchi, T., 2014. Seasonal changes in mesozooplankton swimmers collected by sediment trap moored at a single station on the Northwind Abyssal Plain in the western Arctic Ocean. J. Plankton Res. 36, 490–502. doi:10.1093/plankt/fbt092

McConnaughey, T., McRoy, C.P., 1979. Food-web structure and the fractionation of carbon isotopes in the Bering Sea. Mar. Biol. 53, 257–262. doi:10.1007/BF00952434

McCormack, S.A., Melbourne-Thomas, J., Trebilco, R., Blanchard, J.L., Constable, A., 2017. Simplification of complex ecological networks – species aggregation in Antarctic food web models, in: 22nd International Congress on Modelling and Simulation, Hobart, Tasmania, Australia, 3 to 8 December 2017. pp. 264–270.

McCormack, S.A., Trebilco, R., Blanchard, J.L., Fulton, E.A., Constable, A., 2019. Using stable isotope data to advance marine food web modelling. Rev. Fish Biol. Fish. 4, 1–20. doi:10.1007/s11160-019-09552-4

McCue, M.D., Pollock, E.D., 2008. Stable isotopes may provide evidence for starvation in reptiles. Rapid Commun. Mass Spectrom. 22, 2307–2314. doi:10.1002/rcm

McCutchan, J.H., Lewis, W.M., Kendall, C., McGrath, C.C., 2003. Variation in trophic shift for stable isotope ratios of carbon, nitrogen, and sulfur. Oikos 102, 378–390. doi:10.1034/j.1600-0706.2003.12098.x

McMurrich, J.P., 1886. Notes on the embryology of the gasteropods. Ann. Mag. Nat. Hist. 18, 76–78. doi:10.1080/00222938609459937

McNeil, B.I., Matear, R.J., 2008. Southern Ocean acidification: A tipping point at 450-ppm atmospheric CO_2. Proc. Natl. Acad. Sci. 105, 18860–18864. doi:10.1073/pnas.0806318105

Meinecke, G., Wefer, G., 1990. Seasonal pteropod sedimentation in the Norwegian Sea. Palaeogeogr. Palaeoclimatol. Palaeoecol. 79, 129–147. doi:10.1016/0031-0182(90)90109-K

Michaels, A.F., Silver, M.W., Gowing, M.M., Knauer, G.A., 1990. Cryptic zooplankton "swimmers" in upper ocean sediment traps. Deep Sea Res. Part A, Oceanogr. Res. Pap. 37, 1285–1296. doi:10.1016/0198-0149(90)90043-U

Minagawa, M., Wada, E., 1984. Stepwise enrichment of ^{15}N along food chains: Further evidence and the relation between $\delta^{15}N$ and animal age. Geochim. Cosmochim. Acta 48, 1135–1140. doi:10.1016/0016-7037(84)90204-7

Minutoli, R., Brugnano, C., Granata, A., Zagami, G., Guglielmo, L., 2017. Zooplankton electron transport system activity and biomass in the western Ross Sea (Antarctica) during austral summer 2014. Polar Biol. 40, 1197–1209. doi:10.1007/s00300-016-2043-6

Mohan, R., Verma, K., Mergulhao, L.P., Sinha, D.K., Shanvas, S., Guptha, M.V.S., 2006. Seasonal variation of pteropods from the Western Arabian Sea sediment trap. Geo-Marine Lett. 26, 265–273. doi:10.1007/s00367-006-0035-1

Moran, A.L., Woods, H.A., Shishido, C.M., Lane, S.J., Tobalske, B.W., 2018. Predatory behavior of giant Antarctic sea spiders (*Colossendeis*) in nearshore environments. Invertebr. Biol. 137, 116–123. doi:10.1111/ivb.12210

Morton, J.E.E., 1954. The Biology of *Limacina retroversa*. J. Mar. Assess. U.K. 3, 297–312. doi:10.1017/S002531540000833X

Moteki, M., Odate, T., Hosie, G.W., Takahashi, K.T., Swadling, K.M., Tanimura, A., 2017. Ecosystem studies in the Indian Ocean sector of the Southern Ocean undertaken by the training vessel Umitaka-maru. Polar Sci. 12, 1–4. doi:10.1016/j.polar.2017.04.002

Motoda, S., 1985. Devices of Simple Plankton Apparatus--VII. Bull. Mar. Sci. 37, 776–777.

Mucci, A., 1983. The solubility of calcite and aragonite in seawater at various salinities, temperatures, and one atmosphere total pressure. Am. J. Sci. 283, 780–799. doi:10.2475/ajs.283.7.780

Murphy, E.J., Cavanagh, R.D., Hofmann, E.E., Hill, S.L., Constable, A.J., Costa, D.P., Pinkerton, M.H., Johnston, N.M., Trathan, P.N., Klinck, J.M., Wolf-Gladrow, D.A., Daly, K.L., Maury, O., Doney, S.C., 2012. Developing integrated models of Southern Ocean food webs: Including ecological complexity, accounting for uncertainty and the importance of scale. Prog. Oceanogr. 102, 74–92. doi:10.1016/j.pocean.2012.03.006

Murry, B.A., Farrell, J.M., Teece, M.A., Smyntek, P.M., 2006. Effect of lipid extraction on the interpretation of fish community trophic relationships determined by stable carbon and nitrogen isotopes. Can. J. Fish. Aquat. Sci. 63, 2167–2172. doi:10.1139/f06-116

Newsome, S.D., Rio, Martinez del, C., Bearhop, S., Phillips, D.L., 2007. A niche for isotope ecology. Front. Ecol. Environ. 5, 429–436. doi:10.1890/060150.01

Nielsen, J.M., Clare, E.L., Hayden, B., Brett, M.T., Kratina, P., 2018. Diet tracing in ecology: Method comparison and selection. Methods Ecol. Evol. 9, 278–291. doi:10.1111/2041-210X.12869

Nishizawa, Y., Sasaki, H., Takahashi, K.T., 2016. Interannual variability in euthecosomatous pteropods (*Limacina* spp.) in the Indian sector of the Southern Ocean during austral summer. Antarct. Rec. 60, 35–48.

Noisette, F., Comtet, T., Legrand, E., Bordeyne, F., Davoult, D., Martin, S., 2014. Does encapsulation protect embryos from the effects of ocean acidification? The example of *Crepidula fornicata*. PLoS One 9, 1–11. doi:10.1371/journal.pone.0093021

Noji, T.T., Bathmann, U. V., Von Bodungen, B., Voss, M., Antia, A., Krumbholz, M., Klein, B., Peeken, I., Noji, C.I.M., Rey, F., 1997. Clearance of picoplankton-sized particles and formation of rapidly sinking aggregates by the pteropod, *Limacina retroversa*. J. Plankton Res. 19, 863–875. doi:10.1093/plankt/19.7.863

Oakes, R.L., Peck, V.L., Manno, C., Bralower, T.J., 2018. Impact of preservation techniques on pteropod shell condition. Polar Biol. 1. doi:10.1007/s00300-018-2419-x

Orr, J.C., Fabry, V.J., Aumont, O., Bopp, L., Doney, S.C., Feely, R.A., Gnanadesikan, A., Gruber, N., Ishida, A., Joos, F., Key, R.M., Lindsay, K., Maier-Reimer, E., Matear, R., Monfray, P., Mouchet, A., Najjar, R.G., Plattner, G.K., Rodgers, K.B., Sabine, C.L., Sarmiento, J.L., Schlitzer, R., Slater, R.D., Totterdell, I.J., Weirig, M.F., Yamanaka, Y., Yool, A., 2005. Anthropogenic ocean acidification over the twenty-first century and its impact on calcifying organisms. Nature 437, 681–686. doi:10.1038/nature04095

Orsi, A.H., Whitworth, T., Nowlin, W.D., 1995. On the meridional extent and fronts of the Antarctic Circumpolar Current. Deep. Res. Part I 42, 641–673. doi:10.1016/0967-0637(95)00021-W

Pakhomov, E.A., Froneman, P.W., 2004. Zooplankton dynamics in the eastern Atlantic sector of the Southern Ocean during the austral summer 1997/1998 - Part 2: Grazing impact. Deep. Res. Part II Top. Stud. Oceanogr. 51, 2617–2631. doi:10.1016/j.dsr2.2000.11.002

Pakhomov, E.A., Perissinotto, R., McQuaid, C.D., 1996. Prey composition and daily rations of myctophid fishes in the Southern Ocean. Mar. Ecol. Prog. Ser. 134, 1–14. doi:10.3354/meps134001

Pane, L., Feletti, M., Francomacaro, B., Mariottini, G.L., 2004. Summer coastal zooplankton biomass and copepod community structure near the Italian Terra Nova Base (Terra Nova Bay, Ross Sea, Antarctica). J. Plankton Res. 26, 1479–1488. doi:10.1093/plankt/fbh135

Paranjape, M.A., 1968. The egg mass and veligers of *Limacina helicina* Phipps, in: Veliger. pp. 322–326.

Peck, V.L., Oakes, R.L., Harper, E.M., Manno, C., Tarling, G.A., 2018. Pteropods counter mechanical damage and dissolution through extensive shell repair. Nat. Commun. 9. doi:10.1038/s41467-017-02692-w

Perissinotto, R., 1992. Mesozooplankton size-selectivity and grazing impact on the phytoplankton community of the Prince Edward Archipelago (Southern Ocean). Mar. Ecol. Prog. Ser. 79, 243–258. doi:10.3354/meps079243

Perry, A.L., Low, P.J., Ellis, J.R., Reynolds, J.D., 2005. Climate change and distribution shifts in marine fishes. Science 308, 1912–5. doi:10.1126/science.1111322

Peterson, B., Fry, B., 1987. Stable isotopes in ecosystem studies. Ann. Rev. Ecol. Syst. 18, 293–320. doi:10.1146/annurev.es.18.110187.001453

Phleger, C.F., Nelson, M.M., Mooney, B., Nichols, P.D., 1999. Lipids of abducted Antarctic pteropods, *Spongiobranchaea australis*, and their hyperiid amphipod host. Comp. Biochem. Physiol. Part B Biochem. Mol. Biol. 124, 295–307. doi:10.1016/S0305-0491(99)00120-0

Phleger, C.F., Nelson, M.M., Mooney, B.D., Nichols, P.D., 2001. Interannual variations in the lipids of the Antarctic pteropods *Clione limacina* and *Clio pyramidata*. Comp. Biochem. Physiol. - B Biochem. Mol. Biol. 128, 553–564. doi:10.1016/S1096-4959(00)00356-0

Phleger, C.F., Nichols, P.D., Virtue, P., 1997. Lipids and buoyancy in Southern Ocean pteropods. Lipids 32, 1093–1100. doi:10.1007/s11745-997-0141-x

Pinnegar, J.K., Polunin, N.V.C., 1999. Differential fractionation of $\delta^{13}C$ and $\delta^{15}N$ among fish tissues: Implications for the study of trophic interactions. Funct. Ecol. 13, 225–231. doi:10.1046/j.1365-2435.1999.00301.x

Pomerleau, C., Winkler, G., Sastri, A., Nelson, R.J., Williams, W.J., 2014. The effect of acidification and the combined effects of acidification/lipid extraction on carbon stable isotope ratios for sub-arctic and arctic marine zooplankton species. Polar Biol. 37, 1541–1548. doi:10.1007/s00300-014-1540-8

Post, D.M., 2002. Using stable isotopes to estimate trophic position: models, methos, and assumptions. . Ecology 83, 703–718. doi:Doi 10.2307/3071875

Post, D.M., Layman, C.A., Arrington, D.A., Takimoto, G., Quattrochi, J., Montaña, C.G., 2007. Getting to the fat of the matter: Models, methods and assumptions for dealing with lipids in stable isotope analyses. Oecologia 152, 179–189. doi:10.1007/s00442-006-0630-x

Quezada-Romegialli, C., Jackson, A.L., Hayden, B., Kahilainen, K.K., Lopes, C., Harrod, C., 2018. tRophicPosition, an r package for the Bayesian estimation of trophic position from consumer stable isotope ratios. Methods Ecol. Evol. 9, 1592–1599. doi:10.1111/2041-210X.13009

Raby, D., Lagadeuc, Y., Dodson, J.J., Mingelbier, M., 1994. Relationship between feeding and vertical distribution of bivalve larvae in stratified and mixed waters. Mar. Ecol. Prog. Ser. 103, 275–284. doi:10.3354/meps103275

Rembauville, M., Meilland, J., Ziveri, P., Schiebel, R., Blain, S., Salter, I., 2016. Planktic foraminifer and coccolith contribution to carbonate export fluxes over the central Kerguelen Plateau. Deep Sea Res. Part I Oceanogr. Res. Pap. 111, 91–101. doi:10.1016/j.dsr.2016.02.017

Richoux, N.B., Froneman, P.W., 2009. Plankton trophodynamics at the subtropical convergence,

Southern Ocean. J. Plankton Res. 31, 1059–1073. doi:10.1093/plankt/fbp054

Rines, J.E.B., McFarland, M.N., Donaghay, P.L., Sullivan, J.M., 2010. Thin layers and species-specific characterization of the phytoplankton community in Monterey Bay, California, USA. Cont. Shelf Res. 30, 66–80. doi:10.1016/j.csr.2009.11.001

Rintoul, S.R., 2018. The global influence of localized dynamics in the Southern Ocean. Nature 558, 209–218. doi:10.1038/s41586-018-0182-3

Roberts, D., Hopcroft, R.R., Hosie, G.W., 2014. Southern Ocean Pteropods, in: De Broyer, C., Koubbi, P., Griffiths, H., Raymond, B., d'Udekem d'Acoz, C., Van de Putte, A., Danis, B., David, B., Grant, S., Gutt, J., Held, C., Hosie, G., Huettmann, F., Post, A., Ropert-Coudert, Y. (Eds.), SCAR-Marine Biodiversity Information Network Biogeographic Atlas of the Southern Ocean. Scientific Committee on Antarctic Research, Cambridge, pp. 276–283.

Roberts, D., Howard, W.R., Moy, A.D., Hopcroft, R.R., 2011. Interannual pteropod variability in sediment traps deployed above and below the aragonite saturation horizon in the Sub-Antarctic Southern Ocean. Polar Biol. 3, 1739–1750. doi:10.1007/s00300-011-1024-z

Roberts, Donna, Howard, W.R., Roberts, J.L., Bray, S.G., Moy, A.D., Trull, T.W., Hopcroft, R.R., 2014. Diverse trends in shell weight of three Southern Ocean pteropod taxa collected with Polar Frontal Zone sediment traps from 1997 to 2007. Polar Biol. 37, 1445–1458. doi:10.1007/s00300-014-1534-6

Ropert-Coudert, Y., Chiaradia, A., Ainley, D., Barbosa, A., Boersma, P.D., Brasso, R., Dewar, M., Ellenberg, U., García-Borboroglu, P., Emmerson, L., Hickcox, R., Jenouvrier, S., Kato, A., McIntosh, R.R., Lewis, P., Ramírez, F., Ruoppolo, V., Ryan, P.G., Seddon, P.J., Sherley, R.B., Vanstreels, R.E.T., Waller, L.J., Woehler, E.J., Trathan, P.N., 2019. Happy Feet in a hostile world? The future of penguins depends on proactive management of current and expected threats. Front. Mar. Sci. 6. doi:10.3389/fmars.2019.00248

Rosati, J.Y., Pacheco, V.A., Vankosky, M.A., Vanlaerhoven, S.L., 2015. Estimating the number of eggs in blow fly (Diptera: Calliphoridae) egg masses using photographic analysis. J. Med. Entomol. 52, 658–662. doi:10.1093/jme/tjv053

Ross, R.M., Quetin, L.B., Lascara, C., 1996. Distribution of Antarctic krill and dominant zooplankton west of the Antarctic Peninsula. Found. Ecol. Res. west Antarct. Penins. 70, 199–217. doi:10.1029/AR070p0199

Ross, R.M., Quetin, L.B., Martinson, D.G., Iannuzzi, R.A., Stammerjohn, S.E., Smith, R.C., 2008. Palmer LTER: Patterns of distribution of five dominant zooplankton species in the epipelagic zone west of the Antarctic Peninsula, 1993-2004. Deep. Res. Part II Top. Stud. Oceanogr. 55, 2086–2105. doi:10.1016/j.dsr2.2008.04.037

Runge, J.A., 1987. Measurement of egg production rate of *Calanus finmarchicus* from preserved samples. Can. J. Fish. Aquat. Sci. 44, 2009–2012.

Ryan, C., McHugh, B., Trueman, C.N., Harrod, C., Berrow, S.D., O'Connor, I., 2012. Accounting for the effects of lipids in stable isotope ($\delta^{13}C$ and $\delta^{15}N$ values) analysis of skin and blubber of balaenopterid whales. Rapid Commun. Mass Spectrom. 26, 2745–2754. doi:10.1002/rcm.6394

Ryan, K.G., Tay, M.L., Martin, A., McMinn, A., Davy, S.K., 2011. Chlorophyll fluorescence imaging analysis of the responses of Antarctic bottom-ice algae to light and salinity during melting. J. Exp. Mar. Bio. Ecol. 399, 156–161. doi:10.1016/j.jembe.2011.01.006

Sabine, C.L., Feely, R.A., Gruber, N., Key, R.M., Lee, K., Bullister, J.L., Wanninkhof, R., Wong, C.S., Wallace, D.W.R., Tilbrook, B., Millero, F.J., Peng, T.-H., Kozyr, A., Ono, T., Rios, A.F., 2004. The oceanic sink for anthropogenic CO_2. Science 305, 367–71. doi:10.1126/science.1097403

Sackett, O., Petrou, K., Reedy, B., Grazia, A. De, Hill, R., Doblin, M., Ralph, P., Heraud, P., 2013. Phenotypic plasticity of Southern Ocean diatoms: key to success in the sea ice habitat? PLoS One 8, e81185. doi:10.1371/journal.pone.0081185

Sakurai, H., Moteki, M., Mizobata, K., Shimada, K., Matsuno, K., Okubo, Y., Sano, M., Nirazuka, S., Yamamoto, N., Takao, S., Makabe, R., Takahashi, K., Odate, T., 2018. JARE Data Reports, No. 363 (Marine Biology 64), February 2018. JARE Data Reports 363, 1–13.

Saunders, R.A., Collins, M.A., Shreeve, R., Ward, P., Stowasser, G., Hill, S.L., Tarling, G.A., 2018. Seasonal variation in the predatory impact of myctophids on zooplankton in the Scotia Sea (Southern Ocean). Prog. Oceanogr. 168, 123–144. doi:10.1016/j.pocean.2018.09.017

Schallenberg, C., Bestley, S., Klocker, A., Trull, T.W., Davies, D.M., Gault-Ringold, M., Eriksen, R., Roden, N.P., Sander, S.G., Sumner, M., Townsend, A.T., van der Merwe, P., Westwood, K., Wuttig, K., Bowie, A., 2018. Sustained upwelling of subsurface iron supplies seasonally persistent phytoplankton blooms around the southern Kerguelen Plateau, Southern Ocean. J. Geophys. Res. Ocean. 123, 5986–6003. doi:10.1029/2018JC013932

Schindelin, J., Arganda-Carreras, I., Frise, E., Kaynig, V., Longair, M., Pietzsch, T., Preibisch, S., Rueden, C., Saalfeld, S., Schmid, B., Tinevez, J.-Y., White, D.J., Hartenstein, V., Eliceiri, K., Tomancak, P., Cardona, A., 2012. Fiji: an open-source platform for biological-image analysis. Nat. Methods 9, 676–682. doi:10.1038/nmeth.2019

Schmidt, K., Atkinson, A., Stübing, D., McClelland, J.W., Montoya, J.P., Voss, M., 2003. Trophic relationships among Southern Ocean copepods and krill: Some uses and limitations of a

stable isotope approach. Limnol. Oceanogr. 48, 277–289. doi:10.4319/lo.2003.48.1.0277

Seibel, B.A., Dierssen, H.M., 2003. Cascading trophic impacts of reduced biomass in the Ross Sea, Antarctica: Just the tip of the iceberg? Biol. Bull. 205, 93–97. doi:10.2307/1543229

Seibel, B.A., Maas, A.E., Dierssen, H.M., 2012. Energetic plasticity underlies a variable response to ocean acidification in the pteropod, *Limacina helicina antarctica*. PLoS One 7. doi:10.1371/journal.pone.0030464

Sexton, J.P., Montiel, J., Shay, J.E., Stephens, M.R., Slatyer, R.A., 2017. Evolution of ecological niche breadth. Annu. Rev. Ecol. Evol. Syst. 48, 183–206. doi:10.1146/annurev-ecolsys-110316-023003

Singh, A.D., Conan, S.M.H., 2008. Aragonite pteropod flux to the Somali Basin, NW Arabian Sea. Deep. Res. Part I Oceanogr. Res. Pap. 55, 661–669. doi:10.1016/j.dsr.2008.02.008

Skinner, M.M., Martin, A.A., Moore, B.C., 2016. Is lipid correction necessary in the stable isotope analysis of fish tissues? Rapid Commun. Mass Spectrom. 30, 881–889. doi:10.1002/rcm.7480

Smyntek, P.M., Teece, M.A., Schulz, K.L., Thackeray, S.J., 2007. A standard protocol for stable isotope analysis of zooplankton in aquatic food web research using mass balance correction models. Limnol. Oceanogr. 52, 2135–2146. doi:10.4319/lo.2007.52.5.2135

Sokolov, S., Rintoul, S.R., 2009. Circumpolar structure and distribution of the antarctic circumpolar current fronts: 2. Variability and relationship to sea surface height. J. Geophys. Res. Ocean. 114, 1–15. doi:10.1029/2008JC005248

Soler, G.A., Edgar, G.J., Stuart-Smith, R.D., Smith, A.D.M., Thomson, R.J., 2016. Predicting the diet of coastal fishes at a continental scale based on taxonomy and body size. J. Exp. Mar. Bio. Ecol. 480, 1–7. doi:10.1016/j.jembe.2016.03.017

Stark, J.S., Raymond, T., Deppeler, S.L., Morrison, A.K., 2019. Antarctic Seas, Second Edi. ed, World Seas: an Environmental Evaluation. Elsevier Ltd. doi:10.1016/B978-0-12-805068-2.00002-4

Suprenand, P.M., Ainsworth, C.H., 2017. Trophodynamic effects of climate change-induced alterations to primary production along the western Antarctic Peninsula. Mar. Ecol. Prog. Ser. 569, 37–54. doi:10.3354/meps12100

Svensson, E., Schouten, S., Hopmans, E.C., Middelburg, J.J., Damsté, J.S.S., 2016. Factors controlling the stable nitrogen isotopic composition ($\delta^{15}N$) of Lipids in Marine Animals. PLoS One 11, 1–12. doi:10.1371/journal.pone.0146321

Swanson, H.K., Lysy, M., Power, M., Stasko, A.D., Johnson, J.D., Reist, J.D., 2014. A new probabilistic method for quantifying *n*-dimensional ecological niches and niche overlap.

Ecology 96, 318–324. doi:10.1890/14-0235.1

Sweeting, C.J., Polunin, N.V.C., Jennings, S., 2006. Effects of chemical lipid extraction and arithmetic lipid correction on stable isotope ratios of fish tissues. Rapid Commun. Mass Spectrom. 20, 595–601. doi:10.1002/rcm.2347

Syväranta, J., Lensu, A., Marjomäki, T.J., Oksanen, S., Jones, R.I., 2013. An empirical evaluation of the utility of convex hull and standard ellipse areas for assessing population niche widths from stable isotope data. PLoS One 8, e56094. doi:10.1371/journal.pone.0056094

Syväranta, J., Rautio, M., 2010. Zooplankton, lipids and stable isotopes: importance of seasonal, latitudinal, and taxonomic differences. Can. J. Fish. Aquat. Sci. 67, 1721–1729. doi:10.1139/F10-091

Tarling, G.A., Ward, P., Thorpe, S.E., 2017. Spatial distributions of Southern Ocean mesozooplankton communities have been resilient to long-term surface warming. Glob. Chang. Biol. 1–11. doi:10.1111/gcb.13834

Tarroux, A., Lowther, A.D., Lydersen, C., Kovacs, K.M., 2016. Temporal shift in the isotopic niche of female Antarctic fur seals from Bouvetøya. Polar Res. 35, 1–11. doi:10.3402/polar.v35.31335

Team, R.C., 2014. R: A language and environment for statistical computing.

Teniswood, C.M.H., Roberts, D., Howard, W.R., Bray, S.G., Bradby, J.E., 2016. Microstructural shell strength of the Subantarctic pteropod *Limacina helicina antarctica*. Polar Biol. 39, 1643–1652. doi:10.1007/s00300-016-1888-z

Thabet, A.A., Maas, A.E., Lawson, G.L., Tarrant, A.M., 2015. Life cycle and early development of the thecosomatous pteropod *Limacina retroversa* in the Gulf of Maine, including the effect of elevated CO_2 levels. Mar. Biol. 162, 2235–2249. doi:10.1007/s00227-015-2754-1

Thibodeau, P.S., Steinberg, D.K., Stammerjohn, S.E., Hauri, C., 2019. Environmental controls on pteropod biogeography along the Western Antarctic Peninsula. Limnol. Oceanogr. 64, S240–S256. doi:10.1002/lno.11041

Thomson, P.G., Davidson, A.T., Maher, L., 2016. Increasing CO_2 changes community composition of pico- and nano-sized protists and prokaryotes at a coastal Antarctic site. Mar. Ecol. Prog. Ser. 554, 51–69. doi:10.3354/meps11803

Tieszen, L.L., Boutton, T.W., Tesdahl, K.G., Slade, N.A., 1983. Fractionation and turnover of stable carbon isotopes in animal tissues: Implications for $\delta^{13}C$ analysis of diet. Oecologia 57, 32–37. doi:10.1007/BF00379558

Timms, B. V., Lindsay, S., 2011. Morphometrics of the resting eggs of the fairy shrimp *Branchinella* in Australia (Anostraca: Thamnocephalidae). Proc. Linn. Soc. New South wales

133, 52–68.

Tremblay, M., Sinclair, M., 2007. Sea scallop larvae *Placopecten magellanicus* on Georges Bank: vertical distribution in relation to water column stratification and food. Mar. Ecol. Prog. Ser. 61, 1–15. doi:10.3354/meps061001

Trimborn, S., Thoms, S., Bischof, K., Beszteri, S., 2019. Susceptibility of two Southern Ocean phytoplankton key species to iron limitation and high light. Front. Mar. Sci. 6. doi:10.3389/fmars.2019.00167

Tsurumi, M., Mackas, D.L., Whitney, F.A., DiBacco, C., Galbraith, M.D., Wong, C.S., 2005. Pteropods, eddies, carbon flux, and climate variability in the Alaska Gyre. Deep. Res. Part II Top. Stud. Oceanogr. 52, 1037–1053. doi:10.1016/j.dsr2.2005.02.005

Turner, T.F., Collyer, M.L., Krabbenhoft, T.J., 2010. A general hypothesis-testing framework for stable isotope ratios in ecological studies. Ecology 91, 2227–2233. doi:10.1890/09-1454.1

Urban, M.C., Tewksbury, J.J., Sheldon, K.S., 2012. On a collision course: competition and dispersal differences create no-analogue communities and cause extinctions during climate change. Proc. R. Soc. B Biol. Sci. 279, 2072–2080. doi:10.1098/rspb.2011.2367

van der Spoel, S., Dadon, J.R., Boltovskoy, D., 1999. South Atlantic Zooplankton, Vol.1, in: Boltovskoy, D. (Ed.), South Atlantic Zooplankton, Vol.1. Backhuys Publishers, Leiden, pp. 649–706.

Van Valen, L., 1965. Morphological variation and width of ecological niche. Am. Nat. 99, 377–390. doi:10.1086/282379

Vanderklift, M.A., Ponsard, S., 2003. Sources of variation in consumer-diet $\delta^{15}N$ enrichment: a meta-analysis. Oecologia 136, 169–182. doi:10.1007/s00442-003-1270-z

Venables, W.N., Ripley, B.D., 2002. Random and Mixed Effects, in: Modern Applied Statistics with S. Springer New York, New York, NY, pp. 271–300. doi:10.1007/978-0-387-21706-2_10

Vizzini, S., Martínez-Crego, B., Andolina, C., Massa-Gallucci, A., Connell, S.D., Gambi, M.C., 2017. Ocean acidification as a driver of community simplification via the collapse of higher-order and rise of lower-order consumers. Sci. Rep. 7, 1–10. doi:10.1038/s41598-017-03802-w

Wakabayashi, K., 2017. Embryonic development of the sea butterfly *Desmopterus papilio* (Gastropoda: Thecosomata). Invertebr. Reprod. Dev. 61, 142–146. doi:10.1080/07924259.2017.1311952

Walther, G., Post, E., Convey, P., Menzel, A., Parmesan, C., Beebee, T.J.C., Fromentin, J., I, O.H., Bairlein, F., 2002. Ecological responses to recent climate change. Nature 416, 389–

395.

Wang, K., Hunt, B.P.V., Liang, C., Pauly, D., Pakhomov, E.A., 2017. Reassessment of the life cycle of the pteropod *Limacina helicina* from a high resolution interannual time series in the temperate North Pacific. ICES J. Mar. Sci. 74, 1906–1920. doi:10.1093/icesjms/fsx014

Weldrick, C.K., Trebilco, R., Swadling, K.M., 2019. Can lipid removal affect interpretation of resource partitioning from stable isotopes in Southern Ocean pteropods? Rapid Commun. Mass Spectrom. 569–578. doi:10.1002/rcm.8384

Willis, K., Cottier, F., Kwasniewski, S., Wold, A., Falk-Petersen, S., 2006. The influence of advection on zooplankton community composition in an Arctic fjord (Kongsfjorden, Svalbard). J. Mar. Syst. 61, 39–54. doi:10.1016/j.jmarsys.2005.11.013

Wong, C.S., Whitney, F.A., Crawford, D.W., Iseki, K., Matear, R.J., Johnson, W.K., Page, J.S., Timothy, D., 1999. Seasonal and interannual variability in particle fluxes of carbon, nitrogen and silicon from time series of sediment traps at Ocean Station P, 1982-1993: Relationship to changes in subarctic primary productivity. Deep. Res. Part II Top. Stud. Oceanogr. 46, 2735–2760. doi:10.1016/S0967-0645(99)00082-X

Wood, S.N., 2006. Generalized additive models : An introduction with R. Chapman & Hall/CRC.

Wormuth, J.H., 1981. Vertical distributions and diel migrations of Euthecosomata in the northwest Sargasso Sea. Deep Sea Res. Part A, Oceanogr. Res. Pap. 28, 1493–1515. doi:10.1016/0198-0149(81)90094-7

Xavier, J.C., Brandt, A., Ropert-Coudert, Y., Badhe, R., Gutt, J., Havermans, C., Jones, C., Costa, E.S., Lochte, K., Schloss, I.R., Kennicutt, M.C., Sutherland, W.J., 2016. Future Challenges in Southern Ocean Ecology Research. Front. Mar. Sci. 3, 1–9. doi:10.3389/fmars.2016.00094

Yamamoto-Kawai, M., McLaughlin, F.A., Carmack, E.C., Nishino, S., Shimada, K., Taylor, P.C., Rodger, P.M., Kusalik, P.G., 2009. Aragonite Undersaturation in the Arctic Ocean: Effects of Ocean Acidification and Sea Ice Melt. Science (80-.). 326, 2–4.

Zhang, Ye, Li, C., Yang, G., Wang, Y., Tao, Z., Zhang, Yongshan, Wang, A., 2017. Ontogenetic diet shift in Antarctic krill (*Euphausia superba*) in the Prydz Bay: a stable isotope analysis. Acta Oceanol. Sin. 36, 67–78. doi:10.1007/s13131-017-1049-4

Appendix A

Supplementary materials for Chapter 2

A.1 Supplementary Tables

Table A.1 Averages (± SD) of $\delta^{13}C$ values (‰), $\delta^{15}N$ values (‰) and C:N ratio of untreated samples (bulk) and those chemically treated by lipid extraction (LE) prior to stable isotopes analysis, for different sampling stations. $\Delta\delta^{13}C$ values refer to the difference between LE and bulk $\delta^{13}C$ values. Sample sizes (n) are divided into b = bulk and le = lipid extracted.

Species	station	*n*	$\delta^{13}C_{bulk}$	$\delta^{13}C_{LE}$	$\delta^{15}N_{bulk}$	$\delta^{15}N_{LE}$	$C:N_{bulk}$	$C:N_{LE}$	$\Delta\delta^{13}C$
Clio pyramidata	3	b: 4 le: 2	-28.6 ± 0.4	-25.8 ± 0.5	3.1 ± 0.4	4.2 ± 0.9	4.4 ± 0.5	3.3 ± 0.0	+2.9
	5	b: 8 le: 2	-27.8 ± 0.3	-25.8 ± 0.2	3.4 ± 0.6	4.2 ± 0.1	3.9 ± 0.4	3.4 ± 0.2	+2.0
	12	b: 2 le: 2	-29.1 ± 1.0	-25.4 ± 0.1	3.6 ± 0.3	5.6 ± 0.0	4.2 ± 0.2	3.2 ± 0.0	+3.7
	14	b: 8 le: 13	-27.2 ± 0.3	-25.3 ± 0.5	4.5 ± 0.5	4.4 ± 0.7	3.7 ± 0.1	3.3 ± 0.1	+1.9
	18	b: 3 le: 2	-27.1 ± 0.4	-25.6 ± 0.5	3.5 ± 0.3	3.8 ± 0.1	4.1 ± 0.1	3.6 ± 0.0	+1.6
	29	b: 9 le: 5	-28.2 ± 0.7	-25.2 ± 0.4	3.6 ± 0.9	5.3 ± 0.7	4.1 ± 0.7	3.3 ± 0.0	+3.0

	39	b: 9 le: 3	-27.6 ± 0.8	-25.3 ± 0.4	3.8 ± 0.6	5.2 ± 0.9	3.7 ± 0.1	3.2 ± 0.0	+2.3
	45	b: 4 le: 2	-28.6 ± 0.9	-26.7 ± 0.0	4.1 ± 1.2	4.4 ± 0.4	4.1 ± 0.4	3.3 ± 0.1	+1.9
Clione antarctica	22	b: 3 le: 1	-29.0 ± 0.3	-24.5 ± 0.0	4.4 ± 0.2	7.0 ± 0.0	7.4 ± 0.6	3.3 ± 0.0	+4.5
	43	b: 3 le: 3	-29.5 ± 0.7	-27.0 ± 0.3	4.7 ± 1.4	5.1 ± 0.4	7.1 ± 0.8	4.0 ± 0.0	+2.5
	47	b: 4 le: 2	-28.2 ± 0.4	-27.4 ± 0.0	4.1 ± 0.3	6.3 ± 0.0	7.1 ± 0.5	4.1 ± 0.0	+0.9
Spongiobranchaea australis	40	b: 4 le: 1	-28.0 ± 1.1	-24.0 ± 0.0	5.3 ± 0.3	6.3 ± 0.0	5.2 ± 0.0	3.3 ± 0.0	+4.0
Average		b: 61 le: 38	-28.3 ± 0.8	-25.7 ± 1.0	4.0 ± 0.6	5.1 ± 0.9	5.0 ± 1.5	3.4 ± 0.2	2.6 ± 1.1

Table A.2 One-way MANOVA hypothesis test output for dependent response variables ($\delta^{13}C$ and $\delta^{15}N$ values) and independent variables, species, and treatment (lipid extraction vs. no lipid extraction).

$\delta^{13}C$ x $\delta^{15}N$	Wilk's λ	*F* (df)	*P*
Site	0.367	5.35 (18,148)	1.9x10-9
Species	0.318	28.58 (4,148)	2.2x10-16
Treatment	0.198	150.09 (2,74)	2.2x10-16
Treatment x Species	0.841	3.346 (4,148)	0.012

Table A.3 Summary of multiple pairwise-comparisons made between (1) corrected bulk $\delta^{13}C$ value means derived from each normalization model with the corrected mean derived from our average offset value, and (2) the mean difference between bulk and corrected $\delta^{13}C$ values ($\Delta\delta^{13}C$) derived from each normalization model with the $\Delta\delta^{13}C$ values derived from our average offset value (statistical significance at $\alpha = 0.05$). Details of studied taxa originally used to develop each model are also listed here.

Model	Taxa	Multiple comparison (1)		Multiple comparison (2)	
		Mean $\delta^{13}C_{corr}$	*p*-value	Mean $\Delta\delta^{13}C_{corr}$	*p*-value
This study	Pteropods	-25.66 ± 0.9	--	2.4 ± 0.2	--
Kiljunen et al. (2006)	Marine, freshwater, brackish fishes	-25.80 ± 1.0	0.793	2.3 ± 0.7	0.328
Logan et al. (2008)	Marine & freshwater invertebrates	-27.46 ± 0.9	<0.001	0.6 ± 0.3	<0.001
Post et al. (2007)	Various, aquatic	-27.28 ± 1.1	<0.001	0.8 ± 0.9	<0.001
Smyntek et al. (2007)	Freshwater zooplankton	-26.25 ± 0.9	<0.001	1.8 ± 0.6	<0.001
Syväranta & Rautio (2010)	Freshwater zooplankton	-25.38 ± 1.0	0.073	2.7 ± 0.8	<0.001

Table A.4 Niche analysis summary statistics for each treatment and normalization formula and pteropod species. TA = total area, SEA = standard area ellipse, SEA_c = corrected standard ellipse area (corrected for small sample sizes). Numbers in brackets are Bayesian probability (*p*-value) that metric is larger than that corrected by our average offset value.

Model correction	Summary statistic	*C. pyramidata*	*C. antarctica*	*S. australis*
Bulk	TA	11.50	6.84	1.10
	SEA	1.83 (0.66)	2.42 (0.51)	0.75 (0.50)
	SEAc	1.84	2.58	0.90
This study	TA	9.14	6.84	1.10
	SEA	1.73	2.42	0.75
	SEAc	1.74	2.58	0.90
Kiljunen et al. (2006)	TA	8.78	3.97	0.87
	SEA	1.71 (0.44)	1.59 (0.11)	0.64 (0.38)
	SEAc	1.72	1.69	0.77
Post et al. (2007)	TA	8.73	5.19	0.75
	SEA	1.70 (0.44)	2.17 (0.34)	0.61 (0.34)
	SEAc	1.71	2.26	0.73
Smyntek et al. (2007)	TA	8.78	4.20	0.88
	SEA	1.70(0.43)	1.67 (0.15)	0.64 (0.38)
	SEAc	1.71	1.78	0.77
Logan et al. (2008)	TA	8.77	4.78	0.97

	SEA	1.69 (0.41)	1.68 (0.15)	0.69 (0.44)
	SEAc	1.71	1.79	0.82
(Syväranta and Rautio, 2010)	TA	8.98	5.66	0.77
	SEA	1.75 (0.54)	2.34 (0.45)	0.60 (0.34)
	SEAc	1.76	2.50	0.72

Appendix B

Supplementary materials for Chapter 3

B.1 Supplementary Tables

Table B.1 Summary of multivariate analysis of variance (MANOVA) results for isotopic variations among bulk samples.

Source of variation	$\delta^{13}C$ (‰)				$\delta^{15}N$ (‰)			
	df	SS	MS	*F*	*df*	SS	MS	*F*
Latitude	1	0.39	0.39	0.71^{NS}	1	0.90	0.90	2.71^{NS}
Longitude	1	2.44	2.44	4.42*	1	4.51	4.51	13.50***
Depth	1	2.06	2.06	3.72^{NS}	1	1.32	1.32	3.94*
Species	2	1.36	0.68	1.23^{NS}	2	18.62	9.31	27.84***
Latitude x longitude	1	16.17	16.17	29.25***	1	0.15	0.15	0.44^{NS}
Latitude x depth	1	0.001	0.001	0.002^{NS}	1	2.13	2.13	6.37*
Longitude x depth	1	0.05	0.05	0.09^{NS}	1	0.46	0.46	1.37^{NS}
Latitude x species	2	5.58	2.80	5.05**	2	0.89	0.44	1.33^{NS}
Longitude x species	2	0.39	0.20	0.35^{NS}	2	0.16	0.08	0.24^{NS}

Depth x species	1	1.26	1.26	2.28^{NS}	1	1.18	1.18	3.54^{NS}
Latitude x longitude x depth	1	18.49	18.49	33.46***	1	0.01	0.01	0.01^{NS}
Latitude x longitude x species	1	0.99	0.99	1.79^{NS}	1	0.02	0.02	0.06^{NS}
Latitude x depth x species	1	0.99	0.99	1.80^{NS}	1	1.29	1.29	3.87^{NS}
Longitude x depth x species	1	2.66	2.66	4.80*	1	2.72	2.72	8.14**
Full model	1	0.15	0.15	0.27^{NS}	1	2.57	2.57	7.68**
Residuals	146	80.69	0.55		146	48.80	0.33	

* $P<0.05$; ** $P<0.01$; *** $P<0.001$; *NS* no significant difference

Table B.2 Total area (TA), standard ellipse area (SEA), and SEA corrected for small sample size (SEAc) for each pteropod species and large- and small-fraction POM.

	C. pyramidata	*C. antarctica*	*S. australis*	POM (large)	POM (small)
TA (‰^{2})	7.90	8.15	4.19	1.86	2.18
SEA (‰^{2})	1.66	2.55	2.22	1.22	1.47
SEAc (‰^{2})	1.67	2.67	2.53	1.46	1.71

Table B.3 Niche overlap metric estimates (%) of 10,000 Monte Carlo sampling draws from the prior parameters. Values represent calculations made at 95 and 99 % probabilistic niche region (PNR; α = 0.95, 0.99).

		C. pyramidata	*C. antarctica*	*S. australis*	POM (large)	POM (small)
PNR: 95%	*C. pyramidata*	--	85.60	47.95	0.19	0.14
	C. antarctica	68.35	--	62.44	0.05	0.06
	S. australis	49.68	79.47	--	0.02	0.00
	POM (large)	0.13	0.35	0.03	--	82.68
	POM (small)	0.12	0.32	0.00	74.03	--
PNR: 99%	*C. pyramidata*	--	95.00	64.81	0.65	0.74
	C. antarctica	83.87	--	75.02	0.79	0.86
	S. australis	71.04	89.93	--	0.05	0.03
	POM (large)	0.36	1.37	0.05	--	90.92
	POM (small)	0.40	1.73	0.01	85.00	--

Table B.4 Details of sampling net, mean length (body or shell), length-to-weight equation used (described in Bednaršek et al. 2012), total abundance, and carbon biomass (a product of abundance and DW) estimates for each pteropod species.

Species	RMT	Mean length (mm±SD)	DW Equation	Abundance (ind. m^{-3})	Biomass (mg C m^{-3})	Study
C. pyramidata	8	15.5 (4.3)	$DW = [0.2152 \cdot L^{2.293}] \cdot 0.28$	0.06	1.78	This study
C. antarctica	8	17.8 (3.6)	$DW = [10^{(2.533 \cdot \log(L) - 3.89095) \cdot 10^3}] \cdot 0.28$	0.003	0.005	This study
L. helicina (juvenile)	1	0.44 (0.06)	$DW = 0.137 \cdot D^{1.5005}$	2.69	0.107	Matsuno et al. submitted
L. retroversa	1	1.51 (0.04)	$DW = [0.000194 \cdot L^{2.5473}] \cdot 0.28$	0.14	$2.10e^{-05}$	Matsuno et al. submitted
S. australis	8	14.1 (2.4)	$DW = [10^{(2.533 \cdot \log(L) - 3.89095) \cdot 10^3}] \cdot 0.28$	0.0002	0.0004	This study

B.2 Supplementary Figures

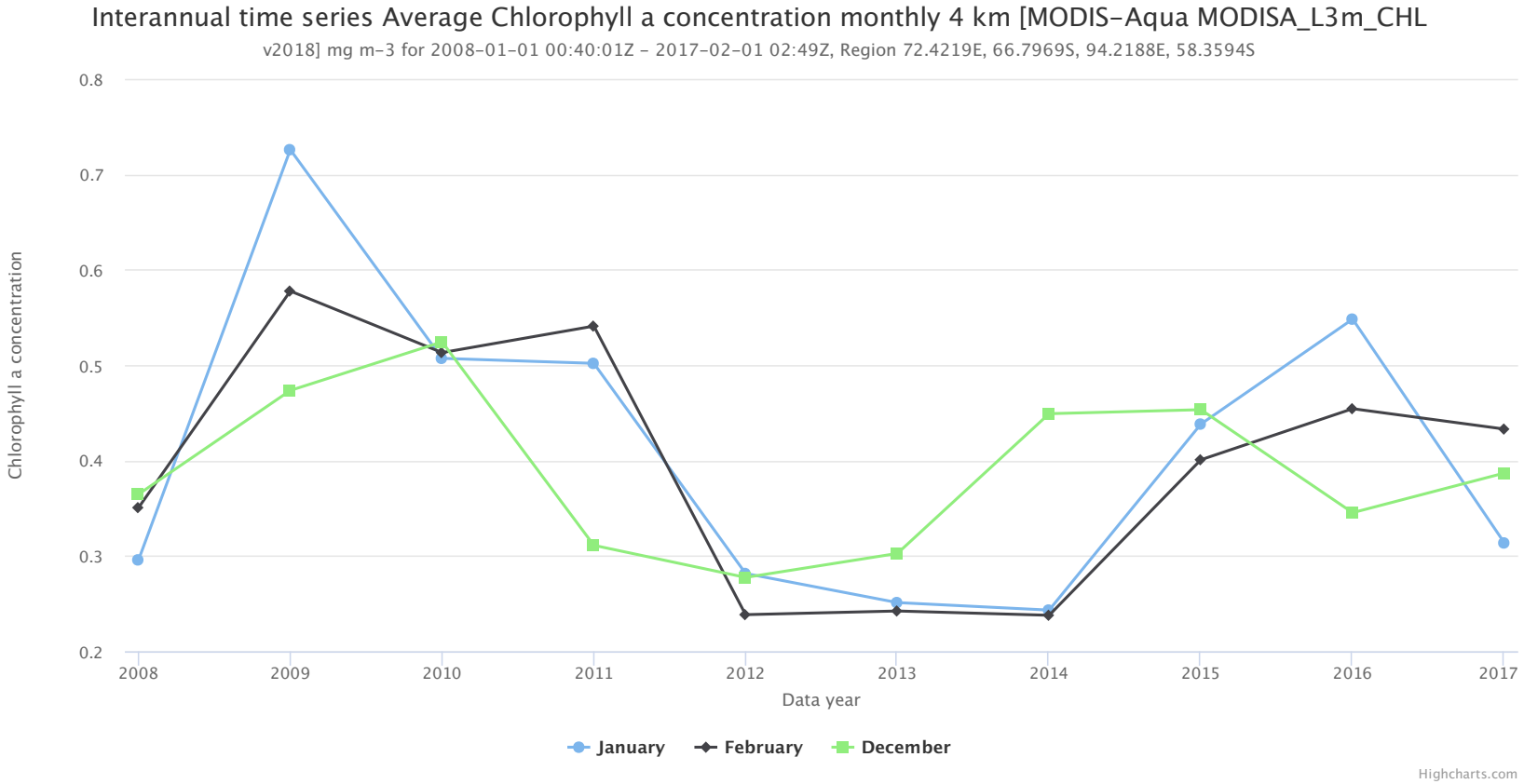

Figure B.1 Interannual monthly time series of average chlorophyll *a* concentrations (mg m^{-3}) for December, January and February (2008-2017), derived from MODIS-Aqua satellite data distributed by NASA (Level 3 binned, 4 km resolution; https://oceandata.sci.gsfc.nasa.gov/MODIS-Aqua/L3BIN/).

Appendix C

Supplementary materials for Chapter 4

C.1 Supplementary Tables

Table C.1 Details of equipment (depth (m) in brackets), sensors, sensor suppliers, and the oceanographic data obtained by each.

Equipment type	Sensor name	Sensor supplier	Oceanographic data
GPS buoy (surface)	ACTW-USB	JFE Advantech Co. Ltd.	Temperature, salinity
Sensor frame 1 (15 m)	Depth sensor	JFE Advantech Co. Ltd.	Depth
	ALW-CMP	JFE Advantech Co. Ltd.	PAR
	ACTW-USB	JFE Advantech Co. Ltd.	Temperature, salinity
	ACLW2-USB	JFE Advantech Co. Ltd.	Chlorophyll, temperature, turbidity
Sensor frame 2 (32 m)	ATD-HR	JFE Advantech Co. Ltd.	Temperature, depth
	ALW-CMP	JFE Advantech Co. Ltd.	PAR
	ACTW-USB	JFE Advantech Co. Ltd.	Temperature, salinity
	ACLW2-USB	JFE Advantech Co. Ltd.	Chlorophyll, temperature, turbidity
Sensor frame 3	ALW-CMP	JFE Advantech Co. Ltd.	PAR

	ALTW-USB	JFE Advantech Co. Ltd.	Temperature, salinity
	ACLW-CMP	JPE Advantech Co. Ltd.	Chlorophyll, temperature, turbidity
Microcat 1 (44 m)	SBE37	SBE	Temperature, salinity
	Depth-sensor	JFE Advantech Co. Ltd.	Depth
	MFL	JFE Advantech Co. Ltd.	Fluorescence, temperature, turbidity
	DEFI2-L	JFE Advantech Co. Ltd.	PAR
Microcat 2 (50 m)	SBE37	SBE	Temperature, salinity
	Depth-sensor	JFE Advantech Co. Ltd.	Depth
Sediment trap 1	A twin trap	NiGK Co.	
	ACT-HR	JFE Advantech Co. Ltd.	Temperature, salinity
ADCP (65 m)	Aquadopp Profiler	Nortek Group	Current
	Depth-sensor	JFE Advantech Co. Ltd.	Depth
Sediment trap 2	A twin trap	NiGK Co.	

Table C.2 Drifter1 pteropod species and age class flux estimated from abundance (ind m^{-2} day^{-1}) per sediment trap cup. Count data in brackets.

Trap cup	*L. helicina antarctica* adult	*L. helicina* juvenile	*L. helicina* veliger	*C. pyramidata* f. *sulcata*	Gymnosome spp.	Egg mass
1	0 (0)	0 (0)	107 (8)	13 (1)	0 (0)	0 (0)
2	0 (0)	0 (0)	282 (21)	0 (0)	13 (1)	0 (0)
3	0 (0)	40 (3)	228 (17)	0 (0)	27 (2)	13 (1)
4	215 (16)	40 (3)	134 (10)	0 (0)	0 (0)	0 (0)
5	228 (17)	27 (2)	899 (67)	0 (0)	0 (0)	27 (2)
6	81 (6)	13 (1)	631 (47)	40 (3)	40 (3)	27 (2)
7	64 (6)	64 (6)	2470 (230)	43 (4)	11 (1)	22 (2)

Table C.3 24hr trap *L. helicina* age class flux estimated from abundance (ind. m^{-2} day^{-1}) per sediment trap cup; F = formalin, L = Lugol's solution. Count data in brackets. There were no other species found in this sampling experiment.

Trap cup	*L. helicina antarctica* adult	*L. helicina* juvenile	*L. helicina* veliger	Egg mass
57 m (F)	282 (5)	113 (2)	452 (8)	57 (1)
57 m (L)	113 (2)	395 (7)	452 (8)	57 (1)
90 m (F)	0 (0)	0 (0)	7115 (126)	0 (0)
90 m (L)	0 (0)	0 (0)	6268 (111)	0 (0)

Table C.4 GLM outputs for the explanatory value of environmental parameters measured for pteropod species and age class fluxes in abundance from sediment trap sensor datasets. The most parsimonious models are selected based on lowest AIC selection criteria. Significant parameters ($p \leq 0.05$) in bold. All GLM's based on negative binomial distribution.

Model Group	Best fit model predictors	Coeff	± SE	*t*-value	*p*	AIC	$pr(X^2)$ model fit
All species/ ages[b] (combined)	fluorescence	-2.23	0.08	-29.4	$9x10^{-5}$	136.4	0.989
	latitude	0.44	0.12	3.50	0.04		
	PIC	0.25	0.02	14.36	$7x10^{-4}$		
	POC	0.08	$5x10^{-3}$	14.43	$7x10^{-4}$		
	zooplankton	$2x10^{-3}$	$9x10^{-6}$	21.94	$2x10^{-4}$		
Adult *L. helicina antarctica*	fluorescence	-15.60	3.34	-4.67	$3x10^{-3}$	64.06	0.934
	salinity	23.69	4.38	5.41	$3x10^{-3}$		
	temperature	-19.24	3.21	-6.00	$2x10^{-3}$		
Juvenile *L. helicina*	fluorescence	-6.02	1.68	-3.59	0.04	66.65	0.172
	gymnosomes	0.07	0.04	2.04	0.13		
	PIC	1.26	0.38	3.28	0.05		
	POC	0.22	0.07	3.22	0.05		
	temperature	-7.41	3.55	-2.08	0.13		
Veliger *L. helicina*	depth	-0.22	0.03	-6.36	0.02	132.29	0.489
	gymnosomes	0.03	0.02	2.25	0.15		
	latitude	4.55	1.26	3.61	0.07		
	POC	-0.08	0.02	-4.64	0.04		
	temperature	-7.42	1.42	-5.22	0.03		

	zooplankton	$3x10^{4}$	$5x10^{-5}$	-29.05	$2x10^{-16}$		
Egg masses	Intercept	$-2x10^{5}$	$4x10^{3}$	-35.66	$8x10^{-4}$	49.40	0.999
	fluorescence	-34.44	9.64	-35.72	$8x10^{-4}$		
	gymnosomes	4.73	0.13	35.53	$8x10^{-4}$		
	juveniles	-1.21	0.03	-35.59	$8x10^{-4}$		
	salinity	$4x10^{3}$	122	35.66	$8x10^{-4}$		
	temperature	$-1x10^{3}$	36.70	-35.50	$8x10^{-4}$		
	zooplankton	-0.02	$8x10^{-4}$	-35.70	$8x10^{-4}$		
C. pyramidata	Intercept	$-2x10^{3}$	38.66	-63.31	$2x10^{-8}$	30.76	0.999
	fluorescence	26.29	0.55	48.15	$7x10^{-8}$		
	longitude	22.87	0.36	63.31	$2x10^{-8}$		
	POC	-4.18	0.08	-53.62	$4x10^{-8}$		
Gymnosomes	Intercept	$7x10^{4}$	144	45.86	$1x10^{-6}$	35.94	0.999
	adults	-5.42	0.12	-45.03	$1x10^{-6}$		
	C. pyramidata	5.51	0.12	44.41	$2x10^{-6}$		
	juveniles	0.50	0.01	47.59	$1x10^{-6}$		
	salinity	$-2x10^{3}$	42.23	-45.85	$2x10^{-6}$		

Table C.5 Pteropod egg mass morphometrics for drifter1 and 24hr trap sampling experiments. 57 m (F) and (L) are sampling cups poisoned with formalin and Lugol's solution, respectively, from the 24-hr sampling experiment.

Sampling cup	Clutch length (mm)	Clutch area (mm)	Clutch-to-Egg ratio	Egg count	Egg area (mm)
3	4.43	6.18	2.18	696	1.64x10-3
5	4.49	4.47	2.32	424	1.17x10-3
5	5.07	6.99	2.04	1106	1.00x10-3
6	4.80	4.47	1.69	692	1.00x10-3
6	4.66	5.11	1.78	807	1.00x10-3
7	5.48	6.56	1.69	653	3.00x10-3
7	4.90	6.06	1.59	893	1.93x10-3
57 m (F)	8.27	18.93	1.34	643	0.014
57 m (L)	4.62	5.52	1.47	605	3.26x10-3

Table C.6 24h sediment trap depth sensor data.

Sensor depth (m)	Maximum depth (m)	Minimum depth (m)	Depth difference (m)	Average depth (m ± SD)
15	16.5	14.4	2.1	15.7 (0.2)
30	32.9	30.3	2.6	31.9 (0.3)
45	45.3	43.0	2.4	44.4 (0.3)
50	51.3	48.2	3.1	50.1 (0.4)
65	67.4	64.3	3.1	66.1 (0.4)

C.2 Supplementary Figures

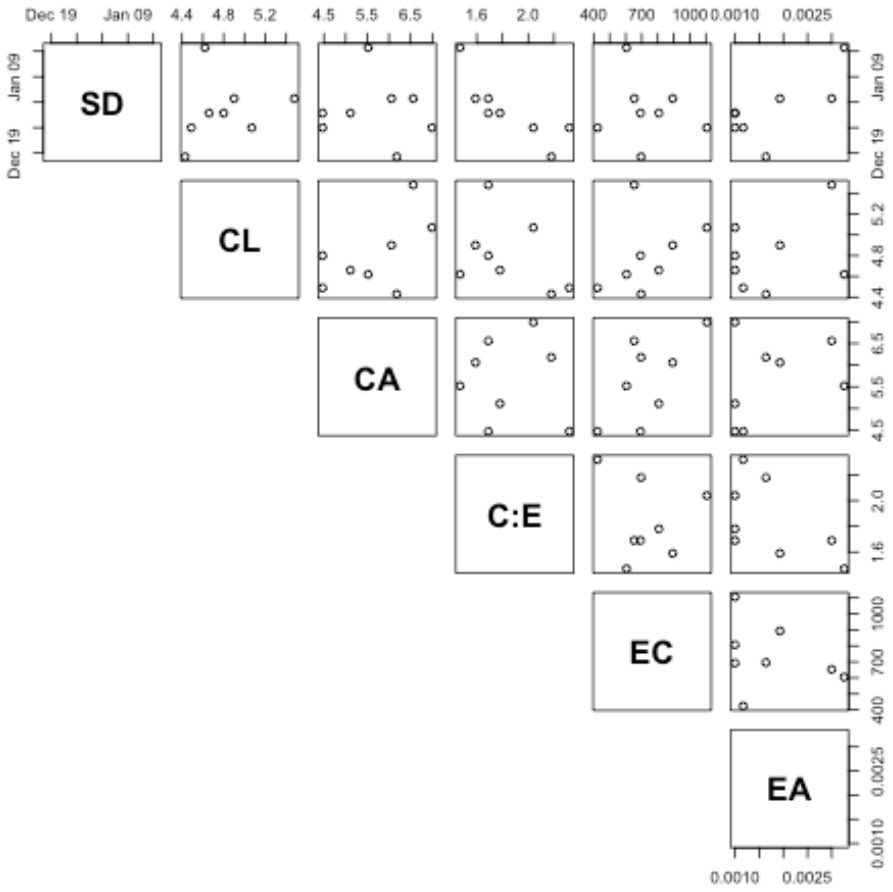

Figure C.1 Multiple pairwise comparisons between each morphometric variable used to describe egg masses from each sampling cup. Variables include: SD = sampling date, CL = clutch length, CA = clutch area, C:E = clutch to egg ratio, EC = egg count, EA = egg area, EDM = Euclidean distance.

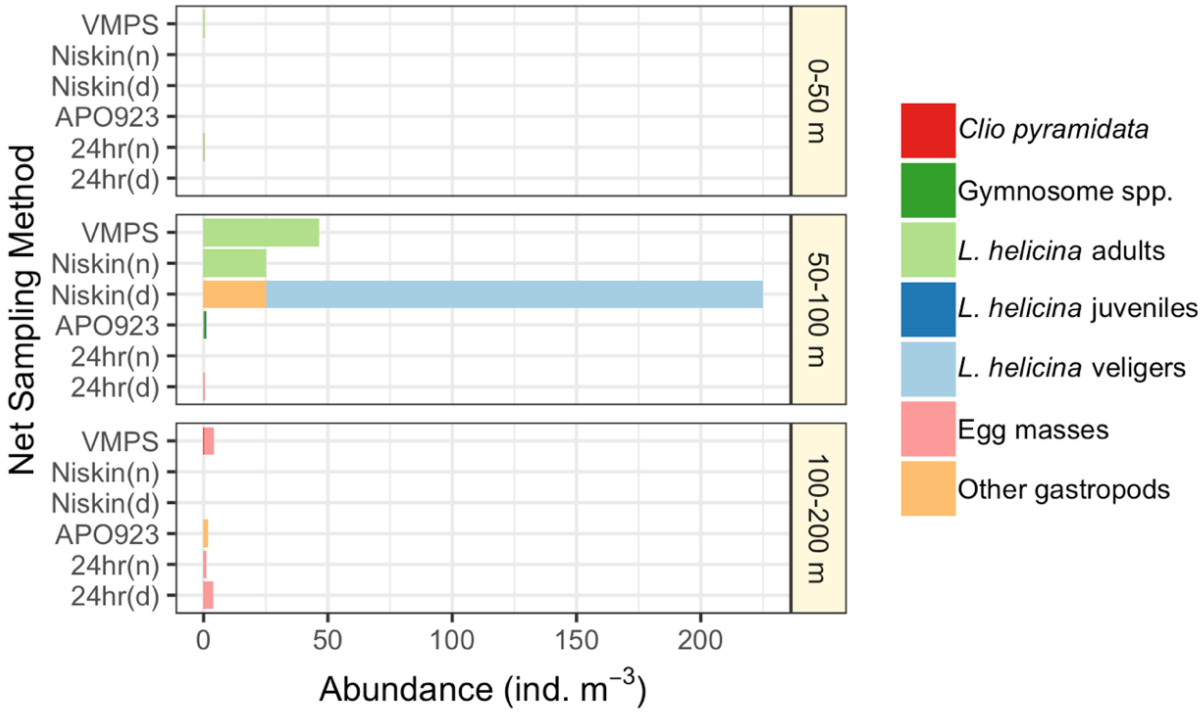

Figure C.2 Log-transformed abundance values from unpublished data for pteropods obtained from various net sampling techniques conducted during the same research program as that presented in this Chapter.

Appendix D

Supplementary materials for Chapter 5

D.1 Supplementary Methods

The following is the protocol that uses ImageJ to enumerate eggs within egg masses:

1. Before eggs can be counted, a binary version of the original image needs to be created. Open the image, then create a duplicate by right-clicking on it and select Duplicate… from the menu. In the resulting dialogue, you can give the image a new name or accept the default (the original image name with –x at the end of it).
2. Select an area around the eggs within the egg mass. Select the "freehand" tool and draw around the region of interest (ROI). Then go to Image > Crop.

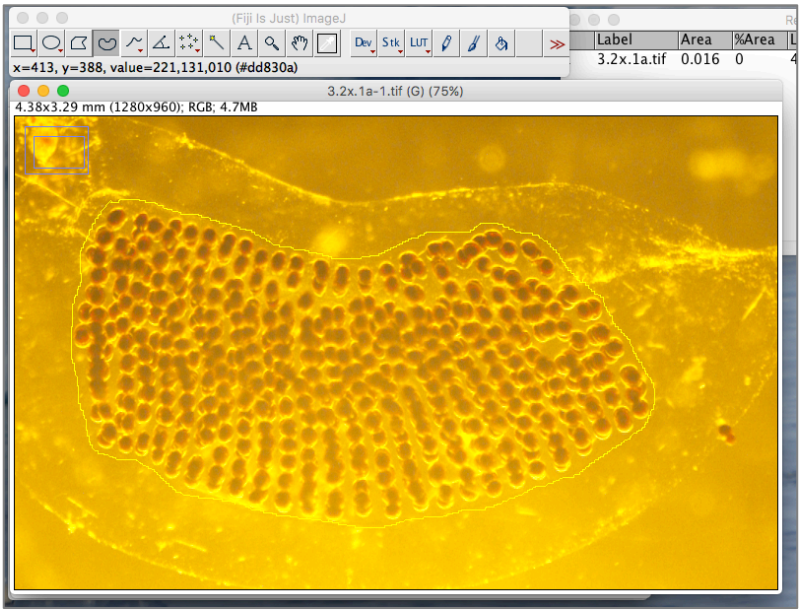

3. Convert image to greyscale. Go to Image > Type > 8-bit.

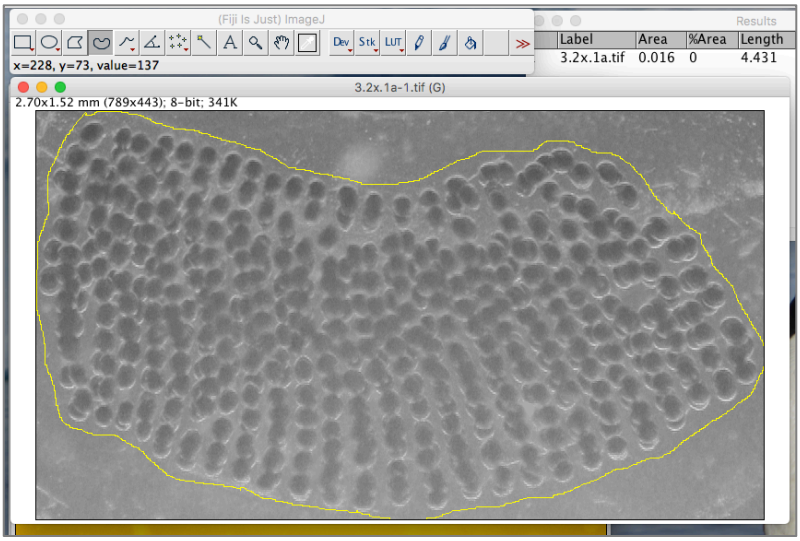

4. Threshold the image. Go to Image > Adjust > Threshold. Tick the Dark Background box and leave all other settings at default.

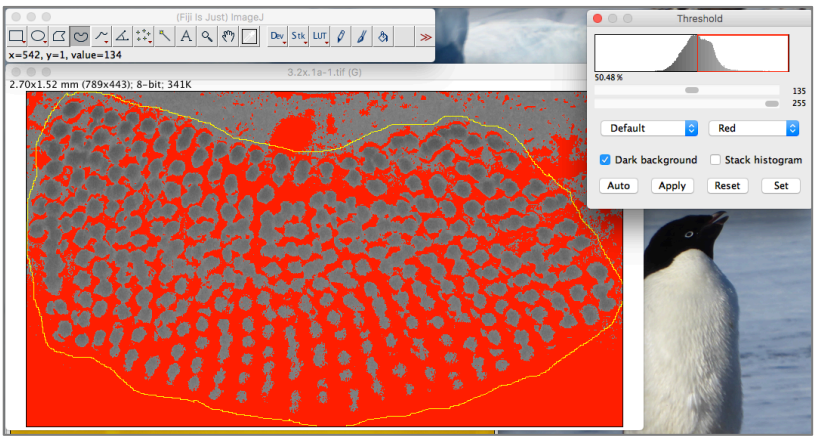

5. Go to Process > Binary > Make Binary or press the Apply button in the threshold window.

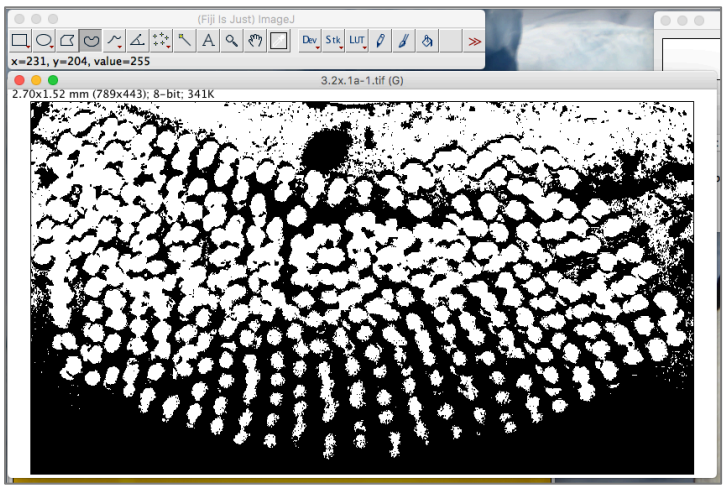

6. The resulting binary image will likely show several eggs that seem fused together. If we were to count this image now, these fused eggs would be counted as one. These can easily be separated by going to Process > Binary > Watershed. The watershed function essentially draws a dividing line between the two objects. Use the "freehand selections" tool to draw around the region of interest.

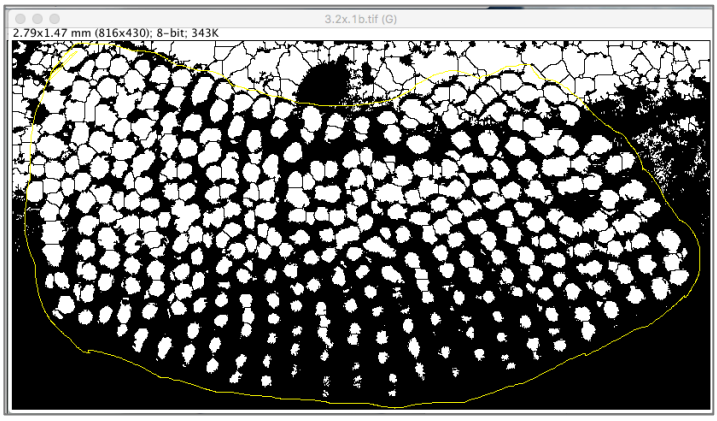

7. To count eggs, go to Analyse > Analyse Particles… In the dialogue box that pops up, leave Size and Circularity at their default values. Set Show: to Outlines, and tick the boxes as per the figure below. Press OK.

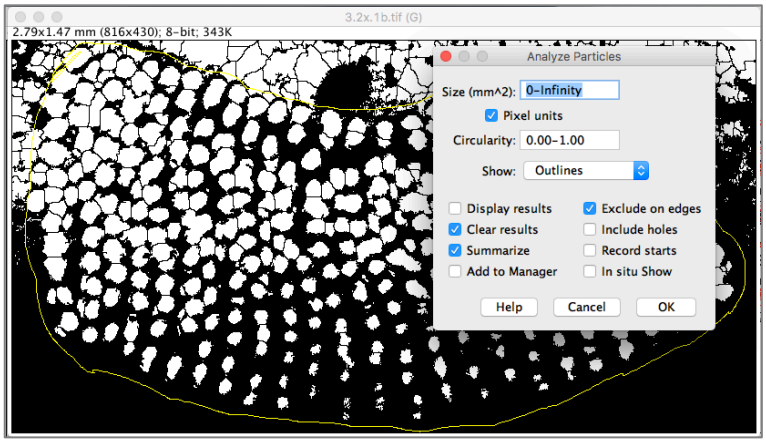

8. The results are displayed in the table and as the outline image. The results show that there are 696 eggs in the image.

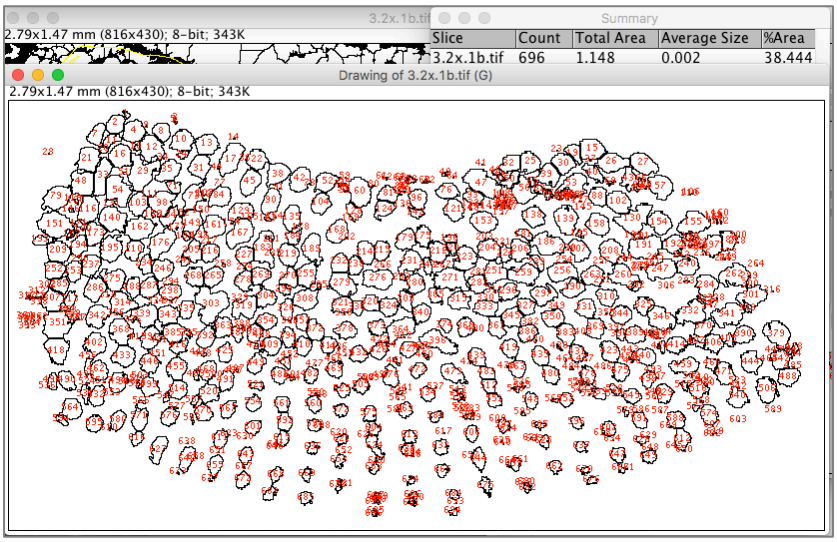

D.2 Supplementary Tables

Table D.1 Details of station and egg mass counts from sites where they were collected.

Station	Voyage	Net gear	Sample date	Longitude (°E)	Latitude (°S)	Egg mass count
16	BROKE-East	RMT	30/1/96	79.97	-66.03	11
27	BROKE-East	RMT	1/2/96	80.01	-64.50	9
R10	K-Axis	RMT	28/1/16	91.53	-62.32	43
R11	K-Axis	RMT	28/1/16	89.67	-62.39	37
R12	K-Axis	RMT	29/1/16	87.79	-62.47	3
R13	K-Axis	RMT	30/1/16	86.11	-62.52	13
R14	K-Axis	RMT	31/1/16	83.87	-62.54	18
R15	K-Axis	RMT	1/2/16	82.03	-62.52	1
R22	K-Axis	RMT	4/2/16	91.38	-65.01	4
R23	K-Axis	RMT	5/2/16	89.80	-64.32	1
R39	K-Axis	RMT	14/2/16	85.85	-60.07	4
R40	K-Axis	RMT	15/2/16	83.59	-60.32	3
R42	K-Axis	RMT	15/2/16	79.93	-60.90	3
C03	KARE20	ORI	9/1/17	110.05	-62.01	48
C07	KARE20	ORI	10/1/17	109.93	-64.24	87

KC6	KARE20	ORI	11/1/17	109.90	-65.16	5
C11	KARE20	ORI	15/1/17	107.96	-63.49	43
C05	KARE20	ORI	16/1/17	109.94	-62.99	55
C06	KARE20	ORI	17/1/17	109.99	-63.50	33

Table D.2 Details on number of egg masses from 24-hr incubation experiments of adult *L. helicina antarctica*.

Site/Date	Bottle ID#	No. egg masses	Adult shell diameter (mm)	Seawater fraction (μm)
C09	37	2	4.185	210
13/1/17	49	3	5.880	210-20
	23	0	4.355	20
	15	1	5.044	210
	77	1	4.728	210-20
	20	0	5.434	20
	84	2	5.039	210
	54	5	6.754	210-20
	62	2	5.338	20
	6	5	5.447	210
	66	3	6.573	210-20
	22	1	6.265	20
C06	84	0	5.477	210
17/1/17	48	13	6.335	210
	58	15	6.440	210
	74	7	6.985	210

Table D.3 Summary of paired *t*-test results of egg and egg mass morphometric traits for each voyage.

Trait	*t*-value		
	BROKE-EAST vs KAXIS	KAXIS vs KARE20	BROKE-EAST vs KARE20
Mass length (mm)	t = -5.3444	t = -0.065677	t = -6.1681
	df = 61.857	df = 134.47	df = 38.177
	$p < 0.001$	$p = 0.9477$	$p < 0.001$
Mass area (mm^2)	t = -6.8343	t = -0.58936	t = -8.291
	df = 81.722	df = 118.19	df = 39.988
	$p < 0.001$	$p < 0.5567$	$p < 0.001$
Clutch area (mm^2)	t = -4.636	t = 2.3351	t = -7.257
	df = 58.841	df = 146.36	df = 38.431
	$p < 0.001$	$p < 0.05$	$p < 0.001$
Clutch area : Egg mass area	t = -4.4366	t = -4.2909	t = -1.654
	df = 73.192	df = 101.2	df = 31.618
	$p < 0.001$	$p < 0.001$	$p = 0.108$
Egg counts	t = -2.2401	t = 1.6663	t = -3.5267
	df = 50.759	df = 163.62	df = 38.377
	$p < 0.05$	$p = 0.09756$	$p < 0.05$
Eggs · mass mm^{-2}	t = 4.0329	t = 1.798	t = 3.3097

	$df = 34.205$	$df = 163.96$	$df = 29.53$
	$p < 0.001$	$p = 0.07402$	$p < 0.05$

D.3 Supplementary Figures

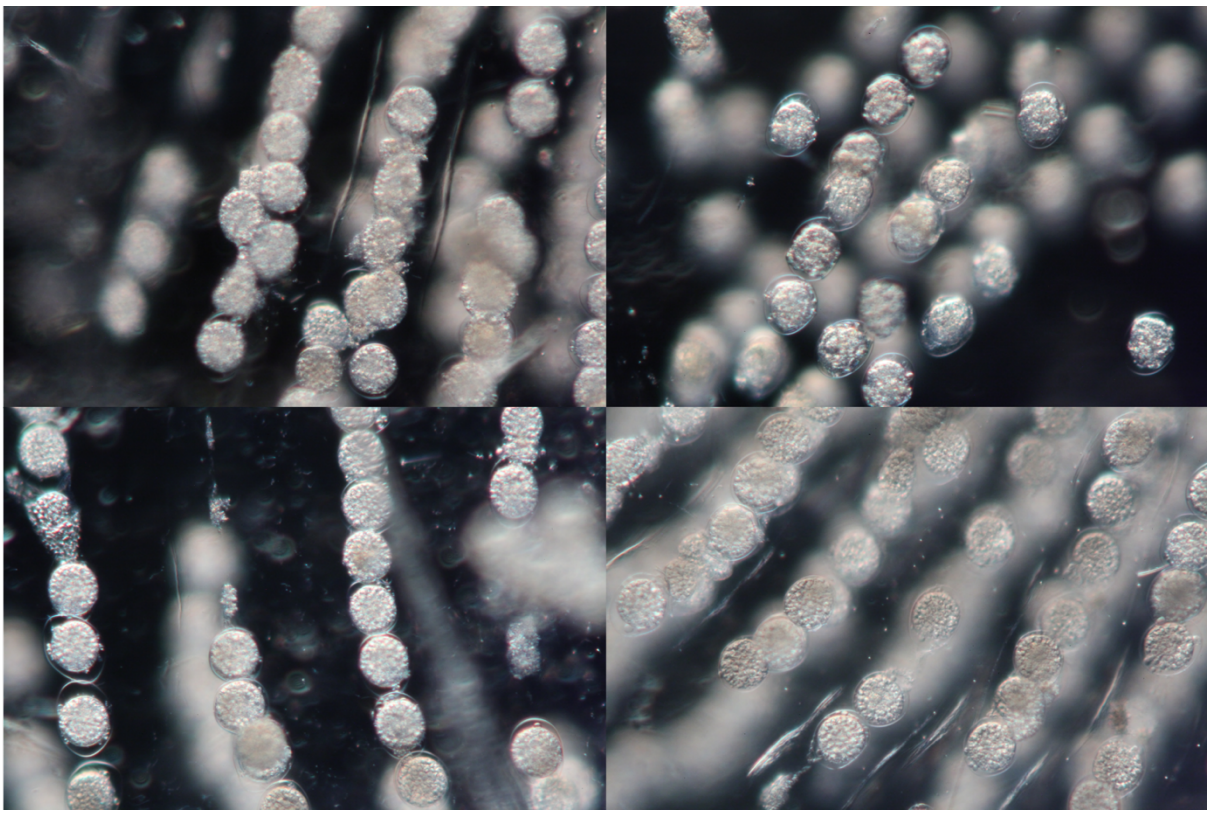

Figure D.1 Composite of images featuring underdeveloped and abnormal embryos.